Enabling the computation of transformation pathways towards a climate-neutral European energy system in high spatial and temporal resolution using a massively parallel solver

Von der Fakultät Energie-, Verfahrens- und Biotechnik der Universität Stuttgart zur Erlangung der Würde eines Doktor-Ingenieurs (Dr.-Ing.) genehmigte Abhandlung

Vorgelegt von

Manuel Wetzel

aus Mutlangen

Hauptberichter:	Prof. Dr. Valentin Bertsch
Mitberichter:	Prof. Dr. Frithjof Staiß
Tag der mündlichen Prüfung:	13.05.2026

Institut für Gebäudeenergetik, Thermotechnik und Energiespeicherung der Universität Stuttgart

2026

Contents

Zusammenfassung 7

Abstract 9

Included publications 11

1 Introduction 15

1.1 Motivation . . . 15

1.2 Energy system modelling . . . 16

1.3 From power system models to long-term transformation pathways . . . 18

1.4 Addressing computational challenges . . . 20

1.5 Research questions and structure . . . 23

2 Methods 25

2.1 Energy system optimisation models . . . 25

2.1.1 The ESOM framework REMix . . . 27

2.1.2 Model formulation and design considerations . . . 29

2.2 Solving methods for linear programs . . . 36

2.2.1 The massively parallel solver PIPS-IPM++ . . . 38

2.2.2 Annotation and decomposition for transformation pathways . . . 39

3 Publications 43

3.1 Overview and contribution to research questions . . . 43

3.2 Publication 1: Green energy carriers and energy sovereignty in a climate neutral European energy system . . . 47

3.3 Publication 2: Understanding the performance impact of a massively parallel solver for energy system optimisation models – a computational experiment using the PIPS-IPM++ solver for REMix instances 63
3.4 Publication 3: From ambition to reality: The impact of limited capacity expansion rates on the transformation pathway to a climate-neutral European energy system 81

4 Extended results **99**
4.1 Benchmarking instances for transformation pathways 99
4.2 Performance comparison for transformation pathways 102

5 Discussion **105**
5.1 Modelling transformation pathways in high temporal and spatial resolution 105
5.2 Overcoming computational boundaries for linear ESOMs 109

6 Conclusions **115**

References **117**

List of abbreviations

AC	alternating current
AC-OPF	alternating current optimal power flow
ADMM	alternating direction method of multipliers
BEV	battery electric vehicle
CAPEX	capital expenditures
CCD	compute complex die
CCX	core complex
CHP	combined heat and power
DLR	Deutsches Zentrum für Luft- und Raumfahrt
CPU	central processing unit
DC-OPF	direct current optimal power flow
EU	European Union
ESOM	energy system optimization model
ERAA	European resource adequacy assessment
FT	Fischer Tropsch
GHG	green house gas
GPU	graphics processing unit
HP	heat pump
HPC	high-performance computing
HPR	Halpern Peaceman-Rachford
IP	interior point
IPCC	Intergovernmental Panel on Climate Change
JSC	Jülich Supercomputing Centre
LP	linear programming
LCA	life cycle assessment
LCOE	levelised cost of electricity
MILP	mixed-integer linear programming
MPI	Message Passing Interface
NUMA	non-uniform memory access
NUTS	Nomenclature des unités territoriales statistiques
NECP	national energy and climate plan
NLP	non-linear programming

OPEX	operational expenditures
OpenMP	Open Multi-Processing
PDHG	primal-dual hybrid gradient
PDLP	primal-dual hybrid gradient for linear programming
PV	photovoltaics
QP	quadratic programming
REMix	Renewable Energy Mix
UC	unit commitment
UK	United Kingdom
VRE	variable renewable energy

Zusammenfassung

Diese Dissertation leistet einen wesentlichen Beitrag zu einer der grundlegenden Herausforderungen auf dem Gebiet der Energiesystemanalyse: die mathematische Lösbarkeit großer linearer Optimierungsmodelle. Insbesondere bei der Erweiterung von Bottom-up Energiesystemoptimierungsmodellen mit hoher räumlicher und zeitlicher Auflösung um Transformationspfade mit perfekter Vorraussicht werden sowohl die grundsätzliche Lösbarkeit als auch die für die Lösung benötigte Rechenzeit zu limitierenden Faktoren. Um diese Herausforderung zu adressieren, wird die Anwendung des massiv-parallelen Solvers PIPS-IPM++ untersucht, durch welchen die Skalierbarkeit und parallele Rechenleistung von Hochleistungsrechnern nutzbar gemacht werden. Die Arbeit erschließt daher einerseits die methodischen und technischen Grundlagen für die Anwendung des Solvers und zeigt andererseits das Potenzial auf, das sich durch dessen Einsatz für die Optimierung von Transformationspfaden des europäischen Energiesystems in hoher räumlicher und zeitlicher Auflösung ergibt.

In einem ersten Schritt wird anhand einer modellgestützten Analyse die Frage untersucht, welche Auswirkungen die Bereitstellung großer Mengen von grünem Wasserstoff innerhalb Europas gegenüber dem Import der erforderlichen Mengen durch strategische Energiepartnerschaften in einem langfristigen, klimaneutralen europäischen Energiesystem hat. Dabei konzentriert sich die Analyse insbesondere auf die räumlichen und zeitlichen Wechselwirkungen zwischen der zeitlich variablen Stromerzeugung aus erneuerbaren Energiequellen und der Wasserstoffproduktion. Die Ergebnisse der Analyse zeigen, dass der Ausbau erneuerbarer Energiequellen und die Umwidmung von Erdgasinfrastrukturen für Wasserstoff von entscheidender Bedeutung sind. Die Ergebnisse verdeutlichen jedoch auch die Grenzen, die sich aus der Optimierung eines einzigen Zieljahres und der räumlichen Auflösung des Modells ergeben. Eine Adressierung dieser Einschränkungen durch eine höhere räumliche Auflösung und die Einbeziehung von Transformationspfaden mit perfekter Vorraussicht steigert jedoch die Größe des Optimierungsproblems erheblich und erfordert neue Lösungsmethoden.

Daher wird in einem zweiten Schritt die Anwendung eines massiv-parallelen Lösers auf Energiesystemmodelle unter Verwendung eines Hochleistungsrechenclusters untersucht. Dabei wird insbesondere das grundlegende Verständnis geschaffen, das erforderlich ist, um den massiv-parallelen Löser PIPS-IPM++ effektiv auf Hochleistungsrechnern einzusetzen. Zudem werden die Auswirkungen auf die Lösungsgeschwindigkeit verschiedener Zerlegungsstrategien für unterschiedliche Modellinstanzen mit variierender Modellgröße und Komplexität des Kapazitätszubaus analysiert. Dieses Rechenexperiment identifiziert einerseits die Anzahl der Zubauentscheidungen und die Gesamtgröße des Modells als die wichtigsten Faktoren für den benötigten Rechenaufwand. Andererseits zeigt es jedoch auch eine signifikante Reduktion der Lösungszeiten um eine Größenordnung unter dem Einsatz der besten Konfiguration für PIPS-IPM++.

In einem dritten Schritt werden die Einschränkungen hinsichtlich der Modellformulierung adressiert, indem die Zieljahr-Optimierung auf einen Transformationspfad mit perfekter Voraussicht ausgeweitet und gleichzeitig die räumliche Auflösung des geografischen Betrachtungsbereichs erhöht wird. Um die Ergebnisse bezüglich des hohen regionsspezifischen Kapazitätsausbaus weiter zu untersuchen, liegt der Fokus auf den länder- und technologiespezifisch erreichbaren jährlichen Kapazitätsausbauraten sowie deren Wechselwirkung mit der heimischen Produktion von grünem Wasserstoff. Die Ergebnisse zeigen, dass diese Zubauraten eine der wichtigsten Annahmen sind, die den Verlauf des gesamten Transformationspfads bestimmen. Ebenso zeigen sie, dass die Erwartungen hinsichtlich zukünftiger Reduktionen der Investitionskosten für Elektrolyseure kurzfristig zu einer verstärkten Nutzung von blauem Wasserstoff führen könnten, die möglicherweise eine langfristige Abhängigkeit von Wasserstoffimporten zur Folge hätte. Eine kurzfristige starke Nutzung von blauem Wasserstoff kann darüber hinaus mittelfristig die erforderlichen Installationsraten für erneuerbare Energien und Elektrolyseure zum Zeitpunkt, an dem sich die techno-ökonomische Rentabilität von blauem zu grünem Wasserstoff verlagert, signifikant steigern.

Im einem vierten Schritt wird die erweiterte Modellformulierung für Transformationspfade mit der Berechnung durch den massiv-parallelen Solver PIPS-IPM++ auf Hochleistungsrechnern kombiniert. Dieses Rechenexperiment liefert weitere Erkenntnisse über die spezifischen Erwägungen der Zerlegungsstrategien für Transformationspfade und demonstriert die Effektivität des Solvers bei der Lösung großer linearer Optimierungsprobleme. Dieses Ergebnis unterstreicht, dass bei einem ausreichenden und grundlegenden Verständnis der Struktur des Optimierungsproblems und der Clusterinfrastruktur die Anwendung massiv-paralleler Löser ein wirksames Mittel sein kann, um die Berechnung von Transformationspfaden mit hoher räumlicher und zeitlicher Auflösung zu ermöglichen.

Abstract

This dissertation provides a significant contribution to one of the fundamental challenges in the field of energy systems analysis: the computational tractability of large-scale linear optimisation models. In particular when extending bottom-up energy system optimisation models with high spatial and temporal resolution by transformation paths with perfect foresight, both the fundamental tractability and the computational time required for the solution become limiting factors. To address this challenge, the application of the massively parallel solver PIPS-IPM++ is investigated, which enables access to the scalability and parallel computing power of high-performance computers. The work therefore develops the methodological and technical basis for the application of the solver and shows the potential that results from its use for the optimisation of transformation paths of the European energy system in high spatial and temporal resolution.

As a first step, a model-based analysis of a long-term, climate-neutral European system explores the implications of providing large quantities of domestic hydrogen or importing the necessary volumes through strategic energy partnerships. The analysis focuses specifically on the spatial and temporal interactions between electricity production from variable renewable energy sources and hydrogen production. Both the crucial role of expanding variable renewable energy technologies and the importance of repurposing natural gas infrastructure towards hydrogen are highlighted in the results of the analysis. However, the results also emphasise limitations relating to target year optimisation and the spatial resolution of the study. Addressing these limitations by considering a higher spatial resolution and including transformation pathways with perfect foresight significantly increases the size of the optimisation problem overall, requiring new methods to solve it.

Therefore, in a second step, the application of a massively parallel solver to energy system models using a high-performance computing cluster is explored. In particular, this establishes the fundamental understanding required to apply the massively parallel solver PIPS-IPM++ effectively on high-performance computers, and analyses the performance implications of different decomposition

strategies for a set of model instances of varying size and varying complexity regarding the capacity expansion decisions. This computational experiment identifies the number of capacity expansion decisions and the overall model size as the key drivers for the computational challenge, but also demonstrates a significant reduction in solution times of one order of magnitude when using the best performing configuration for PIPS-IPM++.

In a third step, the limitations regarding the model formulation are addressed by extending the target-year optimisation to a perfect-foresight transformation pathway while simultaneously increasing the spatial resolution of the geographical scope. To further challenge the findings concerning high country-specific capacity expansion, emphasis is placed on country- and technology-specific achievable annual capacity expansion rates and their interaction with domestic green hydrogen production. The findings reveal that these rates are among the most important assumptions that determine the course of the entire transformation pathway. They also show that expectations regarding future reductions in investment costs for electrolysers could result in an increased use of blue hydrogen in the short term, potentially leading to a long-term dependence on hydrogen imports. Furthermore, a strong short-term utilisation of blue hydrogen can significantly increase the required installation rates for renewable energies and electrolysers in the medium term at the point when the techno-economic profitability shifts from blue to green hydrogen.

In the fourth step, the improved model formulation for transformation pathways is combined with the application of the massively parallel solver PIPS-IPM++. This computational experiment provides further insights into considerations specific to transformation pathways, demonstrating the solver's effectiveness in solving large-scale optimisation problems by reducing the required time by a factor of five. This result highlights that, with a sufficient and fundamental understanding of the problem structure and cluster infrastructure, the application of massively parallel solvers can be an effective means of enabling the computation of transformation pathways at high spatial and temporal resolutions.

Included publications

Peer-reviewed journal contributions by the author included in this thesis.

Publication 1 Manuel Wetzel, Hans Christian Gils, and Valentin Bertsch (2023) *Green energy carriers and energy sovereignty in a climate neutral European energy system*, In Renewable Energy, doi: 10.1016/j. renene.2023.04.015

Publication 2 Manuel Wetzel, Karl-Kiên Cao, and Shima Sasanpour (2025) *Understanding the performance impact of a massively parallel solver for energy system optimization models – a computational experiment using the PIPS-IPM++ solver for REMix instances*, In Sustainable Energy, Grids and Networks, doi: 10.1016/j. segan.2025.101893

Publication 3 Manuel Wetzel, Hans Christian Gils, and Valentin Bertsch (2026) *From ambition to reality: Impact of renewable capacity expansion rates and infrastructure delays on the transformation pathway towards a climate neutral European energy system*, In Renewable Energy, 2026, doi: 10.1016/j.renene.2025.124917

Other peer-reviewed journal contributions by the author not included in this thesis.

Publication 4 Denis Hess, Manuel Wetzel, Karl-Kiên Cao (2018) *Representing node-internal transmission and distribution grids in energy system models*, In Renewable Energy, doi: 10.1016/j. renene.2017.10.041

Publication 5 Karl-Kiên Cao, Kai von Krbek, Manuel Wetzel, Felix Cebulla, Sebastian Schreck (2019) *Classification and Evaluation of Concepts for Improving the Performance of Applied Energy System Optimization Models*, In Energies, doi: 10.3390/en12244656

Publication 6 Mengzhu Xiao, Manuel Wetzel, Thomas Pregger, Sonja Simon, Yvonne Scholz (2020) *Modeling the Supply of Renewable Electricity to Metropolitan Regions in China*, In Energies, doi: 10.3390/en13123042

Publication 7 Ying Deng, Karl-Kiên Cao, Manuel Wetzel, Wenxuan Hu, und Patrick Jochem (2023) *Carbon-neutral power system enabled e-kerosene production in Brazil in 2050*, In Scientific Reports, doi: 10.1038/s41598-023-48559-7

Publication 8 Manuel Wetzel, Eugenio Salvador Arellano Ruiz, Francesco Witte, Jens Schmugge, Shima Sasanpour, Madhura Yeligeti, et al. (2024) *REMix: A GAMS-based framework for optimizing energy system models*, In Journal of Open Source Software, doi: 10.21105/joss.06330

Publication 9 Felix Nitsch, Manuel Wetzel, Hans Christian Gils, Kristina Nienhaus (2024) *The future role of Carnot batteries in Central Europe: Combining energy system and market perspective*, In Journal of Energy Storage, doi: 10.1016/j.est.2024.110959

Publication 10 Maximilian Hoffmann, Bruno U. Schyska, Julian Bartels, Tristan Pelser, Johannes Behrens, Manuel Wetzel, et al. (2024) *A review of mixed-integer linear formulations for framework-based energy system models*, In Advances in Applied Energy, doi: 10.1016/j.adapen.2024.100190

Publication 11 Rafaella Canessa, Rebecca Peer, Manuel Wetzel, Hans Christian Gils, Ashish Gulagi, Christian Breyer, Juan Carlos Osorio-Aravena, Jannik Haas (2025), *From hydro nation to solar giant: New Zealand's renewable build-out and hydrogen export scenarios*, In Environmental Research: Energy, doi: 10.1088/2753-3751/ae2871

Publication 12 Shima Sasanpour, Manuel Wetzel, Karl-Kiên Cao, Hans Christian Gils, Andrés Ramos, *Accelerating Stochastic Energy System Optimization Models: Temporally Split Benders Decomposition*, manuscript submitted to IEEE Transactions on Power Systems

> *As soon as an Analytical Engine exists, it will necessarily guide the future course of the science. Whenever any result is sought by its aid, the question will then arise – by what course of calculation can these results be arrived at by the machine in the shortest time?*

Charles Babbage, *Passages from the Life of a Philosopher*, 1864

1 Introduction

1.1 Motivation

To prevent the long-term and lasting consequences of global warming and reaching tipping points that could further accelerate change, rapid and ambitious reductions in green house gas (GHG) emissions are required. The 6th Assessment Report of the Intergovernmental Panel on Climate Change (IPCC) estimates that the energy sector was responsible for 34% global GHG emissions in 2019, making it the largest contributor [1]. As reducing emissions effectively is a global problem, the adoption of the Paris Agreement in 2015 – the first legally binding international treaty on the mitigation of global warming – was a major success. As countries outlined their contributions to reducing global emissions, the shift towards integrating renewable energy across all sectors became a more concrete. In particular the European Union (EU) and its member states set ambitious targets in the form of national energy and climate plans (NECPs).

Although technological progress and economies of scale in production have made renewables the cheapest option for producing electricity in terms of levelised cost of electricity (LCOE), their integration into the energy system still lags behind the targets of many countries [2]. While in particular the rapid phase-out of fossil fuels via carbon taxing, feed-in tariffs, and quotas can be implemented short-term [3] in particular the long life times and large investment costs of energy infrastructure like power plants, electricity grids, and gas pipelines can slow down the speed of transformation. Similarly, both existing and new fossil fuel infrastructure could further lock in future emissions and jeopardise the climate targets [4], if no appropriate market incentives are provided.

Against the backdrop of the urgent need to decarbonise the energy system rapidly and the long-term nature of energy infrastructure, model-based assessments have emerged as one of the main tools to inform stakeholders. These models encompass a wide range of approaches, each of which is suited to addressing specific research questions and is associated with particular approaches and perspectives

[5]. While these models can vary significantly in terms of their methods, scope and limitations, they share a common goal: to explore the implications of energy regulation, evaluate the impact of technologies and provide policymakers with reliable information to inform decisions regarding the questions about the energy system.

1.2 Energy system modelling

To differentiate between the various energy system models, the categorisation in the academic literature is a valuable starting point. For example, Pfenninger et al. [6] differentiate models based on their fundamental methodology into energy system optimisation models, energy system simulation models, power system models, and electricity market models. Each approach has specific strengths and weaknesses, but also limitations in terms of the insights that can be generated. In particular, for power system optimisation models, the authors further highlight the issue of complexity that needs to be addressed, and emphasise the significant difference in scale between large-scale models covering continental systems at a coarse spatial resolution, and regional models with a much higher resolution.

In a similar classification scheme dedicated to the sub-category of energy system optimization models (ESOMs), Prina et al. [7] distinguish between top-down and bottom-up modelling approaches, where the former are adopted from economists to connect the modelling approach to other macro-economic sectors, while the latter are focused on the individual technical components of the energy system and interconnections between different energy sectors. For instance, models that cover a wide range of technologies and sectors can provide information on the most cost-effective ways to reduce emissions, but face challenges in generating insights into concrete infrastructure decisions. Conversely, power system models with a high spatial resolution allow better approximations for the need for network infrastructure and storage options, but face challenges in providing insights into trade-offs between different sectors and decisions along the transformation horizon. Within the category of bottom-up models, the authors distinguish between short-term and long-term models. They also emphasise the difference between limited foresight, or "myopic foresight", and full foresight, or "perfect foresight", into future changes such as carbon prices and energy demand.

In particular, the specific approach to how much knowledge the model has regarding future developments can have a significant impact on the model results. Keppo and Stubegger [8] note that myopic foresight introduces many potential pitfalls for policymakers like postponing investment into new technologies and higher reliance on technologies that are more expensive in the long run, unless additional constraints are utilised to counteract the lack of foresight. Lambert et al. [9] emphasise the

importance of limiting the extent of knowledge regarding future developments, particularly when modelling unexpected events such as price shocks. While the perfect foresight is an appropriate approach, when it comes to identifying the least-cost ideal system transformation, it is also necessary to consider that this approach does not adequately reflect real world decision-making due to the lack of inclusion of parametric and structural uncertainty [10]. The consideration of long-term transformation pathways introduces additional aspects, which have to be taken into account. Here, for example the depreciation of assets at the end of the optimisation horizon plays a significant role, which can impact the specific timing of investment and decommissioning decisions. Similarly, the weighting between individual years, and therefore also the valuation of future investments is influenced by the socioeconomic discount rate [11].

With further development of different modelling approaches over the years and adaptation of model formulations to answer new research questions, the boundaries between models with a limited sectoral scope and hourly temporal resolution and models with a wide sectoral scope and limited representation of the temporal dimension became more indistinct. Power system models were extended to include further sectors, such as heating and transport, in an effort to answer questions related to sector integration and flexibility requirements in the power sector [12, 13]. Similarly, including additional energy carriers and integrating gas networks became integral to addressing the role of system flexibility via the long-term storage of chemical energy carriers [14, 15]. These extensions each contributed to an increased complexity of the models. To address the resulting computational challenges, aggregation techniques from models with a broader sectoral scope, such as representative weeks and days, have been adopted. More recent classification approaches, exemplified by Ringkjøb et al. [16], distinguish models based on their application cases, considering factors such as spatial and temporal scope, granularity, technological scope, and sectoral scope. In particular, the technological scope in turn also determines the necessary inclusion of energy carriers.

While the range of energy system models collectively ranges from distribution systems to continental energy systems and from short term assessments to long term transformation pathways, no single model can represent the highest level of detail across all dimensions. Focusing on ESOMs, Hoffmann et al. [17] therefore extended the classification of model formulations with the respective impact specific modelling features have on the computational burden. In this study also the fundamental challenge to stay within certain computational limits is highlighted, which mainly depends on key aspects such as the utilisation of integer investment decisions, the formulation of the transformation pathway and the application of complexity reduction techniques. Similar to other publications, like Kotzur et al. [18], it provides an overview of the large field of research on the speed-ups and trade-offs of different complexity reduction techniques along each of the model dimensions.

However, as the link between modelling features and the resulting computational burden remains on a qualitative assessment, there is still a lack of fundamental understanding of the quantitative connection. To overcome this research gap, it is necessary to make systematic comparisons of variations of the same optimisation model – also referred to as "model instances" – with different levels of complexity, in order to properly identify the limitations, particularly with regard to linear optimisation models.

1.3 From power system models to long-term transformation pathways

In order to better understand the emergence and increase in computational challenges prevalent in energy system optimisation models with high spatial and temporal resolutions, it is important to consider how these models have been used and adapted over the decades to address specific research questions.

Even in their earliest form, energy system models relying on linear programming (LP) have been considered as very large optimisation problems. In 1975, Hoffmann and Wood [19] discussed the application of linear programming for energy system models to describe the supply and demand relationships between a wide range of energy carriers. In particular, they highlight the availability of algorithms able to address the large size of the resulting optimisation problems with up to 10,000 variables. Furthermore, they refer to the SRI-Gulf energy model as one of the first energy system models including a network infrastructure with 30 supply regions, 8 demand regions, and 17 time periods [20].

With the technological development and cost reductions for variable renewable energy (VRE) technologies, the prospect of a fully renewable supply for electricity became an increasing focus of research [21, 22, 23]. Here, power system models provided large contributions to the research stream on energy systems based on 100% renewable energy [24], by demonstrating the feasibility of hourly and sub-hourly operation [25] while also considering both the detailed power grid topology and feasibility of network flows using a direct current optimal power flow (DC-OPF) approximation [26]. In particular, the inclusion of hourly time series, which adequately reflect the intermittency of renewable energy technologies, was one of the main driving factors for the increasing size of the resulting energy system models. As the models were primarily focused on the power sector and had fixed exogenous demand, the results showed a significant dependence on spatial and temporal flexibility options. On the spatial dimension, these options were seen in the form of a significant expansion of power lines [27], and on the temporal dimension, in the form of electrical energy storage [12, 28]. The intermittency of VRE generation, in conjunction with inflexible electricity demand, was the main driver of both flexibility

options, leading to immense capacity expansion requirements for power grids and storage systems, particularly for systems relying on 100% renewable electricity[13].

To facilitate the more efficient integration of renewable electricity into the energy system, the research focus shifted towards higher shares of sector integration. In particular, the possibility of direct electrification in the heat and transport sector offered by battery electric vehicles (BEVs) and heat pumps (HPs) and different operational strategies for combined heat and power (CHP) plants provided flexibility on the demand side, while at the same time contributing to the emission reductions outside of the power sector [29]. Furthermore with the Paris climate agreement and the extension of emission reduction targets to other sectors, the role of hydrogen shifted from a chemical energy carrier as a long term storage option to an energy vector with the potential to facilitate the substitution of fossil fuels with hydrogen derived from renewable energy. This required both the comprehensive representation of additional sectors and energy carriers in ESOMs. In particular, the explicit modelling of hydrogen pipeline networks [14, 15, 30] and extension to additional hydrogen derivatives such as green ammonia, green methanol, and green methane significantly contributed to the increase in overall model size and computational challenge. As a point of reference, the resulting optimisation problem addressed in *Publication 1* with hourly resolution for a single target year comprises of 25 million variables, 31 million constraints, and 101 million non-zero elements.

In particular, the integration of hydrogen and hydrogen derivatives into ESOMs and the option to store and transport chemical energy carriers over long distances opened up the discussion on whether imports of energy carriers are an economically viable option in addition to domestic production. In particular research on the global potential to produce hydrogen and Fischer Tropsch (FT) fuels based on electricity from either wind turbines, photovoltaics (PV) systems, or hybrid configurations identified countries with low production costs such as Australia, Chile, and Argentina, among others [31]. While for FT fuels the production cost outweighs the transport cost, making shipping an economically viable option, for imports of hydrogen pipeline-based transport routes from Spain and North Africa to supply countries in Central Europe are more likely [32]. However, there remain large uncertainties with the concrete uptake of a global hydrogen market, which are also reflected by the lack of policy modelling [33]. Therefore, another research gap is the identification of the role of energy import in comparison to domestic production of green hydrogen and the cost-optimal design of capacities and network topology for the European energy system.

Furthermore, the integrated modelling of power and gas networks with the possibility for infrastructure repurposing from natural gas pipelines to hydrogen introduces the challenge of finding the optimal timing for the transformation of pipeline infrastructure. Here, in particular modelling of the

transformation pathways with sufficient foresight can help prevent sub-optimal decisions and avoid stranded investments. This is done in the recent studies of Kountouris et al. [34] and Fleiter et al. [35]. While the approach modelling of transformation pathways with perfect foresight has a significantly longer history, in particular for energy system models with a wide sectoral and technological representation such as TIMES [36, 37] or OSeMOSYS [38], the key difference here comes down to the utilisation of hourly time resolution instead of the representation of the sub-annual time dimension with typical hours and days. In terms of the spatial and temporal scope, both studies are comparable to the ESOM instance addressed in *Publication 3* and the *Extended Results*. Here, the overall size of the optimisation problem reaches up to 200 million variables, 215 million constraints, and 878 million non-zero entries.

To still be able to address the resulting optimisation problems, Fleiter et al. rely on national spatial resolution for European countries aside from Germany and aggregations for smaller countries to manage the computational challenge, while Kountouris et al. rely on rolling horizon approaches. They do, however, provide a reference run utilising perfect foresight with intervals along the transformation pathways reduced to 10-year steps and report an optimisation time of 364 hours, which can be reduced down to 22 hours using the myopic approach. Both studies refer to the computational effort as the key limiting factor requiring these aggregations. Similarly, in *Publication 3*, the overall required time for the optimisation was reduced from 170 hours down to 20 hours per scenario run by using a 3-hourly temporal downsampling. This underlines the significant impact the integration of transformation pathways has on the overall size of the optimisation problem, making transformation pathways in high spatial and temporal resolution particularly challenging to solve without decomposition approaches. Furthermore, this highlights the need to better understand what makes these types of capacity expansion models with transformation pathways and high spatial and temporal resolution particularly hard to solve, and to close the research gap on how to effectively solve these problems without the application of heuristic methods, which may impact the findings.

1.4 Addressing computational challenges

With the increase in overall technological and spatio-temporal scope of the models, likewise, the computational challenges in solving the underlying optimisation models increased. This made it necessary to more critically reflect on the trade-offs between model dimensions to keep the required time for model-based assessment reasonably short. Therefore, in the past, a few distinct fundamental approaches have been developed to address this limitation [18].

To address particular limitations of a single framework, two or more frameworks can be linked together in a model-coupling effort, allowing each of the models to provide detailed insights on a specific aspect that the other model cannot provide and vice versa [39]. The choice of models depends on the concrete research question, for example one ESOM can provide an estimation on the required capacity expansion for a least-cost climate-neutral energy system while an agent-based simulation model then allows the assessment of specific behaviours of individual actors in such a market environment [40, 41]. Likewise, two optimisation models can be coupled addressing different aspects such as the coupling between linear capacity expansion models and non-linear alternating current optimal power flow (AC-OPF) models [39]. While the iterative coupling between models allows for higher focus on the particular strengths and furthermore enables combinations between different problem classes including mixed integer and non-linear aspects, achieving a sufficient convergence between the models can be challenging.

A wide range of complexity reduction methods has been developed, addressing the complexity of individual model dimensions. While some of the methods, such as modelling the system dispatch with representative hours have been an important aspect of integrated energy system models such as TIMES and OsEMOSYS for a long time, they have been also adopted for more infrastructure focused models in various degrees [42, 43]. One of the key aspects, in particular for complexity reduction methods addressing the temporal dimension, is that a certain minimum number of time steps is required to adequately capture the variability of generation profiles for VRE technologies in scenarios with high shares of renewable electricity [42]. To this end, more flexible approaches have been introduced, which allow modelling different sectors in different temporal resolution, for example resolving the power sector in an hourly resolution, while using a 4-hourly downsampling for heat and 24-hourly downsampling for gases and liquid energy carriers [44]. Similarly, the spatial dimension has been addressed to find suitable reduction methods, while capturing adequate network infrastructure [45] and the technological dimension to appropriately cluster technologies with similar characteristics [46].

Mathematical methods to exploit the underlying structure of the optimisation problem can likewise be used to speed up the optimisation. These methods include Benders decomposition, Danzig–Wolf column generation, Lagrangian relaxation, and alternating direction method of multipliers (ADMM), among others. Each method exploits different aspects of the optimisation problem and therefore each is suited to a specific class of problems, but the common denominator is in the iterative and parallel solving of partial problems. Conceptually, this is similar to the model-coupling between two optimisation problems mentioned above, but at least in the case of linear convex optimisation problems, the exact nature of the decomposition enables proving that the algorithm both converges

and leads to the global optimum. For addressing capacity expansion problems, in particular Benders decomposition has been used over several decades. Benders decomposition was originally proposed to address complex mixed-integer linear programming (MILP) problems, which can be solved much more easily by temporarily fixing complicating variables [47]. As this method of exploiting the underlying problem structure proved to be quite effective for planning models in general, it was likewise adapted to capacity expansion models for energy systems. Initially, the application in the field of energy systems was focused on unit commitment (UC) scheduling for hydro and thermal power plants [48], but later on also for solving large-scale multi-stage stochastic capacity expansion problems [49]. More recently, utilisation of the method to decompose the sub-annual temporal dimension with the goal of speeding up large-scale MILP capacity expansion problems has gained traction [50].

Parallel solvers implementing block-structure exploiting parallel interior-point methods, have been one of the more recent methodological additions [51], most likely also due to the wider access to multi-core compute clusters. While the notion, that large-scale stochastic optimisations with sparse matrices can be efficiently exploited, has been presented before [52], Gondzio and Grothey [53] presented a generalised implementation of this methodology for their parallel interior point (IP) solver OOPS to exploit the nested block structures of such problems. In the solver, different matrix structures for sparse, dense and network matrices are used as fundamental building blocks for the problem. A similar object-oriented approach is presented by Gertz and Wright in their solver OOQP [54], which does not exploit any underlying block structure, but offers a generalised framework to represent variables and data structures in a problem-specific fashion. This also was the foundation for PIPS-IPM solver presented by Petra et al. [55], who applied it for the real-time stochastic computation of economic dispatch problems for the US power grid using high performance computers (HPCs). Due to the solver being limited to stochastic optimisation problems, Rehfeldt et al. [56] extended the solver to handle more general problems from the field of ESOMs, allowing the inclusion of constraints linking the individual block structures. They apply the solver to large-scale economic dispatch problems from the ELMOD framework and stylized capacity expansion instances from the SIMPLE framework.[1].

Given the effectiveness of PIPS-IPM++ in solving the large-scale economic dispatch problems with up to 226 million variables, 256 million constraints, and 717 million non-zero elements, one major research gap is whether this solution strategy can be be transferred towards large-scale capacity expansion problems. Furthermore a systematic assessment between the scalability of the solution approach on the two different model types – capacity expansion and economic dispatch – is required in order to show either the direct applicability or identity changes in the decomposition strategy.

[1]The author of this thesis contributed to the development and publication of the SIMPLE framework within the same project. The model code is available as open source at `https://gitlab.com/beam-me/simple-pips`

1.5 Research questions and structure

The analysis of the literature on planning the energy system transformation in Europe shows that certain issues remain unclear. This particularly concerns the feasibility of integrating large volumes of hydrogen into the energy system. Although the use of green hydrogen in the energy system offers a promising way to reduce emissions in cases where direct electrification is not economically viable, the question of whether hydrogen should be produced domestically or imported from countries with high wind and solar potential significantly impacts the required energy infrastructure. Furthermore, a significant increase in the expansion of VRE and electrolysers will be required for high shares of domestic production of green hydrogen, raising questions about the necessary annual expansion rates. The literature review also underlines that novel methods to address the large-scale optimisation resulting from modelling infrastructure transformation pathways at high spatial and temporal resolutions exist. However, the relationship between model structure and resulting solver performance remains unclear, as does the feasibility of applying the method to capacity expansion models at high temporal resolutions. These gaps in existing research motivate the fundamental research question addressed by this thesis.

How can energy system optimisation models be enabled to address the optimisation of transformation pathways in a high spatial and temporal resolution?

Answering this modelling-oriented question allows for the analysis of the key questions on the overall energy system design from a central planner perspective addressed in this work.

- **Research Question 1:** *What is the future role of energy imports in the European energy system compared to domestic production, and what factors are driving this development?*
- **Research Question 2:** *How do limitations in annual capacity expansion rates constrain the large-scale integration of green hydrogen, and what impact do they have on the overall energy system design?*

Furthermore, to effectively apply PIPS-IPM++ to large-scale capacity expansion models with transformation pathways, several questions related to methodology must be considered.

- **Research Question 3:** *Which aspects of ESOMs with a high spatial and temporal resolution cause the computational burden in large-scale applications?*
- **Research Question 4:** *What impact do the decomposition strategy and hardware configuration have on the performance of massively parallel solvers when applied to ESOMs?*

- **Research Question 5:** *In what ways can massively parallel solvers provide performance benefits and overcome hardware limitations when applied to capacity expansion pathways?*

The remainder of this thesis is structured as follows: Chapter 2 outlines the methodological foundation of ESOMs and introduces the specific model formulation of the REMix framework. Furthermore, it introduces the different approaches to solving LPs, and discusses the specific parallelisation approach of PIPS-IPM++ and its implications for the decomposition strategy.

Chapter 3 then first provides an overview of the publications included in this thesis, discussing how they are linked and build upon one another. The model-based assessment of the European energy system begins with *Publication 1*, which introduces the reimplemented energy system model framework REMix and evaluates the trade-offs between domestic supply and energy imports within the European energy system. This analysis focuses specifically on the spatial and temporal interactions between electricity production from variable renewable energy sources and hydrogen production for the target year of 2050.

Publication 2 introduces the fundamental understanding required to effectively apply the massively parallel solver PIPS-IPM++ on high-performance computers and discusses the implications of different decomposition strategies for a set of model instances of varying size and number of capacity expansion decisions.

Publication 3 then extends the formulation from target-year optimisation to a perfect-foresight transformation pathway, while also increasing the spatial resolution of the geographical scope. This publication places a stronger emphasis on the role of per-country and per-technology achievable capacity expansion rates, as well as their interaction with the permitted carbon budget and the role of blue hydrogen.

Chapter 4 builds upon the insights derived in *Publication 2* and expands upon them in the context of applying PIPS-IPM++ to transformation pathways. It thereby demonstrates the effectiveness of this approach for solving large-scale capacity expansion problems and reducing the time required for solving them by a factor of five.

Chapter 5 then addresses the initially posed research questions and considers the implications and limitations of using PIPS-IPM++ to push the computational boundaries, as well as the added value of applying models at a significantly higher resolution. Finally, Chapter 6 concludes by summarising the implications for the research field and outlining future work that can be conducted by building upon the methodology developed in this thesis.

2 Methods

2.1 Energy system optimisation models

To define what an ESOM actually is, it is helpful to follow the classification schemes for general energy system models discussed in Section 1.2. Distinct from simulation and agent-based models, the defining feature of all ESOMs is their shared mathematical programming approach. This involves defining an objective, generating a system of equations and subsequently solving it using an appropriate algorithm. Furthermore, the specific type of optimisation problem can be categorised as LP, MILP, quadratic programming (QP), or non-linear programming (NLP), depending on mathematical formulation, which needs to be chosen according to the features required to answer the specific research question. Similarly, ESOMs can adopt a variety of perspectives, ranging from central planners to distribution system operators and operation planning for individual plants. The following description will mainly focus on the central planner perspective, which is the most prevalent choice for addressing questions about the energy infrastructure on a continental scale, in order to identify optimal future system configurations.

The scope of the defining dimensions and their level of detail are the determining factors in terms of the overall size of the resulting optimisation problem. In the case of multi-node ESOMs, the spatial scope can range from global systems [57] down to national energy systems and district systems [58]. However, while the spatial scope of the system does to a certain degree influence the technical fidelity of the representation of components, such as the need to model discrete investments and therefore use integer variables, the main driver for the spatial size is the spatial resolution defined by the overall number of model regions. While in most cases the representation of regions follows administrative boundaries, such as the Nomenclature des unités territoriales statistiques (NUTS) classification schema used in Europe, other partitioning approaches can be applied based either on the network structure [59] or based on the availability of renewable energy sources [60]. Furthermore, the spatial resolution

of the system has an indirect effect on the number of network connections in the system, which can cause additional scaling to the pure increase of model regions.

In terms of the temporal dimension, it is important to distinguish between the modelling of the optimisation horizon along multiple years and the sub-annual time resolution. This distinction is also usually related to the two main parts of the overall optimisation problem: capacity expansion and economic dispatch. On the optimisation horizon, investment and decommissioning decisions regarding energy infrastructure, as well as other long-term constraints, such as the available carbon budget [61], are taken into account. Here, the specific foresight into future years along the horizon plays a crucial role and can potentially impact the findings [9]. These different approaches can typically be categorised as follows: perfect foresight, where all years along the horizon are optimised simultaneously; myopic rolling horizon approaches, where one or more years are optimised with a limited foresight into the future; target optimisation, where only a single future year is optimised. In particular, for ESOMs with a high spatial and temporal resolution, both target optimisation and single-year myopic pathways are still the most prevalent choice due to the increased computational burden imposed by perfect foresight.

On the sub-annual time resolution there is likewise a wide range of different representations. Most of the power system models used to investigate the possibility to achieve high shares of renewable energy integration, such as REMix [13], PyPSA [29] and oemof [62], started with a fully hourly resolved time series, while in contrast ESOMs with a broader sectoral and technological scope, such as TIMES [36] and OSeMOSYS [38], typically utilised representative hours and days to emulate different load situations classified into seasons, weekdays and peak hours. With this approach, using different weighting factors for different hours allows to ensure that the statistical representation across the full year matches the actual demand time series. In particular, the need to capture the high intermittency of VRE while at the same time to reduce the temporal dimension led to a wide range of representations between the two extremes and a large research stream on the selection and reduction methods [42, 43, 63].

Both the multi-period optimisation horizon and the sub-period time resolution can be extended to reflect stochastic scenarios, accounting for uncertainties in long-term energy demand and techno-economic parameters for system components [64] or to represent a wide range of different weather conditions, which in turn impacts the spatial distribution of VRE across the system [65].

The concrete sectoral scope is mainly defined by the included technologies, which in turn influence the required energy carriers and commodities to be modelled. In particular, the considered end-use demand for different energy carriers is the main driving factor for the detail of the representation.

To satisfy this exogenously given demand, the supply from different producing technologies gets balanced for each model region and time step. Furthermore, spatial and temporal flexibility options, such as power grids, pipelines and energy storage, enable a more efficient energy system design, but further complicate the optimisation. On a conceptual level, a large share of recent implementations of ESOMs follow a component based modelling approach first introduced as energy hubs by Schulze et al. [66]. This approach categorises model components into converters, storage, transfer links, as well as sources and sinks, allowing for easy reuse of modelling components for a wide range of different systems and keeping the modelling framework more maintainable on a software level.

Considering that the overall size of the resulting optimisation problem is primarily determined by the product of the spatial, temporal, and technological dimensions, an increase in any of these dimensions results in a rapid growth in the number of variables, constraints, and non-zero elements. However, since the different model dimensions are largely independent of each other, this scaling results in repeating sub-structures that can be exploited by specialised algorithms, as discussed in more detail in Section 3.1. Due to the large size of the resulting optimisation problem, modellers need to consider fundamental trade-offs between the scope of use-cases, the level of detail of the modelled dimensions, and the conciseness of the model formulation [18].

A concise model formulation requires the removal of superfluous decision variables, which are typically introduced for the convenience of processing model results. Ideally, intermediate variables should be taken care of during the presolve, but this is not always the case, which can lead to the solution taking longer to find [67]. These intermediate variables can be created from partial sums for system costs or commodities with only one associated supply and demand technology. Proper setup of the model formulation and input data adjustments can help remove superfluous variables and constraints, while still making the information available in the results. The ratio of variables to equations before and after presolve can indicate the level of conciseness, but does not guarantee better solver performance.

2.1.1 The ESOM framework REMix

The REMix framework has been developed and utilised as part of several doctoral theses over the years, addressing a wide range of research questions. These include the initial introduction of the model and application for the optimisation of the European power system in high temporal resolution [68], the identification of global renewable energy potentials [69], the integration of BEVs as a flexibility option for the power sector [70], the energy system integration with the heating sector [71], the identification of temporal flexibility demand in the form of energy storage [72], the integration of power-flow

approximations and improvements to the network resolution [73], and the integration of life cycle assessment (LCA) indicators to facilitate multi-criteria optimisation [74].

Similar to the generic energy system optimisation outlined in the previous section, the Renewable Energy Mix (REMix) framework takes the perspective of a central infrastructure planner to typically determine least-cost transformation pathways for future energy scenarios. However, several limitations in the formulation of the model used during the mentioned doctoral theses prevented the extension of the existing framework to address sector-integrated transformation pathways using multiple energy carriers, nor could the parallel solver PIPS-IPM++ be applied effectively given the model structure. Therefore, the author of this thesis fundamentally reimplemented the mathematical formulation of the REMix framework. In a collaborative effort, both the mathematical formulation and additional software for data and result interfacing were made available as open source [75]. The three main motivations behind reimplementing the model, and the connections between these motivations and the included publications, are discussed in the following.

Firstly, the repurposing of infrastructures is an important consideration in multi-sector energy systems, particularly with regard to the transformation of gas networks from natural gas to hydrogen. This aspect and its corresponding model formulation form part of *Publication 1*, which also marks the first application of the newly reimplemented REMix framework to a European energy system with a high temporal resolution. In order to achieve repurposing, the model must allow for the connection between the decommissioning decisions made within the model and the capacity expansion decisions made between different technologies.

Secondly, in order to implement the transformation pathways, the framework must consider the continuity of capacity installations and decommissioning. There are different possible formulations, each of which has a different impact on the overall model complexity. Both the general implementation and application of the transformation pathways are outlined in *Publication 3*, which also highlights the challenge of solving the problem with an hourly resolution due to the immense size of the resulting optimisation matrix.

Thirdly, two aspects must be considered to enable the use of PIPS-IPM++: the implementation of the annotation itself, and providing the most concise model possible by removing superfluous intermediate variables and equations. While the fundamental annotation for PIPS-IPM++ has been formalised as part of *Publication 2*, the concrete implementation in REMix uses the *.stage* suffix of the GAMS modelling language. To achieve a concise model formulation, a highly generalised accounting model was developed to ensure that any overarching constraints are limited to the minimum required, while providing the user with comprehensive systems reporting after the optimisation is finished. Both

aspects – concise model formulation and annotation – are discussed further as part of the description of the mathematical formulation in the following section.

2.1.2 Model formulation and design considerations

Addressing the three key requirements outlined above, the following section presents the REMix framework equations in detail, discussing the challenges and considerations for each part. Similar to the mathematical formulation of other ESOMs discussed in Section 2.1, the REMix model logic follows the same separation into energy-carrier-independent modelling components, as well as into capacity expansion and economic dispatch aspects, on a conceptual level. To facilitate consideration of lumpy investments and adequate modelling of UC for thermal power plants, the three system components (converters, transfer links, and storage) are divided into units and links, each with their respective rated power and storage volume. Within this chapter, the overall definition of the scope and decision variables is introduced first, followed by an explanation of the logic behind the model equations.

Model sets, variables, and parameters

To define the model fundamentally in terms of its spatio-temporal scope and resolution, several sets are introduced. These sets enable a comprehensive description of the model formulation, which is outlined in more detail later in the section.

$t \in T$	time steps
$y \in Y$	model years
$n \in N$	model nodes
$l \in L$	transfer links
$z \in Z$	AC network cycles
$q \in Q$	energy carriers
$a \in A$	converter activities
$p \in P$	technologies
$P_C \subset P$	converter technologies
$P_S \subset P$	storage technologies
$P_L \subset P$	transfer technologies

$i \in I$ system indicators

$I_{obj} \subset I$ indicator declared as objective function

Similarly, a set of decision variables is defined. These represent specific decisions associated with either the capacity expansion formulation or the economic dispatch of the system. Only system indicators describing overarching aspects, such as total system costs, can be associated with both.

$x \geq 0$ number of available units / links

$\Delta x^{+} \geq 0$ units / links expanded

$\Delta x^{-} \geq 0$ units / links decommissioned

$d \geq 0$ dispatch of converter

$e \geq 0$ level of storage

$f^{+} \geq 0$ flow along transfer link

$f^{-} \geq 0$ flow against transfer link

g import and export of energy carriers

j accounting indicator

Furthermore, additional coefficients are required for the concrete parametrisation of the model to describe the techno-economic assumptions for technologies, overarching economic aspects, and specific weighting factors. These ensure that the annualised costs of technologies are comparable, and that the integral sums along the transformation pathways take into account the intervals between model years.

D rated dispatch coefficients

E rated storage coefficients

F rated transfer coefficients

H rated transfer loss coefficients

M incidence matrix between transfer links and model regions

K minimum cycle basis matrix between transfer links and network cycles

J	indicator coefficient matrix
V	activity matrix for converter technologies
W	weighting factor between year intervals
α	availability factor
γ	loss adjusted transfer correction factor
δ	self discharge rate of storage
λ	technical lifetime
χ	link specific reactance

Objective function and indicator accounting

Any linear optimisation problem is primarily defined by the objective function. In the case of ESOMs outlining least-cost transformation pathways, the objective value minimises both capital expenditures (CAPEX) and operational expenditures (OPEX) of the system, as well as their respective contributing costs, such as fuel costs or costs associated with carbon emissions. To incorporate additional constraints for the entire system or sub-regions, this accounting method is generalised to link any accounting indicator with any technical system component. Using this approach, country-specific limits on carbon emissions or firm capacity requirements, for example, can be introduced into the optimisation. Furthermore, this hierarchical accounting framework is designed to generate the fewest constraints possible to minimise the number of linking constraints. While this is usually achieved by the solver during the aggregation phase in the presolve, for PIPS-IPM++ this improves numerical stability during optimisation and reduces communication overhead between blocks.

$$
\begin{aligned}
j_i = \sum_{y \in Y} W_{y,i} \cdot \Bigg(& \sum_{n \in N, p \in P_C \cup P_S} J^{\text{build}}_{i,n,y,p} \cdot \Delta x^{+}_{n,y,p} + J^{\text{fix}}_{i,n,y,p} \cdot x_{n,y,p} + J^{\text{decom}}_{i,n,y,p} \cdot \Delta x^{-}_{n,y,p} && \text{(2.1a)} \\
& + \sum_{l \in L, p \in P_L} J^{\text{build}}_{i,l,y,p} \cdot \Delta x^{+}_{l,y,p} + J^{\text{fix}}_{i,l,y,p} \cdot x_{l,y,p} + J^{\text{decom}}_{i,l,y,p} \cdot \Delta x^{-}_{l,y,p} && \text{(2.1b)} \\
& + \sum_{t \in T, n \in N, p \in P_C, a \in A} J^{\text{var}}_{i,t,n,y,p,a} \cdot d_{t,n,y,p,a} && \text{(2.1c)} \\
& + \sum_{t \in T, l \in L, p \in P_L} J^{\text{flow}}_{i,t,l,y,p} \cdot \left(f^{+}_{t,l,y,p,q} + f^{-}_{t,l,y,p,q} \right) && \text{(2.1d)} \\
& + \sum_{t \in T, n \in N, q \in Q} J^{\text{import}}_{i,t,n,y,q} \cdot g^{+}_{t,n,y,q} + J^{\text{export}}_{i,t,n,y,q} \cdot g^{-}_{t,n,y,q} \Bigg) && \forall i \in I \quad \text{(2.1e)}
\end{aligned}
$$

Capacity expansion

The total number of available converters, storage and links throughout the transformation pathway can be determined based on decisions regarding capacity expansion and decommissioning. Modelling converters, storage technologies, and network links on a per-unit basis further simplifies the switch to mixed-integer formulations, should this be required for a specific use-case. To assess the impact of specific planning decisions relating to technologies, technology-specific capacity corridors can be provided, limiting the minimum and maximum number of units that can be installed in a given model region (see Equations 2.2 and 2.3).

$$\underline{x}_{n,y,p} \leq x_{n,y,p} \leq \overline{x}_{n,y,p} \qquad \forall n \in N, y \in Y, p \in P_C \cup P_S \quad (2.2)$$

$$\underline{x}_{l,y,p} \leq x_{l,y,p} \leq \overline{x}_{l,y,p} \qquad \forall l \in L, y \in Y, p \in P_L \quad (2.3)$$

In order to achieve a consistent and continuous representation of capacities based on expansion and decommissioning decisions, the capacity balance must take into account the total number of units or links from the previous model year and adjust them according to the changes for each subsequent year (see Equations 2.4 and 2.5).

$$x_{n,y,p} = x_{n,y-1,p} + \Delta x^{+}_{n,y,p} - \Delta x^{-}_{n,y,v} \qquad \forall n \in N, y \in Y, p \in P_C \cup P_S \quad (2.4)$$

$$x_{l,y,p} = x_{l,y-1,p} + \Delta x^{+}_{l,y,p} - \Delta x^{-}_{l,y,p} \qquad \forall l \in L, y \in Y, p \in P_L \quad (2.5)$$

Similarly, to ensure that capacities are guaranteed to be decommissioned by the end of their respective lifetimes at the latest, a rolling sum of investment and decommissioning decisions can be used, with an offset corresponding to the lifetime (see Equations 2.6 and 2.7). This formulation allows technologies to be decommissioned pre-emptively, if, for example, the decommissioning decision is connected with another investment decision, such as the repurposing of natural gas infrastructure.

$$\sum_{y' \leq y - \lambda_p} \Delta x^{+}_{n,y',p} \leq \sum_{y' \leq y} \Delta x^{-}_{n,y',p} \qquad \forall n \in N, y \in Y, p \in P_C \cup P_S \quad (2.6)$$

$$\sum_{y' \leq y - \lambda_p} \Delta x^{+}_{l,y',p} \leq \sum_{y' \leq y} \Delta x^{-}_{l,y',p} \qquad \forall l \in L, y \in Y, p \in P_L \quad (2.7)$$

In the special case where converters or links cannot be decommissioned before the end of their technical lifetime, Equations 2.4 to 2.7 can be substituted by Equations 2.8 to 2.9. Rather than continuously

balancing total units and links in conjunction with the rolling horizon formulation for decommissioning, this uses a backwards-looking rolling horizon with an interval equal to the lifetime of the technologies. This approach can only be used for technologies that are not associated with decommissioning costs or repurposing decisions. However, it significantly reduces the number of capacity expansion decisions, as well as the number of linking variables for PIPS-IPM++.

$$x_{n,y,p} = \sum_{y-\lambda_p < y' \leq y} \Delta x^{+}_{n,y',p} \qquad \forall n \in N, y \in Y, p \in P_C \cup P_S \quad (2.8)$$

$$x_{l,y,p} = \sum_{y-\lambda_p < y' \leq y} \Delta x^{+}_{l,y',p} \qquad \forall l \in L, y \in Y, p \in P_L \quad (2.9)$$

Another alternative model formulation for capacity expansion can relax the relationship between the investment decisions and the total number of available units and links (see Equations 2.10 to 2.13). While this formulation can lead to an underestimation of fixed costs associated with the number of existing power plants, as the total number of units can be smaller than the sum of build units, it reduces the tight coupling between the two values. This can benefit the performance of the solving algorithm, as demonstrated in Section 4.2. As with the previous alternative formulation, this approach is only applicable if the technology is not connected to decommissioning and repurposing decisions, and it requires careful consideration, as it effectively enables the decommissioning of capacities free of charge and before the end of their lifetime.

$$x_{n,y,p} \leq x_{n,y-1,p} + \Delta x^{+}_{n,y,p} - \Delta x^{-}_{n,y,v} \qquad \forall n \in N, y \in Y, p \in P_C \cup P_S \quad (2.10)$$

$$x_{l,y,p} \leq x_{l,y-1,p} + \Delta x^{+}_{l,y,p} - \Delta x^{-}_{l,y,p} \qquad \forall l \in L, y \in Y, p \in P_L \quad (2.11)$$

$$x_{n,y,p} \leq \sum_{y-\lambda_v < y' \leq y} \Delta x^{+}_{n,y',p} \qquad \forall n \in N, y \in Y, p \in P_C \cup P_S \quad (2.12)$$

$$x_{l,y,p} \leq \sum_{y-\lambda_v < y' \leq y} \Delta x^{+}_{l,y',p} \qquad \forall l \in L, y \in Y, p \in P_L \quad (2.13)$$

Economic dispatch

In contrast to the capacity expansion model, the economic dispatch model is formulated on the sub-annual time dimension. In particular, the hourly operation of different technologies and the hourly balancing of energy carriers play a crucial role. As before, we can separate the equations based on

their corresponding modelling components, beginning with converters. In REMix, converters can be associated with multiple activities, representing the various operational states of a given technology. For example, a CHP plant can produce only power, only heat, or a combination of power and heat (see Equation 2.14). Summing all activities ensures that the per-unit capacity of the associated converter is not exceeded. Furthermore, the sum of activities can be bounded using either a lower or an upper operation profile, or, in the case of identical values, a fixed operation profile can be ensured.

$$V_{p,a} \cdot \underline{\alpha}_{t,n,y,p} \leq \sum_{a \in A} d_{t,n,y,p,a} \leq V_{p,a} \cdot \overline{\alpha}_{t,n,y,p} \cdot x_{n,y,p} \qquad \forall t \in T, y \in Y, n \in N, p \in P_C \quad (2.14)$$

In the special case that the activities involved are independent of each other and provide no incentive for simultaneous usage – for example, in the case of charging and discharging batteries – the formulation can be adapted to limit each activity independently (see Equation 2.15). In the matrix representation, this generates more equations, but ensures that more non-zero entries are closer to the diagonal, which can improve numerical stability, depending on the solving algorithm. Note that this representation is only valid if no lower profile for the activities is provided, as otherwise all activities would be forced to run simultaneously.

$$V_{p,a} \cdot \underline{\alpha}_{t,n,y,p} \cdot x_{n,y,p} \leq d_{t,n,y,p,a} \leq V_{p,a} \cdot \overline{\alpha}_{t,n,y,p} \cdot x_{n,y,p} \qquad \forall t \in T, y \in Y, n \in N, p \in P_C, a \in A \quad (2.15)$$

For storage technologies, the number of available units limits the maximum state of charge depending on the rated storage volume per unit (see Equation 2.16). Similar to the converter activity, the storage level can be limited using lower and upper profiles to account for applications specific to particular use-cases, such as minimum reservoir filling levels throughout the year.

$$\underline{\alpha}_{t,n,y,p} \cdot x_{n,y,p} \leq e_{t,n,y,p} \leq \overline{\alpha}_{t,n,y,p} \cdot x_{n,y,p} \qquad \forall t \in T, y \in Y, n \in N, p \in P_S \quad (2.16)$$

Similar constraints apply with regard to energy transmission along network links. By default, flows are separated into those along and against the defined link direction (see Equations 2.17 and 2.18). This also enables unidirectional flows to be modelled, as well as different capacities for each direction. Once again, direction-specific profiles can be applied to ensure specific model-exogenous network flows.

$$\underline{\alpha}^{+}_{t,l,y,p} \cdot \gamma_{l,p} \cdot x_{l,y,p} \leq f^{+}_{t,l,y,p} \leq \overline{\alpha}^{+}_{t,l,y,p} \cdot \gamma_{l,p} \cdot x_{l,y,p} \qquad \forall t \in T, y \in Y, l \in L, p \in P_L \quad (2.17)$$

$$\underline{\alpha}^{-}_{t,l,y,p} \cdot \gamma_{l,p} \cdot x_{l,y,p} \leq f^{-}_{t,l,y,p} \leq \overline{\alpha}^{-}_{t,l,y,p} \cdot \gamma_{l,p} \cdot x_{l,y,p} \qquad \forall t \in T, y \in Y, l \in L, p \in P_L \quad (2.18)$$

Opposite to the special case for converter activities, the constraints on network flows can be reformulated into a single equation, reducing the total number of equations in the model formulation (see Equation 2.19). However, this formulation prevents using directional profiles and the usage of a lower flow profile altogether, so special care must be taken when deciding whether this simplification is valid. As before, the impact on solver time depends on the specific algorithm used to solve the optimisation problem, with PIPS-IPM++ benefiting from the sparser formulation.

$$f^{+}_{t,l,y,p} + f^{-}_{t,l,y,p} \leq \overline{\alpha}_{t,l,y,p} \cdot \gamma_{l,p} \cdot x_{l,y,p} \qquad \forall t \in T, y \in Y, l \in L, p \in P_L \quad (2.19)$$

For approximating alternating current (AC) networks, the model contains a DC-OPF formulation based on Kirchhoff's second law (see Equation 2.20. To minimise the number of non-zero entries in the resulting optimisation problem, the network cycle matrix $K_{z,l}$ is computed using a minimum cycle basis approach.

$$\sum_{l \in L} K_{z,l} \cdot \chi_{l,p} \cdot (f^{+}_{t,l,y,p} - f^{-}_{t,l,y,p}) = 0 \qquad \forall t \in T, y \in Y, p \in P_L, z \in Z \quad (2.20)$$

Additional components for sources and sinks can be added to the model to represent flows into and out of the system boundaries, either as an hourly profile, an annual sum, or a combination of both (see Equations 2.21 and 2.22.

$$\underline{g}_{t,n,y,q} \leq g_{t,n,y,q} \leq \overline{g}_{t,n,y,q} \qquad \forall t \in T, n \in N, y \in Y, q \in Q \quad (2.21)$$

$$\underline{G}_{n,y,q} \leq \sum_{t} g_{t,n,y,q} \leq \overline{G}_{n,y,q} \qquad \forall n \in N, y \in Y, q \in Q \quad (2.22)$$

Finally, the balancing equation connects the individual components for each year, time step, model region and energy carrier. Converters are connected to their respective rated activities, ensuring that inputs and outputs are accounted for correctly (see Equation 2.23a). For storage, the state of charge considers any changes for a specific time step as the difference to the previous time step as well as

self-discharge effects (see Equation 2.23b). Network flows are connected to the model regions based on their directionality in the incidence matrix (see Equation 2.23c), while losses are evenly divided between the two connected model regions (see Equation 2.23d). Lastly, any exchange of commodities with the outside of the system boundaries in the form of sources and sinks can be integrated directly into the equation (see Equation 2.23e).

$$\sum_{p \in P_C, a \in A} D_{p,a,q} \cdot d_{t,n,y,p,a} \tag{2.23a}$$

$$+ \sum_{p \in P_S} E_{p,q} \cdot \left(e_{t,n,y,p,q} - (1 - \delta_p) \cdot e_{t-1,n,y,p,q} \right) \tag{2.23b}$$

$$+ \sum_{l \in L, p \in P_L} M_{n,l} \cdot F_{l,q} \cdot \left(f^{+}_{t,l,y,p} - f^{-}_{t,l,y,p} \right) \tag{2.23c}$$

$$- \sum_{l \in L, p \in P_L} \frac{1}{2} \cdot \left| M_{n,l} \right| \cdot H_{l,q} \cdot \left(f^{+}_{t,l,y,p} + f^{-}_{t,l,y,p} \right) \tag{2.23d}$$

$$+ g_{t,n,y,q} = 0 \qquad \forall t \in T, n \in N, y \in Y, q \in Q \tag{2.23e}$$

2.2 Solving methods for linear programs

When it comes to the solving of the LPs generated by any kind of ESOM there are three main methods which need to be considered: the simplex method, the interior-point (IP) method, and first order methods. Each of these methods has particular strengths and weaknesses, which can make them more useful for particular problems, but fundamentally all of them rely on certain mathematical properties of the system of equations to be solved, such as linearity, duality, and convexity. In its simplest form, the primal of any LP can be written as:

$$\begin{aligned} &\text{minimise } c^T x \\ &\text{subject to } Ax \leq b \\ &\qquad x \geq 0 \end{aligned} \tag{2.24}$$

with $x \in \mathbb{R}^n$ representing the decision variables, $c \in \mathbb{R}^n$ representing the cost vector, and $A \in \mathbb{R}^{m,n}$ and $b \in \mathbb{R}^m$ representing the system of constraints. Furthermore, its corresponding dual problem can be formulated as:

$$\begin{aligned} &\text{maximise } b^T y \\ &\text{subject to } A^T y \geq c \\ &\qquad\qquad y \geq 0 \end{aligned} \tag{2.25}$$

with $y \in \mathbb{R}^m$ representing the dual variables associated with the constraints of the primal optimisation problem. Both problem can be brought to equality form by introducing slack variables.

Formalised by Dantzig in 1955 [76], the generalised simplex method enabled a structured and efficient way to solve LPs and laid the groundwork for the field of modern operations research. On a conceptual level, the solution strategy involves creating a basis and iteratively adding non-basic variables. This operation corresponds to following an edge of a polyhedron, which limits the feasible region using the boundary constraints, into the direction of reduced objective values. This procedure is continued until all variables are part of the basis, which indicates that no further reductions in the objective value are possible. While there have been significant advances in the initial simplex algorithm and related methods such as the revised simplex method and the parametric self-dual method [77], in particular the effective parallelization of the algorithm for sparse large-scale LPs has proven to be difficult [78].

In contrast to the simplex method, the fundamental strategy of IP methods, also commonly referred to as barrier methods, involves following a central path through the feasibility space. With its introduction in 1984 by Karmarkar [79], this offered a viable alternative to the simplex method, in particular for large-scale convex optimisation problems. Furthermore, the Cholesky decomposition for the factorization in each iteration can be parallelized and block-sparsity patterns can be exploited, allowing for the better utilisation of modern central processing units (CPUs) [80]. But while the barrier method has been proven to converge in polynomial time [79], in particular the large size of the optimisation problems resulting from the high spatial and temporal resolution can still lead to immense run-times of several days as discussed in Section 1.3. Furthermore, as the method only yields an optimal solution subject to a stopping criterion based on the duality gap between primal and dual problem, an additional simplex method also referred to as crossover may be necessary to recover a basic solution [81]. When it comes to the practical application, an additional problem is the limited scalability with respect to multithreading the factorization, as indicated by decreasing performance with thread counts higher than 16 in computational experiments for problems from the energy domain [56]. Nevertheless, the best performance of large-scale ESOMs to date can still be achieved using the barrier method with crossover disabled [82].

Compared to the simplex and IP methods, first-order methods only recently reappeared due to a series of improvements enabling their wider practical application for LPs [83]. In particular the primal-dual

hybrid gradient (PDHG) and its optimised version for LPs primal-dual hybrid gradient for linear programming (PDLP) [84]. In both methods the primal and dual problems are reformulated into a saddle-point problem, which is then solved using an iterative approach. While first order methods have been applied in various forms in the field of optimisation [85], in particular developments of sparse linear algebra optimised for the massively parallel processing power of graphics processing units (GPUs) was one of the key enabling factors [86]. Similar to PDLP, these benefits of running the algorithm on GPUs have been demonstrated in other first order methods, such as Halpern Peaceman-Rachford (HPR) [87]. This transferability of operations to GPUs stems from the fact, that the methods avoid factorization which in turn ensures a low memory footprint [86]. Theoretically, the sparse nature of ESOMs should allow for increased performance, but similar to the performance experiments conducted in *Publication 2*, a large number of capacity expansion decisions could have a significant impact on the performance. Since the methods have just recently been brought to a competitive state, further investigations, in particular about their performance for ESOMs, are required in the future.

2.2.1 The massively parallel solver PIPS-IPM++

The massively parallel solver PIPS-IPM++ was first introduced by Rehfeldt et al. [56] and further improved by Kempke et al. [88] to provide a solver tailored to ESOMs and able to utilise HPC clusters. While the development and underlying methodology therefore is not part of this thesis, there was a close collaboration during several research projects, which involved in depth discussions about the underlying structure and providing block structure models from the REMix framework to enable the development efforts. Therefore, the description of the solution method presented here is primarily aimed to further the understanding of the required block structures, which is discussed in detail in *Publication 2* and the interpretations of the performance benchmarking done in the *Extended Results*.

In contrast to the methods discussed in the previous section, the solver PIPS-IPM++ relies on a specific matrix structure to be present in the optimisation problem, which is also referred to as arrowhead or doubly bordered block diagonal form. Conceptually, it implements a primal–dual IP algorithm, which solves the augmented system in each of the iterations. The algorithm implements a Schur complement decomposition approach, in which only the formation and solving operations of the global Schur complement can not be performed independently. For the majority of the algorithm, this allows the facilitation of distributed computing and having each of the parallel processes only store a part of the optimisation matrix, avoiding limitations from shared memory when solving large-scale LPs. Furthermore, the algorithm considers a separation of local and global linking constraints, which

can further improve the computational efficiency.

For any ESOM to be solved with PIPS-IPM++, this approach has several implications: Firstly, to utilise the solver a decomposition strategy has to be applied in order to define the double bordered block diagonal form. This process of assigning groups of variables and equations is also referred to as annotation. Each decomposition strategy yields a different number of blocks, linking variables and linking constraints which in turn can significantly impact the overall performance of the solver. The impact of different annotation strategies is discussed in depth in *Publication 2* and quantified in a computational experiment. Secondly, too many linking variables and linking constraints can cause the optimisation problem to become intractable due to the global Schur complement to become too large. This is mainly caused as the size of the Schur complement scales quadratically with the total number of global linking variables and global linking constraints. In contrast, the local linking variables and local linking constraints only contribute to the size with a linear scaling. Therefore, time-based decomposition strategies generally result in a better performance compared to spatial decomposition strategies. Thirdly, as the algorithm comprises of a fully-parallel phase and a non-parallel phase (forming and solving the global Schur complement), it favours a lower number of global linking variables and requires each of the parallel blocks to be similar in size to ensure the computational phase is not limited by individual blocks. Ensuring that the parallel computation is properly load balanced, can be achieved by profiling the CPU utilisation per block as done in the *Extended Results*.

2.2.2 Annotation and decomposition for transformation pathways

While *Publication 2* discusses both the considerations for finding a suitable decomposition strategy and the corresponding configuration of the HPC allocation, the concrete instances only consider the optimisation of a target year. While conceptually similar, the extension towards transformation pathways and utilisation of a different cluster necessitate some adaptations for the computational experiment presented in the *Extended Results*.

In terms of the resulting optimisation matrix, the problems are significantly larger in terms of overall number of variables and time steps due to the high spatial and temporal resolution, but still very sparse when it comes to the number of non-zero elements. Furthermore, in contrast to the decomposition based purely on the time steps, the decomposition into both years and time steps can yield only multiples of 5 blocks corresponding to the 5 model years between 2030 and 2050. While the resulting block structure (see Figure 2.1) therefore is quite similar to the time based decomposition, minor differences can be observed. Firstly, the blocks for each of the years included have slightly different sizes, with increasing sizes for later years. This is caused by the number of additional investment

decision variables which have to be accounted for in later years. While for most technologies a fixed decommissioning at the end of the technical lifetime is assumed, a free decommissioning is required in particular for gas caverns and pipelines, which can be repurposed for the use with hydrogen. Similar to the investment decisions, this also requires more decommissioning decisions to be considered in later model years. Another change compared to the pure temporal decomposition is the pattern of linking constraints which link the storage level between blocks. Due to the circular storage level within one year, the diagonal structure for the local linking constraints is replicated five times. All in all, the structure is quite similar to a pure temporal decomposition and also fulfils the other requirements for PIPS-IPM++ discussed in *Publication 2*, namely similarly sized blocks of comparable computational burden with a low share of global linking variables and constraints.

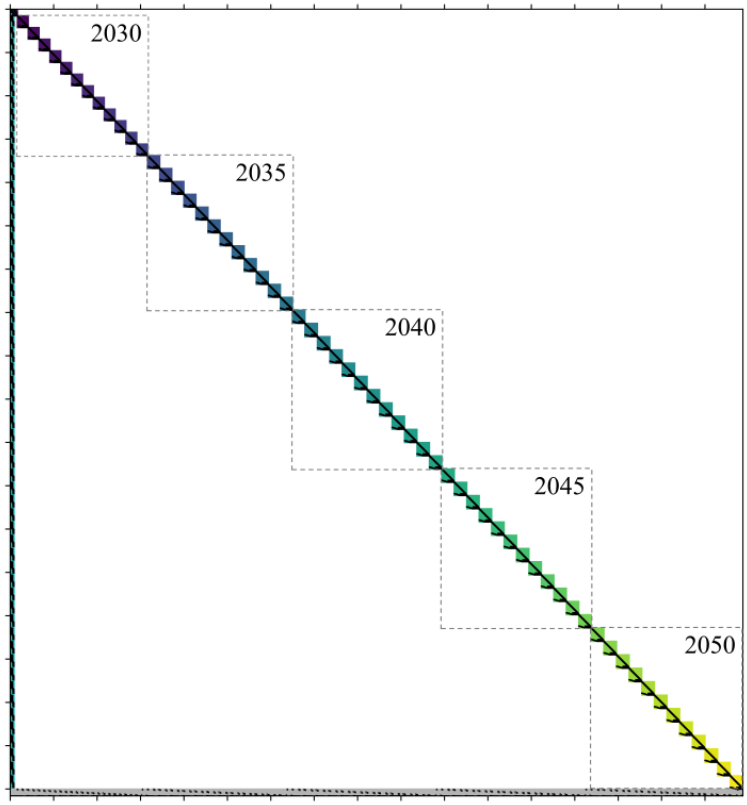


Figure 2.1: Annotation of the model instance with transformation pathway using a total of 60 blocks. For visualisation purposes, the instance is using a subset of the model regions and a 73-hourly downsampling to keep the linking structure visible.

While the computations for *Publication 2* were conducted on the HPC system JUWELS at the Jülich Supercomputing Centre (JSC), the computations for transformation pathways in the *Extended Results* utilise the HPC system CARO at Deutsches Zentrum für Luft- und Raumfahrt (DLR). Furthermore, instead of CPLEX, Gurobi version 12.0.1 was used as a reference for the comparison, due to its lower memory footprint.

When it comes to the available hardware, and therefore the configuration of PIPS-IPM++, some differences need to be considered here: Compared to the Intel Xeon Platinum 8168 CPUs, which contains two non-uniform memory access (NUMA) nodes each, the AMD EPYC 7702 implements a different substructure using eight compute complex dies (CCDs) with two core complexes (CCXs), each containing four cores and 16 MB of L3 cache.[1] As a consequence, the cluster allocation of up to 12 cores-per-block identified in *Publication 2* needs to be adjusted to at most 8 cores-per-block to optimise for cache locality, or 16 cores-per-task to facilitate the usage of two CCXs per block.

Furthermore, given that there are 128 cores per compute node and possible allocation strategies of 4, 8, or 16 cores per block, the maximum number of blocks that can be allocated to each compute node is 32, 16, or 8, respectively. Combined with the fact that the number of blocks should always be a multiple of 5, as discussed previously, this yields a total of 40, 80, or 160 blocks for the pathway instance. Assigning any number of blocks in between would result in partial allocation of the available cores, which may be a reasonable consideration if the memory allocation per block exceeds the total memory available per compute node.

[1] see also the technical specification `https://www.amd.com/content/dam/amd/en/documents/epyc-technical-docs/tuning-guides/amd-epyc-7002-tg-hpc-56827.pdf`

3 Publications

3.1 Overview and contribution to research questions

The included publications each address different aspects of the overarching research question and its associated sub-questions. In particular, *Publication 1* and *3* contextualise the model-based assessment (as indicated by the green background in Figure 3.1) of using ESOMs in outlining pathways to a climate-neutral energy system, as well as examining the role of domestic green hydrogen production in driving the required energy infrastructure. In contrast, *Publication 2* focuses on the technical and methodological aspects of applying the massively parallel solver PIPS-IPM++ (indicated by the blue background in Figure 3.1). To demonstrate the effectiveness of the solver in optimising large-scale pathways, the *Extended Results* then bring together the two research streams, showcasing the performance benefits of applying PIPS-IPM++ to large-scale capacity expansion transformation pathways with high temporal and spatial resolution.

Publication 1 analyses the target system for a climate-neutral energy system in Europe in 2050, focusing on the comparisons between different strategic positions regarding hydrogen imports. The results primarily address Research Question 1 (see Figure 3.2), highlighting the role of repurposing infrastructure for hydrogen to facilitate energy imports. Furthermore, this publication identifies the total VRE expansion and the role of power grids and gas networks as large sources of uncertainty, depending on the scenario context. However, the results of the model-based assessment also demonstrate the limitations of optimising for the target year, as neither the required annual expansion rate for VRE nor the optimal timing for hydrogen repurposing can be identified. In terms of model complexity, the 48 model instances have a limited spatial scope, using national representations for larger European countries and aggregating smaller ones into clusters.

Publication 3 then extends the model-based case study in various ways as specified in Figure 3.1. In particular, it broadens the scope of target year optimisation to encompass a comprehensive

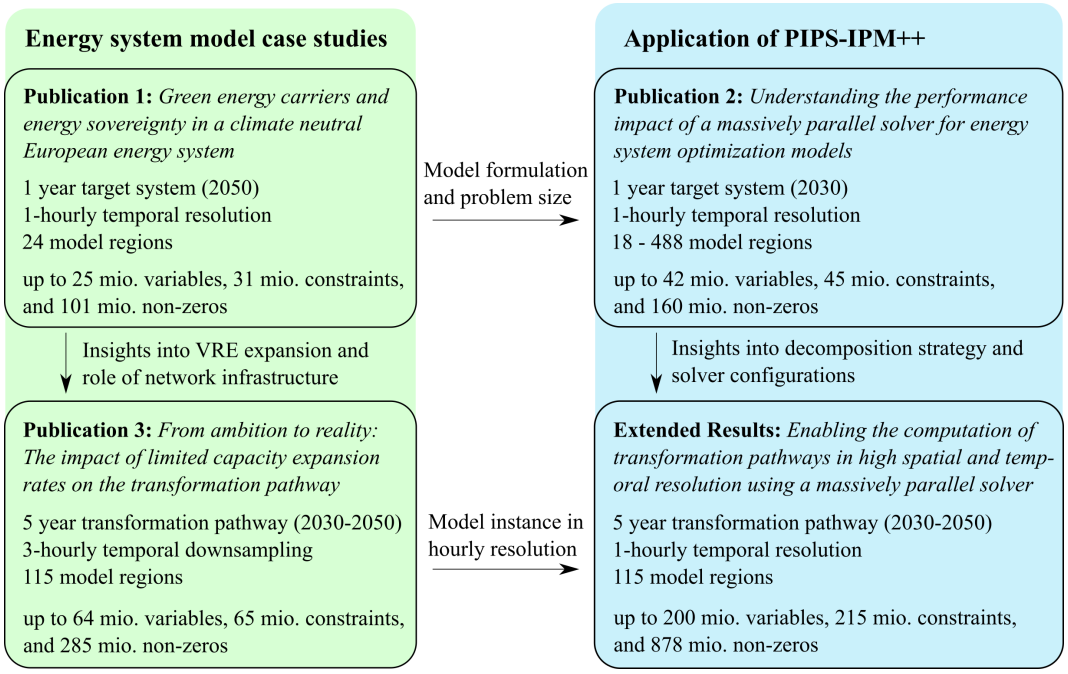


Figure 3.1: Overview of the included publications and their respective model resolution and problem size as an indicator for the associated computational burden. Arrows between the publications indicate how they build upon previous methods and insights.

transformation pathway with perfect foresight. In order to address some of the key uncertainties, the focus is shifted towards the supply side and capacity expansion for VRE and electrolysers. The publication introduces a sub-national resolution, generated based on power and gas network topology, to provide more detailed insights into long-distance energy transmission. Furthermore, it addresses the issue of high country-specific VRE expansion by constraining the national annual capacity expansion rates, thereby addressing the Research Question 2 (see Figure 3.2). Notably, the differentiation into short- and long-term effects, as well as the inclusion of blue hydrogen, provide further insights delivering to Research Question 1. With the transformation pathway divided into five-year steps and the sub-national spatial resolution covering 115 model regions, the resulting optimisation model poses significant computational challenges when using an hourly resolution. This necessitates temporal downsampling to a 3-hourly resolution to enable the total of 30 model instances to be solved in a reasonable time. This reduction in the temporal dimension significantly reduces the time taken to solve the model and further highlights the contribution of the hourly resolution to the computational burden, thereby also contributing towards Research Question 3.

In terms of methodology, *Publication 2* first discusses general complexity reduction techniques that can be utilised in order to reduce the computational burden from ESOMs and contrasts them with mathematical decomposition methods and massively parallel solvers. It then introduces the concept of

annotation and decomposition strategies to effectively apply the solver PIPS-IPM++, and discusses the necessary considerations and hardware configurations for achieving reasonable performance. Similar to *Publication 1*, the systematic computational experiment builds upon the same model formulation and target year optimisation, but focuses strongly on various levels of spatial aggregation to demonstrate the scalability of the solver. In particular, the computational experiment allows addressing Research Question 3 and identifying the differences in computational burden introduced by a large number of capacity expansion decisions. Furthermore, the publication's findings demonstrate a significant reduction in solving time of one order of magnitude across all considered model instances, which makes the solver especially relevant for large-scale optimisation problems. However, the results also highlight that in order to obtain this computational performance, for different problem types different decomposition strategies must be employed, thereby providing the basis for answering Research Question 4 (see Figure 3.2).

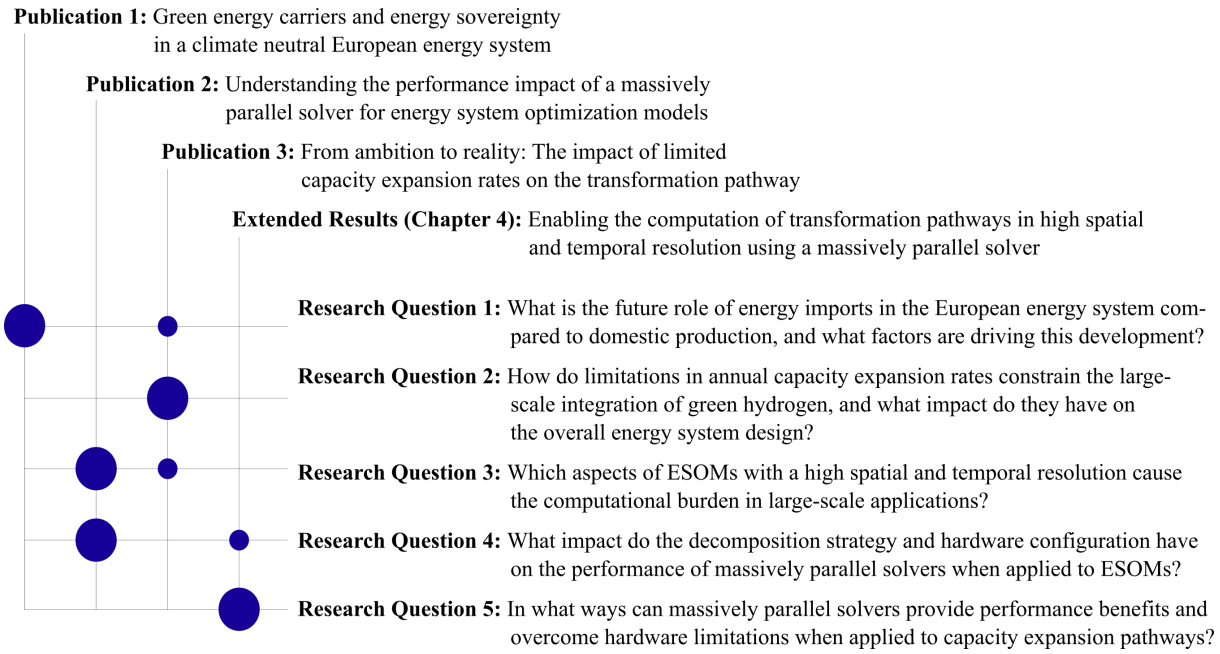


Figure 3.2: Contributions of different publications and extended results to research questions. Major contributions are indicated by large dots, while minor contributions are indicated by small dots.

The *Extended Results* then bring together the findings on effective decomposition strategies and configurations from *Publication 2* with the hourly resolved model instance for *Publication 3*, as shown in Figure 3.1. To improve understanding of the capacity expansion decision ratios further and contribute to the Research Question 4, a systematic assessment of a subset of the full-scope instance is first conducted. This computational experiment confirms the previous observation that, particularly for a large number of capacity expansion decisions, a smaller number of blocks is preferable. Then, using

the identified optimal configuration, the hourly transformation pathway is solved to demonstrate the effectiveness of PIPS-IPM++ in facilitating the computation of transformation pathways to a climate-neutral European energy system with high spatial and temporal resolution. In particular, performance profiling provides the necessary indicators to answer Research Question 5 and demonstrate that utilising PIPS-IPM++ can prevent hardware limitations intrinsic to previous solution approaches on shared memory architectures, in addition to solving optimisation problems faster.

Publication 1: Green energy carriers and energy sovereignty in a climate neutral European energy system

Authors: Manuel Wetzel, Hans Christian Gils, Valentin Bertsch

Published in: Renewable Energy 210, 2023, doi: 10.1016/j. renene.2023.04.015

Methodological advancements: This publication marks the first application of the reimplemented mathematical formulation of the REMix framework (see Section 2.1.1), showcasing the versatility of the generic accounting concept in modelling large-scale ESOMs. Key aspects of the model include the model-endogenous repurposing of both pipelines and cavern storage infrastructure for hydrogen use. Similarly, the accounting framework is used to model the share of domestic generation for each energy carrier in different geographic regions, as well as constraints on total network expansion. Other functionalities, such as transport losses independent of the type of commodity, are used to model gas- and electricity-fuelled compressor stations for pipelines and cavern storage.

Key findings: The results of the model-based case study highlight the crucial role of VRE technologies in a future climate-neutral energy system. They also emphasise the significant uncertainties surrounding their deployment, which vary depending on the scenario context. The publication identifies a close correspondence between VRE capacity installations and regions with favourable wind and solar potential. The results further suggest that electrolysers and synthetic methane production plants are optimally located in close proximity to electricity sources. However, this is only possible if sufficient network infrastructure is in place. Conversely, restricting the expansion of network infrastructure leads to significantly higher system costs. Furthermore, the study identifies the Maghreb region, the Iberian Peninsula, and the British Isles as key regions for hydrogen production, provided imports are permitted. Meanwhile, Germany and Italy emerge as key import regions due to their high energy demand relative to the available area for renewable energy production.

Author contributions: Manuel Wetzel is the main author of this work. He reimplemented the mathematical formulation of the REMix framework, collected the input dataset, performed the optimisation runs, and evaluated the results. Based on these initial results, the authors jointly discussed the findings and conclusions. Following adjustments to the input data and assumptions, Manuel Wetzel drafted the first version of the manuscript, which was then edited by Hans Christian Gils and Valentin Bertsch. Furthermore, Hedda Gardian provided an initial collection of techno-economic data on VRE technologies, while Stefan Kronshage supported in the translation from the energy scenarios to the model inputs. They are both acknowledged in the publication for their work.

Renewable Energy 210 (2023) 591–603

Contents lists available at ScienceDirect

Renewable Energy

journal homepage: www.elsevier.com/locate/renene

Green energy carriers and energy sovereignty in a climate neutral European energy system

Manuel Wetzel [a,*], Hans Christian Gils [a], Valentin Bertsch [b]

[a] German Aerospace Center (DLR), Institute of Networked Energy Systems, Stuttgart, Germany
[b] Chair of Energy Systems and Energy Economics, Ruhr-Universität Bochum, Bochum, Germany

ARTICLE INFO

Keywords:
Energy system modelling
Renewable energy
Sector integration
Green energy carriers
Climate neutrality
REMix

ABSTRACT

Meeting the goals of the Paris Agreement poses significant challenges to provide renewable energy for the power, heating, transport, and industrial sector. Both green hydrogen and methane are considered key energy carriers for reaching these climate targets. However, future needs for an effective infrastructure deployment are highly uncertain, particularly concerning the timely and substantial expansion of renewable electricity generation in Europe. To better understand the trade-offs between domestic production and large-scale energy imports and their corresponding infrastructures needs, we use the energy system optimisation model REMix. We consider different strategic European story lines and constraints on expansion of pipelines and power grids to identify robust capacity targets from a cost optimal perspective. The results indicate that European energy sovereignty is feasible but comes at around 3% higher cost compared to stronger cooperation with resource-rich areas such as the British Isles or the Maghreb region. In contrast, preventing any network expansion lead to an increase of up to 15%. With regard to the extensive adaptations of energy infrastructures required to achieve the emission reduction goal, the timely and substantial expansion of electricity generation from renewable sources in particular is to be regarded as crucial.

1. Introduction

Achieving a climate neutral energy system depends on several key drivers to ensure a successful transition from today's system. The most important drivers include political targets to encourage long-term investments, the technical and economic feasibility of the overall system, and low-cost technologies to convert, transport, and store energy. Furthermore, societal aspects such as public acceptance of energy infrastructures and geostrategic aspects such as the diversity of sources for energy imports have to be considered. Therefore, this study focuses on the technical feasibility of a future European energy system in line with the Paris Agreement while assessing a wide scope of different political constraints and degrees of network expansion for energy transport.

Political commitments towards achieving a climate neutral energy system by 2050 are gaining traction both at the European and national levels. The requirement for a full decarbonisation across all sectors and the technical infeasibility of direct electrification of some energy consumers have recently brought hydrogen and green fuels into focus. To this end both the European Commission (EC) and several European countries have announced strategies dedicated to hydrogen. The strategy of the European Union (EU) puts a strong emphasis on hydrogen as a supporting technology in a system with high shares of renewable electricity and envisions an increase in the total share of hydrogen to 13%–14% in the European energy mix by 2050 [1]. The corresponding Clean Planet study commissioned by the EC emphasises lower than expected costs for renewable energy sources and challenges with respect to carbon capture and sequestration (CCS) technologies as a main driver for low carbon energy carriers such as hydrogen and electrofuels and outlines their respective role in 2050 in line with the emission target according to the Paris Agreement [2].

The study Clean Energy for all Europeans puts further emphasis on strengthening energy sovereignty of the EU [3]. While no clear definition is made, the term is used in the context of reducing imports of fossil fuels, decreasing dependence on external energy suppliers, increasing energy efficiency and positioning the EU as a leader in both development and deployment of renewable energy sources (RES). Westphal [4] further distinguishes between energy sovereignty and security of supply. While a technical robust and resilient system is a prerequisite for both, energy sovereignty is predominantly defined by flexibility, the ability to choose from many options, and reducing dependencies where vulnerabilities can arise. Westphal additionally stresses the difference from energy autarky, as energy partnerships can

* Correspondence to: Curiestraße 4, 70563 Stuttgart, Germany.
E-mail addresses: manuel.wetzel@dlr.de (M. Wetzel), hans-christian.gils@dlr.de (H.C. Gils), valentin.bertsch@ee.rub.de (V. Bertsch).

https://doi.org/10.1016/j.renene.2023.04.015
Received 20 May 2022; Received in revised form 2 March 2023; Accepted 4 April 2023
Available online 5 April 2023
0960-1481/© 2023 Elsevier Ltd. All rights reserved.

List of abbreviations

BEV	Battery electric vehicles
BECCS	Bioenergy with carbon capture and storage
CCGT	Combined cycle gas turbine
CCS	Carbon capture and sequestration
CCU	Carbon capture and utilisation
CDR	Carbon dioxide removal
CHP	Combined heat and power
CSP	Concentrated solar power
DAC	Direct air capture
DACCS	Direct air carbon capture and storage
DACCU	Direct air carbon capture and utilisation
E2P	Energy to power
EC	European Commission
EU	European Union
ESOM	Energy system optimisation model
GHG	Green house gas
HP	Heat pump
HVAC	High voltage alternating current
HVDC	High voltage direct current
LP	Linear programming
LNG	Liquefied natural gas
LH2	Liquid hydrogen
LOHC	Liquid organic hydrogen carriers
MILP	Mixed-integer linear programming
NA	North Africa
NTC	Net transfer capacity
PV	Photovoltaics
RE	Renewable energy
RES	Renewable energy sources
TES	Thermal energy storage
TYNDP	Ten-Year Network Development Plan
VRE	Variable renewable energy

broaden the scope of options. Similarly, Scholten and Bosman [5] argue that a shift towards renewable energy sources will reduce the overall dependence on energy imports and allow for opportunities for domestic sourcing and cross-border trade for balancing. Tröndle et al. [6] assess the possibly of autarky in the European power system on different spatial scales and conclude that especially on sub-national levels significant barriers remain. On the topic of long term energy imports, Hauser [7] compares different approaches towards a diversification of the European gas supply and identify pipelines to suppliers in North Africa (NA) as a no-regret option and the EU-Russian relationship as a main driver or inhibitor of diversification efforts. Frischmuth and Härtel [8] assess potential hydrogen imports and sourcing strategies in the European context and find a high share of 80% of domestic production of hydrogen even at low import costs. Similar findings are presented by Gils et al. [9] for Germany and neighbouring countries.

In the scientific literature there have been model-based assessments of the EU energy system to demonstrate the technical and economic feasibility of carbon neutral power systems. For example, Child et al. [10] analyse an energy system based on 100% RES in the power sector for the European continent by 2050 in line with the Paris Agreement. They underline the role of interconnection capacities in the electrical grid which can lead to overall reduced system cost. This reduction however comes at the cost of increased system-wide interconnection capacity from 63 GW to 262 GW with the largest expansion between France and the British Isles from 2 GW to 45 GW. The study of Hanley et al. [11] focuses on the emergence of hydrogen as part of energy systems on a global, multi-regional and national level highlighting the role hydrogen can play as a key energy carrier across multiple sectors. They identify deep decarbonisation targets, high shares of renewable energy technologies and a lack of development of CCS technologies as key drivers for the market integration of hydrogen. Deane et al. [12] highlight the close dependency between power grids and gas networks and assess the impact of interruptions in gas supply. On a more limited spatial scope Devlin et al. [13] model a joint optimisation of electricity and gas infrastructure for the British Isles and assessing system robustness against possible extreme weather events.

Several key drivers are enabling this push towards green energy carriers such as progressing technological development of PV and water electrolysis which allow for low-cost sustainable production of electricity and hydrogen. While the electrification of demand technologies such as switching to heat pumps and adoption of battery electric vehicles (BEV) offers a rapid way to decarbonise some sectors, other sectors such as the production of steel and concrete and the chemical industry remain more challenging and may rely on hydrogen and methane from sustainable sources [14]. Both hydrogen and methane offer the possibility of storing and transporting large amounts of energy while at the same time enabling higher shares of variable renewable energy (VRE) in the power sector by providing demand side flexibility. This flexibility, however, comes at the additional cost of lower overall efficiencies due to additional conversion steps. Similar effects can also be achieved via other energy carriers such as methanol and ammonia, which are out of the scope of this paper.

Both green hydrogen and green methane provide the opportunity of utilising the existing gas infrastructure of pipelines, storage and liquefied natural gas (LNG) terminals by means of infrastructure repurposing. While historically the sourcing of natural gas depended on oil and gas producing countries, water electrolysis and further methanation via the Sabatier reaction allow for more small-scale regional strategies depending only on low-cost electricity and sufficient water resources. Gorre et al. [15] analyse the technological configuration of such systems in detail and report estimates for techno-economic data in the years 2030 and 2050. Similarly Di Salvo and Wei [16] assess synthetic natural gas production in California highlighting the opportunity of utilising biomass rather than electrolysis. Utilising biomass as resource however is limited in potential.

With both green hydrogen and green methane directly depending on the availability of renewable energy, this requires three main conditions for countries to establish themselves as large-scale producers and exporters for green energy: First, the technical potentials for the installation of renewable energy technologies need to exceed the capacities required for domestic electricity demand. Second, the quality of the renewable potentials in terms of capacity factors needs to be high enough to produce electricity at lower costs compared to other regions. Third, sufficient transport infrastructure for power or gas transmissions is either already available or expanded. Examples for regions that fulfil the first two criteria are the British Isles with the largest offshore wind potentials in Europe as well as the Maghreb region in North Africa where large potentials of direct irradiation can be utilised via CSP and PV. Both regions have high potentials for large-scale low-cost renewable energy, but are separated from the continental European grid by the British Channel, the Mediterranean Sea or the Strait of Gibraltar respectively. This geographical separation is also reflected in the topology of the European power grid and pipeline network and poses additional challenges for the construction and maintenance of energy infrastructure. Therefore, accessing these potentials requires dedicated efforts and investments into either submarine power cables or gas pipelines. Benasla et al. [17] address the opportunity for the Maghreb region to become an energy exporter for countries in Europe in more detail, showing that high voltage direct current (HVDC) lines to enable imports renewable solar can play a significant role as a spatial flexibility option especially for demand centres in and close to Northern Italy. Child et al. [10] estimate the potential annual energy

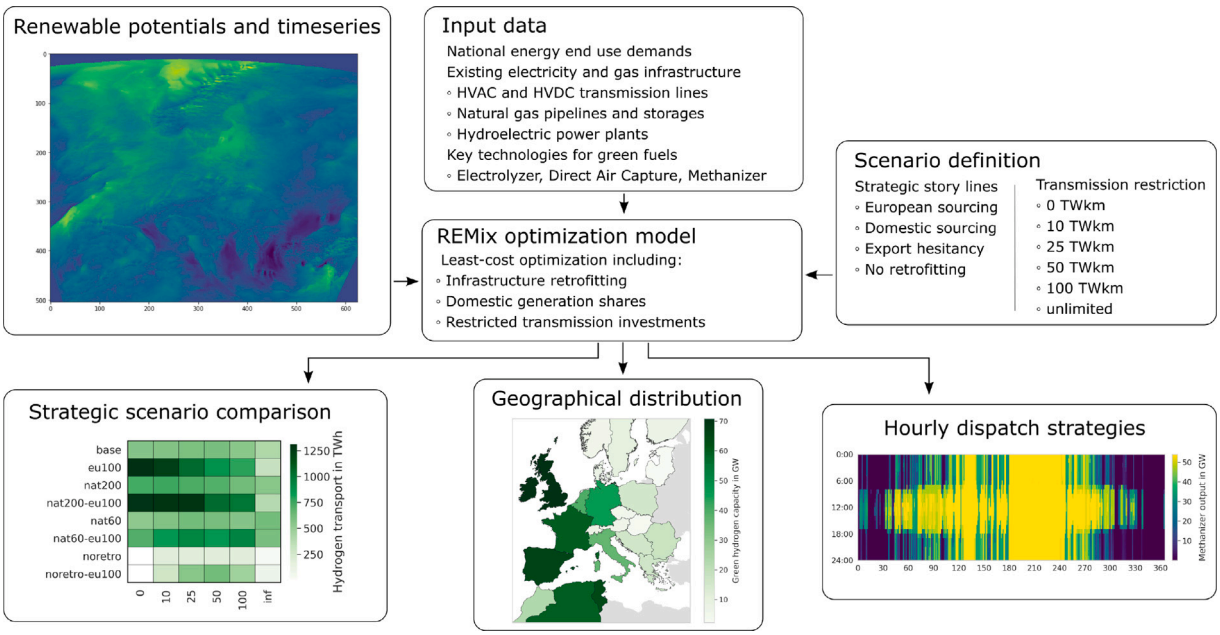


Fig. 1. Overview of the methodological approach.

exports from the British Isles to 194 TWh with a required HVDC transport capacity of 45 GW towards France and 10 GW towards the BeNeLux countries. This has to be seen in contrast to currently existing HVDC capacities connecting the United Kingdom to continental Europe of around 4 GW towards France and 2 GW towards the BeNeLux countries [18]. In addition HVDC lines come with economical risks due to their high investment cost and further legislative challenges such as technical standardisation [19].

Against this background, we analyse two overarching strategies regarding energy import. The first strategy focuses on domestic production and trading in the highly meshed grid in continental Europe (CE), whereas the second puts emphasis on energy partnerships (EP) to enable large scale energy imports from neighbouring regions rich in RES. For a more differentiated view on those two worlds we introduce additional story lines on import and export strategies. Another key dimension for the assessment of future energy systems is the assumed technical feasibility of repurposing existing pipeline for hydrogen as well as restrictions on the allowed degree of network expansion and reinforcement. To this end we employ the energy system optimisation model (ESOM) REMix [20] for a case study to answer the following research questions, that have not been addressed by the existing research described above:

- What is the least-cost spatial distribution of green hydrogen and methane production facilities in an integrated, zero-emission European energy system?
- What investments into renewable energy (RE) capacities and energy transport infrastructure are robust across a broad scope of different sovereignty strategies and limitations on grid expansion?
- What are the optimal energy carriers and main routes for energy transport across the European continent if energy partnerships with the Maghreb region and the British Isles are either promoted or avoided?
- What conclusion for the design of energy systems can be drawn based on the interactions between energy conversion technologies and operational patterns for energy storage technologies?

This paper is structured as follows: Section 2 outlines the general workflow applied for the analysis and gives an overview of the scope of the system as well as the required input data and techno-economic datasets, motivates the considered story lines for the case study, and specifies the model formulation. The results Section 3 is structured in a high level comparison of optimisation results for the different story lines, a more in depth analysis of geographical distribution of technologies, assessment of required network expansion decisions, and hourly operation strategies for the supply and storage technologies. Section 4 puts the research into context of other publications and takes a critical look on limitations which could not be addressed in the scope of this study while Section 5 summarises the key findings and gives an outlook on possible follow-up studies.

2. Methods

2.1. Model scope and input data

The system examined here includes all member states of the European Union, plus Great Britain, Norway, Switzerland, the candidate and potential candidate states in South-eastern Europe, and the Maghreb states of Morocco, Algeria and Tunisia. The British Isles and the Maghreb states are connected to the European mainland via existing power lines and pipelines. The extent to which an annual net import of energy from these countries is possible is defined via the scenarios (Section 2.2). To limit the size of the mathematical problem to be solved, the countries in the study area are partially aggregated to 22 model regions.[1] For these regions, the design of a climate neutral energy supply in 2050 is analysed. The selected year affects the assumptions for energy demand and the techno-economic parameters of the technologies. In all instances the spatial system boundaries are identical and all regions are optimised to keep results comparable across the different story lines. Fig. 1 depicts the methodology and data flows.

In the modelled system, the energy carrier-specific demand is partly specified exogenously and partly a component of the results (Fig. 2). In the heating sector, for example, the demand for useful energy

[1] Algeria, Austria, Balkans East (Bulgaria, Romania), Balkans North (Bosnia and Herzegovina, Croatia, Montenegro, Serbia, Kosovo, Slovenia), Balkans South (Albania, Greece, North Macedonia), Baltics (Estonia, Latvia, Lithuania), BeNeLux (Belgium, Netherlands, Luxembourg), Central East (Hungary, Slovakia), Czech Republic, Denmark, Finland, France, Germany, Iberia (Spain, Portugal), Italy, Morocco, Norway, Poland, Sweden, Switzerland, Tunisia, British Isles (United Kingdom, Ireland).

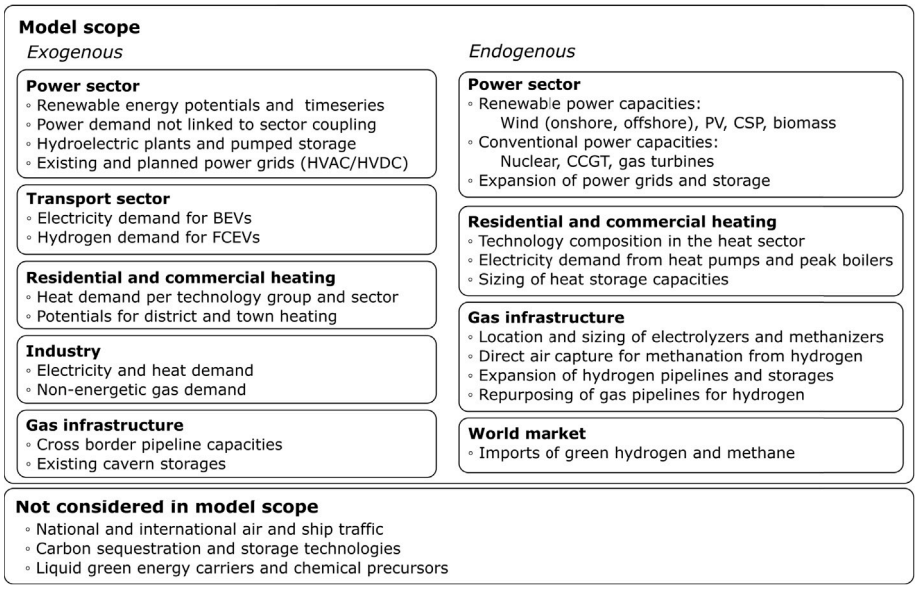


Fig. 2. Outline of the model scope grouped by sectors.

is specified exogenously, divided into the consumer classes industry, large heating networks, small heating networks and buildings. The technologies used to meet this demand are determined endogenously. Depending on the consumer class, different types of combined heat and power (CHP) plants, electric boilers, fuel boilers, and heat pumps (HP) can be considered. A further flexibilisation of the operation of these plants can be realised by endogenous investment in thermal energy storage (TES).

Furthermore, the demand for methane and hydrogen for the transport sector and non-energy use is specified exogenously. It is derived from the *TECH1.5* scenario presented in the Clean Planet study [2]. This demand can increase endogenously through fuel use in the power and heat sectors. For countries which are not included in the original data source we estimate future demand for hydrogen and methane based on a mean value of current and future demand in line with demand projections from the e-Highway 2050 study [21]. From the system perspective, all exogenously given demand for methane is accounted with downstream green house gas (GHG) emissions due to usage in decentral heating systems where CCS and carbon capture and utilisation (CCU) are not economically viable or emissions during the ammonia production for fertilisers. This implies that all methane has to be either sourced from biogas, produced as green methane and from renewable electricity, or imported from a world market for green fuels. Therefore, we model the synthesis of green methane based on direct air capture (DAC) technologies in order to close the carbon cycle. For the case study the techno-economic data for DAC technologies is taken from Fasihi et al. [22] using the conservative capital cost assumptions.

The electricity demand that is not related to flexible sector coupling technologies, i.e. is not used for electric heating, electric driving or hydrogen production, is also specified exogenously. Here, we rely on data from Bruninx et al. [21]. On the electricity supply side, infrastructures are mainly determined endogenously, but existing hydro power plants are considered (Fig. 2) based on datasets generated by the tool power plant matching [23]. Further modifications of the dataset have been done based on the power plant dataset published by the German Bundesnetzagentur [24]. These include run-of-river, reservoir and pumped storage hydro plants.

For the power transmission grid, the existing lines and the planned expansion measures until 2030 are exogenously incorporated as stated in the Ten-Year Network Development Plan (TYNDP) [25]. These can be expanded further endogenously within the allowed boundaries of network expansion (Section 2.2).

In the gas system, existing underground storage facilities are considered according to the GIE database [26] as well as existing transport pipelines based on data from ENTSO-G [27]. An expansion of gas storage is not possible for methane but for hydrogen within the limits specified in [28]. Existing gas pipelines can be repurposed for hydrogen transport, new pipelines can be built either for hydrogen or methane. The assumed cost for pipeline repurposing is taken from [29]. Admixtures of hydrogen and methane are not considered in this analysis.

In addition to increasing capacities of existing connections we also allow new connections between neighbouring countries either via pipeline, overhead landlines or sea cables. The demand and capacity assumptions are supplemented by the techno-economic characteristics of the modelled technologies. These are considered according to [28].

An import of renewable gases can be realised through the utilisation of existing LNG terminals which allow model regions to purchase green gases from the world market at a fixed price of 80 €/MWh for hydrogen and 120 €/MWh for methane (for all energy accounting of hydrogen and methane the lower heating value is used consistently). This demand for methane can also be met by using biogas from agricultural waste. The quality of this gas is assumed to be adequate, but the potential is limited for each model region according to [28].

While electricity and heat supply, including buildings and industry, are fully included in the model, this does not apply to the transport sector. There, only ground-based transport is considered, whereas shipping and air traffic are outside the modelled system.

2.2. Scenario variations

To analyse the impact of different decisions towards energy sovereignty on both the national and European energy systems we utilise the share of domestically sourced energy relative to the regional demand as a key driver. This share is applied to all considered energy carriers individually. Sasanpour et al. [30] present a similar approach in varying self-sufficiency rates, secured capacities and diversity indicators to show a broad range of possible systems. In this analysis, we impose either a lower or an upper limit of domestic supply. While the lower limits ensure a national security of supply for the energy carriers and national contribution towards the mitigation of climate change, the upper limits represent concerns about land use or resource consumption. However, an upper limit can also prevent individual countries from taking up a role as large-scale energy exporter. All limits are based on the annual supply and demand for energy carriers.

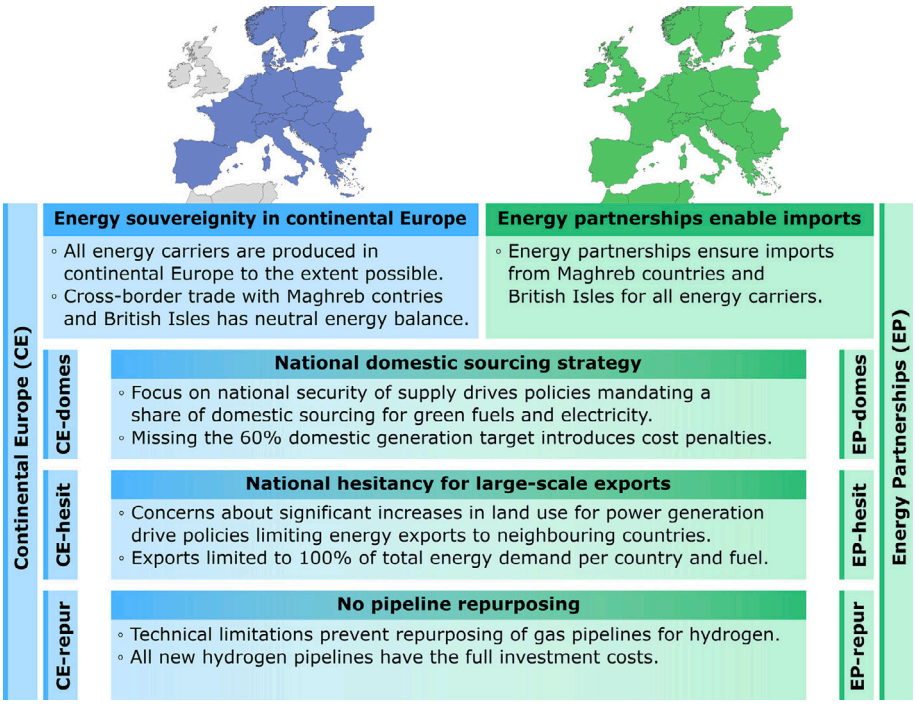


Fig. 3. Considered scenarios derived from the two main story lines on energy sovereignty in continental Europe (CE) and energy partnerships (EP) and 3 sub story lines on export hesitancy (-hesit), domestic sourcing (-domes), and limitations on repurposing (-repur).

Therefore, sub-annual exchange between different model regions is still allowed. Furthermore, to ensure the technical feasibility of the system, imports of hydrogen and methane from a world market are allowed in all scenarios but cause additional penalty costs in the objective function of the optimisation if this leads to violations of the domestic generation shares. All scenario story-lines listed in Fig. 3 are taken into account during the analysis.

In addition to the story-line component on energy sovereignty, a second key driver for the overall energy system design in Europe is the expansion of existing energy transport networks. Schlachtberger et al. [31] present a methodology to evaluate different large-scale network configurations by limiting the overall investment. Due to the methodology of taking the net transfer capacities (NTC) for both the electrical network based on the e-Highway Scenario and for the gas networks based on the ENTSO-G reported values as well as distances between the population-weighted centroids of each model region, we obtain different values compared to the physical network capacities and distances. Based on the modelled infrastructure, existing capacities for natural gas pipelines of 970.3 TWkm, high voltage alternating current (HVAC) grid of 78.5 TWkm and HVDC lines of 27.2 TWkm are exogenously considered as existing infrastructure. The application of NTC reduces the overall considered power network in comparison to other datasets which also account for lines inside national boundaries (e.g. 345.7 TWkm for the HVAC grid as specified in [32]). This also implies an underestimation of the overall investment requirements into grid infrastructure in comparison to studies with a higher spatial resolution. In this analysis, additional expansion of network infrastructure is limited to 0, 10, 25, 50, 100 TWkm per energy carrier in addition to the unrestricted network expansion. This yields 6 different limits on expansion and in conjunction with the eight scenario story-lines (Fig. 3), a total of 48 different scenarios are analysed.

2.3. Model formulation

The energy system optimisation model REMix [20] used in this study allows for finding possible least-cost systems under additional constraints. The overall system costs described in Eq. (1) are composed of the annualised investment cost C_{inv}, fixed and variable operation cost C_{fix} and C_{var} as well as the costs for fuel imports into the model regions C_{fuel}. While the model also supports a formulation as mixed-integer linear programming (MILP), the analysis in this paper is limited to a linear programming (LP) formulation due to the size of the individual optimisation problems and the number of scenarios considered.

$$\min C_{total}$$
$$C_{total} = \sum_{r,p,c} C_{inv,r,p} + C_{fix,r,p} + C_{var,r,p} + C_{fuel,r,c} \quad (1)$$
$$\forall r \in regions, p \in techs, c \in energycarriers$$

In contrast to previous model applications which consider fully separated infrastructures for natural gas and hydrogen [9], we explicitly include the repurposing of natural gas pipelines towards hydrogen as an endogenous model decision. This can be achieved by restricting the investments into repurposed hydrogen pipelines $l_{build,H2repurpose}$ and limiting this variable by the total number of decommissioned natural gas pipelines $l_{decom,CH4}$ on any given pipeline corridor between the model regions r and r' as shown in Eq. (2).

$$l_{build,r,r',H2repurpose} \leq l_{decom,r,r',CH4} \quad (2)$$
$$\forall r, r' \in regions$$

Eq. (3) shows the formulation for considering the domestic generation shares per energy carrier. This equation is only applied to scenarios which consider either upper or lower constraints on the domestic generation dgs_{upper} and dgs_{lower}. We account for the overall generation gen and demand dem of each energy carrier c and technology p without temporal and spatial flexibility options in the form of storage, pipelines and power grids. To ensure feasibility of the optimisation problem, we introduce an additional slack variable for the domestic generation. This slack variable comes with additional penalty costs which prioritise domestic generation of electricity before hydrogen and hydrogen before methane. The prioritisation is motivated firstly by the need to keep electricity demand and supply continuously balanced and secondly due to the increasing electricity demand for water electrolysis and hydrogen demand for the methanation making the achievement of domestic

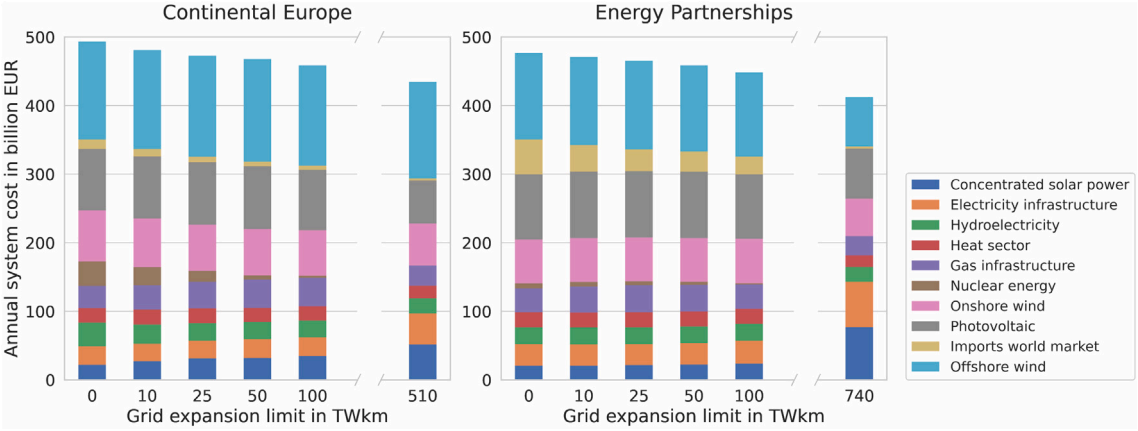


Fig. 4. Overall system costs in billion EUR (y-axis) for the two main story-lines energy sovereignty in continental Europe (CE, left) and energy partnerships (EP, right) along the allowed degree of network expansion (x-axis). The value of the highest degree of network expansion corresponds to the scenario in which network expansion is unlimited.

generation targets more challenging with each additional conversion step.

$$dgs_{lower,r,c} \cdot \sum_{p} dem_{r,p,c} \leq \sum_{t,p} gen_{t,r,p,c}$$
$$\sum_{p} gen_{r,p,c} \leq dgs_{upper,r,c} \cdot \sum_{t,p} dem_{t,r,p,c} \quad (3)$$
$$\forall\, r \in regions, p \in techs, t \in timesteps, c \in energycarriers$$

For the analysis of the energy transport infrastructure requirements, we limit the number of newly constructed power lines and gas pipelines to a given value as shown in Eq. (4). This limit is given individually per energy carrier c and consists of the product of new lines l_{build}, the rated transfer capacity p_{rated}, and the distance between model regions $dist_{r,r'}$.

$$\sum_{r,r',p} l_{build,r,r',p} \cdot p_{rated,p,c} \cdot dist_{r,r'} \leq exp_limit_{c} \quad (4)$$
$$\forall\, r, r' \in regions, p \in techs, c \in energycarriers$$

3. Results and discussion

The evaluation of the cost-minimal solution for 48 scenarios yields a wide range of different systems to explore. While the overall system costs do not significantly vary, the main deviations are attributed to a few technologies (Fig. 4). The system costs are consistently lower for the energy partnership (EP) story-lines than for the continental Europe (CE) sovereignty story lines, on average by 2.8%. The complete omission of network expansion leads to a cost increase by 15.7% in the EP story-line and goes along with the substitution of HVDC lines and CSP plants especially by world market imports and offshore wind power. In the CE story-line, instead, costs increase by 13.5% if no network expansion is allowed, which is mostly related to higher world market imports and VRE capacities, as well as the usage of nuclear power. The maximum network expansion is significantly higher at 740 TWkm in the EP story line compared to the 510 TWkm in the CE story line.

A closer look into the technology specific share of total system costs depicted in Fig. 5 indicates a large variation for a small set of technologies. With green hydrogen mainly produced via water electrolysis and green methane produced via hydrogen and DAC, the main source of all energy carriers is electricity produced from RE technologies. This fundamental role can be seen in the large investments in both onshore and offshore wind energy and PV closely followed by CSP. The costs for hydroelectricity consist of maintenance costs for existing pumped storage and reservoir plants as well as investment costs into new run-of-river plants. The large capacity variation for offshore wind energy in the least cost solutions indicates a high dependence on different

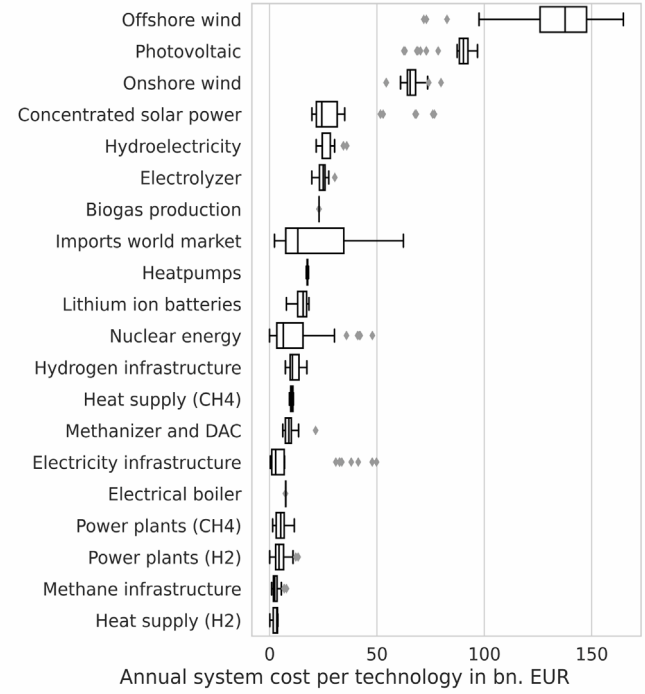


Fig. 5. Contribution of different technology groups (y-axis) to the overall system costs (x-axis) across all 48 combinations of story lines and network restrictions. Higher variations in the box plots indicate more different systems in a subset of all considered scenarios.

scenario narratives and the corresponding policy-driven constraints. Similarly for CSP, we can observe a significantly wider range of investment costs across all scenarios. Notably, also the imports from the world market as well as the utilisation of nuclear energy are subject to a large variation. Furthermore we find that the assumed costs for imports of green energy carriers from a world market are cost competitive towards the techno-economical assumptions for RES and electrolysis for domestic production and pipeline-based imports.

3.1. Implications of strategic decisions

To further analyse the implications of the story-lines and network expansion limitations, we take a closer look at the use of the technologies with the largest variations between the scenarios. This particularly

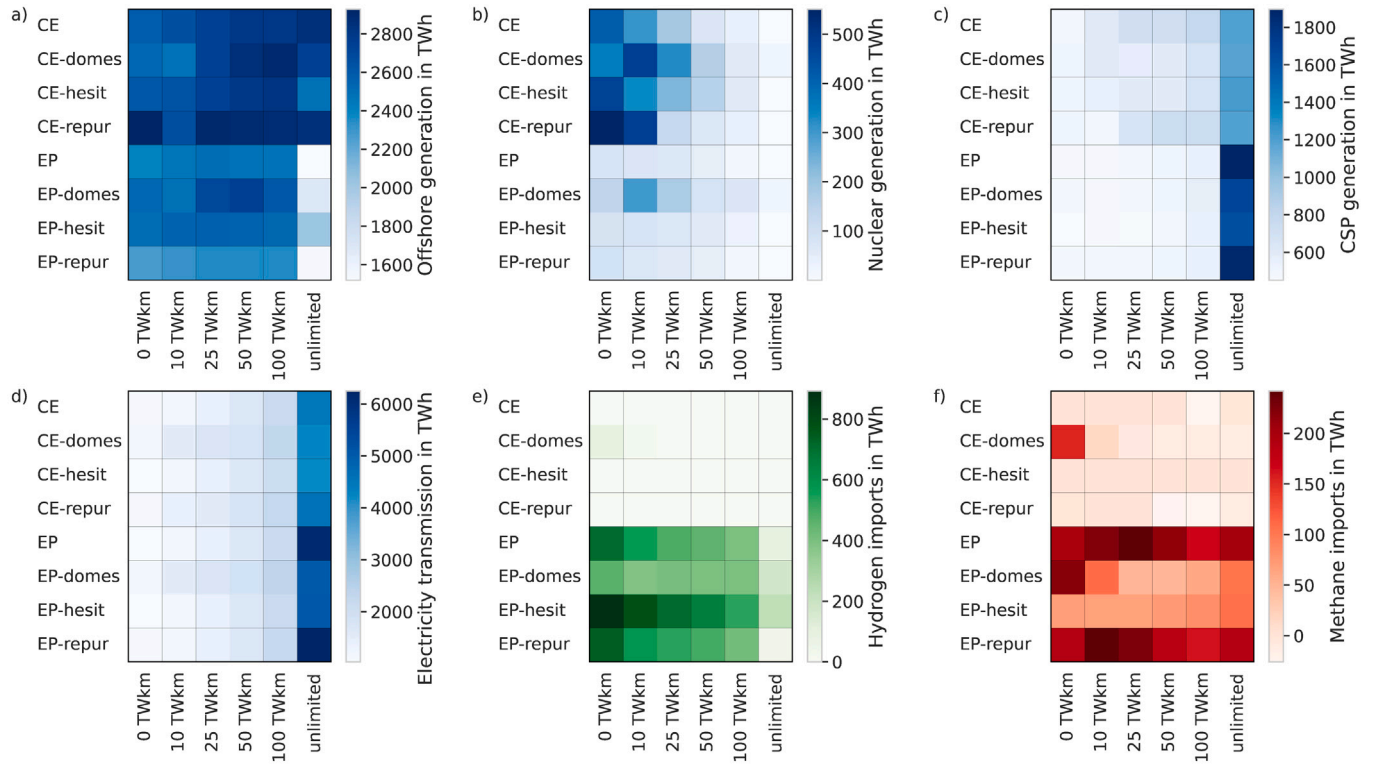


Fig. 6. Evaluation of the selected indicators across the different story-lines (y-axis) and degrees of network expansion (x-axis). The intensity of the heat map (z-axis) corresponds to the level of the indicator. Colours represent the corresponding energy carrier with blue for electricity, green for hydrogen and red for methane. Each heat map has a different scale with some minimum values higher than zero. The individual figures show the annual power generation of offshore wind (a), nuclear power (b) and CSP (c), as well as the annual power transmission (d) and world market imports of hydrogen (e) and methane (f).

concerns the annual power generation by offshore wind, CSP, and nuclear power as well as the dependence on world market imports (Fig. 6).

Offshore wind turbines significantly contribute to the overall electricity generation in most of the scenarios. This is notably reduced by unconstrained network expansion, which favours a higher usage of CSP. Furthermore, there is a preference for offshore wind in the energy sovereignty story-lines as long as a moderate grid expansion is still possible. The strong dependence of CSP usage on grid expansion can be explained by the resource availability of this technology limited to regions in Southern Europe and the Maghreb states. Limiting the overall grid expansions restricts the total share the technology can achieve and shifts the utilisation of CSP towards providing flexible electricity generation on a regional scale with a minimum generation level of around 500 TWh per year. In case of the story-lines including a European energy sovereignty, we observe a slight preference for CSP technologies compared to the non-constrained scenario counterparts.

Substantial investments into nuclear power plants can be observed only in scenarios which combine the European sovereignty story-lines with strong limitations of capacity expansion of networks. This implies that the limited transport range of low-cost VRE electricity leads to relatively higher electricity prices in regions in Eastern Europe and investments into nuclear power plants in the cost optimal solution. An alternative solution can be increased imports of green methane or hydrogen for combined cycle gas turbine (CCGT) power plants, which in turn would lead to overall higher system costs due to the higher fuel costs.

At the assumed prices, the maximum imports of green hydrogen and green methane to continental Europe reach up to 890 TWh and 240 TWh, respectively. In the energy partnership story lines (EP-) the hydrogen imported to continental Europe equals 43% of the overall demand in continental Europe of which 20% can be attributed to energy partnerships and 80% to the world market. Methane imports to continental Europe equals to 53% of the corresponding overall demand, of which the imports are attributed almost completely to energy partnerships with imports from the world market contributing only around 1%. In contrast the story-line focusing on continental Europe (CE-) enforces the complete removal of imports from the system except for the imports required in the case of constraint violations. Furthermore, the increase in hydrogen imports by a factor of two in the story-line with national hesitancy towards large-scale exports indicates an increased reliance on a global hydrogen market. Both the share of energy imports via energy partnerships as well as the ratio between hydrogen and methane are highly dependent on the exogenously assumed prices.

The analysis of the annual energy balances yields three main findings. First, resource-rich areas such as the Maghreb region and the British Isles can offer lower cost production of green energy carriers compared to imports from a global market. This comes back to the additional transport and infrastructure costs for ship-based transports in contrast to existing pipelines and power grids. However, to fully utilise such energy partnerships, large-scale investments into either pipelines or power lines are a prerequisite. Second, prices on a world market exceeding the exogenously assumed prices for the study can increase the shift to regional sourcing of renewable energies and therefore provide incentives for strong European collaboration and investment into transport infrastructure. Third, focusing on European energy sovereignty while at the same time preventing sufficient expansion of transport networks can favour nuclear energy as part of the cost optimal solution. This, in turn, can cause new dependencies on uranium imports for the production of fuel rods. This shift is especially prevalent if national policies prevent the emergence of large-scale energy exports or the expansion of hydrogen networks is limited. Alternatively, imports of green methane from a world market have to be considered as a fallback option at higher overall system costs.

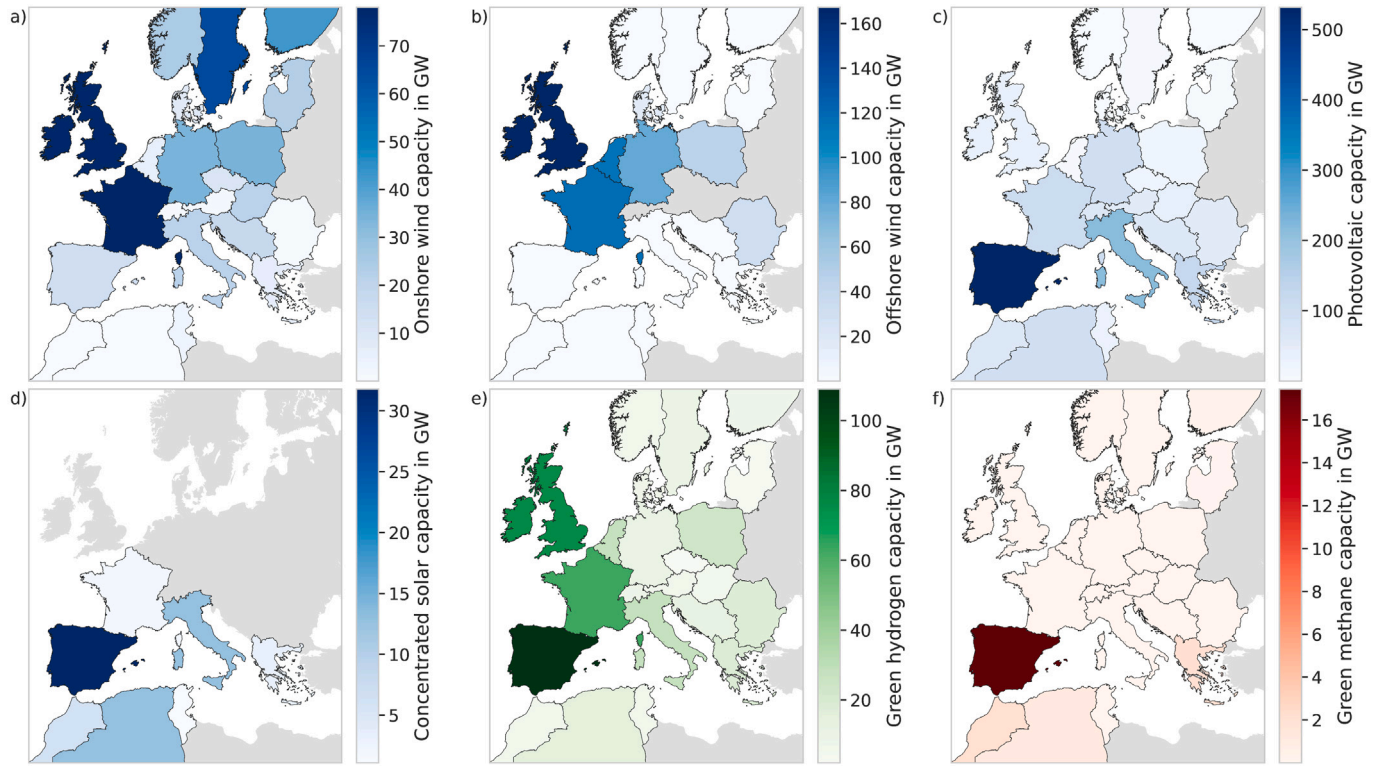


Fig. 7. Regional distribution of robust technology capacities for offshore wind (a), onshore wind (b), PV (c), CSP (d), electrolysers (e) and methanation (f). Colours represent the corresponding energy carrier with blue for electricity, green for hydrogen and red for methane. Robust capacities are calculated via the 10th percentile per region. This means at least the same amount or more capacities are build in 90% of all analysed scenarios across all scenarios and degrees of network expansion. Regions in grey are either outside the model scope or do not have any potential for the corresponding technology.

3.2. Spatial distribution of power and fuel generation

The spatial distribution of power and fuel generation facilities is closely linked to the scenario assumptions. However, minimum capacity values can be derived across the majority of 90% of the scenarios providing a robust lower value for the spatial distribution of different technologies (Fig. 7). The spatial distribution of RE power generation is clearly correlated to the available resource potentials. Offshore wind energy is especially prevalent in the British Isles and shores of the North Sea and Atlantic Ocean, whereas it plays only a marginal role in Northern Europe and the Mediterranean. Hydroelectricity and onshore wind energy are dominant in the Northern countries and a combination of PV and CSP in the Southern countries. There, the low cost VRE power supply from PV is supplemented by thermal energy storage integrated into the CSP power plants. Both PV and onshore wind energy can be found in most model regions, with a slight preference for PV towards the South and wind onshore towards the North. Electrolysers and methanation plants are located close to the electricity sources indicating a preference for transporting gaseous energy carriers across the system while using the electricity grid for spatial balancing of supply and demand according to the overall weather situation across Europe. This assumption is further underlined by the broad distribution of onshore wind and PV across the model regions.

For the VRE capacities, using the 10th percentile method we obtain system wide robust investments of 1.63 TW for PV (compared to 2.44 TW in the scenario with the highest PV capacity), 492 GW for onshore wind energy (compared to 693 GW in the scenario with the highest capacity), and 569 GW for offshore wind energy (compared to 870 GW in the scenario with the highest capacity). As these capacities represent the lower bound for 90% of all considered scenarios, they can be seen as no-regret investment options for the underlying techno-economical assumptions. For electrolysers the spatial distribution of capacities has a larger variance, but around 469 GW are considered robust investments (compared to 860 GW in the scenario with the highest electrolyser capacities). Investments into CSP plants and methanation plants show the highest variance across scenarios. Robust investments amount only to 23.2 GW for methanation and 69.9 GW for CSP plants (compared to a maximum of 169 GW for methanation and 293 GW for CSP in their respective scenarios with the highest capacities).

The required capacity for DAC for the utilisation in the methanation plants ranges from 84.1 $MtCO_2/a$ to 298.3 $MtCO_2/a$ with an annual amount of captured carbon dioxide between 51.5 $MtCO_2/a$ and 210.1 $MtCO_2/a$. Thereof, 45.8 $MtCO_2/a$ are related to the exogenous demand for methane while the remaining part is used for green methane for the utilisation in both in the heating sector and in gas turbines.

3.3. Trade-offs for storage and grid expansion

The possibility to repurpose natural gas networks adds an additional layer of complexity when deciding how the future infrastructure should look like, but can at the same time enable new options potentially limiting public resistance against such infrastructure projects. Fig. 8 shows the comparison of overall storage capacities and new as well as repurposed pipeline capacities for both hydrogen and methane.

The assumption of European energy sovereignty clearly drives investments into hydrogen storage even if repurposing is not possible (top left, CE-repur). At the same time, technical challenges in repurposing lead to an increasing importance of large methane storage facilities (top middle, -repur) and decrease in importance if countries tend towards avoiding large-scale exports (top middle, -hesit). New methane pipelines are installed especially in the European sovereignty story-lines. This is linked to the partial reliance on imports from a world market which require increased pipeline capacities for methane from the Iberian peninsula towards France. Furthermore, we observe a clear order of preferences in the expansion of the energy networks. Expansion of the electricity grid is always the preferred option reaching the imposed limitation across all scenarios (top right). As the

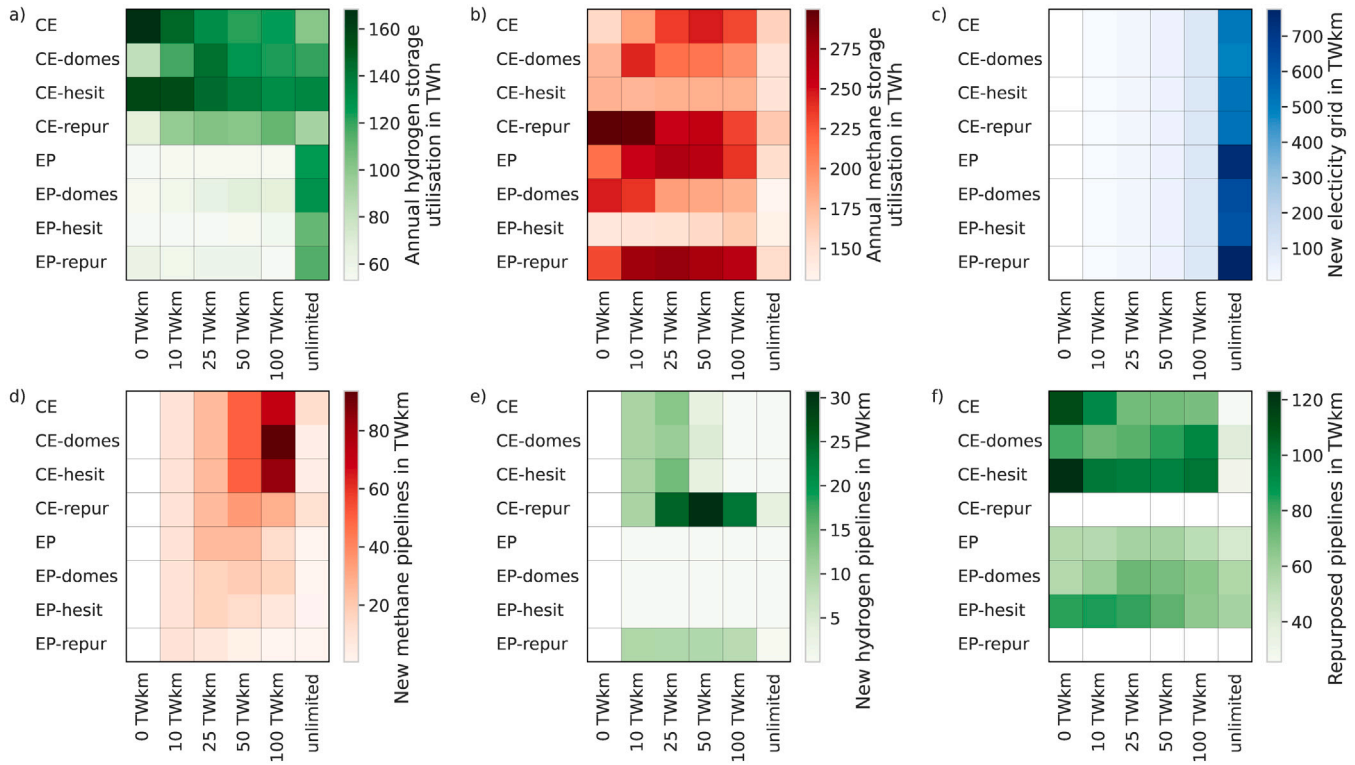


Fig. 8. Comparison of annually used storage volumes and pipeline capacities for hydrogen and methane across the different story-lines (y-axis) and degrees of network expansion (x-axis). The intensity of the heat map (z-axis) corresponds to the level of the indicator. Colours represent the corresponding energy carrier with blue for electricity, green for hydrogen and red for methane. The sub-figures show the storage usage for hydrogen (a) and methane (b), as well as the capacities of new power lines (c), new hydrogen pipelines (d), new methane pipelines (e) and repurposed pipelines (f). Each heat map has a different scale with some minimum values higher than zero.

capacity expansion of power grids becomes increasingly restricted, further investments into methane pipelines are chosen by the model. Again the limit is reached, but only in the story-lines focusing on continental Europe (bottom right, CE-), where no natural gas networks are being repurposed. As last option we see additional investments into new hydrogen pipelines starting at a network expansion constraint of 25 TWkm for each network. New hydrogen pipelines however are relatively small compared due to the option of repurposing from natural gas to hydrogen, which is chosen in all scenarios where it is allowed but plays the largest role when combining the story-lines on sovereignty and national export hesitancy (bottom right, CE-hesit). This combination prevents concentrated regions for production and has a strong reliance on a widespread hydrogen network.

For the analysis of energy flows, we split the scenarios into the group focused on European energy sovereignty and the remaining scenarios. Fig. 9 shows the 67th percentile for the energy flows along each line for each scenario group. The arrows provide the minimum flows observed in one third of the corresponding scenarios. For the European sovereignty case (Fig. 9, top row), we identify two main supply regions. Denmark and Belgium provide both electricity and hydrogen especially to Germany, whereas the Iberian peninsula becomes a main provider for green methane. Due to the large scale production of hydrogen necessary to provide methane to other European countries we can additionally observe hydrogen transport from the Iberian peninsula towards Morocco to better utilise the infrastructure investments. In contrast, in the energy partnership story-line (Fig. 9, bottom row), we can identify an increased role of the Maghreb region in providing electricity, hydrogen, and methane to Europe via Italy. This energy transport route almost fully substitutes the corridor from Spain to France and is extended for energy distribution to countries in Central Europe. For hydrogen, the imports to Germany from neighbouring countries such as Denmark, the Netherlands and Belgium are replaced by imports from the British Isles. Germany, however, still remains dependent on electricity imports from Denmark, although to a lesser extent. In summary, in both scenario groups Germany and Italy are the main energy import countries due to their high energy demand compared to the available area for RES. For Germany, both PV and wind capacities reach their assumed technical potentials of 143 GW and 113 GW, respectively, across all scenarios. For Italy the maximum PV capacity of 215 GW is reached in all scenarios and the maximum wind power capacity of 158 GW in almost all scenarios with a continental Europe energy sovereignty focus.

3.4. Interactions between energy conversion technologies and operational patterns for energy storage technologies

In order to get a deeper understanding of the fundamental system design choices by the optimiser we turn to the hourly dispatch profiles. Here, we can identify a close correlation on the temporal scale between the production of heat, hydrogen and methane and the VRE power generation (Fig. 10). Specifically, we observe a clear correlation between the electricity supply from PV and the utilisation of electrolysers. The operational profile of electrolysers additionally reflects some elements from the feed-in profile of wind energy. This further supports the findings on the spatial correlation between electrolysers and regions with renewable energy resources and suggests on-site production of hydrogen is preferred to electricity transmission and electrolysis close to demand centres. The operation of methanation plants also shows a strong seasonal behaviour. This dispatch shows systematic similarities to the output of CSP plants, which are used in addition to PV generation to supply electricity especially during off-peak hours. This allows for a constant operation profile for the production of methane during the summer months and reduces the need for electrical energy storage. Like hydrogen, the production of green methane also is preferred in close proximity to renewable energy sources. This effect is further amplified by the electricity demand for DAC as the carbon source

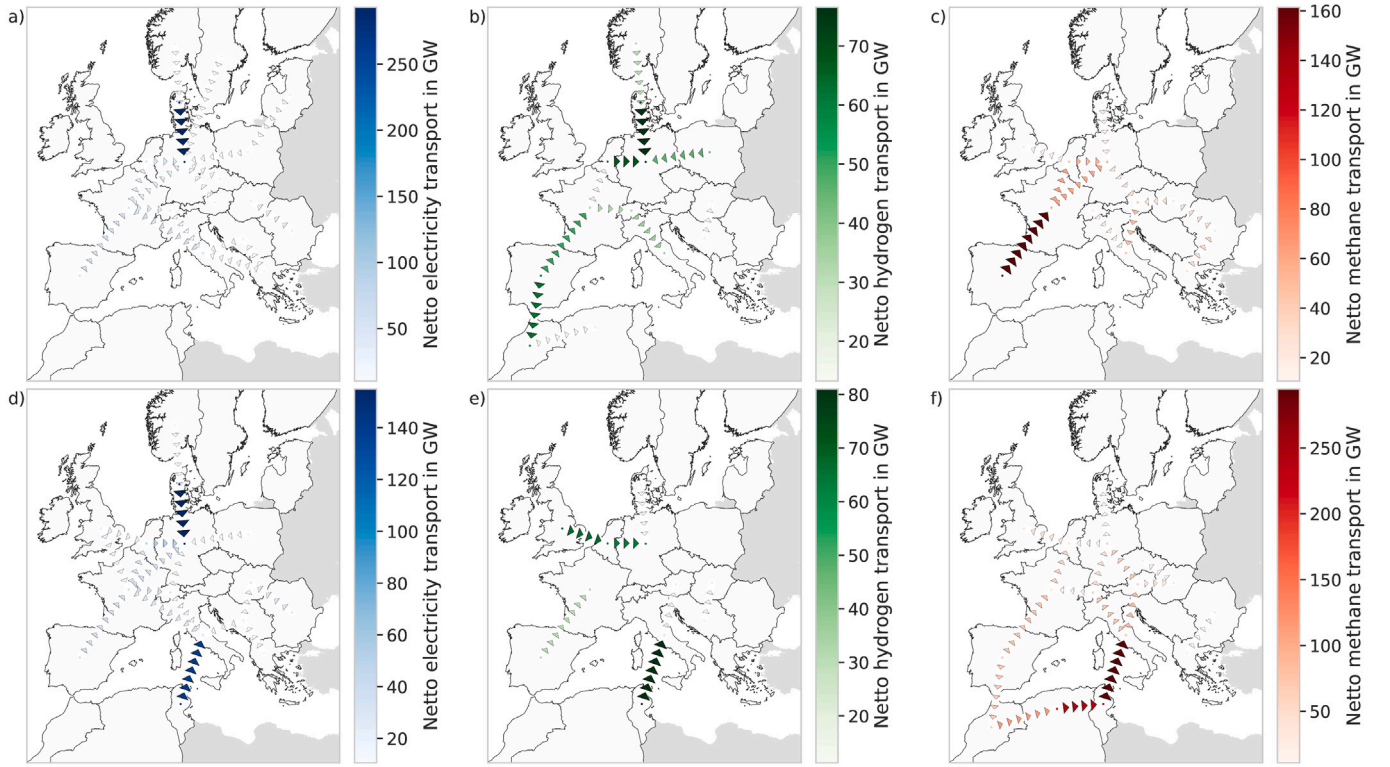


Fig. 9. Regional distribution of robust energy flows across 33% of scenarios for story lines focused on energy sovereignty in continental Europe (CE, top) and predominant focus on energy partnerships (EP, bottom). Colours represent the corresponding energy carrier with blue for electricity (a, d), green for hydrogen (b, e) and red for methane (c, f).

for the methanation process. While production of green methane is predominantly done during the summer, demand for methane from the heating sector increases during the winter. This leads to one of the main challenges of a full climate-neutral energy system which can be observed in the electricity demand for the heating sector. The demand profile has strong seasonal characteristics and can only be partially satisfied using intermittent resources and therefore relies on additional supply via CHP plants and gas turbines. Both backup technologies can use biogas, but can also rely on synthetic gases given sufficient seasonal storage capacities for hydrogen and methane.

When considering the operational patterns of storage technologies there is a close link between charging and availability of VRE resources (Fig. 11). Electricity storage technologies such as pumped hydro storage and batteries are predominantly used for daily shifting from midday to evening hours indicating a balancing function on a local scope. This can be traced back mainly to household demand, electrical heating and inflexible charging of BEV as more flexible consumers such as electrolysers are switched off before the discharging starts. In contrast, Hydrogen storage shows a more intermediate operational pattern which is strongly linked to the hydrogen production from wind power. This interaction with wind power is underlined by the energy to power (E2P) ratios of 10–30 for countries with only hydrogen tanks and 160–300 for countries with good wind resources and access to hydrogen cavern storage potentials such as the British Isles, indicating synergies from siting electrolysers in close proximity to hydrogen storage. In contrast, methane storage shows a strong seasonal utilisation pattern, which is mainly caused by the utilisation of methane in the heating sector. Thus, we observe a continuous filling of the methane storage over the summer months and the lowest level towards the end of the heating period. This seasonally used storage volume amounts to 200–300 TWh, which is substantially exceeded by the current gas cavern capacities of around 1454 TWh. Note that this difference comes in large parts from the perfect foresight method chosen in the modelling approach. In addition to the seasonally used capacities, further capacities for strategic reserves as back-up for industry, CHP and flexible gas turbine power plants will still be necessary in the future, which are not explicitly modelled in our analysis. The siting of the gas storages can be chosen more flexible between either production or demand site if no further conversion steps are done. This can be seen as the majority of hydrogen storage is located in the British Isles, France and Germany while methane storage is located in both the Iberian peninsula and Italy. If hydrogen is used as an intermediate energy carrier for subsequent use in methanation, only a small storage volume is used for buffering purposes.

4. Limitations

This analysis shows different alternatives for a future carbon neutral energy system in Europe, however the modelling of complex systems warrants limitations on the system scope to keep the optimisation problem tractable. In addition limitations on the data side and assumptions on the availability of technologies put additional constraints on the system and therefore also on the possible conclusions.

One of the main limitations posed on optimisation models is related to the number of variables and constraints. During this work we put the emphasis on the hourly dispatch to properly capture the characteristics and interactions of VRE power supply in detail. This on the other hand limits the spatial granularity with impacts on the variability of VRE feed-in and representation of network infrastructure. Bottlenecks in the network infrastructure can only be captured on a national level and not within individual model regions, likewise also spatial balancing inside of model regions is neglected. This effect of spatial resolution on model results has been shown by Frysztacki et al. [33]. To further improve this case study especially a higher spatial resolution and capturing of gas infrastructure as individual model regions would be beneficial. This would allow explicitly capturing the connectivity of infrastructure such as import terminals for LNG and liquid hydrogen (LH2) and gas cavern storage in more detail. Similarly a high resolution modelling of network infrastructures is especially relevant for modelling repurposing natural gas pipelines in a regional context, as a complete switch from natural gas to hydrogen inside a distribution networks and all end users in a

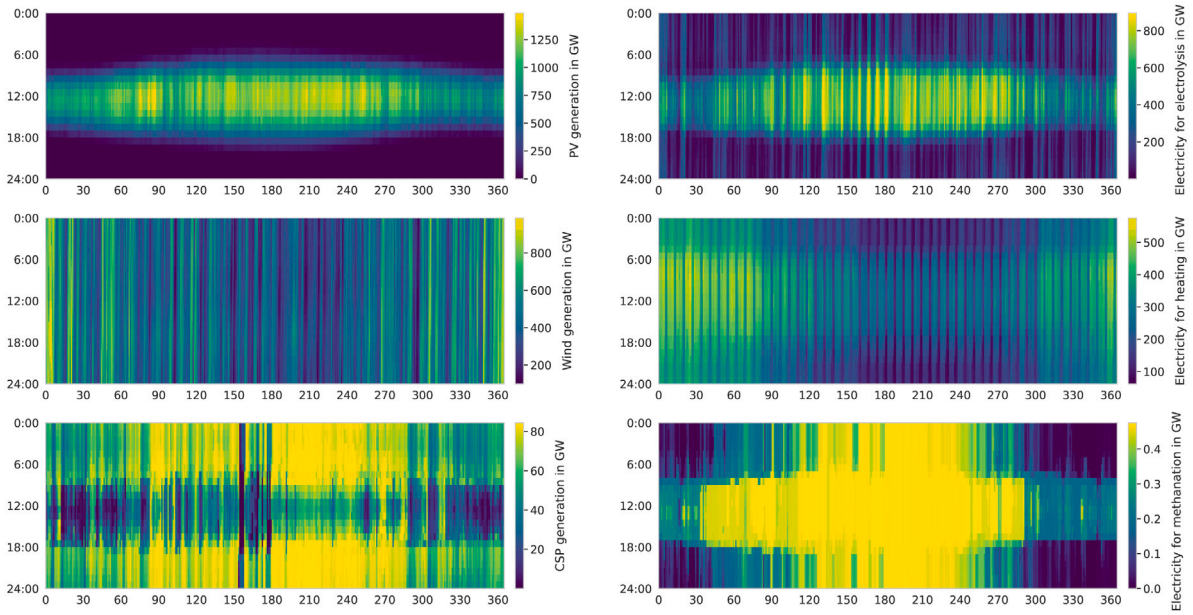


Fig. 10. Hourly dispatch patterns for the main power generation technologies wind energy, PV and CSP (left) and the flexible demand technologies electrolyser, electrical heating and methanation (right). The hours of the day are plotted along the *y*-axis, the days of the year along the *x*-axis. The figures show the story-line focused on energy sovereignty in continental Europe with a moderate grid expansion of 50 TWkm.

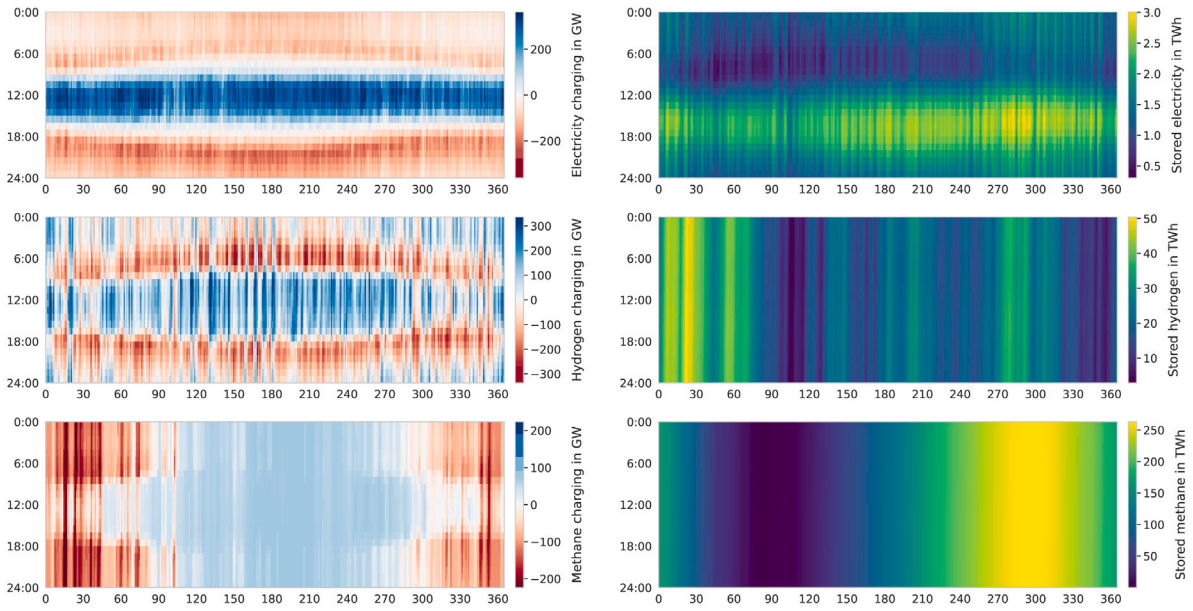


Fig. 11. Hourly storage charging patterns and corresponding storage levels. The hours of the day are plotted along the *y*-axis, the days of the year along the *x*-axis. The figures show the story-line focused on energy sovereignty in continental Europe with a moderate grid expansion of 50 TWkm.

given network is required. To achieve this higher spatial resolution, trade-offs have to be made for example on the temporal resolution via the use of aggregated time slices or typical days such as outlines by Kotzur et al. [34]. The main limitation for this approach is the still remaining challenge to use typical days for systems with high shares of flexible demand and long term energy storage technologies for hydrogen and methane.

In addition to green gaseous energy carriers, to which this study is limited to, liquid energy carriers such as electrofuels offer an additional option for large-scale global transport of energy carriers and can reuse existing petrol infrastructure. Similarly other liquid carriers such as liquid organic hydrogen carriers (LOHC) or ammonia can be utilised as a carrier medium for hydrogen or as a precursor for direct usage in the chemical industry, shifting parts of the value chain to areas rich in RES. In conclusion all additional imports of liquid carriers can reduce the scale of energy supply, but increase import dependence on the other hand.

In the analysis we limited carbon sources to DAC which in turn is only constructed in close proximity to methanation plants. If additionally industrial carbon sources are considered such as cement production, this can have an impact on the optimal locations and cost for green methane production. Similarly, bioenergy with carbon capture and storage (BECCS) was not considered in the study but faces similar problems as CCS in the cement industry or at power plants as adequate storage solutions are required. One possible solutions could be extending the model with additional technologies for carbon capture,

transport and storage similar to studies focusing on systemic cost benefits of CCS technologies [35].

Another large uncertainty is also associated with the techno-economical costs for DAC which assumes a rather strong technological learning of the technology. Realmonte et al. [36] use two integrated assessment models and conclude average scale-up rates for direct air carbon capture and storage (DACCS) of 1.5 $GtCO_2/a$ in the second half of the century after most of the BECCS potential is already utilised. In contrast Fasihi et al. [22] consider only direct air carbon capture and utilisation (DACCU) and estimate the required DAC capacity for the energy sector to scale up earlier with globally installed capacities of 4 $GtCO_2/a$ in 2040 and 7.1 $GtCO_2/a$ in 2050 (15.2 $GtCO_2/a$ if also carbon dioxide removal (CDR) is included). They project levelised costs for carbon capture between 54 and 71 €/tCO_2 for 2050, while in contrast McQueen et al. [37] estimate the levelised costs in the range of 120 and 195 €/tCO_2 at a global cumulative installed capacity of 18 $GtCO_2/a$. This large uncertainly can be attributed to assumptions in initial costs, learning rates, and variable costs for required heat and electricity for the process. With respect to the model results, higher cost assumptions for DAC would not impact the amount of carbon required for satisfying the exogenous methane demand, but could shift the share between hydrogen and methane for both gas turbines and the heating sector towards higher shares of hydrogen.

5. Conclusion

The results of this research show a carbon neutral energy system in continental Europe is technically feasible and leaves several degrees of freedom in the concrete technical and political implementation. The main driver of overall system costs is the allowed degree of network expansion with a cost increase of up to 15% to prevent any additional network expansion and up to 7% if only moderate network expansion is feasible. Forfeiting the option of energy partnerships with the Maghreb region and the British Isles leads to a minor increase in overall system costs of around 3%, but can have a significant impact on the layout of the network infrastructure and siting of methanation plants in the cost optimal solution. For specific pipelines not being part of a wide range of scenarios, this indicated a potential for stranded investments. Therefore, further research is required on robust decisions for the topology of future power grids and gas pipelines.

We identify several technologies which can be considered as robust investments in the least cost systems and under the given assumptions on techno-economic data and demand for hydrogen and methane. This includes 1.63 TW PV mainly built in the Iberian peninsula and Italy, 492 GW onshore wind energy mainly built in the British Isles, France, and Sweden and 570 GW offshore wind energy capacities mainly built in the British Isles, France, and the BeNeLux states. Similarly around 470 GW of electrolyser capacities concentrated in the Iberian peninsula, France and the British Isles are robust investments indicating a preferred production close to RES. This finding is further supported by the temporal correlation between feed-in of renewable electricity and water electrolysis as a flexible demand option. In the case of regions rich in wind resources the balancing is further supported by the use of hydrogen cavern storage on a weekly basis. In contrast, for regions with high solar potential combining PV and CSP allows for low cost production of green methane with a strong seasonal pattern.

With respect to network infrastructure there are three distinct results. First, large shares of CSP can only be enabled if significant investments into the electrical grid (more than 100 TWkm) are feasible and accepted from a societal perspective. Second, if limited network expansion is considered repurposing of natural gas pipelines to hydrogen is a no-regret option. The prevalent hydrogen flows depend mainly on the presumed story lines, but in both cases enable the supply of the two demand centres Germany and Italy. Third, in the case of energy partnerships methane is the prevalent energy carrier, whereas in the continental European system the focus shifts more towards hydrogen including the repurposing of existing natural gas cavern storage sites for hydrogen.

Data availability

Data on model assumptions and results are provided by the corresponding author upon reasonable request.

CRediT authorship contribution statement

Manuel Wetzel: Conceptualization, Methodology, Software, Data curation, Formal analysis, Investigation, Writing – original draft, Writing – review & editing, Visualization. **Hans Christian Gils:** Conceptualization, Data curation, Formal analysis, Investigation, Writing – original draft, Writing – review & editing, Funding acquisition. **Valentin Bertsch:** Supervision, Formal analysis, Investigation, Writing – review & editing.

Declaration of competing interest

The authors declare that they have no known competing financial interests or personal relationships that could have appeared to influence the work reported in this paper.

Acknowledgements

The research for this paper was performed within the projects ‘START’ and ‘Ariadne’ supported by the German Federal Ministry of Education and Research under grant numbers 03EK3046D and 03SFK5B0. The authors thank Stefan Kronshage for his contributions to the demand scenario data, Hedda Gardian for her support in the modelling activities, and all current and former members of the Energy Systems Modelling group of DLR for their continuous contribution to the model input data.

References

[1] European Commission, A hydrogen strategy for a climate-neutral Europe, 2020, URL https://eur-lex.europa.eu/legal-content/EN/TXT/?uri=CELEX:52020DC0301.

[2] European Commission, A Clean Planet for all – A European long-term strategic vision for a prosperous, modern, competitive and climate neutral economy: In-Depth Analysis, 2018.

[3] European Commission, Clean energy for all Europeans, 2019.

[4] Kirsten Westphal, Strategic Sovereignty in Energy Affairs: Reflections on Germany and the EU’s Ability to Act, 2021, http://dx.doi.org/10.18449/2021C07.

[5] Daniel Scholten, Rick Bosman, The geopolitics of renewables; exploring the political implications of renewable energy systems, Technol. Forecast. Soc. Change (ISSN: 00401625) 103 (2016) 273–283, http://dx.doi.org/10.1016/j.techfore.2015.10.014.

[6] Tim Tröndle, Stefan Pfenninger, Johan Lilliestam, Home-made or imported: On the possibility for renewable electricity autarky on all scales in europe, Energy Strategy Rev. (ISSN: 2211467X) 26 (2019) 100388, http://dx.doi.org/10.1016/j.esr.2019.100388.

[7] Philipp Hauser, Does ‘more’ equal ‘better’? – Analyzing the impact of diversification strategies on infrastructure in the European gas market, Energy Policy (ISSN: 03014215) 153 (2021) 112232, http://dx.doi.org/10.1016/j.enpol.2021.112232.

[8] Felix Frischmuth, Philipp Härtel, Hydrogen sourcing strategies and cross-sectoral flexibility trade-offs in net-neutral energy scenarios for Europe, Energy (ISSN: 03605442) 238 (2022) 121598, http://dx.doi.org/10.1016/j.energy.2021.121598.

[9] Hans Christian Gils, Hedda Gardian, Jens Schmugge, Interaction of hydrogen infrastructures with other sector coupling options towards a zero-emission energy system in Germany, Renew. Energy (ISSN: 09601481) 180 (2021) 140–156, http://dx.doi.org/10.1016/j.renene.2021.08.016.

[10] Michael Child, Claudia Kemfert, Dmitrii Bogdanov, Christian Breyer, Flexible electricity generation, grid exchange and storage for the transition to a 100% renewable energy system in Europe, Renew. Energy (ISSN: 09601481) 139 (2019) 80–101, http://dx.doi.org/10.1016/j.renene.2019.02.077.

[11] Emma Hanley, Paul Deane, Brian Ó Gallachóir, The role of hydrogen in low carbon energy futures – A review of existing perspectives, Renew. Sustain. Energy Rev. (ISSN: 13640321) 82 (2018) 3027–3045, http://dx.doi.org/10.1016/j.rser.2017.10.034.

[12] Paul Deane, Maitiú Ó Ciaráin, Brian Ó Gallachóir, An integrated gas and electricity model of the EU energy system to examine supply interruptions, Appl. Energy (ISSN: 03062619) 193 (2017) 479–490, http://dx.doi.org/10.1016/j.apenergy.2017.02.039.

[13] Joseph Devlin, Kang Li, Paraic Higgins, Aoife Foley, A multi vector energy analysis for interconnected power and gas systems, Appl. Energy (ISSN: 03062619) 192 (2017) 315–328, http://dx.doi.org/10.1016/j.apenergy.2016.08.040.

[14] Jakob Wachsmuth, Ali Aydemir, Henning Döscher, Johannes Eckstein, Witold-Roger Poganietz, Davi Ezequiel François, Dirk Scheer, The Potential of Hydrogen for Decarbonising EU Industry, Technical report.

[15] Jachin Gorre, Felix Ortloff, Charlotte van Leeuwen, Production costs for synthetic methane in 2030 and 2050 of an optimized Power-to-Gas plant with intermediate hydrogen storage, Appl. Energy (ISSN: 03062619) 253 (2019) 113594, http://dx.doi.org/10.1016/j.apenergy.2019.113594.

[16] Matteo Di Salvo, Max Wei, Synthesis of natural gas from thermochemical and power-to-gas pathways for industrial sector decarbonization in California, Energy (ISSN: 03605442) 182 (2019) 1250–1264, http://dx.doi.org/10.1016/j.energy.2019.04.212.

[17] Mokhtar Benasla, Denis Hess, Tayeb Allaoui, Mostefa Brahami, Mouloud Denaï, The transition towards a sustainable energy system in Europe: What role can North Africa's solar resources play? Energy Strategy Rev. (ISSN: 2211467X) 24 (2019) 1–13, http://dx.doi.org/10.1016/j.esr.2019.01.007.

[18] TYNDP 2022 Scenario Report - Electricity modelling results, 2021, URL https://2022.entsos-tyndp-scenarios.eu/wp-content/uploads/2022/04/220310_Updated_Electricity_Modelling_Results.xlsx.

[19] Abdulrahman Alassi, Santiago Bañales, Omar Ellabban, Grain Adam, Callum MacIver, HVDC transmission: Technology review, market trends and future outlook, Renew. Sustain. Energy Rev. (ISSN: 13640321) 112 (2019) 530–554, http://dx.doi.org/10.1016/j.rser.2019.04.062.

[20] Hans Christian Gils, Yvonne Scholz, Thomas Pregger, Diego Luca de Tena, Dominik Heide, Integrated modelling of variable renewable energy-based power supply in Europe, Energy (ISSN: 03605442) 123 (2017) 173–188, http://dx.doi.org/10.1016/j.energy.2017.01.115.

[21] Kenneth Bruninx, Dragana Orlic, Dries Couckuyt, Nathalie Grisey, Brahim Betraoui, Niels Traeholt Franck, Gary Keane, Benjamin Hickman, Daniel Huertas-Hernando, Thomas Anderski, et al., e-Highway2050: D2. 1 Data Sets of Scenarios for 2050, Technical report, 2014.

[22] Mahdi Fasihi, Olga Efimova, Christian Breyer, Techno-economic assessment of CO2 direct air capture plants, J. Clean. Prod. (ISSN: 09596526) 224 (2019) 957–980, http://dx.doi.org/10.1016/j.jclepro.2019.03.086.

[23] Fabian Gotzens, Heidi Heinrichs, Jonas Hörsch, Fabian Hofmann, Performing energy modelling exercises in a transparent way – The issue of data quality in power plant databases, Energy Strategy Rev. (ISSN: 2211467X) 23 (2019) 1–12, http://dx.doi.org/10.1016/j.esr.2018.11.004.

[24] Bundesnetzagentur, Kraftwerksliste der Bundesnetzagentur, URL https://www.bundesnetzagentur.de/Kraftwerksliste.

[25] ENTSO-E: TYNDP 2016 – Market modelling data, 2016, URL https://www.entsoe.eu/Documents/TYNDP%20documents/TYNDP%202016/rgips/TYNDP2016%20market%20modelling%20data.xlsx.

[26] Gas Infrastructure Europe, Storage database, 2016, URL https://www.gie.eu/transparency/databases/storage-database/.

[27] ENTSO-G: TYNDP – Market modelling data, 2019, URL https://www.entsog.eu/maps#transmission-capacity-map-2019.

[28] Hans Christian Gils, Hedda Gardian, Thomas Pregger, Johannes Schaffert, Eren Tali, Max Fette, Christine Brandstätt, REMix model input data for the THG95/GHG95 scenario analysed within the MuSeKo project, 2021, URL https://doi.org/10.5281/zenodo.5705414, This dataset was created within the project 'MuSeKo' supported by the German Federal Ministry of Economic Affairs and Energy under grant number 03ET4038.

[29] Guidehouse, European Hydogen Backbone: Analysing Future Demand, Supply and Transport of Hydrogen, Technical report, 2021.

[30] Shima Sasanpour, Karl-Kiên Cao, Hans Christian Gils, Patrick Jochem, Strategic policy targets and the contribution of hydrogen in a 100% renewable European power system, Energy Rep. (ISSN: 23524847) 7 (2021) 4595–4608, http://dx.doi.org/10.1016/j.egyr.2021.07.005.

[31] David Schlachtberger, Tom Brown, Stefan Schramm, Martin Greiner, The benefits of cooperation in a highly renewable European electricity network, Energy (ISSN: 03605442) 134 (2017) 469–481, http://dx.doi.org/10.1016/j.energy.2017.06.004.

[32] Tom Brown, Tobias Bischof-Niemz, Kornelis Blok, Christian Breyer, Henrik Lund, Brian Vad Mathiesen, Response to 'Burden of proof: A comprehensive review of the feasibility of 100% renewable-electricity systems', Renew. Sustain. Energy Rev. (ISSN: 13640321) 92 (2018) 834–847, http://dx.doi.org/10.1016/j.rser.2018.04.113.

[33] Martha Maria Frysztacki, Jonas Hörsch, Veit Hagenmeyer, Tom Brown, The strong effect of network resolution on electricity system models with high shares of wind and solar, Appl. Energy (ISSN: 03062619) 291 (2021) 116726, http://dx.doi.org/10.1016/j.apenergy.2021.116726.

[34] Leander Kotzur, Peter Markewitz, Martin Robinius, Detlef Stolten, Impact of different time series aggregation methods on optimal energy system design, Renew. Energy (ISSN: 09601481) 117 (2018) 474–487, http://dx.doi.org/10.1016/j.renene.2017.10.017.

[35] Franziska Holz, Tim Scherwath, Pedro Del Crespo Granado, Christian Skar, Luis Olmos, Quentin Ploussard, Andrés Ramos, Andrea Herbst, A 2050 perspective on the role for carbon capture and storage in the European power system and industry sector, Energy Econ. (ISSN: 01409883) 104 (2021) 105631, http://dx.doi.org/10.1016/j.eneco.2021.105631.

[36] Giulia Realmonte, Laurent Drouet, Ajay Gambhir, James Glynn, Adam Hawkes, Alexandre C. Köberle, Massimo Tavoni, An inter-model assessment of the role of direct air capture in deep mitigation pathways, Nature Commun. 10 (1) (2019) 3277, http://dx.doi.org/10.1038/s41467-019-10842-5.

[37] Noah McQueen, Katherine Vaz Gomes, Colin McCormick, Katherine Blumanthal, Maxwell Pisciotta, Jennifer Wilcox, A review of direct air capture (DAC): scaling up commercial technologies and innovating for the future, Prog. Energy 3 (3) (2021) 032001, http://dx.doi.org/10.1088/2516-1083/abf1ce.

Publication 2: Understanding the performance impact of a massively parallel solver for energy system optimization models – a computational experiment using the PIPS-IPM++ solver for REMix instances

Authors: Manuel Wetzel, Karl-Kiên Cao, Shima Sasanpour

Published in: Sustainable Energy, Grids and Networks 44, 2025, doi: 10.1016/j. segan.2025.101893

Methodological advancements: This publication provides the first formalised approach to identifying suitable decomposition strategies for applying massively parallel solvers to ESOMs, and quantitatively evaluates the relationship between the size of the overall problem and the number of capacity expansion decisions on solver performance. This is demonstrated using an example application of the REMix model, which further improves the understanding of the underlying complexity of ESOMs and the necessary considerations for applying massively parallel solvers. The methodological contributions include generic annotation and decomposition of models based on contained variables and equations, and hardware considerations to optimise computation allocation on HPC clusters, as well as considerations to optimise solver performance in terms of either shortest time to solve or least computational resources. Furthermore, it outlines the potential transferability to other model frameworks, ensuring the method can be applied to similarly structured energy system optimisation problems.

Key findings: Several key findings emerge from the systematic comparison of the performance of ESOMs. Firstly, the number of capacity expansion decisions and the size of the optimisation problem overall are key drivers of the time taken to solve the problem and the overall computational burden. In particular, a large number of expansion decisions will lead to prohibitively long optimisation times, while problems involving few expansion decisions will more likely be limited by available memory. Secondly, the qualitative difference between capacity expansion and economic dispatch models requires different considerations for configuring the massively parallel solver: economic dispatch models benefit from a larger number of blocks, whereas capacity expansion problems require a limited number of blocks. Thirdly, a direct comparison of state-of-the-art interior-point methods with massively parallel solvers reveals that the latter can reduce the time taken to solve by a factor of ten. As this reduction in time can be observed throughout the different model instances, the largest savings can be achieved with large, complex models such as those used to compute transformation pathways.

Author contributions: Manuel Wetzel is the main author of this work. He implemented the annotation logic into the REMix framework, generated the model instances, ran the computational experiments

on the JUWELS HPC cluster, evaluated and visualised the results, and drafted the first version of the manuscript. Karl-Kiên Cao provided the underlying dataset for the REMix model instances and the different levels of spatial aggregation, based on a previous study, while Shima Sasanpour assisted particularly with the formalisation of the decomposition strategy. The authors jointly revised the manuscript throughout various iterations. Furthermore, Thomas Breuer assisted with the compilation of PIPS-IPM++ and additional dependencies, and Nils-Christian Kempke provided valuable advice on configuration and error resolution. They are both acknowledged in the publication for their work.

Contents lists available at ScienceDirect

Sustainable Energy, Grids and Networks

journal homepage: www.elsevier.com/locate/segan

Understanding the performance impact of a massively parallel solver for energy system optimization models – a computational experiment using the PIPS-IPM++ solver for REMix instances

Manuel Wetzel*, Karl-Kiên Cao, Shima Sasanpour

German Aerospace Center (DLR), Institute of Networked Energy Systems, Stuttgart, Germany

HIGHLIGHTS

- Systematic application of the massively parallel solver PIPS-IPM++ to large-scale capacity expansion problems from the REMix framework reducing the time to solve by about one order of magnitude.
- Identification of the total number of capacity expansion decisions as the primary driver of the computational burden in linear ESOM instances.
- Generation of insights into the optimal decomposition strategy and configuration of PIPS-IPM++ depending on the problem instance to be solved.
- Enable researchers to leverage massively parallel solver on high-performance computing infrastructure, avoid limitations from shared memory, and allow for larger optimization models.

ARTICLE INFO

Keywords:
Energy system analysis
Capacity expansion planning
High performance computing
Linear programming
Massively parallel solvers
Decomposition strategies

ABSTRACT

The complexity in the design of future integrated energy systems is reflected in the modeling tools used to analyze the interactions and synergies between energy technologies. As real-world systems become more interconnected, the complexity of model representations increases, resulting in a greater computational burden to obtain optimal solutions. Several approaches can address this challenge, including making trade-offs between model dimensions, using methods to reduce complexity, performing mathematical decomposition, and applying massively parallel solvers. While most of these approaches have been extensively studied, the application of massively parallel solvers has barely been explored due to their novelty. The main advantage of this approach is that it is well-suited to take advantage of modern high-performance computing infrastructure. Therefore, a more systematic evaluation of the types of model instances and decomposition strategies that can benefit from massively parallel solvers remains necessary. In this study, we identify capacity expansion decisions as the primary driver of computational complexity, particularly within the REMix framework, and demonstrate how to effectively leverage the underlying problem structure of these models. In a computational experiment we evaluate the performance of PIPS-IPM++ against a state-of-the-art interior-point solver. The results show a significant reduction in the total required wall-clock time of about one order of magnitude, as well as a reduction in required computational resources. Our findings provide modelers with the necessary methods and capabilities to solve previously intractable, large-scale problems, thereby increasing the level of detail and explanatory power of energy system optimization models.

1. Introduction

Energy system optimization models (ESOMs) have become widely used tools to gain insight into the interactions between energy technologies and flexibility options in future energy systems. However, accurate modeling of these systems requires a sufficient temporal and spatial resolution to capture the variability of renewable energy sources [1], transmission bottlenecks [2] and need for electrical energy storage expansion [3]. Hence, contemporary large-scale ESOMs translate into mathematical optimization problems involving up to hundreds of millions of variables and constraints, resulting in a high computational

* Corresponding author at: Curiestraße 4, 70563 Stuttgart, Germany.
Email addresses: manuel.wetzel@dlr.de (M. Wetzel), karl-kien.cao@dlr.de (K.-K. Cao), shima.sasanpour@dlr.de (S. Sasanpour).

https://doi.org/10.1016/j.segan.2025.101893
Received 29 January 2025; Received in revised form 23 June 2025; Accepted 1 August 2025

List of abbreviations

AC	alternating current
AC-OPF	alternating current optimal power flow
ESOM	energy system optimization model
FLOP	floating point operation
GPU	graphics processing unit
HPC	high-performance computing
IP	interior-point
IAM	integrated assessment model
JSC	Jülich Supercomputing Centre
LP	linear programming
MILP	mixed-integer linear programming
NUMA	non-uniform memory access
RAM	random access memory
UC	unit commitment
VRE	variable renewable energy

burden. This computational burden is evident in the fact that most modelers opt for clustering and aggregation techniques in either the spatial or temporal resolution [4] as well as the large field of research to systematically improve complexity reduction techniques [5]. The maximum size of ESOMs that can still be solved in a reasonable time frame is mainly determined by the performance of the utilized algorithm and the available hardware. This combination gives an overall threshold, which determines the maximum computational complexity that can still be addressed. However, this reasonable time frame is subjective for each modeler and depends on additional factors like the overall number of runs for a given analysis [6]. For an individual optimization run, there are various approaches that affect the computational burden – trade-offs between model dimensions, aggregation techniques and heuristics, mathematical decomposition, and application of massively parallel solvers. We start by discussing the different influences each of these approaches has on the computational burden and drawbacks that need to be considered by the modeler.

Trade-offs between model dimensions allow one dimension's level of detail to increase at the expense of another dimension's level of detail. For example, simple aggregation techniques can be used to achieve this goal [7]. When using state-of-the-art interior-point (IP) solvers, such shifts allow focusing on a specific aspect of the model while staying within the threshold for computational complexity. More specialized heuristics allow more efficient trade-offs through intelligent reductions in model dimensions [5]. However, like the trade-offs, this approach is also subject to the same overall computational threshold imposed by the available algorithms and hardware. In contrast to the aforementioned approaches, mathematical decomposition allows the computational threshold to be increased by iteratively solving multiple smaller subproblems [8]. Similarly, massively parallel solvers exploit a fundamental block structure of the optimization matrix. This also effectively results in the iterative solving of subproblems but has the advantage that no explicit reformulation of the model logic is required. Both mathematical decomposition and massively parallel solvers can be deployed to distributed memory architectures, enabling the efficient use of high-performance computing (HPC) infrastructure.

1.1. The increasing complexity of ESOMs

Energy system modeling has been widely used to inform policy makers about decisions for a successful energy system transition [9]. The fundamental challenge of decarbonizing energy systems lies in integrating renewable energy resources while ensuring an affordable, secure and sustainable energy supply. All three aspects can be modeled using ESOMs, which enable capacity expansion planning and economic dispatch to be integrated into a single optimization problem [10]. While this integration of capacity expansion planning significantly increases computational complexity [11], it also offers the most valuable insights for planning the energy transition.

One of the most prevalent challenges in modeling large-scale energy systems is the trade-off between two fundamental requirements – maintaining a comprehensive system perspective while at the same time providing a sufficient level of detail. This level of detail can affect either the spatial, the temporal or the technological resolution of the model [4]. Reducing the spatial resolution, for example, can affect the preservation of critical bottlenecks in the network topology, such as high-voltage transmission lines. Consequently, the model may produce overly optimistic solutions. Conversely, increasing the spatial resolution increases computational complexity and potentially leads to time constraints for real-time applications, such as market clearing or network redispatch. There are a large number of different approaches and various degrees of complexity for different formulations of optimization models, but all of them are constrained by the limitation of computational complexity when applying standard IP solvers [8].

Several crucial factors must be considered for future energy systems, requiring a minimum level of detail to be addressed by the ESOM across the different dimensions. In terms of the temporal dimension the correct representation of the availability of variable renewable energy (VRE) sources plays a fundamental role in future energy systems [1]. Due to their variability, hourly and sub-hourly resolutions are required to accurately estimate the need for additional flexibility options, such as transmission networks and storage technologies. Consequently, many ESOMs discretize the temporal dimension of the model into hourly time steps [12].

Similarly, exploring transformation pathways requires the integral consideration of long-term time horizons. For example, this enables the endogenous modeling of optimal CO_2 budget allocation or the inclusion of learning rates for energy technologies [13]. Therefore, a fundamental design choice for ESOMs is whether to include transformation pathways as multi-year optimizations or to use (successive) single-year optimizations. While single-year optimization models focus on the hourly interactions of technologies providing system flexibility, multi-year models typically use representative time slices [8].

At a spatial level, the increasing number of distributed generators and new power consumers requires more accurate modeling of power flows. This modeling must bridge the gap between modeling grid congestion at a regional level and accounting for long-distance energy transmission due to the spatial balancing effects of renewable energy sources [14]. This requires a broad geographical scope, detailed spatial resolution, and accurate representation of network losses, in order to adequately assess energy transmission and identify the need for network expansion [15].

In terms of energy technologies, the expansion of the modeled system is driven by the coupling of energy sectors to decarbonize the heating and transport sectors, primarily through electrification or the provision of synthetic fuels based on renewable energy sources [16]. This introduces a wide range of new technologies and energy vectors to be additionally considered in ESOMs. Similarly, considering hydrogen blending in natural gas pipelines [17] or hydrogen offshore hubs [18] further increases the complexity of capacity expansion decisions in ESOMs.

While reducing the spatial and temporal resolution can often be achieved with limited loss of detail, introducing more sectors and technologies can significantly impact the design of the overall energy system. However, there is still the possibility of aggregating similar technologies [19].

1.2. Heuristics and complexity reduction

As a consequence of this growing complexity in all three dimensions, the size of the model in terms of variables and constraints, as well as the time required to solve it, increases. Many approaches to dealing with the resulting computational limitations can be summarized as heuristics. In this context, heuristics aim to provide either simplifications across one or more dimensions, or multi-stage approaches, where an initial approximation is performed at a low resolution, followed by a consecutive run at a higher resolution. This trade-off between modeling capacity expansion pathways and ensuring a high temporal resolution can be addressed by running two models sequentially. For instance, in Gerbaulet et al. [20], first the capacity expansion is modeled using a low temporal resolution to estimate the overall energy system design. Then, the system's operations are validated by conducting an hourly economic dispatch of power plants at a high temporal resolution.

For models with an hourly resolution in particular, the time dimension is one of the main drivers of complexity and therefore typically the first dimension to be addressed using complexity reduction. This involves reducing the temporal dimension sufficiently (e.g., by identifying representative time periods or merging consecutive hours), while preserving critical information from the input data with an hourly resolution. Kotzur et al. evaluate the impact of several time series aggregation techniques on energy system design (by comparing the resulting objective values) and computational times compared to an ESOM using the full time series data [21]. They conclude that the choice of a specific algorithm does not have a significant impact on the accuracy of a model. However, the authors emphasize that the approaches studied are not recommended for modeling energy systems that rely heavily on energy storage. This finding is also confirmed by Buchholz et al., who use complexity reduction approaches that do not explicitly consider long-term energy storage [22]. The authors point out that investments in flexibility options and thus total system costs are systematically underestimated. Raventos et al. study two different time series aggregation techniques, reporting that chronological clustering better accounts for the operational patterns of energy storage [23].

Similar findings apply to the spatial scale. In a previous study, we demonstrated how such reductions can lead to an underestimation of the share of investment costs for transmission investments, as well as a shifts towards electricity generation with low marginal costs [4]. Although spatial reduction techniques are state-of-the-art in power systems engineering, where network equivalents are used to simplify areas around the study area (i.e., the area of responsibility of a network operator) [24], such approaches are of limited value for ESOMs, which often do not focus on a specific distribution network. The key challenge, therefore, is to define clusters that can be treated as interconnected regions with no internal bottlenecks. Therefore, network clustering approaches are usually used to identify the transmission lines that are most important to maintain in a reduced network representation [25].

In summary, heuristics that aim to reduce the complexity of ESOMs, particularly with regard to the temporal scale, have the potential to significantly reduce computational effort while providing results that are sufficient for specific use cases. Buchholz et al. report reductions in computation time of up to 98 % when ignoring long-term energy storage options [22]. However, systematic evaluations in the literature have mainly been performed with comparatively small ESOMs, since two conditions must be met for such studies. Firstly, a full-scale model must be solved as a benchmark for the complexity reduction method. Secondly, tuning the algorithm and demonstrating scaling effects require a sufficiently large number of runs. To ensure that an algorithm's performance is comparable to the reference solution, these studies must be performed on identical hardware. Therefore, the cumulative computation time for an appropriate benchmark study remains an issue, particularly for systematic studies involving large-scale models [26]. For a broader overview of the various methods of reducing the complexity of energy system models, the reader is referred to [5].

1.3. State of running ESOMs on HPCs

All of the approaches presented so far use single-node, shared-memory architectures to solve the optimization problem. Historically, this approach has worked quite well since available hardware has mainly offered speed increases based on processor clock rates. However, this trend shifted in the early 2000s with the introduction of multi-core processors.[1] Consequently, algorithms had to utilize multi-core architectures to enhance performance. Further scaling of computing resources was achieved by switching from single-node to multi-node computing clusters. This utilization of multiple cores across one or multiple compute nodes can be classified as either parallelization on shared memory architectures (e.g., via OpenMP, Open Multi-Processing, a standard interface for parallel computing on shared memory, multi-core architectures) and parallelization across distributed memory architectures, also referred to as distributed computing (e.g., via MPI, Message Passing Interface, a standard interface for coordinating processes across distributed memory, multi-node architectures). On distributed computing architectures, modelers take advantage of the large number of identical processors for parallel computing, but at the cost of requiring algorithms that are able to utilize the distributed memory. While distributed computing is a quite broad term, modern HPC clusters additionally provide fast communication networks and data storage.

Even without parallel software, HPC can still be used to scale up the optimization of multiple independent model instances in an *embarrassingly parallel* workflow. While this approach is useful for analyzing a broad scenario space, individual model instances still must fit within the hardware limitations of a single compute node. For instance, Sharma et al. [27] perform benchmark analyses with models of the TIMES family [28] and study optimal strategies to allocate multiple independent model instances across compute nodes. The authors also highlight advantages of applying HPC-typical software, such as workload management tools, to perform multiple parameter variations and solve a set of scenarios.

However, solving an ESOM that exceeds the memory capacity of a single compute node requires decomposing the optimization problem into a set of subproblems. Accordingly, such applications must handle the additional communication overhead between subproblems. Various approaches have been presented for operations scheduling [29], often using well-known mathematical decomposition strategies such as Benders decomposition [30] or Dantzig–Wolfe decomposition [31]. Gong et al. use an Augmented Lagrangian Relaxation applied to a combined unit commitment (UC), optimal power flow, and transmission switching problem [32]. They also decompose a coordinated operations planning problem for the gas and electricity sectors in this manner [33]. Göke et al. apply Benders Decomposition to a stochastic two-stage energy system optimization problem where additional enhancement strategies are used to improve the performance of the algorithm [34]. Similarly, to improve the parallelization of Benders Decomposition, Pecci et al. decompose the subproblems along the temporal dimension [35].

In the special case of two-stage stochastic optimization the communication overhead is minimal, making such problems early candidates for the application of HPC. One of the main advantages of stochastic optimization problems is their fundamental structure: the objective is to identify a set of decisions applicable to a broad range of uncertain boundary conditions. If a different solution is allowed for each boundary condition, solving the entire optimization problem is equivalent to solving multiple small optimization problems. The goal, however, is to find a single solution that applies to all problems, so the decision variables span across multiple stochastic scenarios. These variables link the problem structure, preventing the solution of parts individually. Therefore, they are referred to as "linking" or "complicating" variables. Linking

[1] https://github.com/karlrupp/microprocessor-trend-data

variables automatically emerge when the entire problem is decomposed in a particular way.

In terms of application, Papavasiliou et al. decompose a short-term UC problem with a time horizon of 24 hours by Lagrangian relaxation and solve 1,000 independent stochastic scenarios [36]. The authors report reducing the computation time from 120 hours down to 17.5 hours by exploiting the parallelization potential of 1000 processors. In a more recent study Ávila et al. [37] introduce a stochastic optimization problem for transmission system expansion in the European electricity network combining two different decomposition approaches based on the L-shaped method, and bring it to HPC. In contrast to classical decomposition techniques, Lubin et al. present a novel massively parallel interior point solver, PIPS-IPM, which decomposes the stochastic optimization problem along the scenario dimension [38]. This solver is used by Petra et al. to determine the optimal dispatch of power plants in the federal state of Illinois to adequately reflect the probability distribution for electricity generation from wind turbines [39]. The major advantage of these approaches is their scalability, which is one of the most important aspects for distributed memory architectures. Similar scalability was demonstrated by Wang et al. [40], who presented the HiOP solver for addressing nonlinear stochastic optimization problems. This solver was used in one of the first successful attempts at exascale computing with a large number of graphics processing units (GPUs) in the field of power system analysis. More recently, Shin et al. [41] and Swirydowicz [42] both applied massively parallel solvers on GPUs for the optimization of large-scale nonlinear alternating current optimal power flow (AC-OPF) problems. Also outside the field of optimization, novel approaches addressing the increasing complexity of transmission expansion planning are emerging, using convolutional neural networks [43].

However, most of the previously mentioned approaches require either a limited number of linking variables or a limited number of linking constraints for the decomposition of the mathematical formulation. To solve a more generalized type of optimization problem that includes both linking variables and constraints, Rehfeldt et al. [44] extended the PIPS-IPM solver by Lubin et al. to handle both types. For various model instances, they report a speedup factor of up to 67 compared to the best standard IP solver. However, the instances addressed in the study are based on very stylized energy system models and real-world systems for pure economic dispatch models. The authors stress the need to further investigate the solver's performance with model instances showing stronger interconnection between individual subproblems. Similarly, Panos and Hassan apply PIPS-IPM++ to the TIMES model family for two instances and observe a speedup of 4 compared to a standard IP solver [45]. This wide range already indicates a strong connection between the types of optimization problems and the potential for speedups, and a lack of understanding of decomposition approaches and their resulting performance. To date, the PIPS-IPM++ solver has also not yet been applied to large-scale hourly resolved ESOMs, which include a large number of capacity expansion decisions.

1.4. Towards a systematic understanding of computational performance in ESOMs

In summary, solving large-scale ESOMs, which comprise a multitude of capacity expansion decisions is one of the most challenging aspects of outlining pathways for the energy transition. The models aim to identify potential investment opportunities in generation, storage and transmission capacities. This in turn requires methods that can efficiently handle both linking variables and linking constraints. Although several heuristics have been applied to reduce the problem size overall, these heuristics either lead to information loss or require highly model-specific tuning, and they are usually not generalizable. Massively parallel solvers have proven useful in bringing ESOMs to HPC and avoiding hardware limitations. However, their use has been limited to models with a small number of coupling elements. Here, PIPS-IPM++ presents an option to accelerate or even enable the solution of large-scale ESOMs that combine both operational and capacity expansion planning. To better understand the types of problems for which the PIPS-IPM++ solver can be effectively applied, we present its first application to a broad set of model instances to study the overall scaling behavior using real-world instances involving a large number of investment decisions. Thus, our study raises the general question of whether we can obtain similar benefits from applying PIPS-IPM++ to capacity expansion problems and provides the following contributions:

1. We analyze the underlying problem structure for a scalable REMix model instance with varying degrees of capacity expansion planning and economic dispatch, and assess the impact of its complexity on the time and memory needed to solve the problem.
2. We outline the methodological steps that enable modelers to decompose generic ESOMs and solve them using PIPS-IPM++ on distributed memory hardware. To this end, we discuss how different decomposition strategies impact linking elements and the potentially achievable parallelization.
3. We perform a systematic computational experiment on various scalable model instances derived from the REMix framework to compare the performance of PIPS-IPM++ against a state-of-the-art standard IP solver with respect to obtainable solving time speedup, memory reduction, and scaling behavior.

2. Methods

Our research is fundamentally based on a computational experiment. In Sections 2.1 and 2.2, we first present the REMix framework used in this study as well as the parallel solver PIPS-IPM++. Section 2.3 then outlines the necessary block structures, while Section 2.4 presents a systematic approach for the implementation of the decomposition. Section 2.5 then provides a model-specific example and highlights different decomposition strategies for ESOMs.

2.1. The REMix framework

REMix is an open-source framework for energy system optimization modeling.[2] It optimizes the expansion and operation of the energy system from a central planner's perspective with perfect foresight by minimizing the total system costs. The framework consists of a few generalized modules that can represent various technologies across multiple sectors. For most applications, one target year with hourly resolution is formulated as linear programming (LP). However, more advanced features are available such as mixed-integer linear programming (MILP) for UC and investment planning, Pareto fronts, myopic and pathway optimization [46]. Examples of different use-cases of the REMix framework have been published in previous studies [47,48].

As discussed in Section 1.1 from an abstract perspective, REMix is likewise structured in various model dimensions:

$t \in T$	time steps
$y \in Y$	year intervals
$n \in N$	model nodes
$l \in L$	transfer links
$z \in Z$	network cycles
$q \in Q$	energy carriers
$a \in A$	converter activities

[2] https://dlr-ve.gitlab.io/esy/remix/framework

$p \in P$ technologies

$P_C \subset P$ converter technologies

$P_S \subset P$ storage technologies

$P_L \subset P$ transfer technologies

$i \in I$ system indicators

$I_{obj} \subset I$ indicator declared as objective function

The main model variables can be divided into two categories: capacity expansion decisions, which relate to infrastructure investment decisions, and dispatch decisions, which describe how available infrastructure is utilized throughout the year:

$x \geq 0$ number of available units / links

$\Delta x^+ \geq 0$ units / links expanded

$\Delta x^- \geq 0$ units / links decommissioned

$d \geq 0$ dispatch of converter

$e \geq 0$ level of storage

$f^+ \geq 0$ flow along transfer link

$f^- \geq 0$ flow against transfer link

$g^+ \geq 0$ import of energy carriers

$g^- \geq 0$ export of energy carriers

j accounting indicator

Several additional parameters are needed to describe various characteristics of different technologies and the connectivity between transfer links and model regions:

D rated dispatch coefficients

E rated storage coefficients

F rated transfer coefficients

H rated transfer loss coefficients

M incidence matrix between transfer links and model regions

K minimum cycle basis matrix between transfer links and network cycles

J indicator coefficient matrix

V activity matrix for converter technologies

W weighting factor between year intervals

α availability factor

γ loss adjusted transfer correction factor

δ self-discharge rate of storage

λ technical lifetime

χ link-specific reactance

To define an objective function for optimization, various system indicators can be used, which are linked to both the capacity expansion and economic dispatch parts of the model. These indicators can be subdivided into those referring to individual years and those integrating results across multiple years, the latter of which is controlled by the weighting factor W for individual year intervals. Additional bounds can be defined for indicators that are not defined as the objective function to enforce system constraints, such as a limit on carbon emissions.

$$\min j_i \qquad \forall i \in I_{obj} \tag{1}$$

s.t.

$$\underline{j}_i \leq j_i \leq \overline{j}_i \qquad \forall i \in I \setminus I_{obj} \tag{2}$$

$$j_i = \sum_{y \in Y} W_{y,i} \cdot \Bigg(\sum_{n \in N, p \in P_C \cup P_S} J^{\text{build}}_{i,n,y,p} \cdot \Delta x^+_{n,y,p} + J^{\text{fix}}_{i,n,y,p} \cdot x_{n,y,p} + J^{\text{decom}}_{i,n,y,p} \cdot \Delta x^-_{n,y,p} \tag{3a}$$

$$+ \sum_{l \in L, p \in P_L} J^{\text{build}}_{i,l,y,p} \cdot \Delta x^+_{l,y,p} + J^{\text{fix}}_{i,l,y,p} \cdot x_{l,y,p} + J^{\text{decom}}_{i,l,y,p} \cdot \Delta x^-_{l,y,p} \tag{3b}$$

$$+ \sum_{t \in T, n \in N, p \in P_C, a \in A} J^{\text{var}}_{i,t,n,y,p,a} \cdot d_{t,n,y,p,a} \tag{3c}$$

$$+ \sum_{t \in T, l \in L, p \in P_L} J^{\text{flow}}_{i,t,l,y,p} \cdot \left(f^+_{t,l,y,p,q} + f^-_{t,l,y,p,q} \right) \tag{3d}$$

$$+ \sum_{t \in T, n \in N, q \in Q} J^{\text{import}}_{i,t,n,y,q} \cdot g^+_{t,n,y,q} + J^{\text{export}}_{i,t,n,y,q} \cdot g^-_{t,n,y,q} \Bigg) \qquad \forall i \in I \tag{3e}$$

The capacity expansion model of REMix can be described using the lower and upper bounds of the converter and storage units and of the transfer links,

$$\underline{x}_{n,y,p} \leq x_{n,y,p} \leq \overline{x}_{n,y,p} \qquad \forall n \in N, y \in Y, p \in P_C \cup P_S \tag{4}$$

$$\underline{x}_{l,y,p} \leq x_{l,y,p} \leq \overline{x}_{l,y,p} \qquad \forall l \in L, y \in Y, p \in P_L \tag{5}$$

the continuity equation considering existing units from the previous year's intervals and changes in the number of units due to new investment and decommissioning decisions,

$$x_{n,y,p} = x_{n,y-1,p} + \Delta x^+_{n,y,p} - \Delta x^-_{n,y,v} \qquad \forall n \in N, y \in Y, p \in P_C \cup P_S \tag{6}$$

$$x_{l,y,p} = x_{l,y-1,p} + \Delta x^+_{l,y,p} - \Delta x^-_{l,y,p} \qquad \forall l \in L, y \in Y, p \in P_L \tag{7}$$

and the equations enforcing the decommissioning of units and links after the end of their respective lifetime λ:

$$\sum_{y' \leq y - \lambda_v} \Delta x^+_{n,y',p} \leq \sum_{y' \leq y} \Delta x^-_{n,y',p} \qquad \forall n \in N, y \in Y, p \in P_C \cup P_S \tag{8}$$

$$\sum_{y' \leq y - \lambda_l} \Delta x^+_{l,y',p} \leq \sum_{y' \leq y} \Delta x^-_{l,y',p} \qquad \forall l \in L, y \in Y, p \in P_L \tag{9}$$

The number of available units limits the dispatch of different activities for converters,

$$\sum_{a \in A} d_{t,n,y,p,a} \leq V_{p,a} \cdot \alpha_{t,n,y,p} \cdot x_{n,y,p} \qquad \forall t \in T, y \in Y, n \in N, p \in P_C \tag{10}$$

the maximum level of storage reservoirs,

$$e_{t,n,y,p} \leq \alpha_{t,n,y,p} \cdot x_{n,y,p} \qquad \forall t \in T, y \in Y, n \in N, p \in P_S \tag{11}$$

and the flows of energy carriers throughout the network:

$$f^+_{t,l,y,p} \leq \alpha_{t,l,y,p} \cdot \gamma_{l,p} \cdot x_{l,y,p} \qquad \forall t \in T, y \in Y, l \in L, p \in P_L \tag{12}$$

$$f^-_{t,l,y,p} \leq \alpha_{t,l,y,p} \cdot \gamma_{l,p} \cdot x_{l,y,p} \qquad \forall t \in T, y \in Y, l \in L, p \in P_L \tag{13}$$

In addition to the flow constraints based on the network capacity, a direct current optimal power flow (DC-OPF) formulation is used to linearly approximate alternating current (AC) networks:

$$\sum_{l \in L} K_{z,l} \cdot \chi_{l,p} \cdot (f^+_{t,l,y,p} - f^-_{t,l,y,p}) = 0 \qquad \forall t \in T, y \in Y, p \in P_L, z \in Z \tag{14}$$

Both the availability of fuels and the exogenous demand for energy carriers are defined through the bounds on imports and exports across

the system boundary:

$$\underline{g}^{+}_{t,n,y,q} \leq g^{+}_{t,n,y,q} \leq \overline{g}^{+}_{t,n,y,q} \qquad \forall t \in T, n \in N, y \in Y, q \in Q \quad (15)$$

$$\underline{g}^{-}_{t,n,y,q} \leq g^{-}_{t,n,y,q} \leq \overline{g}^{-}_{t,n,y,q} \qquad \forall t \in T, n \in N, y \in Y, q \in Q \quad (16)$$

The nodal conservation of energy carriers is enforced by the balancing equation for all model regions and time steps. This equation includes inputs and outputs into the converters (17a), flows across transfer links in the network (17c) and associated losses, which are evenly distributed to both connected model regions (17d), the change in storage levels and their respective self-discharge (17b), and imports and exports of energy carriers across the system borders (17e). Note that for the storage level the reference to the previous time step $t-1$ behaves in a cyclical fashion in which the predecessor of the first time step is equal to the last time step of the set T:

$$\sum_{p \in P_C, a \in A} D_{p,a,q} \cdot d_{t,n,y,p,a} \quad (17a)$$

$$+ \sum_{p \in P_S} E_{p,q} \cdot \left(e_{t,n,y,p,q} - (1-\delta_p) \cdot e_{t-1,n,y,p,q} \right) \quad (17b)$$

$$+ \sum_{l \in L, p \in P_L} M_{n,l} \cdot F_{l,q} \cdot \left(f^{+}_{t,l,y,p} - f^{-}_{t,l,y,p} \right) \quad (17c)$$

$$- \sum_{l \in L, p \in P_L} \frac{1}{2} \cdot |M_{n,l}| \cdot H_{l,q} \cdot \left(f^{+}_{t,l,y,p} + f^{-}_{t,l,y,p} \right) \quad (17d)$$

$$+ \left(g^{+}_{t,n,y,q} - g^{-}_{t,n,y,q} \right) = 0 \qquad \forall t \in T, n \in N, y \in Y, q \in Q \quad (17e)$$

Applying the optimization to a single target year significantly simplifies the Eqs. (4)–(9). Similarly, if the expansion and decommissioning of power plants are not permitted, the available units $x_{n,y,p}$ and links $x_{l,y,p}$ can be treated as fixed variables and are reduced to constant factors in Eqs. (10)–(13), effectively resulting in a pure economic dispatch model. The equations shown are the minimum requirement to model the basic functionality of the general ESOMs and are even in the reduced form for a single target year sufficient to demonstrate the increase in computational complexity of the model with a fixed number of time steps $|T|$ and increasing the number of model regions $|N|$ and transfer links $|L|$.

2.2. The parallel solver PIPS-IPM++

As mentioned in Section 1, the original implementation of PIPS-IPM was specifically designed to solve stochastic optimization problems on HPCs. The algorithm effectively leverages the block structure of the underlying problem quite well and is adept at handling the linking variables that connect the stochastic dimension of optimization problems. For instance, in [38], these are the decision variables related to the power generation limits, which must be consistent across all scenarios. In contrast, the decomposition of arbitrary optimization problems generated by ESOMs leads not only to linking variables, but also to linking constraints. For instance, incorporating limits on annual CO_2 emissions as constraints in such models yields constraints across all model regions and time steps. For this particular reason, Rehfeldt et al. extended their version of PIPS-IPM, called PIPS-IPM++, to apply to linear programs with both linking variables and linking constraints and presented the improvements in [44]. Fundamentally, the solver uses a primal-dual IP method to solve the augmented system of an LP with arrowhead structure. This arrowhead structure can be created via a permutation of the optimization matrix, resulting in a structure in which most of the non-zero entries are close to the diagonal of the matrix and the remaining non-zero entries are close to the left and top borders of the matrix. This property is intrinsic to almost all ESOMs with a high temporal resolution, as discussed further in Section 2.3. The solver's increased parallelism and computational performance stem from the distributed computation of the local Schur complement for each block in the structure. For a more detailed description of the algorithm, see the initial introduction in [39] and [44].

Since PIPS-IPM++ can also use information about the adjacency of blocks, it is necessary to distinguish between globally linking constraints and variables and locally linking constraints and variables. Constraints that are contained in fewer than four blocks are considered locally linking and can be treated differently by the solver. All other constraints are considered globally linking. The same metrics apply to both local and global linking variables. Building upon this, Kempke et al. extended this version with a hierarchical approach that splits the linear system, allowing it to solve larger models with a large number of local constraints [49]. Initial benchmark analyses have demonstrated that PIPS-IPM++ can outperform standard IP solver software for both generic and real-world ESOMs [50]. Moreover, the reported results show that PIPS-IPM++ is even able to obtain solutions where other solvers cannot. However, the degree of parallelization and thus the ability to accelerate ESOMs depends on several parameters, such as the choice of underlying problem structure. As we demonstrate during the computational experiment, there are some fundamental aspects to consider based on the model instance at hand in order to obtain reasonable performance when applying PIPS-IPM++.

In contrast to standard IP solver, a slightly different workflow is required in order to benefit from distributed memory architectures and to obtain optimal performance with PIPS-IPM++. Fig. 1 shows a comparison of the two workflows and highlights the necessary considerations for parallelism. The HPC cluster used in the computational experiment has dual-socket compute nodes with 2 CPUs per node. Since each socket has its own memory controller, only half of the memory is locally accessible by each CPU. Accessing the remaining memory requires cross-socket communication, which decreases access speeds. This concept of non-uniform memory access (NUMA) needs to be considered when distributing any computations on HPC systems. In the case of the standard IP solver on shared memory (left side), only one compute node can be used. Furthermore, using more than half of the total memory can decrease the solver's overall performance due to cross-socket communication. For PIPS-IPM++ additional preparation steps are required. First, in this case, annotation describes the assignment of variables and equations to blocks, a topic discussed further in Section 2.4. Then, splitting and distributing the matrix is required to prevent parallel threads from simultaneously reading the same input file, which could cause a bottleneck. Up to 12 cores can be used for each block with the fastest memory access, or up to 24 cores can be used while still preventing cross-socket communication. Please note that the exact number of cores for each case depends on the CPU architecture and memory layout specific to the HPC cluster.

2.3. Matrix structures in ESOMs

The objective function of linear programs is typically formulated in the form $c^T x$ representing either a minimization or maximization of the decision variables x multiplied by a cost vector c. In the case of ESOMs this objective function is usually a minimization of total system costs as shown in Eq. (1). In addition to the decision variables the model contains equations in the form of $Ax \leq b$ which limit the dispatch of power plants to their rated capacity, for example. The non-zero entries of the matrix A therefore provide useful insights into the connectivity between variables and equations. These non-zero elements can be used to represent any optimization problem visually (see Fig. 2(a)). In this visualization, each row represents an equation, and each column represents a variable. Black dots indicate non-zero entries and show whether a given constraint contains a given variable. The rows and columns of the matrix can be permuted without altering the underlying optimization problem, creating a block-structured matrix (see Fig. 2(c)). This block structure is required by the parallel solver PIPS-IPM++ and allows us to treat each of the blocks P_1 to P_k as a partial optimization problem. The linking

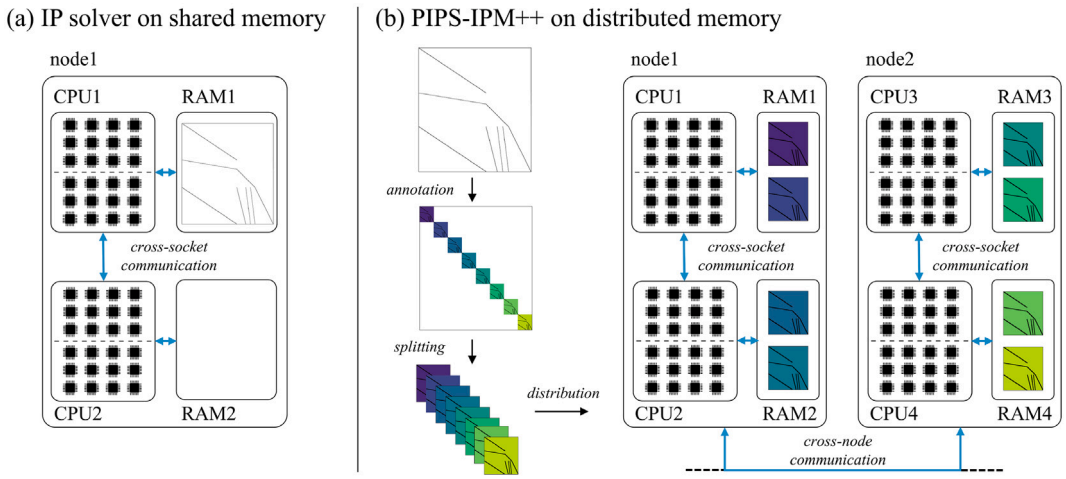
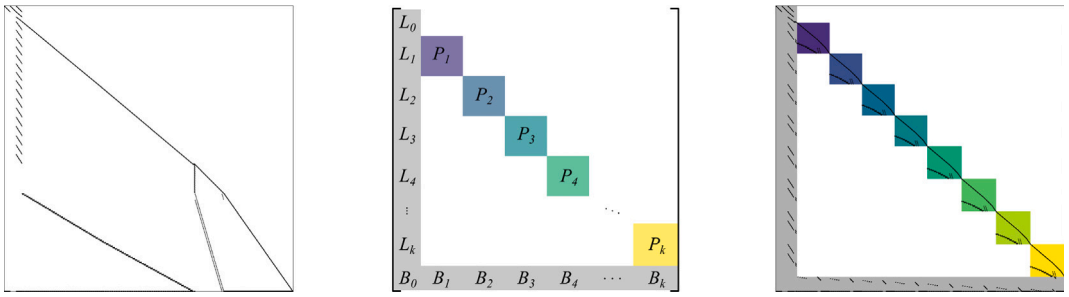


Fig. 1. Stylized representation of the differences in the workflow and hardware utilization between PIPS-IPM++ operating on distributed memory architectures and standard IP solvers. Blue arrows indicate communication pathways at the CPU, node, and cluster levels. The dashed line indicates CPU-internal core subdivisions. (a) IP solver on shared memory: Ideally, the matrix can be stored in the memory addressable by a single socket, otherwise cross-socket communication can decrease performance due to non-uniform memory access. (b) PIPS-IPM++ on distributed memory. The problem is first annotated, then split and finally distributed and solved on several nodes and CPUs. The blocks can be evenly distributed throughout the system, allowing for fast access and mitigating memory limitations.



(a) Original matrix of instance (b) Stylized arrowhead matrix structure (c) Annotated model instance

Fig. 2. Matrix structure representations for a small scale instance with 5 model regions and 16 time steps. (a) Representation of the matrix structure using the non-zero coefficients. (b) Required matrix structure for PIPS-IPM++ with colored blocks highlighting the diagonal sub-matrices and gray blocks highlighting sub-matrices for linking elements. (c) Permutation of the original matrix structure to match the matrix structure required by PIPS-IPM++.

variables and equations in L_0 to L_k and B_0 to B_k are used between parallel iteration steps to update the bounds for each partial optimization problem. In other words, each block represents a subproblem computed by one of many processes running in parallel. Thus, the greater the number of blocks, the greater the number of parallel processes that can be used.

However, the number of blocks – and thus the degree of parallelism – is limited by the additional elements connecting the blocks. Some variables appear in equations across multiple blocks, creating additional interlinkages. These linking variables are shown on the left-hand side of Fig. 2(b) as L_1 to L_k. Similarly, equations can contain variables from multiple blocks. These linking equations can be found at the bottom of the arrowhead matrix in blocks B_0 to B_k. Both types of linking structures impose an overhead cost on the parallel solver. In extreme cases, this communication overhead can outweigh the performance gain from parallel computing. Therefore, the goal of pre-structuring the matrix is to find appropriate decomposition strategies and optimize the number of blocks.

2.4. Block structure generation

Depending on the chosen decomposition strategy, this pre-structuring can result in various arrowhead structures. Despite the large number of possible decompositions, there are several points to consider for the effective application of PIPS-IPM++. First, the number of blocks corresponds to the maximum achievable parallelism. Therefore, we try to generate structures with a large number of diagonal blocks. Second, the more linking elements there are in the block structure, the greater the communication overhead during the non-parallel phase of the solver. These two effects create a trade-off between the speedup gained from parallelization and the slowing effect of communication, which is further explored in the computational experiment presented in Section 3.

In order to generate a specific block structure for PIPS-IPM++, a decomposition strategy must first be defined. This strategy comprises the mapping between two sets: the set of decomposition elements D, which are related to the model variables based on the decisions the variables represent, and the set of blocks $\mathcal{K}$ we want to generate. In a temporal decomposition strategy, for example, the set of decomposition elements is the set of all time steps considered in the model. The mapping can then, for example, assign hours 1 to 24 to block 1, hours 25 to 48 to block 2, and so on. For the partitioning of the variables, each variable is checked to see if it is associated with a decomposition element. For example, a variable can represent the dispatch of a power plant in hour 12. If a variable is associated with an element of the decomposition strategy, it belongs to the parallel blocks P_1 to P_k and the corresponding linking equations B_1 to B_k, with the block k depending on the mapping from

decomposition elements to blocks. If a variable is not associated with an element in the strategy, then it belongs to the linking variables of the blocks L_0 to L_k and B_0. To determine the partitioning of the constraints, the annotation of the variables must be evaluated. If a constraint contains only linking variables, then it is an L_0-constraint contained in the top-left block, L_0. If a constraint contains only variables from a single block and optionally linking variables, it is assigned to the respective parallel block, P_1 to P_k. If a constraint contains variables from multiple parallel blocks, then it is a linking constraint contained in blocks B_0 to B_k. More formally, it can be described via the following partitioning algorithm.

1. **Definition of the decomposition strategy**
   With $D = \{1, 2, \dots, D\}$ as the set of decomposition elements and $\mathcal{K} = \{1, 2, \dots, K\}$ as the set of blocks, $s : D \to \mathcal{K}$ is the user-defined decomposition strategy assigning each decomposition element to a block.
2. **Annotation of the variables**
   With $\mathcal{X} = \{x_1, x_2, \dots, x_j\}$ as the set of all decision variables, the variables can be partitioned as follows:

$$\mathcal{X}_k = \{x \in \mathcal{X} \mid x \text{ is associated with } d \text{ such that } s(d) = k\} \quad \forall k \in \mathcal{K}$$
$$\mathcal{X}^{\text{linking}} = \mathcal{X} \setminus \bigcup_{k \in \mathcal{K}} \mathcal{X}_k$$

3. **Annotation of the constraints**
   With $\mathcal{C} = \{c_1, c_2, \dots, c_i\}$ as the set of all constraints and $\mathcal{X}_c \subseteq \mathcal{X}$ as the subset of decision variables with non-zero coefficients in constraint c, the constraints can be partitioned as follows:

$$C^{L_0} = \left\{c \in \mathcal{C} \mid \mathcal{X}_c \subseteq \mathcal{X}^{\text{linking}}\right\}$$
$$C_k = \left\{c \in \mathcal{C} \setminus C^{L_0} \mid \mathcal{X}_c \subseteq \mathcal{X}_k \cup \mathcal{X}^{\text{linking}}\right\} \quad \forall k \in \mathcal{K}$$
$$C^{\text{linking}} = \mathcal{C} \setminus \left(C^{L_0} \cup \bigcup_{k \in \mathcal{K}} C_k\right)$$

4. **Assignment of variables and constraints to matrix blocks**
   With $A_{c,x}$ as the coefficients in the original matrix A for constraint c and variable x, the matrix can be partitioned for the structure required by PIPS-IPM++ as follows:

$$L_0 = \left\{A_{c,x} \mid c \in C^{L_0} \wedge x \in \mathcal{X}^{\text{linking}}\right\}$$
$$L_k = \left\{A_{c,x} \mid c \in C_k \wedge x \in \mathcal{X}^{\text{linking}}\right\} \quad \forall k \in \mathcal{K}$$
$$P_k = \left\{A_{c,x} \mid c \in C_k \wedge x \in \mathcal{X}_k\right\} \quad \forall k \in \mathcal{K}$$
$$B_0 = \left\{A_{c,x} \mid c \in C^{\text{linking}} \wedge x \in \mathcal{X}^{\text{linking}}\right\}$$
$$B_k = \left\{A_{c,x} \mid c \in C^{\text{linking}} \wedge x \in \mathcal{X}_k\right\} \quad \forall k \in \mathcal{K}$$

2.5. Decomposition strategies

Due to the high spatial and temporal resolution of the ESOMs, decomposing along these dimensions is the most promising way to generate a large number of blocks k:

- In the case of spatial decomposition, individual model regions can be treated as parallel blocks. However, these blocks are still connected by hourly variables that representing energy transmission between model regions and by constraints affecting multiple model regions, such as a global CO_2 budget.
- In the case of temporal decomposition, multiple time steps can be grouped into blocks, allowing for a uniform sizing of the parallel blocks. This type of decomposition establishes investment decisions as the linking variables and creates additional linking constraints for the storage level continuity and annual limitations, such as CO_2 budgets.

Table 1 shows the commonly used constraints and variables in ESOMs and the number of linking variables and constraints generated depending on the decomposition strategy. The last row provides an estimation of the scaling behavior of the linking elements. When using a spatial decomposition approach, the number of linking elements depends primarily on the size of the time dimension ($|T|$) and the total number of lines ($|L|$) between model regions. For a temporal decomposition, the number of linking constraints and variables depends mainly on the number of model regions ($|N|$) times the number of transmission and storage technologies ($|P_C| + |P_S|$) and the number of transfer links ($|L|$) times the number of transfer technologies ($|P_L|$). Note that if capacity expansion and decommissioning decisions are not allowed for a specific model region or technology, these decisions do not factor into the number of linking variables. Therefore, in the special case of a pure economic dispatch model, as described in Section 2.1, combined with a temporal decomposition, there are no linking variables.

A decomposition by time steps can be beneficial if the level of detail on the temporal scale outpaces the spatial scale. Additionally, when using HPC, it is essential to consider load balancing across multiple compute nodes and, consequently, to create similarly sized blocks. This is similar to two of the requirements of Lagrangian relaxation, in which the quality of the diagonal structure can be determined by granularity (a large number of blocks) and homogeneity (equally sized blocks) [51]. In the case of a spatial decomposition, each model region is usually connected to a various number of generation and demand technologies, resulting in unequally sized blocks. In contrast, the overall number of time steps can be equally and more flexibly assigned to the number of blocks chosen, allowing for a more thorough assessment of the scaling behavior between solver performance and the number of blocks. For this reason, and because the number of time steps is significantly greater than the number of model regions, we select the temporal decomposition strategy for the computational experiment in Section 3.

Table 1
Estimation of linking constraints and variables for spatial and temporal decomposition of a generic ESOM. The entries correspond to the factor by which the the number of linking elements increases per constraint or variable. k denotes the number of blocks, $|T|$ the number of time steps, $|N|$ the number of regions, $|L|$ the number of network links, $|P_{C,L,S}|$ the number of converter, network, and storage technologies, respectively.

		spatial decomposition	temporal decomposition
constraint	global annual constraint, e.g. CO_2 limit	1	1
	regional annual constraint, e.g. CO_2 limit	–	$\|N\|$
	conservation of energy carriers	–	$\|N\| \cdot \|P_S\| \cdot k$
	limitation of transfer flows	$\|T\| \cdot \|L\| \cdot \|P_L\|$	–
variable	available converter units	–	$\|N\| \cdot \|P_C\|$
	available storage units	–	$\|N\| \cdot \|P_S\|$
	available transfer links	$\|L\| \cdot \|P_L\|$	$\|L\| \cdot \|P_L\|$
	transfer flows	$\|T\| \cdot \|L\| \cdot \|P_L\|$	–
	scaling of linking elements	$\sim (2 \cdot \|T\| + 1) \cdot \|L\| \cdot \|P_L\|$	$\sim (1 + k) \cdot \|N\| \cdot \|P_S\| + \|N\| \cdot \|P_C\| + \|L\| \cdot \|P_L\|$

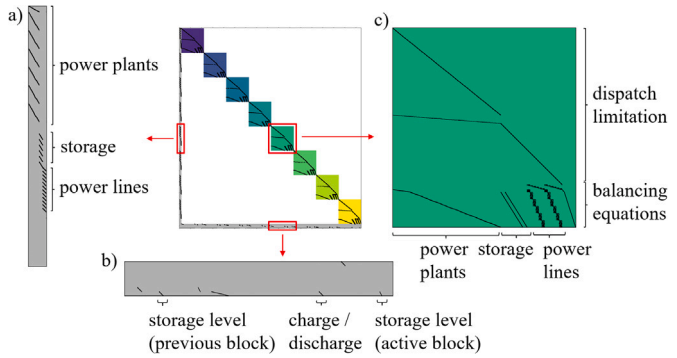


Fig. 3. Structure of a temporally decomposed optimization matrix which includes the following sub-matrices: (a) L_1 to L_k containing linking variables, (b) B_1 to B_k containing linking constraints, (c) P_1 to P_k containing the block-specific independent part of the decomposed optimization problem.

Fig. 3 shows an ESOM temporally decomposed into 8 blocks. Most of the equations and variables are non-linking, so they can be easily separated into parallel blocks, as indicated in the block matrix in (c). However, a few equations significantly impact the number of linking variables and constraints. These equations are:

- Globally linking constraint (e.g., CO_2-limit): An annual limitation on carbon emissions $\bar{j}_{CO_2}$ results in a globally linking constraint, since the emissions resulting from the utilization of fossil fuels in each time step and model region are summed up as modeled in Eq. (3a)).
- Globally linking variable (e.g., capacity expansion): If investment decisions are considered in the optimization the capacities of each technology represent linking variables. For example, they have an impact on the dispatch in each time step, as modeled in Eqs. (10)–(13) (see Fig. 3 (a)).
- Locally linking constraint (e.g., storage level): Storage technologies introduce locally linking constraints to the optimization. Equation (17b) enforces conservation of energy carriers and therefore also links the storage level of any time step to the storage level of the previous one (see Fig. 3 (b)).

3. Computational experiment

In this section, we will first provide a summary of the case study, followed by more details on the model instances for the computational experiment in Section 3.1. Second, in Section 3.2 we motivate the selection of performance indicators that are relevant in the context of assessing ESOMs in the context of HPC. Third, in Section 3.3 we describe the used hardware, software, and solver-specific configurations.

3.1. Model instance

This paper uses a model instance based on the work of Cao et al. [52] that focuses on the capacity expansion in the power sector. The model includes existing capacities for renewable and conventional power plants, as well as lithium-ion battery, pumped hydro storage, and the transmission grid. An annual CO_2 budget limits the operation of conventional power plants. Each year is modeled with full hourly resolution, resulting in 8,760 sequential time steps. At the highest spatial resolution, Germany is considered with 477 model regions representing substations and grid junctions including a total of 643 transmission lines. Additionally, the 11 neighboring countries are included with one model region each, and their electricity imports and exports to Germany are fixed based on historical time series. The base model with the highest spatial resolution and full expansion planning has been published as open data.[3] Although minor data updates have been implemented compared to the model instances used in this study, they do not affect the findings regarding computational performance.

Starting from the base model instance, we use hierarchical clustering [4] to derive a subset of spatial aggregations to investigate the performance of the solver for a broad set of model instances. For our computational experiment, we use eight levels of aggregation with 18 to 488 model regions. Additionally, we vary the degree of complexity by defining three levels of capacity expansion planning typical for energy systems research: i) disabled (economic dispatch optimization, *disp*), ii) enabled only for renewable power generators (generation expansion planning, *expRE*), and iii) enabled for renewable power generators, storage units, and transmission lines (full expansion planning, *expAll*). Combining these three levels with eight different spatial aggregations results in a total of 24 model instances. Table 2 lists the number of constraints, variables and non-zeros for each of these instances.

To decide which decomposition strategy to use, the rule of thumb from the Table 1 for estimating the number of linking elements can be applied to the full-size model. In the case of a spatial decomposition, the large number of time steps significantly increases the number of linking variables for power flows to about 22 million. With a temporal decomposition and an estimate of 100 time blocks, however, the number of linking constraints for the storage level is only about 0.1 million. This confirms our expectation from Section 2.4, that for REMix and other hourly resolved ESOMs, a temporal decomposition is advantageous when using PIPS-IPM++.

3.2. Performance indicators

For energy system modelers, one of the most important metrics is the wall-clock time required to solve a given optimization problem. A short wall-clock time significantly reduces the overall analysis workflow time because solving the problem is usually the most time-consuming step, except for initial data collection. During the setup of a given case study, for example, several workflow cycles are required to calibrate the model correctly and to detect and correct possible errors in the input data. Even if computation across multiple compute nodes is possible for a large-scale scenario analysis, the minimum run time of the analysis as a whole is limited by the longest single run.

Another key metric to consider is the amount of random access memory (RAM) required to store the optimization problem matrix on a shared memory system. Although there is some overhead caused by the optimization method itself, it scales quite linearly within a given problem class. As a result, energy system modelers face an upper bound on maximum problem sizes depending on available hardware. One way to circumvent this limitation is to simplify the problem's overall complexity through aggregation on the temporal, spatial, or technological scale, as previously discussed in Section 1.2. If simplifications cannot be made, or if the goal is to solve a reference run at the highest possible resolution, memory can still be a limiting factor for standard IP solvers using shared memory hardware. In contrast, decomposition approaches and block-structure solvers allow smaller chunks of the optimization matrix to be stored in memory.

From an HPC usage perspective, another key metric is the number of core hours required to solve the problem, in the following also referred to as compute. The number of core hours gives an indication of how much computational effort was required to solve any specific problem. In the context of HPCs, core hours usually also represent the budget that is granted in publicly funded compute clusters or paid for in commercial clusters. Therefore, it is important to develop an awareness of how much compute is required in order to run in a highly parallel environment.

Due to the overall scaling behavior of the optimization problem, all three factors – wall-clock time, RAM demand, and core hours – are highly correlated, but they offer trade-offs when using parallel solvers.

[3] https://gitlab.com/dlr-ve/esy/remix/projects/powger

Table 2
Model instances for the computational experiment and sizes of their corresponding optimization matrices.

regions	constraints [mio]			variables [mio]			dense columns [tsd]			non-zeros [mio]		
	disp	*expRE*	*expAll*	*disp*	*expRE*	*expAll*	*disp*	*expRE*	*expAll*	*disp*	*expRE*	*expAll*
18	2.60	3.00	3.24	2.44	2.83	3.07	0.00	0.10	0.16	8.57	10.46	12.07
30	3.96	4.63	4.98	3.71	4.37	4.72	0.00	0.15	0.24	13.02	16.07	18.48
60	6.90	8.23	8.85	6.44	7.77	8.38	0.00	0.26	0.44	22.35	28.13	32.48
90	9.17	11.15	12.03	8.53	10.51	11.39	0.00	0.35	0.60	29.52	37.80	43.96
120	11.49	14.13	15.27	10.70	13.34	14.48	0.00	0.44	0.76	36.74	47.54	55.49
240	18.99	24.13	26.32	17.71	22.85	25.04	0.00	0.74	1.33	59.65	79.84	94.52
360	23.85	31.03	34.19	21.66	28.84	32.00	0.00	0.91	1.74	73.78	101.36	122.30
488	31.11	40.75	45.04	28.51	38.15	42.44	0.00	1.19	2.29	95.94	132.81	160.67

Decomposing the problem into more blocks allows for a higher degree of parallelism, reducing wall-clock time and RAM requirements per block. Conversely, more blocks increase the number of link variables and constraints generated per block, in turn leading to increased communication overhead when exchanging information between different blocks. To investigate this trade-off, we use the temporal decomposition strategy introduced in Section 2.5 to demonstrate scaling across a range of different block numbers.

3.3. Software setup and hardware

All runs of the computational experiments were performed on the JUWELS cluster at Jülich Supercomputing Centre (JSC) with 2,271 standard nodes, each with two Intel Xeon Platinum 8168 and 96 GB of DDR4 memory, and 240 large memory nodes with the same CPUs but 192 GB of memory.[4] All compute nodes are connected via an InfiniBand EDR network.

The runs with the standard IP solver as the reference case were performed using GAMS 39.1 and CPLEX 22.1. For all runs we used an interior-point method with crossover disabled, which generally seems to provide the best performance for large and complex ESOMs [53]. Other additional settings have been applied based on previous experiences with the REMix model.[5] Sharma et al. report the highest reductions in overall solve time for their model until up to 12 cores, and a slightly less steep reduction between 12 and 35 cores [27]. In order to make use of both a high solver performance and limit the number of cores to allow for running multiple instances on the same machine we utilize 8 cores for the runs with the standard IP solver and take into account the theoretical farming factor. This factor describes how many similar jobs could be run simultaneously on a single compute node given the limitation of 48 physical cores and 192 GB of RAM. When running small-scale models 8 cores are taken into account for the calculation of the compute because memory is not limiting, and 6 instances can be run simultaneously. However, for large model instances, when shared memory is limited, the additional cores cannot be allocated for parallel runs, resulting in a farming factor of 1.

Another option to consider for the solvers is the stopping criterion used by the optimization algorithm. For interior point methods this is usually the duality gap between the primal and dual objectives of the LP. For ESOMs solved as linear problems a sufficient gap tends to be in the range of 10^{-8} to 10^{-4} depending on the optimization problem at hand. For many ESOMs the area around the optimal solution tends to be rather flat due to the large number of marginally different decisions. Therefore, lowering the precision is a reasonable strategy to reduce wall-clock time, albeit at the expense of being slightly off the global optimum. In all runs of the computational experiment, the stopping criterion is set to a tolerance of 10^{-5} between the primal and dual objectives.

The parallel solver PIPS-IPM++ was compiled using the Intel Compiler and ParaStationMPI. The optional library PARDISO 7.2 [54] was used as a sparse direct solver, though other options, such as MA57 [55], can also be used. For PIPS-IPM++ the default settings for the convergence criteria have been used, requiring a μ value below 10^{-6} and a relative residual norm below 10^{-4}. Additional PIPS-IPM++-specific options are required to set PARDISO as the direct solver when multiple direct solvers are available during compilation.[6] As discussed in Section 2.4, the two main drivers of the overall performance of PIPS-IPM++ are the number of blocks into which the problem is decomposed into and the utilized hardware per block. To fully utilize all available 48 cores per compute node and account for NUMA cache locality for the dual-socket CPU nodes, we split the number of blocks into multiples of 12 and allocate 4 cores for each block. This results in a total of 72, 96, 144, and 192 blocks, while utilizing 6, 12 and 24 compute nodes respectively.

4. Results and discussion

The results of this paper are structured as follows: Section 4.1 analyzes the scaling behavior of the model instances with respect to different model sizes and levels of complexity using a standard IP solver. Section 4.2 derives the ideal configurations of the parallel solver PIPS-IPM++ in terms of optimal number of blocks for decomposition and utilized hardware nodes. Section 4.3 then brings together the model instances and the optimal configuration for PIPS-IPM++ from the previous sections to compare PIPS-IPM++ to the standard IP solver in terms of key performance indicators.

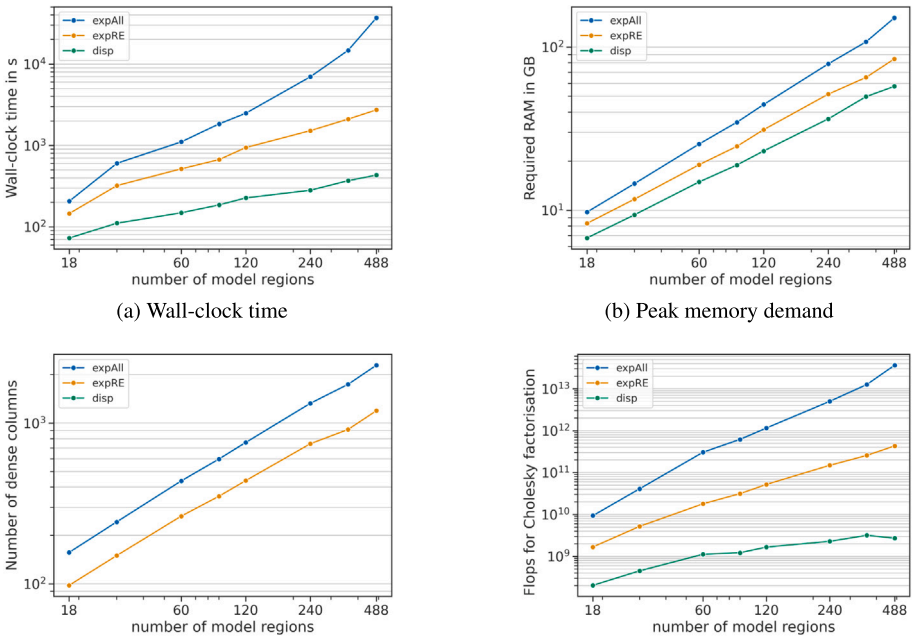
4.1. Complexity of ESOMs

Fig. 4 shows the comparison of the runs performed using a standard IP solver for the 24 instances described in Section 3.1. As expected, Fig. 4(a) shows an overall increase in the wall-clock time as the number of model regions increases. Similarly, the overall complexity of the problem in terms of capacity expansion decisions significantly impacts the results. The difference between the types of capacity expansion becomes more pronounced when a larger number of model regions is considered. The increasing difference in solving times can be explained by the additional complexity due to capacity expansion decisions indicated by the number of dense columns (see Fig. 4(c)). Dense columns in the coefficient matrix result from variables that appear in many equations, such as limitations on dispatch relative to capacity expansion. These variables

[4] https://www.fz-juelich.de/en/ias/jsc/systems/supercomputers/juwels

[5] The following CPLEX solver options have been used for the computational experiment:
lpmethod 4 (select interior point method)
predual −1 (pass only the primal problem to the pre-solver)
barorder 3 (use nested dissection for the matrix ordering)
barepcomp 1e-5 (set stopping criteria to 10^{-5})
solutiontype 2 (disable crossover, as no basic solution is required).

[6] The following PIPS-IPM++ solver options have been used to set PARDISO as the direct sparse solver:
LINEAR_ROOT_SOLVER 3 int
LINEAR_SUB_ROOT_SOLVER 3 int
LINEAR_LEAF_SOLVER 3 int



(a) Wall-clock time (b) Peak memory demand

(c) Number of dense columns (d) Compute estimation per iteration

Fig. 4. Scaling across the different instances while using a standard IP solver. Note that both x and y axis are displayed with a logarithmic scaling. (a) Wall-clock time: For all expansion variations, the wall-clock time increases exponentially with more model regions. The *expAll* variation has the steepest ascent. (b) Peak memory demand: The higher the complexity of the expansion variation, the higher the memory demand and the exponential increase. (c) Number of dense columns: This metric is only applicable for the two variations with expansion variables. (d) Compute estimation via FLOPs for Cholesky factorization: Especially the *expAll* variation shows the highest exponential increase with a higher spatial resolution.

are comparable to linking variables and are identified in standard IP solvers to be treated differently during presolve. For the *disp* instance, the presolver can remove all dense variables, resulting in a reduced complexity. For the other instances, *expAll* and *expRE*, the curves show clear scaling behavior with respect to the number of model regions. However, the curves are shifted relative to each other, as *expAll* allows investments in storage technologies and power lines, in addition to renewable power plants, whereas *expRE* only allows investments into renewable power plants. For the largest analyzed instance this amounts to 2290 dense columns for *expAll*, 1194 for *expRE* and 0 for *disp*.

The number of dense columns also affects the total number of variables, constraints and non-zeros in the optimization problem because each investment decision results in dispatch decisions for every hour of the model. The overall size of the optimization matrix is one of the main drivers of the required memory (see Fig. 4(b)). For the largest instance size the total memory requirement ranges from 57 GB to 151 GB depending on the complexity of investment decisions. This memory demand corresponds to the number of variables after presolve, which ranges from 14.4 million to 37.1 million. We consider the number of variables because it is larger than the number of constraints. This allows us to derive an estimate of memory per variable, ranging from 3.96 to 4.07 GB per million variables after presolve, indicating a theoretical limitation of a few hundred million variables on current shared memory architectures.

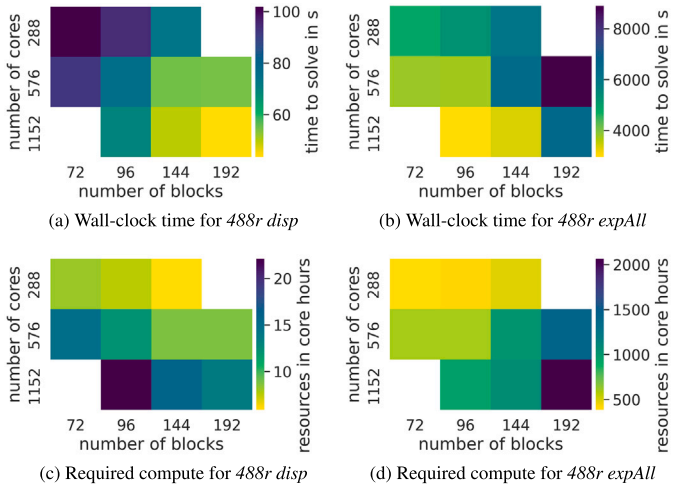
Another helpful metric for estimating the total runtime of the optimization in barrier algorithms is the number of floating point operations (FLOPs) for the Cholesky factorization. This value provides a rough estimate of how much time each iteration will take. However, the total time required to solve the problem depends on the maximum achievable FLOPs of the hardware and the total number of barrier iterations required for the solution. Fig. 4(d) shows the number of FLOPs required per iteration across all instances, indicating a clear difference in computational effort for each barrier iteration depending on the instance's complexity.

In summary, we can clearly establish a connection between the overall size of the optimization problem and the number of capacity expansion decisions as the primary drivers of model complexity. A comparison of the scaling behaviors for memory and wall-clock time indicates that, with a larger number of investment decisions, the increase in wall-clock time significantly outpaces the increase in memory requirement. Therefore, even if the shared memory suffices for the computation, the theoretical example with several hundred million variables is expected to require multiple days of wall-clock time to solve.

4.2. Solver tuning for PIPS-IPM++

To identify the ideal configurations for the model decomposition and the hardware, we run the same model instances using a range of different configurations as outlined in Section 3.3. Fig. 5 shows a clear difference between the two large-scale instances (*disp* on the left, *expAll* on the right). The top figures show the time to solve for different configurations in terms of chosen number of blocks and cores. As expected, a larger number of cores results in faster solution times at the expense of additional computing power. However, the figure also highlights the risk of choosing non-optimal configurations, which can result in up to three times longer solution times compared to the best configuration.

For the economic dispatch instance the fastest time to solution is achieved with both a large number of cores and a large number of blocks. This suggests that the model complexity, due to linking variables and constraints, is not the limiting factor and even higher speedups would be possible if more blocks and cores are utilized. Conversely, the best performance when dealing with a large number of investment decisions is achieved with a high number of cores and a low number of blocks. This indicates an additional limitation of the algorithm's overall parallelism. In this case, the bottleneck for the performance is not in solving the individual blocks, but rather the computation of the global Schur complement and overall communication due to the additional linking structures of the underlying problem.



(a) Wall-clock time for *488r disp*

(b) Wall-clock time for *488r expAll*

(c) Required compute for *488r disp*

(d) Required compute for *488r expAll*

Fig. 5. Time to solve and required compute for the different model instances and hardware configurations using PIPS-IPM++. Lower time to solve and lower compute resources are favorable. (a) The *disp* variation achieves the lowest wall-clock time with more cores and a higher number of blocks. (b) The *expAll* variation benefits from more cores when minimizing wall-clock time, however, fewer blocks are favorable. (c) The compute of the *disp* variation is the lowest with more blocks and a lower number of cores. (d) The *expAll* variation requires the least compute with fewer blocks and cores.

These findings provide a good initial estimate for the configuration of PIPS-IPM++ depending on the optimization problem to be solved. The optimal configuration also depends on the overall goal of deploying PIPS-IPM++: decreasing wall-clock time, increasing efficiency in terms of computation, or preventing limitations from the shared memory architectures. Furthermore, these results provide an explanation for the significant differences in speedup observed in the previous two applications of PIPS-IPM++ by Rehfeldt et al. and Panos and Hassan, as reported in their respective studies [44,45]. Rehfeldt et al. observed the highest speedup, a factor of 67, for the *ELMOD_EU16* instance with 876 blocks and 1,752 CPU cores. While the model instances do have around 300,000 linking constraints, they have only very few global linking variables. Therefore, they are similar to the large *disp* instances presented in this study, which also benefited from a larger number of CPU cores. Panos and Hassan, on the other hand, report a speedup of factor 4 for their model instance *288_22_8*, which contains 162,169 linking constraints and 16,783 linking variables which is higher than the largest *expAll* instance considered here. Due to the different model structure, they used 88 blocks and 88 CPU cores.

4.3. Solver comparison with PIPS-IPM++

Bringing together the results of the complexity analysis using standard IP solvers in Section 4.1 and the assessment of different configurations for PIPS-IPM++ in Section 4.2, we can evaluate the relative performance between the two. While the reference solution using the standard IP solver provides only one data point for time to solve and compute (Fig. 4), the different configurations for PIPS-IPM++ provide a range of data points for solution time and compute (Fig. 5). For the following comparison, we will assume prior knowledge of the optimal configuration for PIPS-IPM++ in terms of the shortest time to solve and the least compute, respectively.

Fig. 6 shows the time required to solve and the necessary compute for all instances considered in this study. It illustrates the effect of using the most suitable PIPS-IPM++ configuration instead of the standard IP solver. A significant reduction in time to solve, roughly one magnitude, can be observed across all instances. The greatest reductions are possible for the economic dispatch instances with small numbers of model regions. For instances with the largest number of model regions, regardless of model complexity, the time required to solve can be reduced by one order of magnitude by using PIPS-IPM++ instead of the standard IP solver. However, this speedup comes at the cost of slightly increased compute and furthermore requires prior knowledge of the optimal PIPS-IPM++ configuration. Only for the instances *expAll* with 488 model regions is it roughly on par. This is mainly due to the farming factor that we considered, which significantly favors the standard IP solver if memory is not a limiting factor.

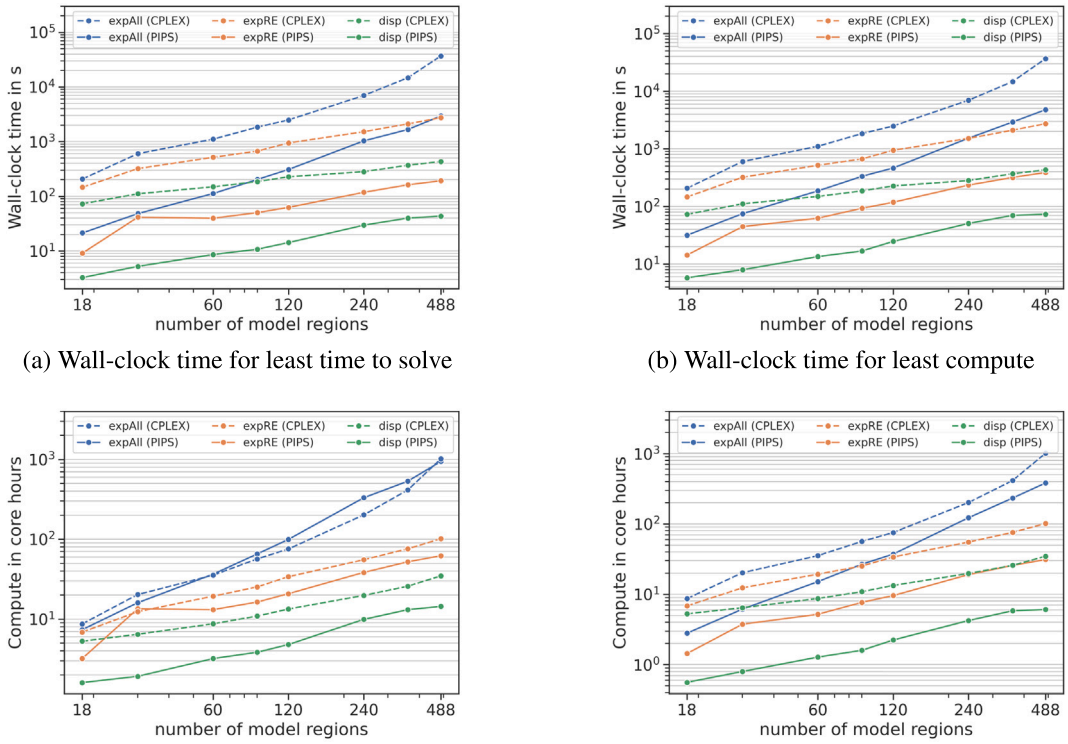
The speedup achieved via the application of PIPS-IPM++ can also be expressed in terms of solving larger models within a similar time frame. For the model instance *disp*, the greatest difference is observed when solving the 488 region instance faster than the 18 region instance using the standard IP solver. However, since the absolute solution time is still in the range of minutes, the real-world savings are negligible. In contrast, the savings in wall-clock time for the instance *expRE* allow one to increase the number of regions from 60 to 240 or from 90 to 360, respectively. On average, model instances can increase fourfold with a similar wall-clock time to solve, significantly pushing the limits of computational complexity.

Switching to a comparison of the most efficient solution in terms of required compute, we observe similar findings to those of the shortest time to solve. Fig. 6(b) shows that all instances can be solved faster using PIPS-IPM++. Additionally, the required compute to solve the same instances is reduced across all model instances. This is especially relevant for the full capacity expansion instances. For the 488 model regions instance, we observe a 13 % reduction in solve time, while saving 22 % of compute compared to the standard IP solver. These results further support the conclusion that applying PIPS-IPM++ can provide the greatest benefits for large, complex models. Table 3 shows the solving time and compute for all scenarios and regions, as well as for both solvers and the different PIPS-IPM++ configurations.

5. Limitations

Strictly speaking, the findings of this study are only applicable to the REMix framework. However, the results align with findings from previous applications, suggesting some degree of transferability to other ESOMs. Considering all applications thus far, the performance of PIPS-IPM++ highly depends on a suitable algebraic model formulation, the total number of blocks and the linking structure between blocks. In the case of non-optimal configurations for PIPS-IPM++, the computational benefits can quickly diminish. Similarly, access to hardware with sufficient performance to take advantage of the high degree of parallelism can be a limiting factor.

Based on the reported findings for ELMOD [56], the Swiss TIMES model [57], and REMix [46], we can formulate some general expectations for other ESOMs: For models with a high temporal resolution, chronologically ordered time steps, and limited interlinkages between time steps, such as PyPSA [58], oemof [59], Backbone [60], Balmorel [61], and AnyMod [62], we expect similar performance benefits from PIPS-IPM++, under the assumption of a similar ratio between time steps and investment decisions, and of a well-performing configuration. When it comes to models using representative time slices, such as OSeMOSYS [63], GENeSYS-MOD [64], and models from the TIMES family, the ratio between investment decisions and the number of time steps makes it more challenging to apply PIPS-IPM++. Furthermore, aspects such as international energy trade can make a sufficient decomposition into blocks challenging, since they are usually represented on an annual rather than sub-annual timescale. Applying different decomposition strategies may therefore be more appropriate for these types of models. Regarding integrated assessment models (IAMs), such as Message$_{ix}$ [65] and REMIND [66], we expect similar challenges, because these models focus on additional aspects, such as the overall economy and environmental impact. IAMs also typically consider more



(a) Wall-clock time for least time to solve

(b) Wall-clock time for least compute

(c) Required compute for least time to solve

(d) Required compute for least compute

Fig. 6. Time to solve and required compute for the three model instances solved with the standard IP solver and PIPS-IPM++. Sub-figures (a) and (c) utilize the PIPS-IPM++ configuration optimized for the least time to solve. Sub-figures (b) and (d) utilize the PIPS-IPM++ configuration optimized for the least compute. Lower time to solve and lower compute resources are better. Note that both x and y axis are displayed with a logarithmic scaling.

Table 3
Wall-clock time and compute for all scenarios and regions. Comparison between CPLEX and different configurations for PIPS-IPM++. Depending on the configuration either the solving time or the compute is minimized for PIPS-IPM++.

scenario	regions	CPLEX		PIPS-IPM++ (shortest time)		PIPS-IPM++ (least compute)	
		time [s]	compute [core h]	time [s]	compute [core h]	time [s]	compute [core h]
disp	18	73	5.28	3.25	1.60	5.25	0.56
	30	111	6.45	5.23	1.92	7.95	0.80
	60	149	8.72	8.62	3.20	13.48	1.28
	90	186	10.91	10.73	3.84	16.81	1.60
	120	227	13.36	14.22	4.80	24.68	2.24
	240	282	19.79	29.61	9.92	50.62	4.24
	360	369	25.81	39.90	13.12	69.93	5.84
	488	433	34.80	43.46	14.40	73.33	6.08
expRE	18	146	6.85	9.12	3.20	14.34	1.44
	30	321	12.37	41.47	13.44	44.55	3.76
	60	517	19.33	39.69	13.12	62.45	5.20
	90	670	25.28	50.25	16.32	92.92	7.68
	120	943	33.95	62.65	20.80	117.99	9.60
	240	1519	55.33	118.06	38.40	234.74	19.04
	360	2109	75.87	162.19	52.16	318.73	25.76
	488	2733	101.55	192.44	62.08	387.57	31.20
expAll	18	207	8.69	21.33	7.36	31.65	2.80
	30	603	20.29	48.27	16.00	74.69	6.16
	60	1108	35.44	112.32	36.48	185.92	15.12
	90	1839	56.59	202.60	65.28	333.10	26.80
	120	2489	75.52	309.26	99.52	464.43	37.28
	240	6973	201.81	1030.94	330.56	1530.5	122.56
	360	14723	414.11	1665.62	533.44	2915.69	233.36
	488	36897	1015.47	2944.78	942.72	4791.47	383.44

nonlinear and nonconvex interactions, which may prevent the application of PIPS-IPM++ altogether. Ultimately, future research is needed to demonstrate the generalized transferability of our findings and show concrete performance benefits across a wide range of ESOM frameworks and model instances with different levels of complexity.

The performance of PIPS-IPM++ can be significantly affected not only by the software, but also by the available hardware, such as the CPU and memory per compute node, as well as by proper software configuration, such as thread pinning. Therefore, the findings of this study should be considered in the context of the used HPC until the solver has been applied to a wider range of clusters. Additionally, computational experiments may be influenced by other factors, such as simultaneous computational loads on the same nodes or general loads on the communication network. Although we applied simple countermeasures, such as allocating complete compute nodes for each run, variations caused by simultaneous load can affect the results. Ideally, computational experiments are performed with multiple runs per test and on different hardware to ensure the reliability of the results. For this study, however, such a design was not possible due to limited access to HPC clusters and the prohibitively large number of computational resources required to obtain statistical significance for the large model instances.

It should also be noted that, in its current state, PIPS-IPM++ has strict requirements regarding the provided optimization problems. These requirements must be addressed by the modeler until adequate heuristics are incorporated into the solver itself. For example, this concerns rank-deficient matrices, which standard IP solvers can automatically presolve but which PIPS-IPM++ currently cannot handle due to challenges in preserving the block structure during the presolve. This can render PIPS-IPM++ impossible to apply to some of the aforementioned problems.

6. Conclusion and outlook

This study evaluates a broad spectrum of scalable energy system model instances generated with the REMix framework. It shows the direct link between the size and complexity of the model instances and their corresponding computational requirements. Specifically, the number of investment decisions significantly impacts the required wall-clock time, while the total number of variables and constraints primarily drives the memory demand. These findings also suggest that, as the size increases, pure economic dispatch problems are more likely to be limited by available shared memory, while capacity expansion problems are more likely to be limited by the time required to obtain a solution.

We further demonstrate that decomposing the problem and utilizing the massively parallel solver PIPS-IPM++ can significantly reduce solution times and prevent limitations imposed by shared memory architectures, given both access to sufficient HPC hardware and a well performing configuration. However, the optimal configuration of PIPS-IPM++ depends heavily on the specific model instance to be solved and the emphasis placed on either the least wall-clock time or the least compute time. The number of blocks into which the optimization problem is decomposed and the number of cores used for the parallel solving process must be adjusted accordingly. For instances with few investment decisions, a large number of blocks is advisable. For instances with a large number of investment decisions, a smaller number of blocks should be used. If the primary goal is to reduce the wall-clock time to solve an instance, utilizing more cores is beneficial. Conversely, reducing the required compute can be achieved by reducing the number of utilized cores.

The observed speedups are in line with previous applications of PIPS-IPM++ which demonstrated significant speedups for pure economic dispatch models [44] and a limited speedups for models with a greater emphasis on capacity expansion planning [45]. In our application, the greatest benefits are obtained for large, complex instances, where solving with standard IP solvers on a shared memory architecture is challenging or impossible. First, the speedup achieved by PIPS-IPM++ allows more scenarios to be solved in the same amount of time. Thus, the challenge of multiple uncertainties associated with scenario studies of large energy systems can be addressed more effectively [6]. Second, the ability to switch to distributed memory machines avoids the memory limitations previously encountered on shared memory machines, as only part of the full optimization matrix needs to be stored in local memory [44]. This is particularly relevant for using modern HPC infrastructure, as the emphasis is generally on high parallelization and throughput, and individual compute nodes have limited memory.

When it comes to the question of whether to adopt the use of PIPS-IPM++, several key conditions must be met. First, access to a multi-node computing cluster is recommended or, alternatively, cutting-edge CPUs with more than 256 cores on shared memory systems. This translates to approximately 120 blocks with two cores per block or 60 blocks with four cores per block, which seems like a reasonable lower entry point. Furthermore, due to the additional overhead of annotating and splitting the problem, using PIPS-IPM++ is only recommended for models that exceed several hours of solve time with standard IP solvers or that exceed the available shared memory. Additionally, extra time must be factored in to determine well-performing configurations in terms of the number of blocks and cores used. Regarding the trade-off between configurations optimized for the shortest time or the least compute, the decision depends heavily on the specific usage scenario. The former is especially relevant for academic HPC systems, which often have constraints on the maximum time allowed for each computing job. The latter is potentially more suitable for users running PIPS-IPM++ in cloud computing environments, where computing costs are charged based on usage. In both cases, we expect users to benefit most from significant reductions in the time it takes to solve large linear optimization problems.

Against the background of ever-increasing model complexity and the prevalent design of modern HPC infrastructure, massively parallel solvers for general optimization problems, such as PIPS-IPM++, offer clear advantages compared to other current approaches. While many of these solvers are still in the early stages of research, they have the potential to significantly benefit many different ESOM frameworks in the long term. However, additional development efforts are required for PIPS-IPM++ specifically in terms of numerical stability, testing across multiple platforms, and lowering the entry barrier for using the solver. Regarding the development of ESOM frameworks, different annotations and classes of problem instances must be explored in the future. Some of the most promising approaches that could significantly benefit from the application of solvers like PIPS-IPM++ are capacity expansion planning problems with stochastic economic dispatch, as well as the computation of long-term transformation pathways with perfect foresight. These approaches share a decomposition into capacity expansion and economic dispatch along the time dimension, offering a large number of blocks while keeping the total number of linking variables and constraints relatively low. Going forward, this allows for the efficient solution of increasingly large model instances, such as the assessment of resource adequacy for renewable capacities [37,67] and the outlining of long-term transitions toward systems with high shares of renewable energy technologies and high degrees of sector integration at high temporal resolution [17].

CRediT authorship contribution statement

Manuel Wetzel: Writing – original draft, Visualization, Software, Methodology, Formal analysis, Conceptualization. **Karl-Kiên Cao:** Writing – review & editing, Project administration, Funding acquisition, Formal analysis, Data curation, Conceptualization. **Shima Sasanpour:** Writing – review & editing, Visualization, Investigation.

Declaration of competing interest

The authors declare that they have no known competing financial interests or personal relationships that could have appeared to influence the work reported in this paper.

Acknowledgments

The research for this paper was performed within the projects 'BEAM-ME' and 'UNSEEN' supported by the German Federal Ministry for Economic Affairs and Energy under grant numbers 03ET4023A and 03EI1004A.

The authors gratefully acknowledge the Gauss Centre for Supercomputing e.V. (www.gauss-centre.eu) for funding this project by providing computing time through the John von Neumann Institute for Computing (NIC) on the GCS Supercomputer JUWELS at Jülich Supercomputing Centre (JSC).

Furthermore, the authors thank the developers of PIPS-IPM++ D. Rehfeldt and N. Kempke for providing insights into the solver and debugging encountered errors, F. Fiand for establishing the GAMS/PIPS++ Solverlink and supporting the annotation and optimization of the REMix model, and T. Breuer for his support in utilizing the JUWELS HPC. In addition, we would like to thank all current and former members of the Energy Systems Modeling group at DLR for their continuous contributions to the modeling framework REMix and the input data for the model instances, in particular G. Recht and H. C. Gils, who reviewed the manuscript, J. Buschmann, who contributed to the input data collection for the model instance, and F. Borggrefe, who contributed to the funding acquisition.

Data availability

Model instances from the computational experiment, as well as HPC-specific scripts and configurations, can be provided by the corresponding author upon request.

References

[1] K. Phillips, J.A. Moncada, H. Ergun, E. Delarue, Spatial representation of renewable technologies in generation expansion planning models, Applied Energy 342 (121092) (2023) https://doi.org/10.1016/j.apenergy.2023.121092.

[2] M.M. Frysztacki, J. Hörsch, V. Hagenmeyer, T. Brown, The strong effect of network resolution on electricity system models with high shares of wind and solar, Appl. Energy 291 (116726) (2021) https://doi.org/10.1016/j.apenergy.2021.116726.

[3] J. Haas, F. Cebulla, K. Cao, W. Nowak, R. Palma-Behnke, C. Rahmann, P. Mancarella, Challenges and trends of energy storage expansion planning for flexibility provision in low-carbon power systems – a review, Renew. Sustain. Energy Rev. 80 (2017) 603–619, https://doi.org/10.1016/j.rser.2017.05.201.

[4] K.-K. Cao, K. von Krbek, M. Wetzel, F. Cebulla, S. Schreck, Classification and evaluation of concepts for improving the performance of applied energy system optimization models, Energies 12 (24) (2019) 4656.

[5] L. Kotzur, L. Nolting, M. Hoffmann, T. Groß, A. Smolenko, J. Priesmann, H. Büsing, R. Beer, F. Kullmann, B. Singh, A. Praktiknjo, D. Stolten, M. Robinius, A modeler's guide to handle complexity in energy systems optimization, Adv. Appl. Energy 4 (100063) (2021) https://doi.org/10.1016/j.adapen.2021.100063.

[6] K.-K. Cao, U. Frey, T. Breuer, M. Wetzel, S. Sasanpour, J. Buschmann, K. von Krbek, A. Böhme, A multi-perspective approach for exploring the scenario space of future power systems, in: International Conference on Operations Research - OR 2022, Springer, Aug 2022. URL https://elib.dlr.de/188202/.

[7] B.A. Frew, M.Z. Jacobson, Temporal and spatial tradeoffs in power system modeling with assumptions about storage: an application of the POWER model, Energy 117 (2016) 198–213, https://doi.org/10.1016/j.energy.2016.10.074.

[8] M. Hoffmann, B.U. Schyska, J. Bartels, T. Pelser, J. Behrens, M. Wetzel, H.C. Gils, C.-F. Tang, M. Tillmanns, J. Stock, A. Xhonneux, L. Kotzur, A. Praktiknjo, T. Vogt, P. Jochem, J. Linßen, J.M. Weinand, D. Stolten, A review of mixed-integer linear formulations for framework-based energy system models, Adv. Appl. Energy 16 (100190) (2024) https://doi.org/10.1016/j.adapen.2024.100190.

[9] G. Savvidis, K. Siala, C. Weissbart, L. Schmidt, F. Borggrefe, S. Kumar, K. Pittel, R. Madlener, K. Hufendiek, The gap between energy policy challenges and model capabilities, Energy Policy 125 (2019) 503–520, https://doi.org/10.1016/j.enpol.2018.10.033.

[10] J. DeCarolis, H. Daly, P. Dodds, I. Keppo, L. Francis, W. McDowall, S. Pye, N. Strachan, E. Trutnevyte, W. Usher, M. Winning, S. Yeh, M. Zeyringer, Formalizing best practice for energy system optimization modelling, Appl. Energy 194 (2017) 184–198, https://doi.org/10.1016/j.apenergy.2017.03.001.

[11] J. Wales, A. Zolan, T. Flamand, A. Newman, Decomposing a renewable energy design and dispatch model, Optim. Eng. 26 (1) (2025) 613–653.

[12] A. Zerrahn, W.-P. Schill, Long-run power storage requirements for high shares of renewables: review and a new model, Renew. Sustain. Energy Rev. 79 (2017) 1518–1534.

[13] C.F. Heuberger, E.S. Rubin, I. Staffell, N. Shah, N.M. Dowell, Power capacity expansion planning considering endogenous technology cost learning, Appl. Energy 204 (2017) 831–845, https://doi.org/10.1016/j.apenergy.2017.07.075.

[14] P.V. Gomes, J.T. Saraiva, State-of-the-art of transmission expansion planning: a survey from restructuring to renewable and distributed electricity markets, Int. J. Electr. Power Energy Syst. 111 (2019) 411–424.

[15] F. Neumann, V. Hagenmeyer, T. Brown, Assessments of linear power flow and transmission loss approximations in coordinated capacity expansion problems, Appl. Energy 314 (118859) (2022) https://doi.org/10.1016/j.apenergy.2022.118859.

[16] T. Brown, D. Schlachtberger, A. Kies, S. Schramm, M. Greiner, Synergies of sector coupling and transmission reinforcement in a cost-optimised, highly renewable European energy system, Energy 160 (2018a) 720–739.

[17] J. Hanto, P. Herpich, K. Löffler, K. Hainsch, N. Moskalenko, S. Schmidt, Assessing the implications of hydrogen blending on the European energy system towards 2050, Adv. Appl. Energy 13 (100161) (2024) https://doi.org/10.1016/j.adapen.2023.100161.

[18] R. Martínez-Gordón, M. Sánchez-Diéguez, A. Fattahi, G. Morales-España, J. Sijm, A. Faaij, Modelling a highly decarbonised North Sea energy system in 2050: a multi-national approach, Adv. Appl. Energy 5 (100080) (2022) https://doi.org/10.1016/j.adapen.2021.100080.

[19] J. Priesmann, L. Nolting, A. Praktiknjo, Are complex energy system models more accurate? An intra-model comparison of power system optimization models, Appl. Energy 255 (113783) (2019).

[20] C. Gerbaulet, C. von Hirschhausen, C. Kemfert, C. Lorenz, P.-Y. Oei, European electricity sector decarbonization under different levels of foresight, Renew. Energy 141 (2019) 973–987.

[21] L. Kotzur, P. Markewitz, M. Robinius, D. Stolten, Impact of different time series aggregation methods on optimal energy system design, Renew. Energy 117 (2018) 474–487.

[22] S. Buchholz, M. Gamst, D. Pisinger, A comparative study of time aggregation techniques in relation to power capacity expansion modeling, Top 27 (2019) 353–405.

[23] O. Raventós, J. Bartels, Evaluation of temporal complexity reduction techniques applied to storage expansion planning in power system models, Energies 13 (4) (2020) 988.

[24] A. Akhavein, M.F. Firuzabad, R. Billinton, D. Farokhzad, Review of reduction techniques in the determination of composite system adequacy equivalents, Electr. Power Syst. Res. 80 (12) (2010) 1385–1393, https://doi.org/10.1016/j.epsr.2010.06.002.

[25] M.M. Frysztacki, G. Recht, T. Brown, A comparison of clustering methods for the spatial reduction of renewable electricity optimisation models of Europe, Energy Inform. 5 (1) (2022) 1–28.

[26] M. Macmillan, K. Eurek, W. Cole, M.D. Bazilian, Solving a large energy system optimization model using an open-source solver, Energy Strat. Rev. 38 (100755) (2021).

[27] T. Sharma, J. Glynn, E. Panos, P. Deane, M. Gargiulo, F. Rogan, B.Ó. Gallachóir, High performance computing for energy system optimization models: enhancing the energy policy tool kit, Energy Policy 128 (2019) 66–74, https://doi.org/10.1016/j.enpol.2018.12.055.

[28] G. Giannakidis, B.G. Maryse Labriet, G. Tosato, Informing energy and climate policies using energy systems models, Springer International Publishing, Switzerland. Doi 10 (1007) (2015) 978–983.

[29] Y. Chen, Z. Huang, S. Jin, L. Ang, Computing for power system operation and planning: then, now, and the future, iEnergy 1 (3) (2022) https://doi.org/10.23919/IEN.2022.0037.

[30] A.J. Conejo, E. Castillo, R. Minguez, R. Garcia-Bertrand, Decomposition Techniques in Mathematical Programming: Engineering and Science Applications., Springer Science & Business Media, 2006.

[31] A. Flores-Quiroz, K. Strunz, A distributed computing framework for multi-stage stochastic planning of renewable power systems with energy storage as flexibility option, Appl. Energy 291 (116736) (2021) https://doi.org/10.1016/j.apenergy.2021.116736.

[32] L. Gong, C. Wang, C. Zhang, F. Yong, High-performance computing based fully parallel security-constrained unit commitment with dispatchable transmission network, IEEE Trans. Power Syst. 34 (2) (2019) https://doi.org/10.1109/TPWRS.2018.2876025.

[33] L. Gong, Y. Peng, C. Zhang, F. Yong, Fully parallel optimization of coordinated electricity and natural gas systems on high-performance computing, IEEE Trans. Smart Grid 14 (5) (2023) https://doi.org/10.1109/TSG.2023.3235247.

[34] L. Göke, F. Schmidt, M. Kendziorski, Stabilized Benders decomposition for energy planning under climate uncertainty, Eur. J. Oper. Res. 316 (1) (2024) 183–199.

[35] F. Pecci, J.D. Jenkins, Regularized Benders decomposition for high performance capacity expansion models, in: IEEE Transactions on Power Systems, 2025.

[36] A. Papavasiliou, S.S. Oren, B. Rountree, Applying high performance computing to transmission-constrained stochastic unit commitment for renewable energy integration, IEEE Trans. Power Syst. 30 (3) (2014) 1109–1120.

[37] D. Ávila, A. Papavasiliou, M. Junca, L. Exizidis, Applying high-performance computing to the European resource adequacy Assessment, IEEE Trans. Power Syst. 39 (2) (2024) 3785–3797, https://doi.org/10.1109/TPWRS.2023.3304717.

[38] M. Lubin, C.G. Petra, M. Anitescu, V. Zavala, Scalable stochastic optimization of complex energy systems, in: Proceedings of 2011 International Conference for High Performance Computing, Networking, Storage and Analysis, 2011, pp. 1–64.

[39] C.G. Petra, O. Schenk, M. Anitescu, Real-time stochastic optimization of complex energy systems on high-performance computers, Comput. Sci. Eng. 16 (5) (2014).

[40] J. Wang, N.-Y. Chiang, C.G. Petra, An asynchronous distributed-memory optimization solver for two-stage stochastic programming problems, in: 2021 20th International Symposium on Parallel and Distributed Computing (ISPDC), 2021, pp. 33–40, https://doi.org/10.1109/ISPDC52870.2021.9521613.
[41] S. Shin, M. Anitescu, F. Pacaud, Accelerating optimal power flow with GPUS: SIMD abstraction of nonlinear programs and condensed-space interior-point methods, Electr. Power Syst. Res. 236 (110651) (2024). ISSN 03787796, https://doi.org/10.1016/j.epsr.2024.110651.
[42] K. Świrydowicz, N. Koukpaizan, T. Ribizel, F. Göbel, S. Abhyankar, H. Anzt, S. Peleš, GPU-resident sparse direct linear solvers for alternating current optimal power flow analysis, Int. J. Electr. Power Energy Syst. 155 (109517) (2024). ISSN 01420615, https://doi.org/10.1016/j.ijepes.2023.109517.
[43] J. Dong, J. Cao, Y. Lu, Y. Zhang, L. Jiulong, X. Chongshan, D. Zheng, S. Han, Transmission expansion planning: a deep learning approach, Sustain. Energy Grids Netw. 41 (101585) (2025) https://doi.org/10.1016/j.segan.2024.101585.
[44] D. Rehfeldt, H. Hobbie, D. Schönheit, T. Koch, D. Möst, A. Gleixner, A massively parallel interior-point solver for LPs with generalized arrowhead structure, and applications to energy system models, Eur. J. Oper. Res. 296 (1) (2022).
[45] E. Panos, A. Hassan, Accelerating the performance of large-scale times models in the modelling of sustainable development goals, In M. Labriet; K. Espegren; G. Giannakidis, B.Ó. Gallachóir (Eds.), Aligning the Energy Transition with the Sustainable Development Goals, vol. 101, Springer Nature Switzerland and Imprint Springer, Cham, 2024. ISBN pp. 67–95, 9783031588976 , https://doi.org/10.1007/978-3-031-58897-6_4 of *Lecture Notes in Energy*.
[46] M. Wetzel, E.S.A. Ruiz, F. Witte, J. Schmugge, S. Sasanpour, M. Yeligeti, F. Miorelli, J. Buschmann, K.-K. Cao, N. Wulff, H. Gardian, A. Rubbert, B. Fuchs, Y. Scholz, H.C. Gils, REMix: a GAMS-based framework for optimizing energy system models, J. Open Source Softw. 9 (99) (2024) https://doi.org/10.21105/joss.06330.
[47] H.C. Gils, H. Gardian, J. Schmugge, Interaction of Hydrogen infrastructures with other sector coupling options towards a zero-emission energy system in Germany, Renew. Energy 180 (2021) 140–156, https://doi.org/10.1016/j.renene.2021.08.016.
[48] M. Wetzel, H.C. Gils, V. Bertsch, Green energy carriers and energy sovereignty in a climate neutral European energy system, Renew. Energy 210 (2023) 591–603.
[49] C.K. Nils, PIPS-IPM++ – a massively parallel interior-point method, in: Operations Research 2021, International Conference of the Swiss, German and Austrian Operations Research Societies (SVOR/ASRO, GOR EV, ÖGOR), University of Bern, Switzerland, August 31–September 3, 2021.
[50] K.-K. Cao, M. Wetzel, N.-C. Kempke, T. Koch, Pushing computational boundaries: solving integrated investment planning problems for large-scale energy systems with PIPS-IPM++, in: Operations Research 2021, 2021. URL https://elib.dlr.de/143744/.
[51] T. Khaniyev, S. Elhedhli, F.S. Erenay, Structure detection in mixed-integer programs, Inf. J. Comput. 30 (3) (2018) https://doi.org/10.1287/ijoc.2017.0797.
[52] K.-K. Cao, J. Metzdorf, S. Birbalta, Incorporating power transmission bottlenecks into aggregated energy system models, Sustainability 10 (6) (2018) 1916,.
[53] M. Bröchin, B. Pickering, T. Tröndle, S. Pfenninger, Harder, better, faster, stronger: understanding and improving the tractability of large energy system models, Energy. Sustain. Soc. 14 (1) (2024) https://doi.org/10.1186/s13705-024-00458-z.
[54] O. Schenk, K. Gärtner, Solving unsymmetric sparse systems of linear equations with PARDISO, Futur. Gener. Comput. Syst. 20 (3) (2004). ISSN 0167739X, https://doi.org/10.1016/j.future.2003.07.011.
[55] S.D. Iain, MA57 – a code for the solution of sparse symmetric definite and indefinite systems, ACM Trans. Math. Softw. 30 (2) (2004) 118–144.
[56] F.U. Leuthold, H. Weigt, C. von Hirschhausen, A large-scale spatial optimization model of the European electricity market, Netw. Spat. Econ. 12 (1) (2012). ISSN 1566-113X, https://doi.org/10.1007/s11067-010-9148-1.
[57] R. Kannan, H. Turton, A long-term electricity dispatch model with the TIMES framework, Environ. Model. Assess. 18 (3) (2013). ISSN 1420-2026, https://doi.org/10.1007/s10666-012-9346-y.
[58] T. Brown, J. Hörsch, D. Schlachtberger, PyPSA: Python for power system analysis, J. Open Res. Softw. 6 (1) (2018b) https://doi.org/10.5334/jors.188.
[59] S. Hilpert, C. Kaldemeyer, U. Krien, S. Günther, C. Wingenbach, G. Plessmann, The Open Energy Modelling Framework (oemof) - a new approach to facilitate open science in energy system modelling, Energy Strat. Rev. 22 (2018) 16–25. ISSN 2211467X, https://doi.org/10.1016/j.esr.2018.07.001.
[60] N. Helistö, J. Kiviluoma, J. Ikäheimo, T. Rasku, E. Rinne, C. O'Dwyer, L. Ran, D. Flynn, Backbone—an adaptable energy systems modelling framework, Energies 12 (17) (2019) https://doi.org/10.3390/en12173388.
[61] F. Wiese, R. Bramstoft, H. Koduvere, A.P. Alonso, O. Balyk, J.G. Kirkerud, Å.G. Tveten, T.F. Bolkesjø, M. Münster, H. Ravn, Balmorel open source energy system model, Energy Strat. Rev. 20 (2018) 26–34. ISSN 2211467X, https://doi.org/10.1016/j.esr.2018.01.003.
[62] L. Göke, Anymod.jl: a Julia package for creating energy system models, SoftwareX 16 (100871) (2021). ISSN 23527110, https://doi.org/10.1016/j.softx.2021.100871.
[63] M. Howells, H. Rogner, N. Strachan, C. Heaps, H. Huntington, S. Kypreos, A. Hughes, S. Silveira, J. DeCarolis, M. Bazillian, A. Roehrl, OSeMOSYS: the open source energy modeling system, Energy Policy 39 (10) (2011). ISSN 03014215, https://doi.org/10.1016/j.enpol.2011.06.033.
[64] K. Löffler, K. Hainsch, T. Burandt, P.-Y. Oei, C. Kemfert, C. von Hirschhausen, Designing a model for the global energy system – GENeSYS-MOD: an application of the open-source energy modeling system (OSeMOSYS), Energies 10 (10) (2017) 1468, https://doi.org/10.3390/en10101468.
[65] D. Huppmann, M. Gidden, O. Fricko, P. Kolp, C. Orthofer, M. Pimmer, N. Kushin, A. Vinca, A. Mastrucci, K. Riahi, V. Krey, The MESSAGE Integrated assessment model and the IX modeling platform (IXMP): an open framework for Integrated and cross-cutting analysis of energy, climate, the environment, and sustainable development, Environ. Model. Softw. 112 (2019) 143–156. ISSN 13648152, https://doi.org/10.1016/j.envsoft.2018.11.012.
[66] L. Baumstark, N. Bauer, F. Benke, C. Bertram, B. Stephen, C.C. Gong, J.P. Dietrich, A. Dirnaichner, A. Giannousakis, J. Hilaire, D. Klein, J. Koch, M. Leimbach, A. Levesque, S. Madeddu, A. Malik, A. Merfort, L. Merfort, A. Odenweller, M. Pehl, R.C. Pietzcker, F. Piontek, S. Rauner, R. Rodrigues, M. Rottoli, F. Schreyer, A. Schultes, B. Soergel, Dominika Soergel, Jessica Strefler, Falko Ueckerdt, Elmar Kriegler, and Gunnar Luderer. REMIND2.1: transformation and innovation dynamics of the energy-economic system within climate and sustainability limits, Geosci. Model Dev. 14 (10) (2021) https://doi.org/10.5194/gmd-14-6571-2021.
[67] T.H. Ruggles, E. Virgüez, N. Reich, J. Dowling, H. Bloomfield, E.G.A. Antonini, S.J. Davis, N.S. Lewis, K. Caldeira, Planning reliable wind- and solar-based electricity systems, Adv. Appl. Energy 15 (100185) (2024) https://doi.org/10.1016/j.adapen.2024.100185.

Publication 3: From ambition to reality: The impact of limited capacity expansion rates on the transformation pathway to a climate-neutral European energy system

Authors: Manuel Wetzel, Hans Christian Gils, Valentin Bertsch

Published in: Renewable Energy 258, 2026, doi: 10.1016/j.renene.2025.124917

Methodological advancements: This publication is the first of its kind to address energy system transformation pathways in high temporal and sub-national spatial resolutions, as well as providing detailed network infrastructure, in order to facilitate both pipeline- and port-based energy imports. A novel approach using a community finding algorithm is employed to derive the network topology for joint power and gas infrastructure, maintaining high-capacity long-distance transmission lines throughout the network. In terms of wind turbine expansion, three different classes of wind turbine are utilised for the computation of feed-in profiles based on their respective IEC classification. The study considers the optimal timing for investment, decommissioning and repurposing decisions for energy infrastructure using the capacity model of the reimplemented mathematical formulation. Furthermore, the generic accounting framework of the REMix framework is used to model limitations on national annual capacity expansion rates and VRE capacity expansion targets for individual countries and the Ostend region.

Key findings: The publication emphasises the pivotal role of annual capacity expansion rates and their substantial influence on energy system design. In particular, the high country concentrations, which were also previously observed in *Publication 1*, are significantly limited and compensated for through spatial and technological shifts. This primarily reduces the capacity of installed onshore wind energy in the UK in the short term and installed PV capacities in Spain in the long term. Furthermore, the integration of transformation pathways reveals a crucial interaction between green and blue hydrogen production. Assuming unconstrained capacity expansion, the expectation of decreasing costs for electrolysers and VRE technologies leads to the early adoption of blue hydrogen production from natural gas and a shift in investment in electrolysers to later years. Consequently, this results in a significant investment peak for both electrolysers and PV when the economic conditions for switching from blue to green hydrogen are met. A similar interaction is observed in terms of imports of energy carriers, requiring higher shares of imported hydrogen due to the delayed expansion of electrolysers. Regarding the required network topology, a strong dependence on the relative pricing of different import sources is evident. However, both hydrogen imports and fully domestic production

pipelines connecting regions with good VRE potential to seasonal cavern storage sites are found to be an important design choice across all scenarios.

Author contributions: Manuel Wetzel is the main author of this work. He implemented the mathematical formulation for the transformation pathway, designed the community finding algorithm to generate the network topology, processed the generation profiles for VRE in high spatial resolution, and collected the techno-economic assumptions for the included technologies. Using this comprehensive dataset, he ran the model-based analysis, evaluated and visualised the findings, and wrote the first draft of the manuscript. The authors then jointly discussed the findings and conclusions leading to some further iterations of the model-based assessment. Hans Christian Gils and Valentin Bertsch then edited the manuscript and helped refine the conclusions. Furthermore, Stefan Kronshage provided the demand scenarios, Hans Christian Gils translated the energy scenarios into model inputs, and Jens Schmugge contributed to discussions on the model assumptions. Stefan Kronshage und Jens Schmugge are acknowledged in the publication for their work.

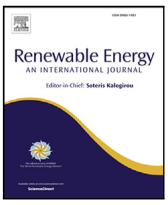
Renewable Energy 258 (2026) 124917



Contents lists available at ScienceDirect

Renewable Energy

journal homepage: www.elsevier.com/locate/renene





From ambition to reality: The impact of limited capacity expansion rates on the transformation pathway to a climate-neutral European energy system

Manuel Wetzel [a,*], Hans Christian Gils [a], Valentin Bertsch [b]

[a] German Aerospace Center (DLR), Institute of Networked Energy Systems, Stuttgart, Germany
[b] Chair of Energy Systems and Energy Economics, Ruhr-Universität Bochum, Bochum, Germany

ARTICLE INFO

Keywords:
Energy system modelling
Transformation pathways
Capacity expansion rates
Green hydrogen
Network topology
REMix

ABSTRACT

The rapid expansion of renewable energy technologies is essential for the successful transition to a climate-neutral European energy system. This is particularly important for producing large quantities of green hydrogen to decarbonise hard-to-abate sectors. However, the annual expansion rate of renewable energy technologies could hinder this transformation. These limitations can stem from various sources, including policy incentives that influence investment decisions, import supply chains, and critical materials. To evaluate the potential impact of these limitations on the transformation pathway, we present a model-based scenario analysis with high temporal and subnational spatial resolution, which explicitly considers import corridors for energy carriers. Our results show that, when national limits on expansion rates are considered, hydrogen production shifts from southern Spain to Germany. Furthermore, our results highlight the need to balance green and blue hydrogen production to avoid an escalation in the required scale-up of photovoltaic and wind technologies. Analysing hydrogen import options reveals their significant impact on network topology. Here, the focus should be on connecting regions rich in renewable resources to hydrogen cavern storage sites. Our findings emphasise the need for European coordination to facilitate the development of sufficient energy infrastructure for a successful transformation.

1. Introduction

Achieving climate neutrality in the European energy system by 2050 will require fundamental changes to energy infrastructure and carriers. Green hydrogen is expected to play an important role in hard-to-abate sectors, such as industry and transport [1]. However, given the short timeframe until 2050, one of the biggest risks to successful implementation is the speed at which the energy system can be transformed [2].

The transition to hydrogen must be coordinated across the entire system, from scaling up electrolysers and renewable energy on the supply side, the conversion of infrastructure for hydrogen transport and storage, and the adoption of green energy carriers on the demand side. Aside from the technical implementation, coordination and harmonisation of the different national regulatory and legal frameworks is required. All of these elements are associated with uncertainties, resulting in a wide range of risks that could affect the transformation path and alter how the system might evolve in the short and long term [3]. This challenge is further exacerbated by the large number of different stakeholders involved in the transition towards hydrogen as a key energy carrier [4].

In this paper, we assess the performance of energy transformation pathways towards a climate-neutral energy system in Europe. Specifically, we focus on the techno-economic implementation of hydrogen infrastructure, assessing the impact of varying annual expansion rates for renewable energy technologies and networks. This is achieved by computing the least-cost energy system transformation pathways with high spatial and temporal detail for a variety of scenarios. To take into account various factors influencing the transformation, we consider three clusters of challenges, namely production-side scale-up, system transformation inertia, and long-term strategic uncertainties, as specified in the following.

1.1. Scaling-up capacities

With the increasing deployment of variable renewable energy (VRE) technologies for power generation amounting to a global annual expansion of photovoltaics (PV) capacity by 426 GW and wind turbine capacity by 116 GW in 2023 [5], the vision of a climate-neutral energy system is becoming a reality. However, as renewable energy sources in 2024 still only contributed 31.9% (15% from VRE) to global electricity

* Correspondence to: Curiestraße 4, 70563 Stuttgart, Germany.
E-mail addresses: manuel.wetzel@dlr.de (M. Wetzel), hans-christian.gils@dlr.de (H.C. Gils), valentin.bertsch@rub.de (V. Bertsch).

https://doi.org/10.1016/j.renene.2025.124917
Received 24 June 2025; Received in revised form 21 October 2025; Accepted 6 November 2025
Available online 1 December 2025
0960-1481/© 2025 The Authors. Published by Elsevier Ltd. This is an open access article under the CC BY license (http://creativecommons.org/licenses/by/4.0/).

List of abbreviations

ATR	Autothermal reforming
BEV	Battery electric vehicles
BECCS	Bioenergy with carbon capture and storage
CDR	Carbon dioxide removal
CCS	Carbon capture and storage
CSP	Concentrated solar power
DAC	Direct air capture
DEA	Danish Energy Agency
CETO	Clean Energy Technology Observatory
EU	European Union
ESOM	Energy system optimisation model
GASP	Global Atlas for Siting Parameters
IEA	International Energy Agency
JRC	Joint Research Centre
LNG	Liquefied natural gas
NECP	National energy and climate plan
NG	Natural gas
PECD	Pan-European Climate Database
PV	Photovoltaics
RFNBO	Renewable fuel of non-biological origin
SAF	Sustainable aviation fuel
SMR	Steam methane reforming
SNG	Synthetic natural gas
UK	United Kingdom
VRE	Variable renewable energy

generation and 41.6% (19.5%) in Europe [6] there is a long way to go, in particular when it comes to the direct and indirect electrification of hard-to-abate sectors. This relates to the fundamental challenge of scaling up investments in and deployment of VRE technologies, as well as electrolysers for green hydrogen production.

The dynamics associated with this scale-up have previously been described for renewable capacities using S-curve approaches to capture logistic-type growth behaviour, reflecting the different formation, growth, and saturation phases based on historical expansion rates [7]. However, particularly for model-based assessments, including upper limits on annual growth rates and generalising to a wide range of model regions remains challenging due to data availability [8]. Furthermore, there is a close interaction between the growth of renewable technologies and the emergence of a hydrogen market. While diminishing revenues from simultaneous feed-in from VRE are discussed as a possible cause of growth saturation [9], demand-side flexibility from electrolysis can mitigate this problem but depends heavily on the dynamics of hydrogen market uptake [10]. This strong interdependence further complicates quantitative assessment and extrapolation for the future.

Furthermore, additional factors can limit this scale-up, such as the availability of energy technologies in the form of PV panels and electrolyser stacks, as well as more indirect factors, such as the availability of skilled workers [11], permitting procedures [5], long-term planning for grid integration [5], and access to critical materials [12]. These factors must be considered for each technology individually. In the case of PV, the main challenge is Europe's high import dependency, accounting for up to 90% of the main components, such as solar cells and electronics for inverters [13]. For wind energy, domestic production of wind turbines accounts for the entire offshore market and 88% of the onshore market, but reliance on a single country for critical raw materials remains a key issue [14]. In 2024, European capacities for domestic electrolyser manufacturing amounted up to 10.2 GW_{H_2}/a with additional 2.7 GW_{H_2}/a under construction [15], still lagging behind the stated goal of an annual electrolyser manufacturing capacity of 17.5 GW_{H_2}/a by 2025.

1.2. Inertia of systems transformation

Infrastructure projects take a long time from planning to completion, and their effects on system design can last for several decades [16], requiring long-term planning. Many uncertainties must be considered during the planning phase, such as the future development of energy carrier demand. This is further complicated in the case of natural gas (NG) and hydrogen (H_2), as they compete with each other for the same pipeline infrastructure. This leads not only to timing and capacity conflicts regarding the repurposing of pipelines, but also to significant challenges with respect to regional gas distribution systems. These systems may become financially unviable or require complete conversion to hydrogen, affecting all end consumers simultaneously. This, in turn, could result in higher overall costs than those associated with electrification or the use of synthetic methane [17].

A large number of European countries provide political targets for the expansion of VRE technologies as part of their national energy and climate plans (NECPs), which are agreements between the European Union (EU) and its member states on the planned development of capacities, the share of renewable energy, and the phasing out of fossil fuels. Therefore, another factor influencing system inertia is the regulatory framework and investment incentives used by countries to meet their targets. Ambitious targets, in turn, require the early and continuous expansion of renewable technologies [18].

Against this background, the modelling of perfect foresight transformation pathways can provide additional insights to distinguish between stranded investments and bridging technologies [19], and ensure that the transformation begins early enough to meet national capacity targets. Additionally, possible end-of-life synergies can be considered during the optimisation. For example, the offshore production of hydrogen could switch from blue to green after gas fields have been depleted, or the economic phase-out is triggered by reduced electrolyser costs and higher carbon prices [20].

1.3. Long-term uncertainties and import strategy

For VRE and electrolysers, future uncertainties primarily concern the potential for increased efficiency and reduced costs through technological development and the use of innovative materials. In contrast, there is greater uncertainty regarding the technological viability of other technologies. These include direct air capture (DAC) [21,22] to enable the production of synthetic fuels, the combination autothermal reforming (ATR) and carbon capture and storage (CCS) for the production of blue hydrogen with a high capture rate [20], and technologies for the long-distance transport of hydrogen, such as liquid hydrogen (LH_2) ships and the corresponding port infrastructure [23]. While prototypes of these technologies exist, their large-scale implementation remains to be proven.

Another highly uncertain and impactful aspect is the uptake of a global hydrogen market [24]. This encompasses not only available volumes and prices at European ports, but also global competition and supply routes. In the short term especially, importing hydrogen via pipelines can be cheaper than ship-based imports. However, pipeline-based imports to Europe are limited to a few countries. Similarly, the required pipeline system, cavern storage, and strategic positioning in relation to domestic production will differ significantly depending on the establishment of a global hydrogen market.

In this case, having prior knowledge of import options during perfect foresight optimisation allows for the consideration of future hydrogen availability. However, this approach provides limited information on how the system can adapt to different scenarios. To estimate the range of possible systems, we consider different extremes, where cost shifts are observable or certain supply technologies are excluded.

1.4. Modelling transformation pathways in high spatial and temporal resolution

Providing insights to inform decisions relating to the scaling up of capacities, systems inertia, and long-term uncertainties can be achieved by computing transformation pathway scenarios using energy system optimisation models (ESOMs). These models have become a widely used method of providing decision-makers with a range of alternatives and important considerations [25]. This extends to a large number of studies showing the viability of climate-neutral systems in 2050 with high VRE shares [26], the future role of hydrogen in the European energy system [3,19,27], and a possible realisation of a global hydrogen trade system [28]. All underlying studies demonstrate the need for a significant increase in VRE capacity, as well as the efficient use of transmission networks and storage systems to balance energy carriers spatially and temporally.

In general, representation of transformation pathways ESOMs falls under three categories: optimisation of target years; transformation pathways with myopic foresight; or transformation pathways with perfect foresight. An additional consideration of high technological, temporal, and spatial detail of the modelled system drives the size of the resulting optimisation problem, often leading to computational challenges. To deal with this challenge, trade-offs between different model dimensions are required [29].

The strength of target year optimisation lies in its high spatial and temporal resolution, which provides insights into long-term static systems. Typically, large contributions from VRE technologies are part of the least-cost solution, and the strong effect of spatial and temporal balancing in the form of power grids, gas pipelines, and energy storage can be observed [30]. This approach is especially useful for assessing the overall design and operation of the energy infrastructure and detailed network topology. However, the single-year nature of the optimisation limits the insights into optimal timing.

Target year models can be extended to a myopic approach across multiple model years, to obtain some information about the transformation pathway. Capacities from a target year optimisation are considered in each of the subsequent years. This rolling horizon approach can include either a single year per iteration, or include one or more years of foresight into the future. However, considering longer periods of foresight, again, leads to larger optimisation problems and greater computational challenges. Conversely, shorter periods of foresight can result in more stranded investments if transformation pathways are optimised without sufficient foresight [31].

In contrast, pathway optimisation models with perfect foresight typically use aggregation methods for the temporal dimension. These methods use representative days or peak hours to model demand peaks [32], thereby managing the computational burden. However, this creates new challenges when it comes to representing long-term energy storage technologies, such as gas caverns, and the intermittent nature of VRE [33]. Conservative estimation of VRE technologies, in particular, leads to a significantly higher utilisation of gas-fired power plants during peak hours compared to hourly resolved models with high spatial resolution, accounting for up to 10% of annual electricity generation in 2050 [34]. Similarly, models that implement endogenous learning require transformation pathways with perfect foresight, but due to the necessity of using mixed integer formulations, they have to accept even stricter limitations in their spatial and temporal resolution [35].

In their recently published work, Fleiter et al. [3] assess a wide range of possible hydrogen demand scenarios for the European energy system until 2050. To achieve this, they employed perfect foresight pathway optimisation with a high temporal resolution. To stay within computational limitations, they opt for a spatial resolution at country level and group smaller countries such as the Baltic States and the Balkans together. However, this approach restricts their ability to provide insights into network requirements and the spatial allocation of energy conversion and storage technologies across Europe.

1.5. Contribution and research questions

Our contribution to the existing literature involves modelling of transformation pathways for the European energy system between 2030 and 2050 at a subnational level and with detailed temporal resolution, focusing specifically on hydrogen supply infrastructure. A key novelty in model design, compared to earlier work, is the explicit modelling of port infrastructure as part of the gas network for energy imports. The application of the model focuses on the often-overlooked issue of limited capacity expansion rates for VRE, which could impede the transformation, particularly with regard to the provision of substantial amounts of domestic hydrogen. Our model-based analysis addresses the following research questions:

- How do the realisable VRE expansion rates and the available CO_2 emissions budgets influence the use of different technologies for providing electricity, hydrogen and methane along the transformation path to 2050?
- Are the national targets for VRE expansion in line with realisable renewable energy expansion rates, and do these targets enable substantial shares of domestic hydrogen production in Europe and individual countries?
- How do delays in the hydrogen network deployment and availability of import options affect the optimal system design, and how do these factors interact with the VRE expansion rates?

To answer these research questions, we systematically analyse a wide range of scenarios using a comprehensive ESOM framework. The scenarios comprise a variety of assumptions regarding national limitations on the expansion rates for VRE technologies, the permitted carbon budget for transformation pathways, different political targets for VRE capacities, short-term network infrastructure delays, and long-term uncertainties associated with hydrogen import.

The remainder of this paper is structured as follows: Section 2 outlines the model formulation and the general input data which are used across all scenarios. Section 3 provides an overview of the scenarios and the assumptions on the annual capacity expansion rates considered in this study. Section 4 presents the results from the model-based assessment and contextualises the findings within the broader scope of similar modelling activities. Section 5 critically reflects on the limitations of the study and outlines possible future research directions to address. Finally, Section 6 summarises the key findings and draws conclusions from them.

2. Model scope and input data

To evaluate the impact of different scenarios on the most cost-effective pathway towards climate neutrality, we employ the open-source energy system modelling framework REMix [36]. This framework is used to create a detailed model of the European energy system and calculate the most cost-effective transformation pathways. These pathways consider the integrated optimisation of capacity expansion and economic dispatch in five-year increments from 2030 to 2050. All considered years are optimised simultaneously using a perfect foresight approach to limit stranded investments and pre-emptive overshoot of the permitted carbon budget. The model covers all EU countries located in continental Europe, as well as Switzerland, Norway, the British Isles, and the EU membership candidate countries in south-east Europe (Fig. 1). The model explicitly considers all infrastructures for producing, storing, and transporting electricity, hydrogen, and methane. Energy demand in the industry, heating, and transport sectors is considered based on their respective energy carriers.

2.1. Pathway methodology

To model the overall system cost along the transformation pathway, REMix uses the logic that all costs are annualised and refinanced over the technical lifetime of the infrastructure, in order to make investments between technologies comparable and to correctly account for the end of the optimisation horizon. Similar to other studies on transformation pathways [37,38], a socioeconomic discount rate of 2% and a cost of capital of 8% are used for the weighting between different technologies and model years. The highly generalised accounting model in REMix enables detailed constraints to be established in a simplified manner by associating indicators with various components of the optimisation model. Several of required modelling features used in this study, such as carbon budgets, limits on annual capacity expansion rates and capacity targets can be derived from it, as described below. For a more detailed nomenclature of the mathematical model description see Appendix.

Eq. (1) provides the generalised accounting form, which comprises contributions from the expansion and decommissioning of energy conversion units, and fixed costs of existing power plants (1a). Similar contributions are considered for network infrastructure (1b). The remaining terms relate to dispatch decisions made during infrastructure operation. It considers contributions from conversion activities, such as power generation (1c), energy transfers between model regions (1d), and imports or exports across the system boundaries (1e).

$$j_i = \sum_{y\in Y} W_{y,i} \cdot \Bigg(\sum_{n\in N, p\in P} J^{\text{build}}_{i,n,y,p} \cdot \Delta x^{+}_{n,y,p} + J^{\text{fix}}_{i,n,y,p} \cdot x_{n,y,p} + J^{\text{decom}}_{i,n,y,p} \cdot \Delta x^{-}_{n,y,p} \tag{1a}$$

$$+ \sum_{l\in L, p\in P_L} J^{\text{build}}_{i,l,y,p} \cdot \Delta x^{+}_{l,y,p} + J^{\text{fix}}_{i,l,y,p} \cdot x_{l,y,p} + J^{\text{decom}}_{i,l,y,p} \cdot \Delta x^{-}_{l,y,p} \tag{1b}$$

$$+ \sum_{t\in T, n\in N, p\in P_C, a\in A} J^{\text{var}}_{i,t,n,y,p,a} \cdot d_{t,n,y,p,a} \tag{1c}$$

$$+ \sum_{t\in T, l\in L, p\in P_L} J^{\text{flow}}_{i,t,l,y,p} \cdot \left(f^{+}_{t,l,y,p,q} + f^{-}_{t,l,y,p,q} \right) \tag{1d}$$

$$+ \sum_{t\in T, n\in N, q\in Q} J^{\text{import}}_{i,t,n,y,q} \cdot g^{+}_{t,n,y,q} + J^{\text{export}}_{i,t,n,y,q} \cdot g^{-}_{t,n,y,q} \Bigg) \tag{1e}$$

$$\forall i \in I$$

To keep track of the total number of installed technologies, Eq. (2) provides a balance of the added and decommissioned capacities throughout the transformation pathway. To ensure that capacities are decommissioned, Eq. (3) sums up both the added and decommissioned capacities up to any given year, offset by the maximum lifetime of the technology in question. This formulation allows capacities to be decommissioned flexibly, while ensuring that plants are decommissioned by the end of their respective lifetimes at the latest.

$$x_{n,y,p} = x_{n,y-1,p} + \Delta x^{+}_{n,y,p} - \Delta x^{-}_{n,y,v} \qquad \forall n \in N, y \in Y, p \in P \tag{2}$$

$$\sum_{y'\le y-\lambda_v} \Delta x^{+}_{n,y',p} \le \sum_{y'\le y} \Delta x^{-}_{n,y',p} \qquad \forall n \in N, y \in Y, p \in P \tag{3}$$

If capacities can only be decommissioned at the end of their lifetime, without repurposing or decommissioning costs being taken into account, Eqs. (2) and (3) can be substituted by Eq. (4), which uses a backward-looking rolling horizon over the lifetime to limit the number of decision variables and reduce the computational burden.

$$x_{n,y,p} = \sum_{y-\lambda_v<y'\le y} \Delta x^{+}_{n,y',p} \qquad \forall n \in N, y \in Y, p \in P \tag{4}$$

The limitations on carbon budgets and the available gas reserves from offshore fields in Eq. (5) can be derived from the generalised accounting by using the relevant factors for carbon-emitting activities and gas extraction. The weighting factor ensures that annual emissions are scaled up to account for a time period of five years.

$$\sum_{y\in Y} W_{y,CO_2} \cdot \Bigg(\sum_{t\in T, n\in N, p\in P_C, a\in A} J^{\text{var}}_{CO_2,t,n,y,p,a} \cdot d_{t,n,y,p,a} + \sum_{t\in T, n\in N, q\in Q} J^{\text{import}}_{CO_2,t,n,y,q} \cdot g^{+}_{t,n,y,q} + J^{\text{export}}_{CO_2,t,n,y,q} \cdot g^{-}_{t,n,y,q} \Bigg) \le J^{CO_2 budget} \tag{5}$$

Similarly, annual capacity expansion rates can be constrained on a per-country and per-year basis by Eq. (6).

$$\Delta x^{+}_{n,y,p} \le X^{max}_{n,y,p} \qquad \forall n \in N, y \in Y, p \in P \tag{6}$$

Likewise, capacity targets can be specified including their corresponding slack variables. The slack variables enable the determination of the capacity gap between stated policy and maximum expansion under limited expansion rates, as shown in Eq. (7)

$$x_{n,y,p} + x^{slack}_{n,y,p} \ge X^{target}_{n,y,p} \qquad \forall n \in N, y \in Y, p \in P \tag{7}$$

2.2. Input data and assumptions

For the annual energy demands we generate a dataset for all European countries based on the *Clean Planet for All* study by the European Commission [39]. Here, we consider a demand-side scenario H_2 which focuses on the increased use of hydrogen, particularly in the industrial and transport sectors and, to a limited extent, in space heating. We treat the demand scenarios as model-exogenous input to derive the required infrastructure transformations for supply, storage, and transmission across the system. The annual demand data is distributed into hourly profiles for electricity, hydrogen, and methane using the extremOS profiles [40] and is aggregated from NUTS3 areas to the model regions used in this study.

The existing network between model regions is derived from the sci2Grid_gas dataset [41] and the ENTSO-E grid map, which was created using an updated version of GridKit [42]. These two high-resolution networks are combined into a single network graph by adding edges between power and gas nodes in close proximity. The network topology is then partitioned using a community-finding algorithm, which is calibrated to identify the most relevant long-distance and large-capacity transfer options for electricity and gas. This ensures the network adequately reflects the pan-European transmission infrastructure, while also enabling national boundaries to be maintained and larger European countries to be divided into multiple regions based on their respective network topology. This preserves both cross-border and internal transmission bottlenecks. The resulting European network comprises 83 regions, including sub-national regions in 16 countries. In addition to these regions, the model explicitly incorporates 28 LNG terminals, four import nodes and two offshore hubs using a reduced set of technologies.

In terms of existing gas infrastructure, the capacities of LNG terminals and cavern storage are based on the sci2grid dataset and are connected to the gas network via their respective pipeline connections. Natural gas cavern storage sites and pipeline infrastructure can be decommissioned before the end of their technical lifetime to enable the model endogenous repurposing towards hydrogen, as described in a previous study [43]. Imports of gases via pipelines from outside the scope of the model are permitted based on realised gas imports in 2024, as provided by the ENTSO-G gas flow dashboard [44]. Imports of natural gas amounted to 107 TWh_{CH_4} from Algeria to Spain, 223 TWh_{CH_4} from Tunisia to Italy, 322 TWh_{CH_4} from Turkey to Greece and Bulgaria, and 169 TWh_{CH_4} from Ukraine to Slovakia. We assume that, by 2030, only 20% of energy imports can come from green hydrogen or synthetic methane, with this volumetric share gradually increasing to 100% by 2045. (0.2, 0.3, 0.5, 1.0, 1.0 for the 5-year intervals between 2030 and 2050). Alternatively, blue hydrogen can be produced from steam methane reforming (SMR) and ATR with CCS and transported through pipelines repurposed for hydrogen.

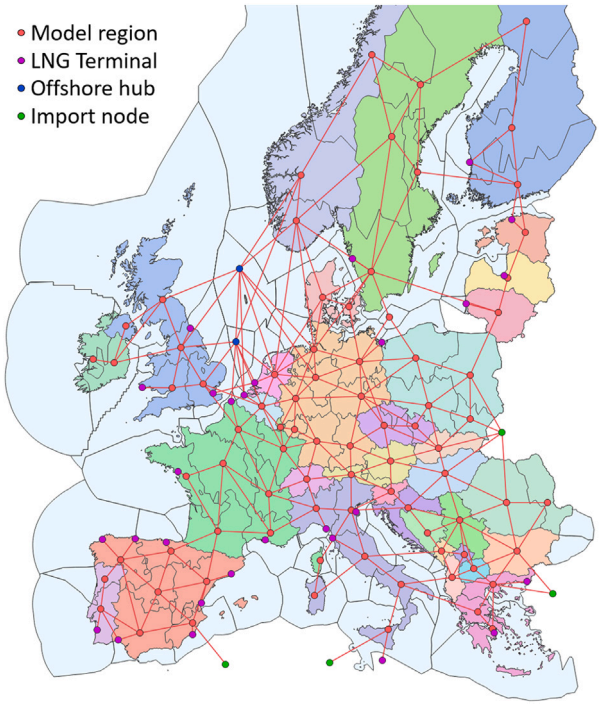


Fig. 1. Geographical scope and network topology of the case study. Model regions (red vertices) contain the full set of technologies for capacity expansion and hourly energy demand. LNG terminals (purple vertices), offshore hubs (blue vertices), and import nodes (green vertices) contain no energy demand and a reduced set of technologies. Network corridors (red edges) represent existing grid and pipeline connections that can be further expanded or, in the case of natural gas pipelines, repurposed for hydrogen use.

Similarly, the extraction and distribution of natural gas from the North Sea via offshore pipelines is based on recent production levels. The maximum permitted extraction of natural gas is based on the 2024 annual production volumes of 192 TWh for the United Kingdom and 1225 TWh for Norway [44], which is mapped to the two offshore hubs in the North Sea. The duration for which the offshore natural gas reserves will last is highly uncertain and depends significantly on additional exploration activities, which in turn depend on future policies and incentives for blue hydrogen. To estimate the overall energy amounts that can be freely allocated along the transformation pathway, we assume remaining extraction times of 5 and 15 years for the gas fields in the UK and Norwegian gas fields, respectively.

In order to enable model-endogenous investment in hydrogen offshore hubs, the North Sea area and the island of Bornholm are included as separate regions. Infrastructure expansion can take the form of either wind farms connected via undersea cables or direct offshore electrolysis with transport via pipeline infrastructure [45]. Additionally, the offshore hubs in the North Sea are used for the domestic extraction of natural gas, which can be converted to grey or blue hydrogen via SMR and ATR. Blue hydrogen can be produced via SMR-CCS with a carbon capture rate of 56% or ATR-CCS with a carbon capture rate of 90%, as detailed in the supplementary information provided by Ueckerdt et al. [20]. To better observe the timing between the technologies, the capacity expansion of ATR-CCS is only permitted from the second modelling year (2035) onwards. While carbon networks are also gaining increasing attention as a potential CCS option in industry [46], this study only considers blue hydrogen production in close proximity to gas extraction sites [47].

The existing capacities of conventional power plants are based on data from the Global Nuclear Power Tracker [48], the Global Oil and Gas Plant Tracker [49], and Beyond Fossil Fuels for coal plants [50]. These capacities are then allocated to subnational clusters using Voronoi polygons derived from the network nodes. Similarly, hydro capacities are derived from the Joint Research Centre (JRC) hydropower dataset [51] using normalised hourly profiles from the Pan-European Climate Database (PECD) [52]. Capacities for existing VRE technologies are taken from Eurostat [53], grouped into five-year intervals for capacity expansion, and allocated to model regions based on spatial distribution factors derived from the region specific maximum permitted installation for PV and wind turbines. The techno-economic assumptions for most technologies are taken from technology catalogues provided by the Danish Energy Agency (DEA) [54]. To ensure security of supply for electricity, for each of the model regions the capacity for firm-capacity power plants, such as gas-fired turbines using either synthetic methane or hydrogen, must be at least as high as the peak hour of the inflexible electricity demand.

Renewable energy power generation profiles are calculated using the COSMO-REA6 weather reanalysis [55] and the CORINE land cover dataset [56], in order to account for suitable and restricted areas for the expansion of renewable energy technologies. For wind turbines, the potential is categorised according to IEC 61400 classes using geospatial information from the Global Atlas for Siting Parameters (GASP) project [57]. The power curves are modelled using data from three different Vestas turbines (V112, V124, V136) with hub heights (91.5 m, 117 m, 155 m) corresponding to turbines with similar power densities. To reflect the wide range of conditions affecting VRE generation profiles, the weather years between 2012 and 2016 from the REA6 reanalysis are mapped, in chronological order, to the model years between 2030 and 2050 along the transformation pathway.

3. Scenario design

To answer the research questions raised in Section 1, we design a multi-layer scenario approach in which the different key parameters influencing the transformation pathways of the European energy system are varied. To identify a wide range of possible pathways towards climate neutrality, we consider the following variations: (1) the available carbon budget for power generation and downstream emissions for industry and heating, (2) the achievable speed for capacity expansion of VRE technologies across Europe, (3) the achievement of policy targets for renewable energy technologies as outlined in European and national policies such as the NECPs and the Ostend Declaration,[1] (4) possible delays in expanding the European network infrastructure, particularly in repurposing existing pipelines for hydrogen, and (5) the available volumes and prices of future pipeline- and port-based hydrogen imports.

These five aspects are grouped into three categories according to the research questions to be answered, and their respective scenario assumptions are specified below. Section 3.1 is dedicated to the interaction between the available CO_2 budget and achievable VRE expansion rates. Section 3.2 builds on this by explaining how the political expansion targets are incorporated into the model. Finally, Section 3.3 provides the assumptions for the delays in developing hydrogen networks and the availability of various import options. The subsequent model results in Section 4 follow the same structure. Fig. 2 summarises this structure and the key variations per scenario dimension.

[1] The Ostend Declaration is an agreement on the joint expansion of offshore wind energy and infrastructure between the European countries bordering the North Sea [58]. These countries include the United Kingdom (UK), Ireland, France, Belgium, the Netherlands, Germany, Denmark, and Norway.

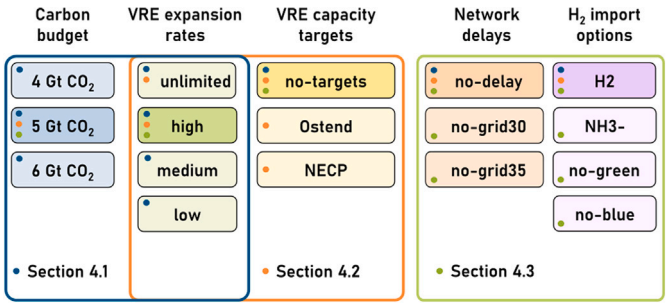


Fig. 2. Overview of the scenario variation combinations in this study. The coloured dots indicate the variations considered in each of the results sections, while the coloured boxes indicate the key variations each section focuses on.

3.1. Carbon budgets and VRE expansion rates

The cumulative carbon emissions in the time frame between 2030 and 2050 are one of the main drivers of the speed of transformation, as achieving a lower cumulative sum requires more ambitious and rapid emissions reductions and faster VRE expansion. Taking into account downstream emissions from the model-exogenous demand for methane, the cumulative baseline for the carbon budget is 5.5 Gt_{CO_2}. If the allowed cumulative carbon budget is higher than this baseline, additional emissions from fossil power plants or the production of grey and blue hydrogen is possible. Conversely, a lower cumulative carbon budget requires additional use of DAC in order to produce synthetic methane and close the carbon cycle. Against this baseline, we consider three different variations of 4, 5, and 6 Gt_{CO_2} as an available cumulative carbon budget across all model years, providing scenarios with different levels of ambition for reducing emissions.

The achievable annual capacity expansion rates are extrapolated based on the International Energy Agency (IEA) report on the expected progress of renewable energy technologies [5]. The study considers various influencing factors, such as historical expansion rates, falling investment costs, policy incentives and manufacturing capacities. While the outlook only provides information on the expected expansion between 2024 and 2030, any progress or delays will affect subsequent decades. Therefore, we use this dataset as a per-country baseline, limiting the expansion of VRE technologies while increasing the capacity expansion rates towards later model years to account for future efforts. Specifically, we derive a *high* expansion scenario based on the accelerated case, using the following factors for the five model years between 2030 and 2050: 1.0, 1.2, 1.5, 2.0, 2.0. For the scenarios *medium* and *low* scenarios, we use the main case as a baseline with the following factors: 1.0, 1.2, 1.5, 2.0 and 2.0, and 0.8, 1.0, 1.2, 1.5 and 2.0, respectively. The resulting annual expansion rates for each model year and country with the highest expected expansion rate for each VRE technology are listed in Table 1. To assess the impact of limited expansion rates, we also consider an *unlimited* scenario, in which annual capacity expansion rates are not constrained.

3.2. Political VRE expansion targets

To consider the stated policy targets for the expansion of VRE in European countries, we utilise the dataset from the EU NECP tracker compiled by Ember [59]. In terms of capacity targets for PV Germany has the most ambitious targets by far, with 215 GW by 2030 and 400 GW by 2040, followed by Spain with 95 GW and Italy with 79 GW, both of which are planned to be reached by 2030. A similar pattern emerges for onshore wind energy: Germany aims to reach 115 GW by 2030 and 160 GW by 2040, followed by France with 37 GW by 2030 and Italy with 26 GW by 2030. While the NECPs outline additional targets, such as the phase-out of fossil power plants and target shares for renewable electricity, we only consider the targets for VRE expansion.

With regard to the joint expansion of offshore wind energy in the North Sea, as set out in the Ostend Declaration [58], equally ambitious targets have been agreed upon. The joint targets to be reached across all participating countries are 120 GW by 2030 and 300 GW by 2050. Country-specific contributions for 2030 are led by the UK with 30 GW, followed by Germany with 26 GW and the Netherlands with 21 GW. By 2050, Germany's target is 66 GW, followed by the Netherlands with 50 GW, Denmark with 35 GW, and Norway with 30 GW.

Although the capacity targets for NECPs and the Ostend Declaration should be considered simultaneously, we are treating them as separate scenarios to better isolate their respective impacts on spatial shifts in domestic hydrogen production. To ensure that capacity targets are met despite delays caused by limited annual capacity expansion rates, slack variables are introduced to penalise any capacity gaps between the total installed capacity and the target capacity. For intermediate years without explicit capacity targets, the most recent active target remains in place.

3.3. Network expansion delays and hydrogen import options

With regard to infrastructure delays, we consider the three variations *no-delay*, *no-grid30*, and *no-grid35*. In the first variation, capacity expansion for power grids and pipelines (including the repurposing of natural gas pipelines for hydrogen) is permitted in all model years. In contrast, the two latter variations prevent the short-term expansion in the model years 2030 and 2030 to 2035, respectively. While the expansion of new hydrogen pipelines along the corridors between model regions is unlimited, repurposing natural gas pipelines for hydrogen use requires the same number of natural gas pipelines to be decommissioned in the same model year and corridor. However, repurposing comes at a significantly lower cost of 1.1 M€/km compared to 3.4 M€/km, when investing into new hydrogen pipelines [60].

In terms of hydrogen import costs, we consider the variations H_2, NH_3-, *no-blue*, and *no-green*. H_2 reflects the baseline assumptions on hydrogen prices, taking into account all available sources. Pipeline-based imports can enter the system via the import nodes, ship-based imports are facilitated in the LNG terminal nodes, and extraction of NG takes place in the offshore hubs.

The large uncertainty surrounding the costs of producing and importing green hydrogen can be seen in previous literature estimates. Weißenburger et al. compare a range of literature values for hydrogen imports to Germany, deriving several price pathways ranging from 80–250 €/MWh_{H_2} in 2030 to 50–165 €/MWh_{H_2} in 2050, with the largest number of literature values for 2050 clustered between 50–90 €/MWh_{H_2} [61]. Similarly, Schmitz et al. provide price pathways ranging from 69–149 €/MWh_{H_2} for hydrogen and 92–186 €/MWh_{CH_4} for synthetic methane in 2030 and respectively 73–98 €/MWh_{H_2} and 95–134 €/MWh_{CH_4} in 2050 [62]. However, it should be noted that in the study by Schmitz et al. only the high-price scenario is based entirely on green hydrogen; the medium-price scenario considers a mix of green and blue hydrogen, and the low-price scenario assumes only blue hydrogen.

The TYDNP 2024 scenarios are significantly more optimistic, assuming that by 2040, the cost of hydrogen will range between 27–73 €/MWh_{H_2} depending on the scenario and country of origin [63]. The dataset also provides long-term import cost estimates for ship-based hydrogen imports using ammonia (NH_3) as a transport vector, derived using a global import assessment tool. This yields reference values for hydrogen imports at European ports of 138, 108, and 87 €/MWh_{H_2} for the years 2030, 2040 and 2050, respectively. Furthermore, the cost range is differentiated between the two scenarios, resulting in a range of hydrogen importing costs between 69–104 €/MWh_{H_2} in 2050.

Table 2 provides an overview of the import costs assumed in this study, which have been derived in part from the above-mentioned

Table 1
Assumptions on the maximum annual expansion rate in GW/a for the scenarios *low* and *high* and the European countries with the highest annual capacity expansion of VRE for each technology.

		Scenario *low*					Scenario *high*				
		2030	2035	2040	2045	2050	2030	2035	2040	2045	2050
PV utility scale	Germany	11.1	13.9	16.6	20.8	27.7	15.8	18.9	23.7	31.6	31.6
	Spain	3.9	4.9	5.8	7.3	9.7	8.5	10.2	12.8	17.0	17.0
	United Kingdom	3.6	4.5	5.4	6.8	9.0	5.8	6.9	8.7	11.6	11.6
	France	2.3	2.9	3.5	4.3	5.8	4.3	5.2	6.5	8.7	8.7
PV distributed	Germany	9.6	12.0	14.4	18.0	24.0	16.3	19.6	24.5	32.6	32.6
	Italy	4.8	6.1	7.3	9.1	12.1	7.3	8.7	10.9	14.5	14.5
	Netherlands	3.6	4.5	5.4	6.8	9.0	5.2	6.2	7.7	10.3	10.3
	France	3.0	3.7	4.4	5.5	7.4	4.2	5.1	6.3	8.4	8.4
Wind onshore	Germany	6.2	7.8	9.3	11.6	15.5	9.8	11.7	14.7	19.6	19.6
	United Kingdom	2.2	2.7	3.2	4.0	5.4	3.3	3.9	4.9	6.5	6.5
	France	2.0	2.4	2.9	3.7	4.9	2.9	3.5	4.3	5.8	5.8
	Italy	1.6	2.1	2.5	3.1	4.1	2.8	3.4	4.2	5.6	5.6
Wind offshore	Germany	2.0	2.6	3.1	3.8	5.1	4.6	5.5	6.8	9.1	9.1
	United Kingdom	3.1	3.8	4.6	5.8	7.7	4.2	5.1	6.4	8.5	8.5
	Netherlands	1.3	1.6	2.0	2.5	3.3	2.0	2.4	3.1	4.1	4.1
	Denmark	1.0	1.2	1.4	1.8	2.4	1.6	1.9	2.4	3.2	3.2

Table 2
Assumptions on import costs for energy carriers and model years for the base scenario H_2, the reduced cost scenario for a global hydrogen market using ammonia as transport vector NH_3- and the scenario without imports of green energy carriers *no-green*. Costs for H_2 and NH_3 are given as €/MWh_{H_2}, while costs for LNG, NG, and SNG are given as €/MWh_{CH_4}. Values for the intermediate years 2035 and 2045 are interpolated using the geometric mean.

Scenario	Import source	2030	2035	2040	2045	2050
H_2	H_2 (pipeline)	94	84	75	67	60
	NH_3 (ship)	138	122	108	97	87
	LNG (ship)	56	56	56	56	56
	NG (extraction)	28	28	28	28	28
	NG (pipeline)	28	28	28	28	28
	SNG (pipeline)	129	119	108	100	93
NH_3-	NH_3 (ship)	97	86	76	68	61
no-green	H_2 (pipeline)	–	–	–	–	–
	NH_3 (ship)	–	–	–	–	–
	SNG (pipeline)	–	–	–	–	–

sources. Additional adjustments have been made to ensure that energy carriers reflect their respective end use in the model, and that no further conversions to other energy carriers are economically viable. The scenario NH_3- assumes the availability of ship-based hydrogen imports, which are cost competitive to pipeline-based imports.

To evaluate the impact of fully domestic production on the transformation pathway, the *no-green* scenario assumes that no green hydrogen or fuels derived from it are imported. Similarly, the *no-blue* scenario evaluates the impact on the transformation pathway if blue hydrogen is not utilised on a large scale.

4. Results and discussion

The structure of this section follows the research questions (Section 1) and scenario design (Section 3). First, we analyse the impact of carbon budgets and VRE expansion rates on the system design (Section 4.1). The results of this section provide insights into how the carbon budget affects the pace of transformation, potentially causing peaks in the required annual capacity expansion rate. Similarly, national limits on annual capacity expansion lead to significant spatial shifts in the siting for VRE and electrolysers. This is then related to the stated political targets for VRE expansion (Section 4.2), where we find that not all national targets can be met at limited expansion rates and observe a similar spatial shift in VRE technologies induced by capacity targets. Finally, we address challenges posed by delayed network expansion and the unavailability of hydrogen supply options (Section 4.3), highlighting the strong influence of import prices on network topology and providing insights into seasonal hydrogen storage patterns for high shares of domestic electrolysis.

4.1. Impact of limited capacity expansion rates and available carbon budget

The most significant systematic changes to the transformation pathways are caused by the permitted cumulative carbon budget. This is the main factor that determines how quickly and ambitiously the system needs to transform. As discussed in Section 2, the exogenously assumed methane demand results in downstream emissions of 5.5 Gt_{CO_2}. If the carbon budget is higher than this threshold, more options for the conversion of natural gas to hydrogen via SMR become available. Conversely, a more restricted carbon budget has the opposite effect by forcing the model to utilise either domestically produced synthetic methane from the Sabatier process or import synthetic or biogenic methane from outside the system boundaries, due to a lack of endogenous carbon dioxide removal (CDR) options within the model.

Fig. 3 shows the system-wide energy balances for the energy carriers methane (top), hydrogen (middle), and electricity (bottom). As expected, stricter limitations on the carbon budget (4-6 Gt_{CO_2} from left to right) require a higher annual expansion rate for electrolysers to provide green hydrogen for increased synthetic methane production. Similarly, a shift in imported fuels from natural gas to green methane via existing pipeline infrastructure can be observed. In the 5 Gt_{CO_2} scenario, the assumed limits on annual green methane imports are almost sufficient to realise the reduction in downstream carbon emissions. For achieving the 4 Gt_{CO_2} budget, domestic production of synthetic methane is required between 2030 and 2040.

Further changes to the system are caused by the different annual capacity expansion limitations. While all scenarios utilise blue hydrogen from ATR-CCS as soon as the technology is available in the model year 2035, only the scenario with a 6 Gt_{CO_2} limit uses SMR-CCS to start producing blue hydrogen in 2030. In the case of the unconstrained annual capacity expansion (*unlimited*), the utilisation of blue hydrogen is generally lower compared to scenarios with restricted expansion of VRE technologies. This is due to the reduced ability to rely on domestic green hydrogen production, which is caused by the lack of electricity from VRE to support this indirect electrification.

However, the overall amount of blue hydrogen produced varies with more restrictive expansion rates of VRE, as does the amount of natural gas reserves utilised in the different model years. With strongly limited VRE expansion (*low*), more offshore gas capacity is reserved for the production of blue hydrogen in later decades. With unconstrained annual capacity expansion (*unlimited*), blue hydrogen is utilised more

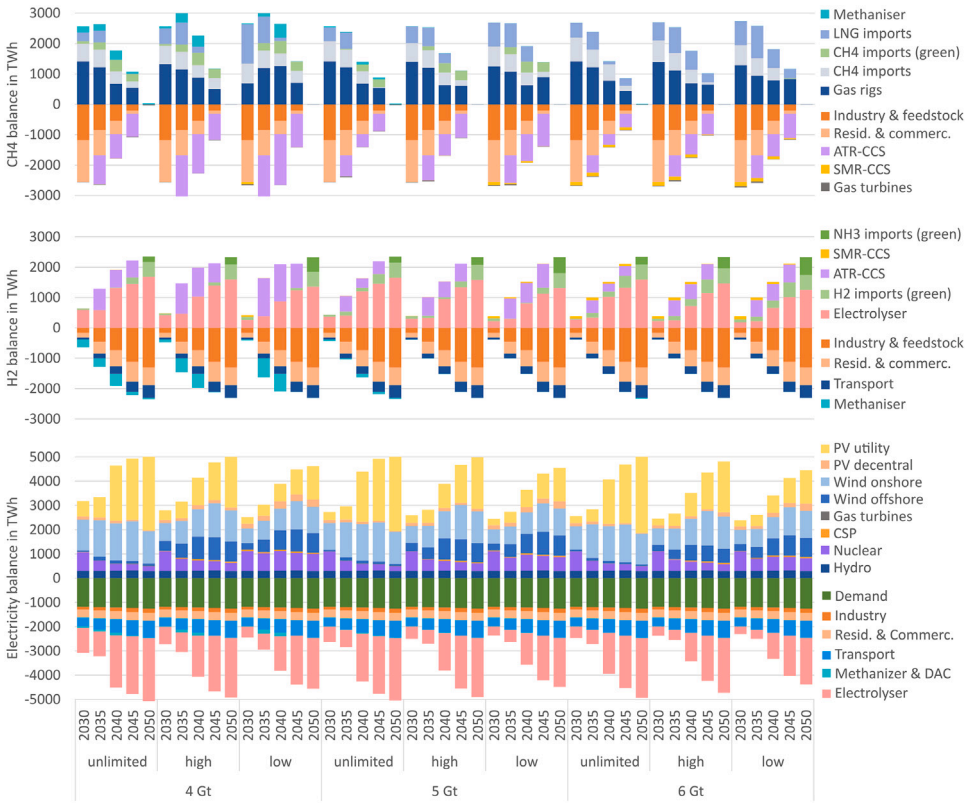


Fig. 3. Energy balances for supply and demand of methane (top), hydrogen (middle), and electricity (bottom) along the transformation pathway for scenarios with different carbon budgets (*4 Gt*, *5 Gt*, and *6 Gt*) and limited annual capacity expansion rates (*unlimited*, *high*, and *low*). Note that the y-axis scaling differs for the different energy carriers.

in the short term (i.e. until 2035) as soon as the technology becomes available. One possible reason for this is the expectation of decreasing investment costs for the electrolyser and VRE technologies in later years. This allocation exacerbates the required rate of capacity expansion rate in 2040 resulting in 55 GW_{H_2}/a for electrolyser plants and 249 GW/a for utility-scale PV.

In general, the reduced expansion of utility-scale PV and onshore wind energy leads to a shift towards other renewable technologies, such as distributed PV and offshore wind. In the case of the scenario *4 Gt low*, where this effect is most pronounced, offshore wind turbines contribute 918 TWh/a to the annual electricity generation, while distributed PV contributes 276 TWh/a. Alongside these shifts in VRE technologies, the main increase in power generation is observed in nuclear power plants, which remain at a similar production level to those seen today. In contrast, with unlimited VRE capacity expansion nuclear power plants are gradually phased out of the system. Despite the additional investments required for reserve capacity, the system-wide utilisation of gas-fired power plants remains below 16 TWh/a in all scenarios, indicating that the flexibility provided by electrolysers, power grids, and electricity storage systems is sufficient to compensate for the intermittency of VRE.

This systematic shift in VRE expansion likewise affects the spatial allocation of investments, as illustrated in Fig. 4. In 2035, an unconstrained expansion of capacity leads to onshore wind energy in the North Sea region, particularly in Scotland, becoming the main contributor to electricity generation, providing 182 TWh/a (compared to a total onshore wind production of 371 TWh/a across the UK and a Europe-wide electricity production from VRE of 2240 TWh/a). For PV, the main contributions come from Spain (149 TWh/a) and Italy (101 TWh/a). However, this concentration of generation in a few resource-rich areas becomes less prevalent when limitations on the capacity expansion are considered. While these regions still account for a large proportion of the overall electricity generation, additional capacity expansion shifts towards Germany, for both onshore wind in the north and PV capacities in the south.

In terms of the spatial distribution of VRE and electrolyser technologies in 2050, the focus shifts heavily towards utility-scale PV due to the low cost of electricity for green hydrogen production. This is particularly evident in regions of Southern Spain, where up to 292 TWh_{H_2}/a of hydrogen are produced per year (out of a total of 432 TWh_{H_2}/a in Spain and 1654 TWh_{H_2}/a across Europe) in the unconstrained case. However, this high spatial concentration decreases significantly under limited capacity expansion rates. This results in an annual hydrogen production across Spain of 249 TWh_{H_2}/a when considering the optimistic capacity (*high*), and 154 TWh_{H_2}/a in the pessimistic case (*low*). Conversely, the *high* limitation leads to an increase in the long-term annual hydrogen production in the UK (297 TWh/a), Germany (287 TWh/a), and France (129 TWh/a).

This suggests that earlier studies may have overestimated the role of individual regions in producing large quantities of hydrogen, given that these studies did not impose limits on the expansion of renewable energy. This can be observed, for example, in the model results of Fleiter et al. [3] who identified a similar pattern involving the production of green hydrogen in the British Isles in 2030 (up to 21 GW_{H_2}) and in the Iberian Peninsula in 2050 (up to 207 GW_{H_2}). In our study, limiting capacity expansion for these regions to the *high* case results in reductions from 42 GW_{H_2} down to 12 GW_{H_2} for the British Isles, and from 158 GW_{H_2} down to 99 GW_{H_2} for the Iberian Peninsula.

Regarding the required increase in electrolyser production, Victoria et al. estimate that 500 TWh of green hydrogen production are required in Europe by 2030 to achieve a carbon budget that would result in a high likelihood of staying within the 1.5 degree target for global warming [2]. Under the assumed limited expansion rates, our results indicate that a domestic production of green hydrogen up to 415 TWh/a is feasible in 2030, in the most optimistic case.

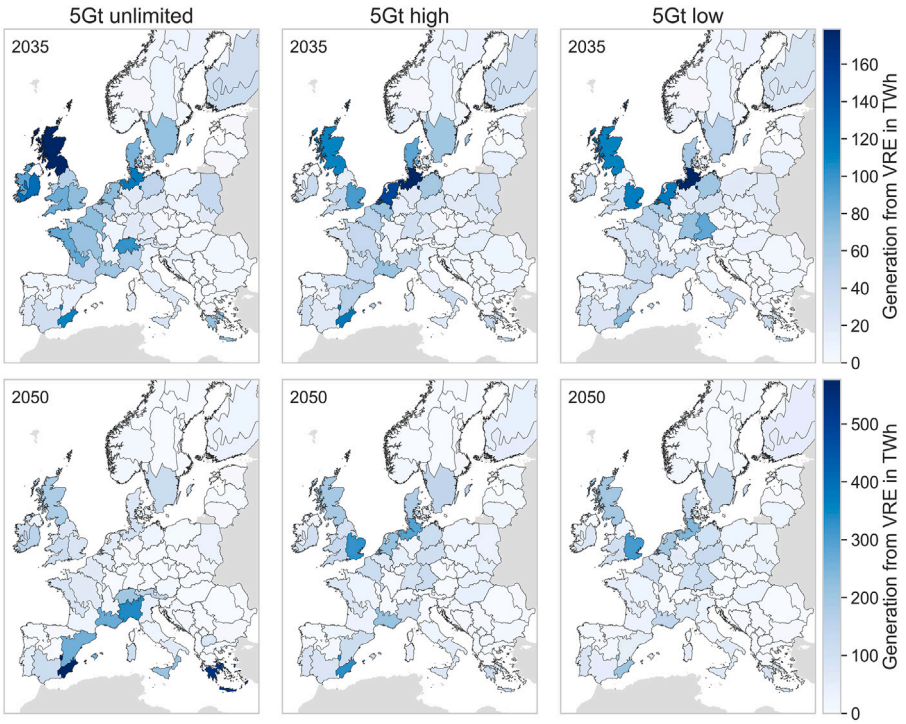


Fig. 4. Spatial distribution of annual VRE generation under different limitations on capacity expansion limitations and a fixed carbon budget for the years 2035 and 2050. In 2035, the system-wide VRE generation totals 2240 TWh/a, 2035 TWh/a, and 1877 TWh/a for the *unlimited*, *high*, *low* scenarios, respectively. In 2050, it totals 4695 TWh/a, 4368 TWh/a, and 3675 TWh/a, respectively.

4.2. Political targets and achievable expansion rates for renewable energy technologies

If the annual expansion rate is limited, a key question is whether the current political VRE capacity targets can still be achieved. Furthermore, a successful implementation of the NECPs and the Ostend Declaration is expected to influence both the timing and spatial distribution of VRE expansion, and therefore also the location of hydrogen production.

Our results show that the long-term NECP capacity targets for 2050 can be met at all limited expansion rates. However, the short- and medium-term targets are at risk of delay in the scenarios involving limited capacity expansion (*medium* and *low*). In the *medium* scenario, the gap between total installations and capacity targets amounts to 40 GW for PV in Spain in 2030, 46 GW for onshore wind in Germany in 2030, and 40 GW for onshore wind in Spain in 2035. Stronger limitations on the annual expansion of VRE capacities (*low*) would delay the achievement of the NECP targets until the year 2045.

The *Ostend* scenario reveals a significant discrepancy between the capacity expansion achieved in the past and the ambitious goals set for 2030 and beyond. In Norway, 3 GW and 30 GW of offshore wind are targeted for the years 2030 and 2050, respectively. The first floating offshore wind farm, with an 88 MW capacity, began operating in 2023. However, as the reference dataset for annual capacity does not anticipate any offshore installations in Norway, the capacity gap remains across all scenarios and model years. For the UK, the Netherlands, and Ireland the capacity gap between stated policy and model results begins in 2030 at 28 GW, 8.2 GW, and 3.7 GW, respectively, even in the *high* scenario. While the UK and the Netherlands close the gap in 2040 and 2035, respectively, Ireland's capacity gap remains throughout all model years and ultimately reaches 13 GW due to higher targets in 2050.

Fig. 5 shows how different capacity targets impact the spatial distribution of annual domestic hydrogen production. Compared to the *high* scenario, the scenarios with an unconstrained annual capacity expansion show a significantly greater difference to their respective *no-targets* baseline. This suggests that the reference solution already involves a high spatial concentration of electrolyser technologies and that limiting annual capacity expansion rates and modelling capacity targets both have a systemic effect on the spatial distribution of electrolysers.

In both the *NECP* and *Ostend* scenarios, increasing electricity production in specific geographic regions affects the location of electrolysers. This is most evident in northern Germany in both 2035 and 2050, where there is a significant increase in hydrogen electrolysis. Similarly, the capacity targets reduce the hydrogen production in southern Spain in 2050, although Spain remains the country with the highest production in all scenarios. Unlike the *NECP* scenario, the *Ostend* scenario includes a greater contribution to the domestic hydrogen supply from the UK in both 2035 and 2050.

In the *Ostend* scenario, the model allocates some electrolyser capacity to offshore regions. However, with an annual production of just 35–43 TWh/a in 2050, offshore hydrogen production is quite limited compared to the total hydrogen production of 1776 TWh/a and 1628 TWh/a for the *5 Gt unlimited Ostend* and *5 Gt high Ostend* scenarios. This is consistent with the findings of Gea-Bermúdez et al. [64], who found that electrolyser capacities are predominantly installed onshore before 2050.

4.3. Impact of hydrogen import strategy and network delays

While the network delays up to 2030 (nogrid30) have only a minor impact on the system, network delays for hydrogen pipelines until 2035 (*nogrid35*) prevent access to green and blue hydrogen from the North Sea and import nodes. Fig. 6 shows the more widespread distribution of electrolysers across regions, facilitating production close to demand sites. Consequently, the spatial distribution of VRE technologies is also influenced, utilising resource-rich regions close to demand sites and the existing electricity grid. As spatial balancing between model regions via hydrogen networks is not possible in this scenario, the required electrolyser capacity increases significantly in 2030 from 64 GW_{H_2} to 92 GW_{H_2} if hydrogen infrastructure is slightly delayed (*nogrid30*) and

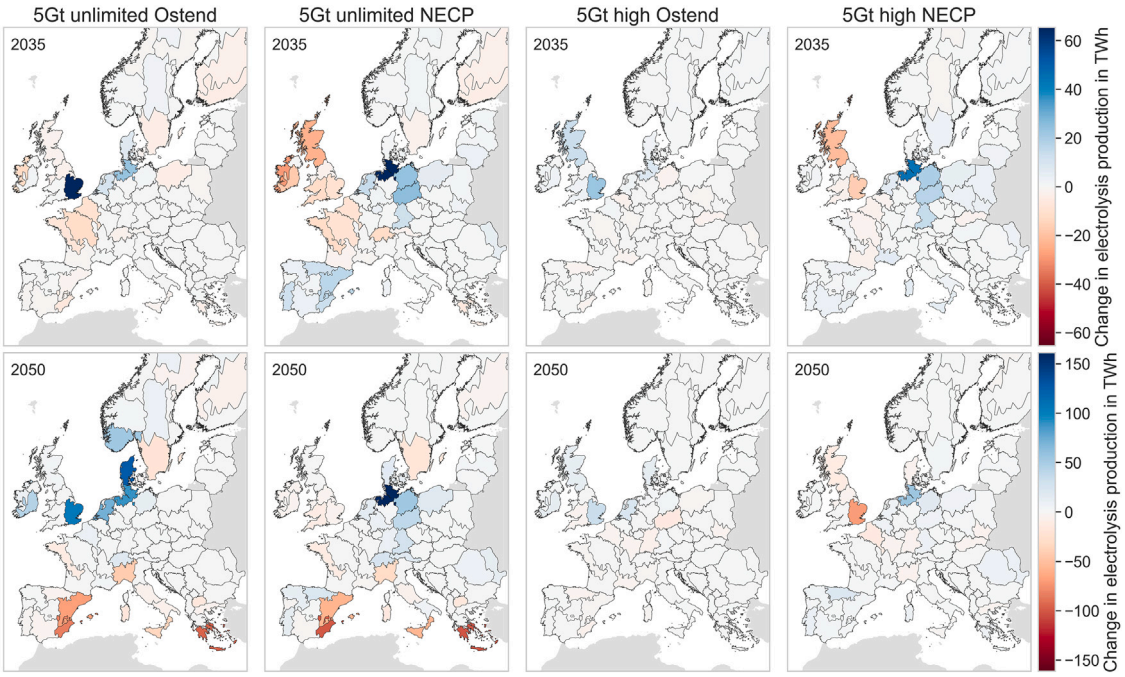


Fig. 5. Impact of *NECP* and *Ostend* capacity targets for a 5 Gt_{CO_2} carbon budget and considering the *unlimited* (left figures) and *high* scenarios (right figures) compared to their respective *no-targets* counterparts. Annual domestic hydrogen production in 2035 for the *no-targets* reference amounts to 377 TWh in the *unlimited* scenario and 248 TWh in the *high* scenario. For 2050 the reference values amount to 1620 TWh and 1381 TWh, respectively.

to 167 GW_{H_2} if network delays are expected to continue until 2035 (*nogrid35*).

A similar shift in the siting of hydrogen production can be observed in the scenario *no-blue*, in which greater emphasis is given to onshore wind in the North Sea area to compensate for the offshore production of blue hydrogen. However, hydrogen production is also set to increase significantly across various regions in France, reaching up to 130 TWh_{H_2}/a in 2035. In the NH_3- and *no-green* scenarios, the short-term impact compared to the H_2 scenario is limited, as the affected hydrogen import options are not yet cost-competitive with domestic production.

The largest reduction in domestic production in 2050 is seen in the scenario where the cost of port-based hydrogen imports is similar to that of pipeline-based imports (NH_3-). Shorter transport routes for hydrogen imports reduce domestic hydrogen production, particularly in regions close to LNG terminals. While the significant overlap between regions with good VRE potential and regions in close proximity to LNG terminals poses challenges for the economic efficiency of domestic production, it also offers synergies in terms of infrastructure.

Conversely, in a scenario where the import of green hydrogen or hydrogen derivatives is prohibited (*no-green*), we observe the repurposing of blue hydrogen offshore infrastructure to green hydrogen production by 2050. The existing offshore infrastructure can facilitate up to 94 TWh_{H_2}/a electrolysis from offshore wind energy and supply neighbouring countries via pipelines. Similarly, to compensate for the lack of green hydrogen imports from Turkey and Tunisia, there is an increase in domestic hydrogen production in Greece and Sardinia.

With a carbon budget of 5 Gt_{CO_2} and limited expansion rates (*high*), the results further show that providing sufficient domestic green hydrogen can be challenging. In both scenarios, in which green imports or blue hydrogen production are prevented, the slack variable for the carbon budget is utilised to a small degree. This suggests that, given the assumed speed of transformation in hydrogen demand, some additional green imports or blue hydrogen production is necessary, even if VRE expansion is limited to the optimistic scenario.

Similar to the changes in the spatial distribution of electrolyser production, the import strategy and hydrogen prices influence the topology of the network needed for hydrogen transfer, as shown in Fig. 7. In 2035, the topology is primarily determined by the option of utilising blue hydrogen production in the North Sea. Additionally, capacities for hydrogen transfer along the import corridors from Algeria, Tunisia, and Turkey are established early on.

In 2050, significant variations in topology are evident, primarily centred on import corridors (H_2 and *no-blue*), connections between LNG terminals (NH_3-), and inter-European hydrogen transfer (*no-green*). A common feature of the scenarios is the hydrogen transfer route between Southern Spain and demand centres in the North Sea area. To a lesser extent, this also includes corridors along Italy and the route connecting Greece to Central Europe.

The choice of hydrogen strategy and import routes significantly impacts the interaction between domestic hydrogen production and storage utilisation. Fig. 8 shows this interaction on an hourly basis, comparing domestic production, imports, and storage levels in caverns and pressurised tanks. Given that the model framework has perfect foresight for each hour of every year, the total storage capacity reflects only the volume of storage necessary for effectively balancing the supply and demand of hydrogen over the course of a year. This results in storage being completely full at the end of summer and completely empty at the end of winter, as no uncertainties on the demand or supply side are considered. In reality, however, additional strategic reserve capacities are required to account for uncertainties in demand, extreme weather events, delays in hydrogen imports and other supply chain disruptions.

As expected, there is a clear correlation between the overall share of domestic production and the required seasonal storage. When green hydrogen imports are avoided (*no-green*, right figures), the storage must be able to provide the full seasonal shift, relying on a more consistent balance between solar PV and wind energy as electricity sources. Conversely, when cheap hydrogen imports are available (NH_3-, left figures), domestic hydrogen production mainly utilises the best solar potential, reducing reliance on imports during the summer months.

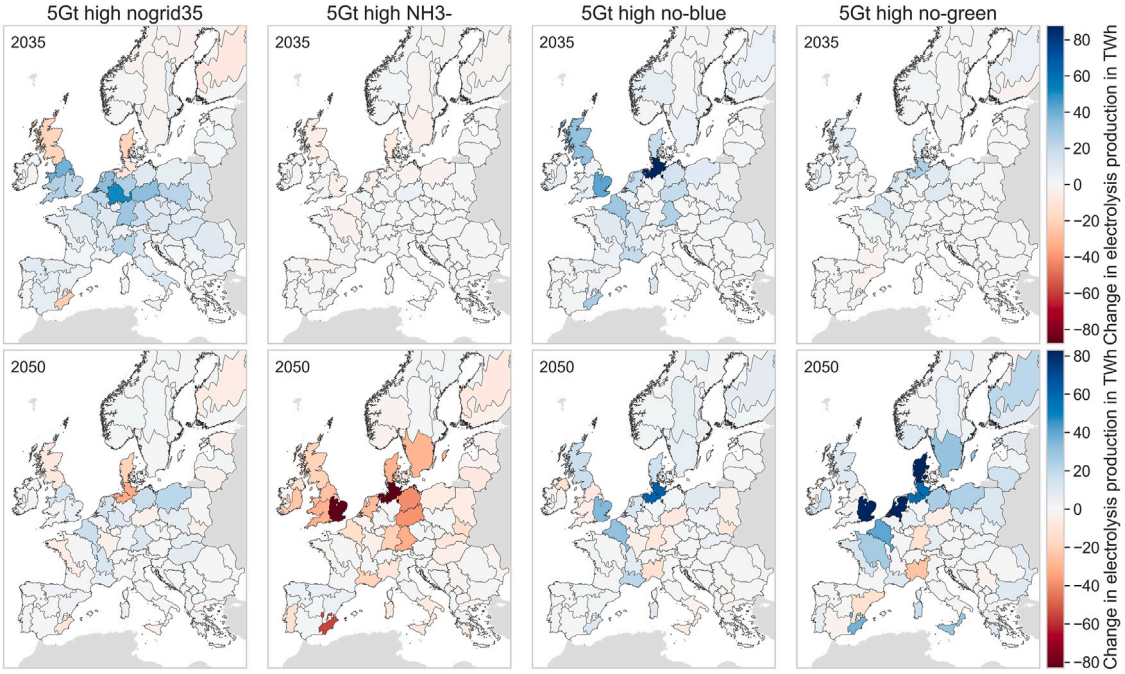


Fig. 6. Impact of the network delays scenario (*no-grid35*) and hydrogen import scenarios (NH_3-, *no-blue*, and *no-green*) compared to their respective H_2 reference for limited annual expansion rates (*high*) and a 5 Gt_{CO_2} carbon budget. Annual domestic hydrogen production in 2035 for the *5 Gt H2 high* reference scenario amounts to 332 TWh in 2035 and 1579 TWh in 2050.

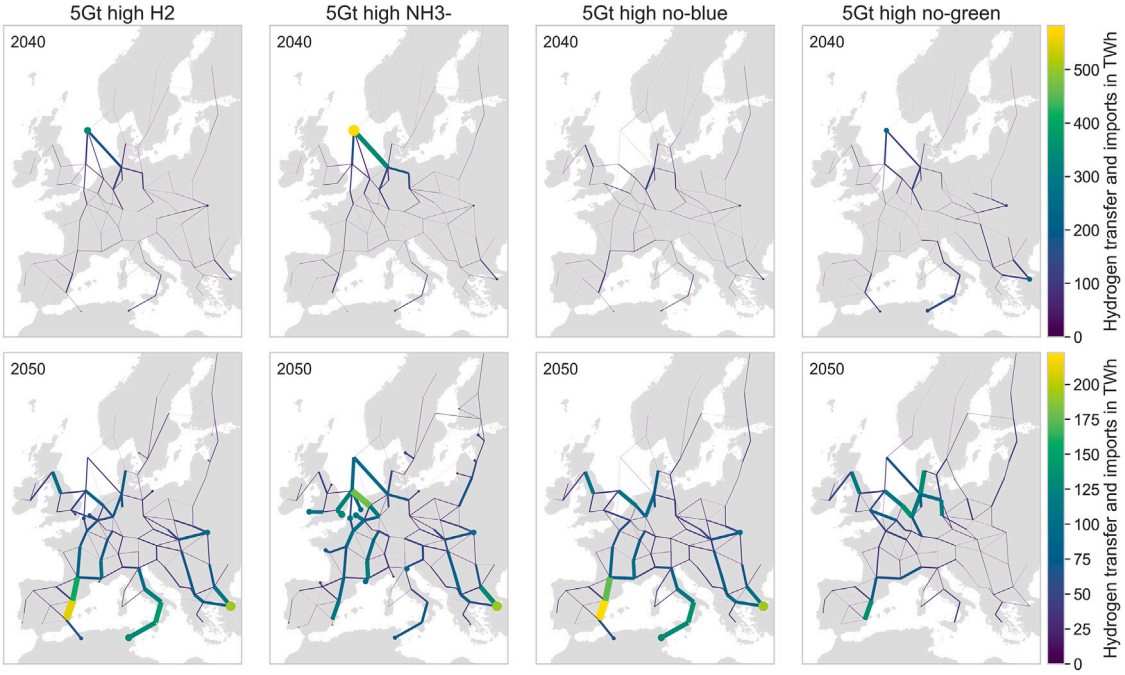


Fig. 7. Annual hydrogen network flows and imports from outside the system boundaries across different import scenarios. Note, that the import sources depicted as coloured circles can be either blue hydrogen from ATR-CCS or green hydrogen from electrolysis, or a combination of the two, depending on the conditions of the scenario. In 2040, the annual hydrogen transport throughout the system accounts for 2793 TWh/a, 3330 TWh/a, 2141 TWh/a, and 3002 TWh the scenarios H_2, NH_3-, *no-blue*, and *no-green*, respectively. For 2050, the annual hydrogen transport totals 4690 TWh/a, 5554 TWh/a, 4562 TWh/a, and 3308 TWh/a, respectively.

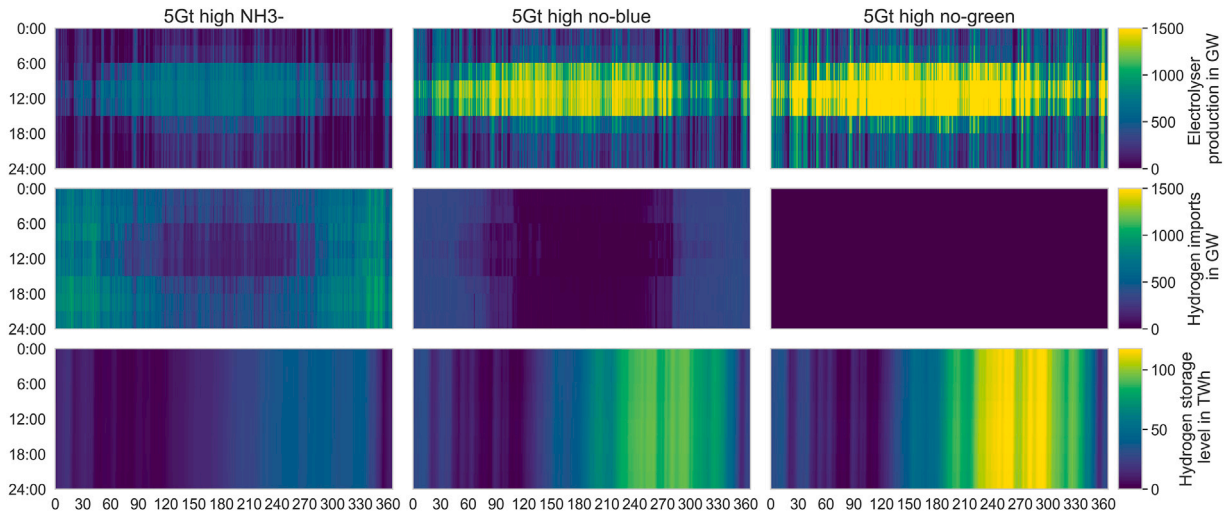


Fig. 8. Hourly utilisation of domestic electrolysers (top row), hydrogen imports (middle row), and seasonal storage level of for hydrogen caverns and pressurised hydrogen tanks (bottom row) across three different hydrogen import scenarios NH_3- (left column), *no-blue* (middle column), and *no-green* (right column). Note the difference in axis scaling between the domestic hydrogen production and hydrogen import (GW_{H_2}) and the storage level (TWh_{H_2}).

This scenario also results in lower storage requirements for seasonal balancing, but shifts the risk to import availability and potential price spikes.

The base scenario and the scenario without blue hydrogen (*no-blue*, middle figures) combine aspects of the two extreme cases previously discussed. Domestic hydrogen electrolysis in summer enables full domestic production for half the year, while seasonal hydrogen imports in winter reduce Europe's overall peak hydrogen storage requirement. For countries aiming to export hydrogen, this seasonal behaviour could favour imports from the Southern Hemisphere – for example Chile, South Africa and Australia.

The required hydrogen storage capacity of up to 160 TWh is similar in magnitude compared to the findings of Fleiter et al. [3], who observed a maximum hydrogen storage capacity of 215–300 TWh with the same one-cycle seasonal operational pattern. This large storage volume also enables a better integration of VRE by providing short-term flexibility in the power sector via electrolysers.

5. Limitations and outlook

There are various aspects outside the scope of this study that may influence the overall findings of the model-based analysis. While input data, such as future technology costs and overall demand trends, are always subject to large uncertainties, this section discusses the study's specific limitations. These limitations can be grouped into three categories: sectoral scope, technological scope, and fundamental modelling approach.

A major limitation of the study is that it did not consider the possibility of large-scale domestic hydrogen production for renewable fuels of non-biological origin (RFNBOs). These are expected to play a crucial role in decarbonising aviation and shipping. However, large uncertainties remain regarding market competition between different carriers, particularly with regard to bio-jet, as well as aspects of the regulatory framework. While the EU currently mandates a 70% share for sustainable aviation fuels (SAFs) of and a 35% share for RFNBOs for the aviation sector in 2050 [65], the national implementation of these targets and the possibility of importing these fuels remains uncertain. Significant RFNBO production in Europe would necessitate accelerated VRE expansion. Follow-up assessments should address the uncertainty surrounding the additional demand for hydrogen in the context of limited capacity expansion rates. Similarly, a better understanding and alignment of the dynamics between the potential re-acceleration of VRE expansion [7] and the scale-up of the hydrogen market [10] is required.

In terms of the technological scope of the study, aside from indirect electrification via hydrogen, there is a lack of detailed endogenous sector coupling options. This leads to an underestimation of flexibility options. In the power system, electrolysis, power grids, and battery storage systems offer the greatest flexibility. However, given the increasing market penetration of battery electric vehicles (BEVs), electric heat pumps, and smart meters, overall demand-side flexibility is expected to grow substantially. While the chosen model resolution is sufficient for addressing questions related to the deployment of large infrastructures, future model-based assessments need to consider demand-side flexibility in more detail.

While the technologies included in the model allow for the production of synthetic methane, there are no explicit CDR options, such as bioenergy with carbon capture and storage (BECCS) [66] or the utilisation of carbon as feedstock for the chemical industry [67]. Including these technologies, as well as carbon emission reduction strategies in other sectors, would enable a more comprehensive consideration of the overall carbon budget and cross-sectoral effects. Similarly, including pipelines for transporting and storing CO_2 could alter the overall emission trajectory. Extending the modelling period to 2070, while allowing for temporary overshooting to be compensated for later, would provide further insight into the allocation of the carbon budget across different sectors, particularly those not considered in this study.

The annual capacity expansion rates assumed in this study likewise are subject to limitations that must be considered when interpreting the model results. As the increase is only extrapolated based on an estimated short-term expansion rate, the analysis does not consider the dynamic effects of scaling up between different technologies or countries. This was demonstrated in the model results with regard to the expansion of offshore wind technologies in the North Sea. To provide a clearer picture of the solution space, more in-depth research is required into the limiting factors on a per-country and per-technology basis. These factors include the future availability of skilled workers, import dependence for technologies, components and raw materials, market incentives and societal impact, as outlined in the Clean Energy Technology Observatory (CETO) reports [13,14,68].

In terms of the modelling approach, the uncertainty surrounding the hydrogen strategy and imports is only considered through deterministic scenarios. Stochastic or robust optimisation could provide additional

insights, for example, into a more robust and adaptable topology for the hydrogen pipeline network, and into hedging strategies against high import prices. Similarly, selecting only five different weather years and mapping them across the transformation pathway may introduce bias into the spatial allocation of investment between solar and wind technologies [69].

More generally, system-wide least-cost optimisation lacks the multitude of perspectives from individual actors and their investment incentives. At a system level, this can result in an overestimation of VRE sites with high capacity factors and long-distance transmission throughout the system. In contrast, regional actors will always invest in VRE and electrolyser technologies if doing so benefits them in their market situation. Although the model results suggest clear co-location of electrolyser capacities and VRE sources, future studies need to further investigate the integration of these technologies at the level of regional energy systems, taking into account the perspectives of local actors.

To allow for the wide range of scenarios, the temporal dimension is downsampled to a 3-hourly resolution, which leads to a significant reduction in solution time from 170 h down to 20 h per scenario. Previous studies have shown that a downsampling to 3-hourly resolution is still suitable for energy system models, as it adequately captures the intermittency of high shares of VRE [70]. To assess the impact of the temporal downsampling, a 1-hourly resolution run is conducted for the *5 Gt high no-targets no-delay* H_2 scenario as reference. For the year 2050, the key differences between the two runs confirm that the main differences lie in flexibility options, with a system-wide increase in battery converter capacities of 18 GW (17.4% increase) and utilisation of 34 TWh (19.4% increase). Similarly, the capacity of hydrogen buffer storage units in Southern Europe increases by 37 GW (11.8% increase) and their utilisation increases by 8.6 TWh (13.7% increase). Furthermore, reductions are observable in the annual electricity supply from concentrated solar power (CSP) by 15 TWh (6.2% decrease) and PV by 18 TWh (1% decrease), while offshore wind energy increases by 7 TWh (18.5% increase). Taking into account the differences in required short-term flexibility options, this suggests that the downsampling results are reasonable compared to the overall uncertainties in the input data.

6. Conclusions

First and foremost, the findings of this study highlight the crucial role of achieving high annual VRE capacity expansion rates in the successful transformation towards a climate-neutral energy system. While modelling transformation pathways with high spatial and temporal resolution and perfect foresight can ensure that sufficient capacities are reached through early investment, it also reveals the systematic impact of national limits on annual expansion rates. Therefore, energy system modellers must carefully consider limitations on annual expansion rates and associated uncertainties, not only when modelling transformation pathways, but also when modelling target years. This also requires more in-depth investigations into the interplay between the various factors that can potentially limit future annual expansion rates, enabling the move away from pure extrapolation and adopting a stronger, scenario-based approach with a solid foundation of data.

Regarding the stated policies, we can observe that some targets, such as the NECP targets for onshore wind energy and PV in Spain and Germany, require a significant acceleration in the annual capacity expansion compared to the *high* baseline. While there is a risk of missing these particular targets, the overarching goal of achieving a climate-neutral energy system by 2050 remains feasible, if capacity expansion is distributed across more European countries. In order to achieve this, a clear European strategy is required to incentivise more countries to contribute to VRE capacity expansion. This would mitigate the risk of individual countries lagging behind and ensure a sufficient European hydrogen network to enable spatial balancing across borders. The expansion of VRE and networks must be closely coordinated and monitored to ensure electrolysers can be deployed on a regional level providing demand-side flexibility, while the hydrogen network enables access to hydrogen cavern storage sites for seasonal balancing.

The co-location of VRE capacities and electrolysers throughout all scenario variations also demonstrates the value that hydrogen can offer in terms of system integration. Flexible operation of systems comprising a renewable electricity source, buffer storage, and an electrolyser reduces reliance on the power grid and contributes to overall system stability. Given both the co-location and matching operational patterns of VRE technologies and electrolysers, we can also conclude that policies, such as the RFNBO classification, in terms of temporal and geographical matching, can be seen as being in line with the operational patterns required to integrate large shares of VRE into the system.

Regarding the use of blue hydrogen, we conclude that a strong reliance in the short term poses a significant risk to achieving the carbon budget. This is because it delays the required expansion of VRE and electrolyser capacities to later years, based on the expectation of lower future investment costs. Consequently, this delay necessitates a faster rate of annual capacity expansion for the transition to green hydrogen in 2040. Similarly, over-reliance on blue hydrogen can induce an increased dependency on energy imports in the long term if it results in reduced investment in domestic electrolyser capacities.

Therefore, incentives for hydrogen production and demand should focus solely on green hydrogen, as this indirectly facilitates the rapid expansion of VRE. Although blue hydrogen could substantially increase hydrogen usage in industry by 2035, this would only be possible without affecting the carbon budget if sufficiently high capture rates for ATR-CCS can be achieved. When considering the trade-off between blue and green hydrogen, competition for investment funds must be taken into account. Similarly, if the provision of blue hydrogen relies on repurposing existing pipelines, this could delay the installation and network connection of green hydrogen production facilities, leading to a medium-term dependency on fossil fuels and exacerbating the need to expand VRE capacities.

Based on the model results, ensuring a long-term, fully domestic supply of green hydrogen requires a significant increase in annual capacity expansion to 51 GW/a for PV and 49 GW/a for onshore wind energy across Europe. Until 2050, the annual expansion rate for PV needs to almost triple to 139 GW/a, while the level of around 50 GW/a for onshore wind needs to be consistently maintained throughout this period. However, the exact peak of the maximum capacity expansion rate varies depending on the scenario and could happen earlier if CCS with high capture rates is not technically or economically viable.

In terms of hydrogen network infrastructure, the clear impact of the relative costs of import sources on the overall network topology is evident. This suggests that the expected costs and volumes require further investigation. However, assuming high levels of domestic hydrogen production, a common pattern emerges across the topologies: connecting large hydrogen supply regions to cavern storage systems along the route from southern Spain to the North Sea area appears to be a viable option and would allow existing LNG terminals to be connected along this corridor. Additionally, smaller sized hydrogen network capacities are required to connect spatially distributed electrolysers to seasonal hydrogen storage sites.

In summary, VRE capacity expansion rates and the reasons for their limitations are one of the crucial determining factors for a successful energy transition and must be adequately considered in modelling activities. This is particularly relevant if the aim is to produce large quantities of green hydrogen domestically, as failing to achieve the required expansion rates would result in a reliance on imports of hydrogen or the long-term use of blue hydrogen derived from fossil fuels. Adequate measures must be implemented to ensure that the burden of rapid VRE expansion is shared across a large number of European countries, and that sufficient hydrogen network capacity is in place to enable access to seasonal hydrogen storage sites. Going forward, additional effort is needed to better understand the reasons and conditions that could prevent the rapid expansion of VRE, and to adequately and proactively address the associated risks.

CRediT authorship contribution statement

Manuel Wetzel: Writing – review & editing, Writing – original draft, Visualization, Software, Methodology, Investigation, Formal analysis, Data curation, Conceptualization. **Hans Christian Gils:** Writing – review & editing, Writing – original draft, Investigation, Funding acquisition, Formal analysis, Data curation, Conceptualization. **Valentin Bertsch:** Writing – review & editing, Supervision, Investigation, Formal analysis.

Declaration of competing interest

The authors declare that they have no known competing financial interests or personal relationships that could have appeared to influence the work reported in this paper.

Acknowledgements

The research for this paper was partly conducted in the context of the project 'HINT', which is supported by the German Federal Ministry of Research, Technology and Space under grant number 03SF0690, and the project 'ARTESIS', which is supported by the German Federal Ministry of Economic Affairs and Energy under grant number 03EI1067A.

The authors thank Stefan Kronshage for his contributions to the demand scenario data, Jens Schmugge and Hedda Gardian for their support in the data collection and modelling activities, and all current and former members of the Energy Systems Modelling group of DLR for their continuous contribution to the input data and model framework.

Furthermore, the authors gratefully acknowledge the scientific support and HPC resources provided by the German Aerospace Center (DLR). The HPC system CARO is partially funded by the "Ministry of Science and Culture of Lower Saxony" and the "German Federal Ministry for Economic Affairs and Energy".

Appendix. Model nomenclature

Model dimensions

$t \in T$	time steps
$y \in Y$	year intervals
$n \in N$	model nodes
$l \in L$	transfer links
$q \in Q$	energy carriers
$a \in A$	converter activities
$p \in P$	technologies
$i \in I$	system indicators

Model variables

$x \geq 0$	number of available units/links
$\Delta x^+ \geq 0$	number of commissioned units/links
$\Delta x^- \geq 0$	number of decommissioned units/links
$d \geq 0$	utilisation of converter activities
$f^+ \geq 0$	flow along transfer link
$f^- \geq 0$	flow against transfer link
$g^+ \geq 0$	import of energy carriers
$g^- \geq 0$	export of energy carriers
j	accounting indicator variable

Model parameters

J	indicator coefficient matrix
W	weighting factor between year intervals
X	number of target units/links
λ	technical lifetime

References

[1] Nathan Johnson, Michael Liebreich, Daniel M. Kammen, Paul Ekins, Russell McKenna, Iain Staffell, Realistic roles for hydrogen in the future energy transition, Nat. Rev. Clean Technol. (2025) http://dx.doi.org/10.1038/s44359-025-00050-4.

[2] Marta Victoria, Elisabeth Zeyen, Tom Brown, Speed of technological transformations required in Europe to achieve different climate goals, Joule 6 (5) (2022) 1066–1086, http://dx.doi.org/10.1016/j.joule.2022.04.016.

[3] Tobias Fleiter, Joshua Fragoso, Benjamin Lux, Şirin Alibaş, Khaled Al-Dabbas, Pia Manz, Felix Neuner, Bastian Weißenburger, Matthias Rehfeldt, Frank Sensfuß, Hydrogen infrastructure in the future CO2-neutral European energy system – How does the demand for hydrogen affect the need for infrastructure? Energy Technol. (ISSN: 2194-4288) 13 (2) (2025) http://dx.doi.org/10.1002/ente.202300981.

[4] David Schlund, Simon Schulte, Tobias Sprenger, The who's who of a hydrogen market ramp-up: A stakeholder analysis for Germany, Renew. Sustain. Energy Rev. (ISSN: 13640321) 154 (2022) 111810, http://dx.doi.org/10.1016/j.rser.2021.111810.

[5] International Energy Agency, Renewables 2024, 2025.

[6] Ember, Yearly electricity data 2024, 2025, URL https://ember-energy.org/data/yearly-electricity-data/.

[7] Aleh Cherp, Vadim Vinichenko, Jale Tosun, Joel A. Gordon, Jessica Jewell, National growth dynamics of wind and solar power compared to the growth required for global climate targets, Nat. Energy 6 (7) (2021) 742–754.

[8] Oliver Linsel, Philipp Herpich, Konstantin Löffler, Valentin Bertsch, Quantifying renewable capacity expansion limitations in energy system modelling and their impact on future hydrogen production, in: 2025 21st International Conference on the European Energy Market, EEM, IEEE, 2025, pp. 1–8.

[9] J.P. Hansen, P.A. Narbel, D.L. Aksnes, Limits to growth in the renewable energy sector, Renew. Sustain. Energy Rev. 70 (2017) 769–774.

[10] Adrian Odenweller, Falko Ueckerdt, Gregory F. Nemet, Miha Jensterle, Gunnar Luderer, Probabilistic feasibility space of scaling up green hydrogen supply, Nat. Energy 7 (9) (2022) 854–865, http://dx.doi.org/10.1038/s41560-022-01097-4.

[11] Chris Briggs, Alison Atherton, Jeremy Gill, Rusty Langdon, Jay Rutovitz, Kriti Nagrath, Building a 'Fair and Fast' energy transition? Renewable energy employment, skill shortages and social licence in regional areas, Renew. Sustain. Energy Transit. (ISSN: 2667095X) 2 (2022) 100039, http://dx.doi.org/10.1016/j.rset.2022.100039.

[12] Tobias Naegler, Sebastian Rauner, Alois Dirnaichner, Patrick Jochem, Steffen Schlosser, Gunnar Luderer, Raw material demand and geopolitical risk in carbon-neutral futures, Energy Policy (ISSN: 03014215) 204 (2025) 114622, http://dx.doi.org/10.1016/j.enpol.2025.114622.

[13] European Commission, Clean Energy Technology Observatory, Overall strategic analysis of clean energy technology in the European Union: 2024, Publications Office, Luxembourg, ISBN: 9789268210154, 2025, http://dx.doi.org/10.2760/3507717.

[14] European Commission, Clean Energy Technology Observatory: Wind energy in the European Union: 2024 Status Report on Technology Development, Trends, Value Chains and Markets, Publications Office, Luxembourg, ISBN: 9789268209967, 2024, http://dx.doi.org/10.2760/0882709.

[15] IPCEI Hydrogen, Electrolyser manufacturing capacity, 2024, URL https://ipcei.observatory.clean-hydrogen.europa.eu/hydrogen-landscape/technology-manufacturing/electrolyser-manufacturing-capacity.

[16] Anurag Gumber, Riccardo Zana, Bjarne Steffen, A global analysis of renewable energy project commissioning timelines, Appl. Energy (ISSN: 03062619) 358 (2024) 122563, http://dx.doi.org/10.1016/j.apenergy.2023.122563.

[17] Johannes Giehl, Jeremias Hollnagel, Joachim Müller-Kirchenbauer, Assessment of using hydrogen in gas distribution grids, Int. J. Hydrog. Energy (ISSN: 03603199) 48 (42) (2023) 16037–16047, http://dx.doi.org/10.1016/j.ijhydene.2023.01.060.

[18] Marta Victoria, Kun Zhu, Tom Brown, Gorm B. Andresen, Martin Greiner, Early decarbonisation of the European energy system pays off, Nat. Commun. 11 (1) (2020) 6223, http://dx.doi.org/10.1038/s41467-020-20015-4.

[19] Ioannis Kountouris, Rasmus Bramstoft, Theis Madsen, Juan Gea-Bermúdez, Marie Münster, Dogan Keles, A unified European hydrogen infrastructure planning to support the rapid scale-up of hydrogen production, Nat. Commun. 15 (1) (2024) 5517, http://dx.doi.org/10.1038/s41467-024-49867-w.

[20] Falko Ueckerdt, Philipp C. Verpoort, Rahul Anantharaman, Christian Bauer, Fiona Beck, Thomas Longden, Simon Roussanaly, On the cost competitiveness of blue and green hydrogen, Joule 8 (1) (2024) 104–128, http://dx.doi.org/10.1016/j.joule.2023.12.004.
[21] Lukas Küng, Silvan Aeschlimann, Charithea Charalambous, Fergus McIlwaine, John Young, Noah Shannon, Karen Strassel, Cara Nichole Maesano, Rudy Kahsar, Daniel Pike, Mijndert van der Spek, Susana Garcia, A roadmap for achieving scalable, safe, and low-cost direct air carbon capture and storage, Energy Environ. Sci. (ISSN: 1754-5692) 16 (10) (2023) 4280–4304, http://dx.doi.org/10.1039/D3EE01008B.
[22] Filippo Bisotti, Karl Anders Hoff, Anette Mathisen, Jon Hovland, Direct air capture (DAC) deployment: A review of the industrial deployment, Chem. Eng. Sci. (ISSN: 00092509) 283 (2024) 119416, http://dx.doi.org/10.1016/j.ces.2023.119416.
[23] Peggy Shu-Ling Chen, Hongjun Fan, Hossein Enshaei, Wei Zhang, Wenming Shi, Nagi Abdussamie, Takashi Miwa, Zhuohua Qu, Zaili Yang, A review on ports' readiness to facilitate international hydrogen trade, Int. J. Hydrog. Energy (ISSN: 03603199) 48 (46) (2023) 17351–17369, http://dx.doi.org/10.1016/j.ijhydene.2023.01.220.
[24] Mona Wappler, Dilek Unguder, Xing Lu, Hendrik Ohlmeyer, Hannah Teschke, Wiebke Lueke, Building the green hydrogen market – Current state and outlook on green hydrogen demand and electrolyzer manufacturing, Int. J. Hydrog. Energy (ISSN: 03603199) 47 (79) (2022) 33551–33570, http://dx.doi.org/10.1016/j.ijhydene.2022.07.253.
[25] Stefan Pfenninger, Adam Hawkes, James Keirstead, Energy systems modeling for twenty-first century energy challenges, Renew. Sustain. Energy Rev. (ISSN: 13640321) 33 (2014) 74–86, http://dx.doi.org/10.1016/j.rser.2014.02.003.
[26] Christian Breyer, Siavash Khalili, Dmitrii Bogdanov, Manish Ram, Ayobami Solomon Oyewo, Arman Aghahosseini, Ashish Gulagi, A.A. Solomon, Dominik Keiner, Gabriel Lopez, Poul Alberg Ostergaard, Henrik Lund, Brian V. Mathiesen, Mark Z. Jacobson, Marta Victoria, Sven Teske, Thomas Pregger, Vasilis Fthenakis, Marco Raugei, Hannele Holttinen, Ugo Bardi, Auke Hoekstra, Benjamin K. Sovacool, On the history and future of 100% renewable energy systems research, IEEE Access 10 (2022) 78176–78218, http://dx.doi.org/10.1109/ACCESS.2022.3193402.
[27] Fabian Neumann, Elisabeth Zeyen, Marta Victoria, Tom Brown, The potential role of a hydrogen network in Europe, Joule 7 (8) (2023) 1793–1817, http://dx.doi.org/10.1016/j.joule.2023.06.016.
[28] Jana Fakhreddine, Paul E. Dodds, Isabela Butnar, Global hydrogen trade pathways: A review of modelling advances and challenges, Int. J. Hydrog. Energy (ISSN: 03603199) 129 (2025) 236–252, http://dx.doi.org/10.1016/j.ijhydene.2025.04.203.
[29] Maximilian Hoffmann, Bruno U. Schyska, Julian Bartels, Tristan Pelser, Johannes Behrens, Manuel Wetzel, Hans Christian Gils, Chuen-Fung Tang, Marius Tillmanns, Jan Stock, André Xhonneux, Leander Kotzur, Aaron Praktiknjo, Thomas Vogt, Patrick Jochem, Jochen Linßen, Jann M. Weinand, Detlef Stolten, A review of mixed-integer linear formulations for framework-based energy system models, Adv. Appl. Energy (ISSN: 26667924) 16 (2024) 100190, http://dx.doi.org/10.1016/j.adapen.2024.100190.
[30] Martha Maria Frysztacki, Jonas Hörsch, Veit Hagenmeyer, Tom Brown, The strong effect of network resolution on electricity system models with high shares of wind and solar, Appl. Energy (ISSN: 03062619) 291 (2021) 116726, http://dx.doi.org/10.1016/j.apenergy.2021.116726.
[31] C. Gerbaulet, C. von Hirschhausen, C. Kemfert, C. Lorenz, P.-Y. Oei, European electricity sector decarbonization under different levels of foresight, Renew. Energy (ISSN: 09601481) 141 (2019) 973–987, http://dx.doi.org/10.1016/j.renene.2019.02.099.
[32] Karlo Hainsch, Thorsten Burandt, Konstantin Loffler, Claudia Kemfert, Pao-Yu Oei, Christian von Hirschhausen, Emission pathways towards a low-carbon energy system for Europe: A model-based analysis of decarbonization scenarios, Energy J. (ISSN: 0195-6574) 42 (5) (2021) 41–66, http://dx.doi.org/10.5547/01956574.42.5.khai.
[33] Leonard Göke, Mario Kendziorski, Adequacy of time-series reduction for renewable energy systems, Energy (ISSN: 03605442) 238 (2022) 121701, http://dx.doi.org/10.1016/j.energy.2021.121701.
[34] Stefan L. Luxembourg, Steven S. Salim, Koen Smekens, Francesco Dalla Longa, Bob van der Zwaan, TIMES-Europe: An integrated energy system model for analyzing Europe's energy and climate challenges, Environ. Model. Assess. (ISSN: 1420-2026) 30 (1) (2025) 1–19, http://dx.doi.org/10.1007/s10666-024-09976-8.
[35] Elisabeth Zeyen, Marta Victoria, Tom Brown, Endogenous learning for green hydrogen in a sector-coupled energy model for Europe, Nat. Commun. 14 (1) (2023) 3743, http://dx.doi.org/10.1038/s41467-023-39397-2.
[36] Manuel Wetzel, Eugenio Salvador Arellano Ruiz, Francesco Witte, Jens Schmugge, Shima Sasanpour, Madhura Yeligeti, Fabia Miorelli, Jan Buschmann, Karl-Kiên Cao, Niklas Wulff, Hedda Gardian, Alexander Rubbert, Benjamin Fuchs, Yvonne Scholz, Hans Christian Gils, REMix: A GAMS-based framework for optimizing energy system models, J. Open Source Softw. 9 (99) (2024) 6330, http://dx.doi.org/10.21105/joss.06330.
[37] Konstantin Löffler, Social discounting, social costs of carbon, and their use in energy system models, Environ. Res. Lett. 16 (10) (2021) 104005, http://dx.doi.org/10.1088/1748-9326/ac228a.
[38] Mathias Mier, Valeriya Azarova, Investment cost specifications revisited, Energy Policy (ISSN: 03014215) 188 (2024) 114058, http://dx.doi.org/10.1016/j.enpol.2024.114058.
[39] European Commission, A clean planet for all: A European long-term strategic vision for a prosperous, modern, competitive and climate neutral economy, 2018, URL https://eur-lex.Europa.eu/legal-content/EN/TXT/?uri=CELEX:52018DC0773.
[40] Andrej Guminski, Claudia Fiedler, Stephan Kigle, Christoph Pellinger, Patrick Dossow, Kirstin Ganz, Fabian Jetter, Timo Kern, Timo Limmer, Alexander Murmann, Janis Reinhard, Tapio Schmidt-Achert, Serafin von Roon, eXtremOS summary report, 2021, http://dx.doi.org/10.34805/FFE-24-21.
[41] Jan Diettrich, Adam Pluta, Wided Medjroubi, Sci2grid_gas IGGIELGN, 2021, http://dx.doi.org/10.5281/zenodo.4767098.
[42] Bart Wiegmans, GridKit: GridKit 1.0 'for scientists', 2016, http://dx.doi.org/10.5281/ZENODO.47263.
[43] Manuel Wetzel, Hans Christian Gils, Valentin Bertsch, Green energy carriers and energy sovereignty in a climate neutral European energy system, Renew. Energy (ISSN: 09601481) 210 (2023) 591–603, http://dx.doi.org/10.1016/j.renene.2023.04.015.
[44] ENTSO-G, Gas flow dashboard, 2025, URL https://gasdashboard.entsog.eu/#map-flows.
[45] Malte Jansen, Connor Duffy, Tim C. Green, Iain Staffell, Island in the Sea: The prospects and impacts of an offshore wind power hub in the North Sea, Adv. Appl. Energy (ISSN: 26667924) 6 (2022) 100090, http://dx.doi.org/10.1016/j.adapen.2022.100090.
[46] Drazen Tumara, Andreas Uihlein, Ignacio Hidalgo, Shaping the future CO2 transport network for Europe, ISBN: 9789268120590, 2024, http://dx.doi.org/10.2760/582433, URL https://op.europa.eu/o/opportal-service/download-handler?identifier=b761e384-c4e3-11ee-95d9-01aa75ed71a1&format=pdf&language=en&productionSystem=cellar&part=.
[47] Osama Massarweh, Maha Al-khuzaei, Manal Al-Shafi, Yusuf Bicer, Ahmad S. Abushaikha, Blue hydrogen production from natural gas reservoirs: A review of application and feasibility, J. CO2 Util. (ISSN: 22129820) 70 (2023) 102438, http://dx.doi.org/10.1016/j.jcou.2023.102438.
[48] Global Energy Monitor, Global nuclear power tracker, 2024, URL https://globalenergymonitor.org/projects/global-nuclear-power-tracker/.
[49] Global Energy Monitor, Global oil and gas plant tracker, 2024, URL https://globalenergymonitor.org/projects/global-oil-gas-plant-tracker/.
[50] Beyond Fossil Fuels, Europe coal plants database, 2024, URL https://beyondfossilfuels.org/wp-content/uploads/2025/05/2025-04-30-BeyondFossilFuels-Europe_Coal_Plants_Database.xlsx.
[51] European Commission, Joint Research Centre, JRC hydro-power database, 2019, URL http://data.Europa.eu/89h/52b00441-d3e0-44e0-8281-fda86a63546d.
[52] Copernicus C3S, Climate and energy related variables from the pan-European climate database derived from reanalysis and climate projections, 2024, http://dx.doi.org/10.24381/cds.f323c5ec.
[53] Eurostat, Electricity production capacities for renewables and wastes, 2024, URL https://ec.europa.eu/eurostat/databrowser/product/page/NRG_INF_EPCRW.
[54] Danish Energy Agency, Technology catalogues, 2024, URL https://ens.dk/en/analyses-and-statistics/technology-catalogues.
[55] C. Bollmeyer, J.D. Keller, C. Ohlwein, S. Wahl, S. Crewell, P. Friederichs, A. Hense, J. Keune, S. Kneifel, I. Pscheidt, S. Redl, S. Steinke, Towards a high–resolution regional reanalysis for the European CORDEX domain, Q. J. R. Meteorol. Soc. (ISSN: 0035-9009) 141 (686) (2015) 1–15, http://dx.doi.org/10.1002/qj.2486.
[56] European Environment Agency, CORINE Land Cover 2018 (raster 100 m), Europe, 6-yearly - version 2020_20u1, May 2020, 2019.
[57] Xiaoli Guo Larsén, Neil Davis, Ásta Hannesdóttir, Mark Kelly, Lasse Svenningsen, René Slot, Marc Imberger, Bjarke Tobias Olsen, Rogier Floors, The global atlas for siting parameters project: Extreme wind, turbulence, and turbine classes, Wind. Energy (ISSN: 1095-4244) 25 (11) (2022) 1841–1859, http://dx.doi.org/10.1002/we.2771.
[58] Ostend Declaration, Ostend Declaration of energy ministers: The North Seas as Europe's green power plant, 2023, URL https://assets.publishing.service.gov.uk/media/65ae7a62fd784b0010e0c65d/ostend-energy-ministers-declaration-north-sea-as-green-power-plant.pdf.
[59] Ember, Live EU NECP tracker, 2025, URL https://ember-energy.org/data/live-eu-necp-tracker.
[60] Gas for Climate, Assessing the benefits of a pan-European hydrogen transmission network, 2023, URL https://gasforclimate2050.eu/wp-content/uploads/2023/12/GfC_PanEU_230320_received_230323_published_final.pdf.
[61] Bastian Weißenburger, Martin Wietschel, Benjamin Lux, Matthias Rehfeldt, The long term price elastic demand of hydrogen – A multi-model analysis for Germany, Energy Strat. Rev. (ISSN: 2211467X) 54 (2024) 101432, http://dx.doi.org/10.1016/j.esr.2024.101432.
[62] Richard Schmitz, Julian Brandes, Hannah Nolte, Christoph Kost, Benjamin Lux, Michael Haendel, Anne Held, Implications of hydrogen import prices for the German energy system in a model-comparison experiment, Int. J. Hydrog. Energy (ISSN: 03603199) 63 (2024) 566–579, http://dx.doi.org/10.1016/j.ijhydene.2024.03.210.

[63] ENTSOG & ENTSO-E, TYNDP 2024 scenarios methodology report: Final version January 2025, 2025, URL https://2024.entsos-tyndp-scenarios.eu/wp-content/uploads/2025/01/TYNDP_2024_Scenarios_Methodology_Report_Final_Version_250128.pdf.

[64] Juan Gea-Bermúdez, Rasmus Bramstoft, Matti Koivisto, Lena Kitzing, Andrés Ramos, Going offshore or not: Where to generate hydrogen in future integrated energy systems? Energy Policy (ISSN: 03014215) 174 (2023) 113382, http://dx.doi.org/10.1016/j.enpol.2022.113382.

[65] European Commission, Commission Delegated Regulation (EU) 2023/1184 of 10 February 2023 supplementing Directive (EU) 2018/2001 of the European Parliament and of the Council by establishing a Union methodology setting out detailed rules for the production of renewable fuels of non-biological origin: 2023/1184, 2023, URL https://eur-lex.Europa.eu/eli/reg_del/2023/1184/2024-06-10.

[66] Lorenzo Rosa, Daniel L. Sanchez, Marco Mazzotti, Assessment of carbon dioxide removal potential via BECCS in a carbon-neutral Europe, Energy Environ. Sci. (ISSN: 1754-5692) 14 (5) (2021) 3086–3097, http://dx.doi.org/10.1039/D1EE00642H.

[67] Alexander Otto, Thomas Grube, Sebastian Schiebahn, Detlef Stolten, Closing the loop: captured CO2 as a feedstock in the chemical industry, Energy Environ. Sci. (ISSN: 1754-5692) 8 (11) (2015) 3283–3297, http://dx.doi.org/10.1039/C5EE02591E.

[68] European Commission, Clean Energy Technology Observatory: Photovoltaics in the European Union: 2024 Status Report on Technology Development, Trends, Value Chains and Markets, Publications Office, Luxembourg, ISBN: 9789268209936, 2024, http://dx.doi.org/10.2760/1812909.

[69] Tyler H. Ruggles, Edgar Virgüez, Natasha Reich, Jacqueline Dowling, Hannah Bloomfield, Enrico G.A. Antonini, Steven J. Davis, Nathan S. Lewis, Ken Caldeira, Planning reliable wind- and solar-based electricity systems, Adv. Appl. Energy (ISSN: 26667924) 15 (2024) 100185, http://dx.doi.org/10.1016/j.adapen.2024.100185.

[70] Stefan Pfenninger, Dealing with multiple decades of hourly wind and PV time series in energy models: A comparison of methods to reduce time resolution and the planning implications of inter-annual variability, Appl. Energy (ISSN: 03062619) 197 (2017) 1–13, http://dx.doi.org/10.1016/j.apenergy.2017.03.051.

4
Extended results

4.1 Benchmarking instances for transformation pathways

As discussed in Section 2.2.2, transformation pathways are connected to a different annotation and involve a greater number of investment decisions than those considered in *Publication 2*. Therefore, the first step in finding a well-performing PIPS-IPM++ configuration for solving the fully resolved model from *Publication 3* is to assess the scaling behaviour of different smaller versions of the full-resolution model. To this end, the three variations of spatial scope *subFR* (only France), *subCWE* (only central western Europe), and *subEU* (full spatial scope), are combined with variations of a temporal downsampling method *1h*, *3h*, *8h*, *24h*, and *73h*. Similar to the scaling experiment in *Publication 2*, this enables a wide range of different problem sizes, with different ratios of capacity expansion and economic dispatch decisions, to be evaluated (see Table 4.1).

Table 4.1: Model instances with a reduced spatial and temporal scope for the benchmarking experiment and sizes of their corresponding optimisation matrices.

	subFR			subCWE			subEU		
metric	1h	3h	8h	3h	8h	24h	8h	24h	73h
model regions	10	10	10	43	43	43	115	115	115
time steps	43,800	14,600	5,475	14,600	5,475	1,825	5,475	1,825	600
expansion decisions	1,130	1,130	1,130	4,549	4,549	4,549	12,857	12,857	12,857
mio. variables	16.7	5.6	2.1	23.8	9.1	3.1	25.4	8.6	2.9
mio. constraints	13.8	4.6	1.7	19.2	7.3	2.5	20.6	7.0	2.3
mio. non-zeros	67.2	22.5	8.5	98.7	37.4	12.6	104.5	35.2	11.6

Further analysis of the performance profiling of the three instances confirms the findings of *Publication 2* that a greater number of blocks is more effective for problems involving a low number of capacity

expansion decisions, whereas a smaller number of blocks is more effective for problems involving a high number of capacity expansion decisions. In the case of 1,130 capacity expansion variables, the configuration using 160 blocks achieves a better performance than the configuration using 80 blocks, despite the total amount of hardware resources being the same in both cases. This can be explained by limitations in the computation occurring during the parallel phase, as performance profiling across all Message Passing Interface (MPI) ranks suggests (see Figure 4.1). In this computation, each block is allocated to one MPI task, and each task has access to a number of cores equal to the total number of cores divided by the number of MPI tasks.

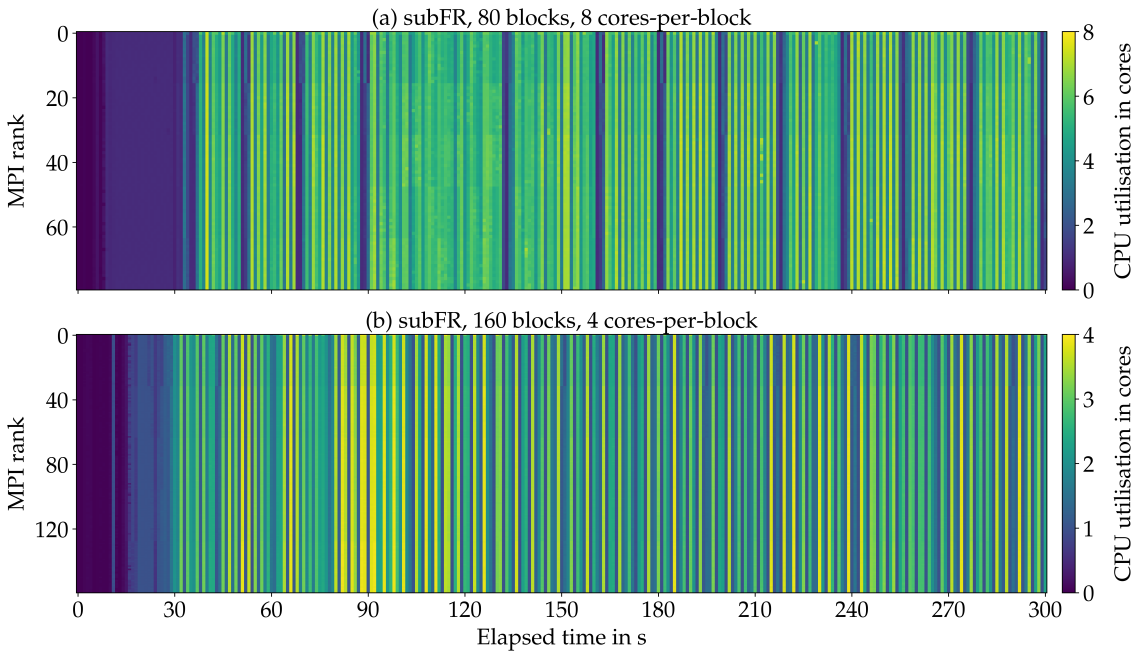


Figure 4.1: Performance profile of the core utilisation of each MPI rank for the benchmarking instance *subFR* with a cut-off at 300 seconds. Although both configurations demonstrate a high degree of parallelism, the configuration with 160 blocks (a) achieves slightly faster iteration times than the configuration with 80 blocks (b).

In contrast, the performance of the benchmarking instance with 12,857 capacity expansion variables, is limited due to the global computation performed on MPI rank 0 (see Figure 4.2). Reducing the total number of blocks from 80 to 40, allows the non-parallel phase to utilise more cores via Open Multi-Processing (OpenMP) parallelisation, thereby reducing the time per iteration, as indicated by the higher frequency of iterations in the parallel phase. This further highlights the importance of capacity expansion variables and the resulting global linking variables as potential bottlenecks. In particular, the 8-hourly downsampling helps to isolate this effect, as it largely trivialises the economic dispatch part of the problem.

A similar picture emerges when comparing the overall convergence behaviour of the *subEU* model

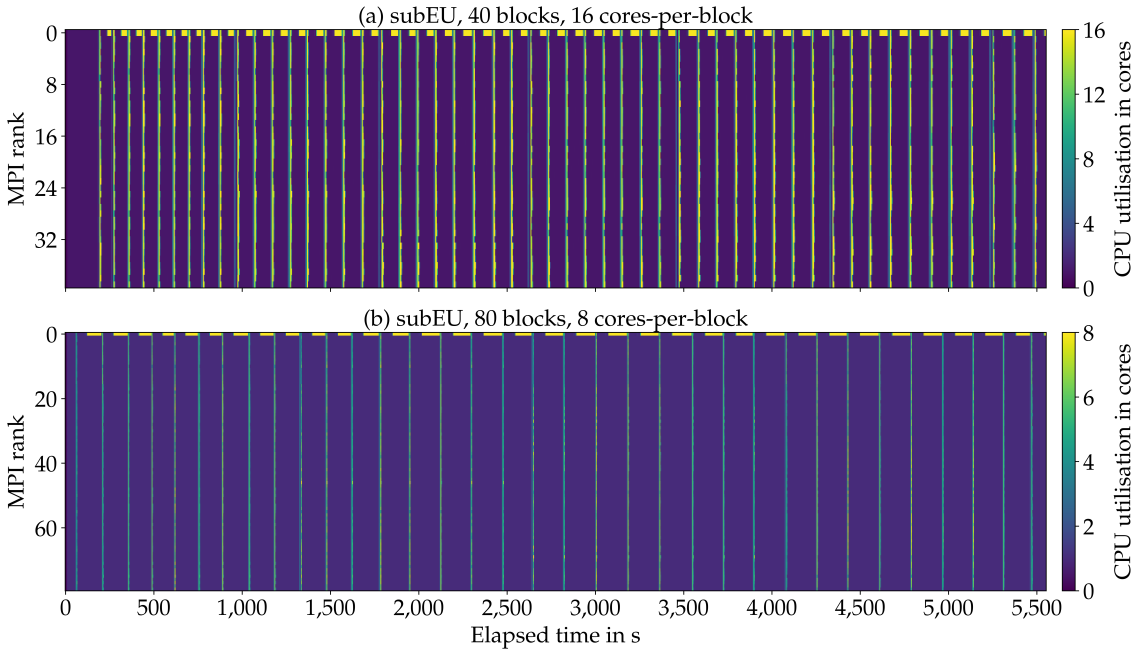


Figure 4.2: Performance profile indicating core utilisation of each MPI rank for the benchmarking instance *subEU* with a cut-off at 5,550 seconds. The computation of the instance with 40 blocks (a) has a significantly shorter time per iteration compared to configuration with 80 blocks (b).

instance, as measured by the complementarity gap μ (see Figure 4.3). For all three levels of temporal downsampling, the 40-block decomposition strategy (indicated by the solid line) converges fastest, followed by the 80-block and 160-block strategies. The same limitation effect due to the global phase on MPI rank 0, as previously discussed, can be demonstrated within each of the downsampling strategies. For the *73h* downsampling, depicted in red, the convergence time roughly doubles with each reduction in the number of cores available per task. Furthermore, the results reveal a noteworthy scaling property with regard to the sub-annual temporal resolution. While the change in downsampling method from *73h* to *8h* increases the number of time steps of the optimisation problem by a factor of about 9, the corresponding change in time to reach the stopping criteria increases by only a factor of 2.2.

Some additional observations were made during the testing of different model formulations and solver-specific PIPS-IPM++ options. In general, the standard IP solver benefited from a more compact formulation when it comes to the activities for converters and the flow along transmission lines (see Section 2.1.2), while conversely PIPS-IPM++ benefited more from a sparse formulation. Additionally, placing explicit bounds on the variables to increase model tightness improved convergence in PIPS-IPM++, whereas it made no difference to the standard IP solvers due to the more advanced bound tightening during presolve. PIPS-IPM++ internally also implements methods for the sparsifying matrices by deleting entries close to zero [56], which can improve the overall speed at the expense

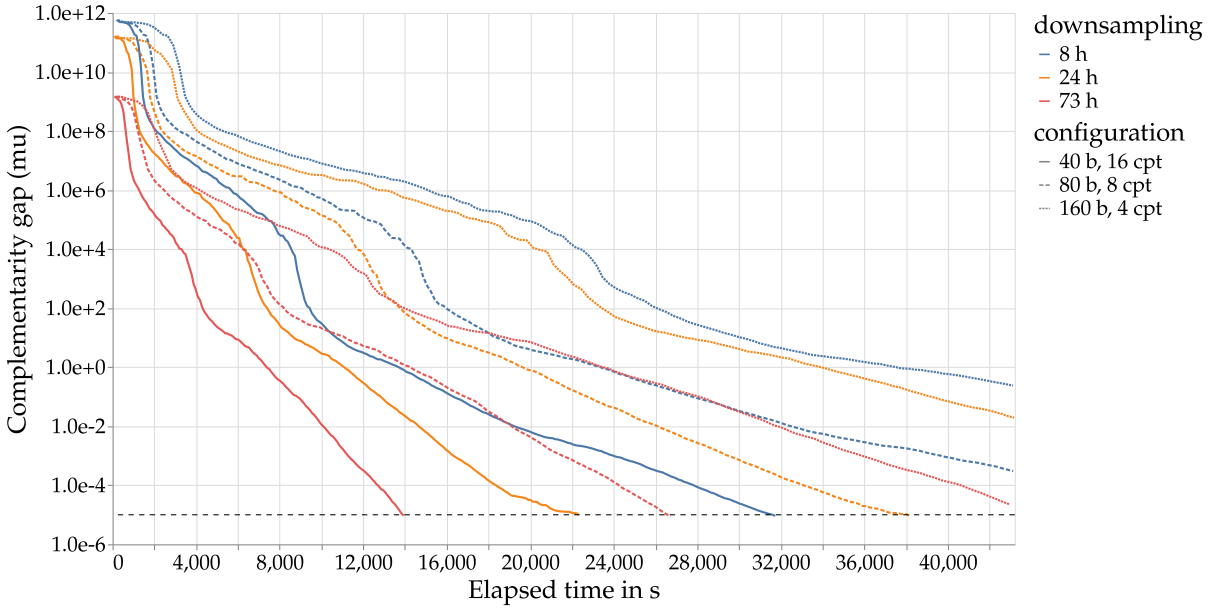


Figure 4.3: Convergence profile for the benchmarking instance *subEU* for different downsampling resolutions indicated by the colour and number of blocks generated by the decomposition strategy indicated by the line type. The y-axis shows the complementarity gap using a logarithmic scale, with the the stopping criteria indicated by the dashed black line.

of numerical precision. In the instances considered here, however, it had the opposite effect, so the corresponding options were deactivated.[1]

4.2 Performance comparison for transformation pathways

For the fully resolved hourly instance from *Publication 2* both the model instances with a decomposition strategy with blocks and 16 cores per block and 80 blocks and 8 cores per block are tested, based on the configurations identified as the best choices for the benchmarking model. While the configurations with 40 blocks and 80 blocks perform similarly in terms of total time for the optimisation, additional differences emerge. The main difference is observable in the significantly later start of the interior point iterations when using 40 blocks. This is caused by the larger matrices for each of the blocks and the lack of parallelization during the presolve and startup. Furthermore, while the 80 block instance starts with the iterations around 3.5 hours earlier, at the end of the profiling interval a shift in the computational burden emerges. In particular, the lower frequency of iterations indicates that the

[1]The following PIPS-IPM++ options can be used to configure the deactivation of sparsification during preconditioning:
PRECONDITION_DISTRIBUTED false bool
PRECONDITION_SPARSE false bool

global phase on MPI rank 0 becomes a limiting factor later on due to the lower available CPU cores per block.

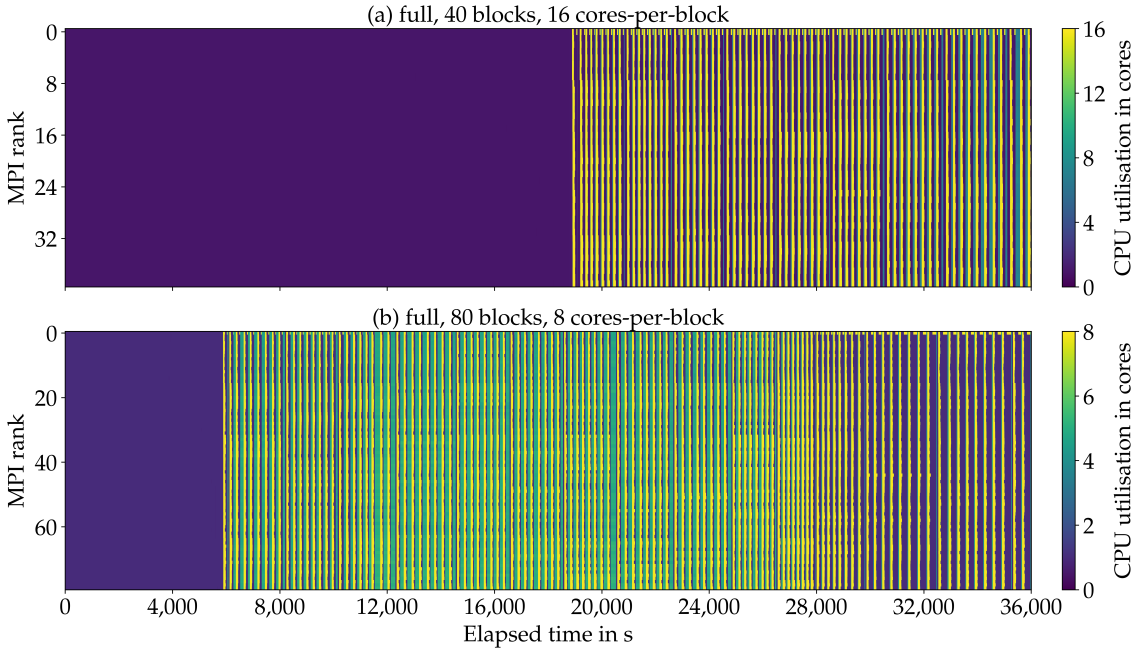


Figure 4.4: Performance profile indicating core utilisation of each MPI rank for the full model instance with a cut-off at 10 hours. The computation of the instance with 40 blocks (a) has a significantly shorter time per iteration compared to configuration with 80 blocks (b).

When it comes to the comparison against a standard IP method on a shared memory node as summarized in Table 4.2, several key differences can be observed: Firstly, the overall wall clock time can be significantly reduced from 171 hours down to 40 hours by using the distributed computing approach. If the simplifications on the formulation of capacities can be applied, a further reduction down to 31.6 hours is possible. The findings of the computation of the large-scale transformation therefore support the conclusions reached in *Publication 2* and demonstrate, that even for significantly larger optimisation problems a reasonable speed-up factor between 4 and 5 can be achieved, if the system is configured correctly.

Secondly, the computational results also support the hypothesis formulated in *Publication 2* that compute time, rather than available memory, becomes the main bottleneck for large-scale capacity expansion problems. Although the 1 TB of memory available on the compute node was sufficient for the standard IP solver, which had a peak memory demand of 680 GB, cross-socket communication may have impacted the solver's performance. In contrast, the peak memory demand for the application of PIPS-IPM++ underlines one of the main advantages: As the distributed computing enables storing the overall optimisation matrix across multiple compute nodes, the peak memory demand per node can be reduced. The comparison between the 40 block and 80 block instances shows that, while the former

ends up with larger blocks it still results in a lower memory footprint, as the latter allocates more MPI processes per node, thereby increasing overhead. However, both approaches allow preventing limitations with respect to the peak memory prevalent in the case of the standard solver on shared memory.

Table 4.2: Full resolution model instances, sizes of their corresponding optimisation problems, utilised hardware and computational performance indicators.

metric	standard IP	PIPS-IPM++	PIPS-IPM++	PIPS-IPM++ (cap. inequ.)[1]
model regions	115	115	115	115
time steps	43,800	43,800	43,800	43,800
expansion decisions	12,857	12,857	12,857	12,857
mio. variables (presolved)	199.5 (192.3)	199.5 (193.2)	199.5 (193.2)	199.5 (193.2)
mio. constraints (presolved)	194.2 (181.5)	215.0 (203.8)	215.0 (203.8)	215.0 (203.8)
mio. non-zeros (presolved)	856.7 (824.3)	877.5 (846.0)	877.5 (846.0)	877.5 (846.0)
blocks	-	80	40	40
compute nodes	1	5	5	5
CPU resources in cores	16	640	640	640
peak memory per node in GB	680	375	284	284
time to solve in s	615,522	148,222	143,987	113,823
compute in core-h	21,885 [2]	26,350	25,597	20,235

[1] Using the relaxed capacity formulation described in Section 2.1.2

[2] While the standard IP solver effectively uses only 16 cores, the full cores per node were used for the calculation of the compute due to memory being the limiting factor (see the discussion on farming factors in *Publication 2*)

Lastly, the relaxation of the capacity equalities leads to an underestimation of 1.2% in overall system cost, but still adequately captures the transformation pathway reasonably well. Therefore, the further reduction of the overall compute time of 21% (translating to an absolute reduction of 8.4 hours) against the already significantly faster solution with PIPS-IPM++ can be a well-founded consideration, if the exactness of decommissioning decisions does not play a major role for the research question at hand.

5 Discussion

The collective results from *Publication 1* to *3* and the *Extended Results* demonstrate that the reimplementation of the REMix framework and the application of PIPS-IPM++ can, in fact, enable the solution of large-scale capacity expansion pathways within a reasonable timeframe. In particular, the choice of concrete case studies on the interactions between annual capacity expansion rates and domestic hydrogen production highlights the benefits that the application offers for research into energy systems in practice. To put the findings into context, first, Section 5.1 discusses the key insights for the initially posed research questions and outlines associated limitations of the model-based application of capacity expansion pathways towards a climate-neutral energy system. Section 5.2 then addresses the method-oriented research questions, further discussing the insights with respect to the decomposition strategy and solver configuration, as well as limitations and future use-cases that could also benefit from the application of massively parallel solvers.

5.1 Modelling transformation pathways in high temporal and spatial resolution

What is the future role of energy imports in the European energy system compared to domestic production, and what factors are driving this development?

Regarding the future role of energy imports, the results of the model-based analysis in *Publication 1* suggest that, while a fully domestic supply of green energy carriers is possible, strategic energy partnerships could contribute to reducing total system costs by around 3%, confirming similar findings from studies on strategic energy partnerships with North Africa [89]. The model results also indicate that for high shares of domestic hydrogen production, seasonal storage in the form of gas caverns is required to facilitate surplus generation in summer with an overall storage demand of up to 300 TWh,

confirming results from studies with a similar methodology [35]. Furthermore, the model results suggest significant PV capacity expansion in the Iberian Peninsula and North Africa, as well as substantial onshore wind capacity in the British Isles. This corroborates the findings of other studies on hydrogen integration [15].

Taking into account the results from *Publication 3*, some of these findings are partially confirmed and some are partially challenged. In particular, the introduction of transformation pathways provides further distinction in terms of capacity expansion along the transformation pathway, showing that, in the short term, the addition of onshore wind energy in the United Kingdom (UK) and, in the long term, the supply from PV in southern Spain is preferable. While these findings on country concentrations for VRE are in line with previous findings [35], the introduction of country- and technology-specific annual capacity expansion rates reduces high concentrations of capacity expansion in favour of more distributed expansion across Europe. As a consequence, these limitations lead to lower investment in electrolysers, thereby increasing the share of imported hydrogen and green methane. In the case of high expansion rates, fully avoiding green energy imports increases the overall system costs of the transformation by 16%, as a consequence of a significantly higher competition between direct electrification and indirect electrification via hydrogen. Similar effects of limitations on VRE expansion leading to increased energy imports can be observed in myopic expansion pathways [90].

Furthermore, the modelling results from both *Publications 1* and *3* highlight the strong impact that hydrogen import cost assumptions play for the optimal network topology. In a wide range of scenarios, in particular the corridors from North Africa and Turkey are expanded to facilitate pipeline-based imports of hydrogen towards Central Europe. If a global hydrogen market with competitive prices emerges, the infrastructure shifts towards higher shares of port based imports. While the overall design of the energy system in a least-cost optimisation approach naturally reflects these highly pronounced solutions, additional aspects have to be considered when it comes to a joint European import strategy: First and foremost, the reliance on pipeline-based imports, while economically attractive, can lead to high reliance on individual exporting countries [91]. Therefore, any import strategy should place additional emphasis on further diversifying import sources, for example via port-based imports, allowing for the access to more hydrogen exporting countries. However, in particular when it comes to facilitating a global hydrogen market further international regulations and standardisation are necessary [87].

Similarly, the grid topology in all the considered scenarios with significant domestic production of hydrogen includes key corridors between European countries. These ensure access to hydrogen storage caverns for seasonal balancing. This confirms the results of previous work focussing on the network

topology for a fully domestic supply of green hydrogen [30]. Facilitating the necessary regulations and infrastructure for cross-border projects therefore also requires a close coordination on a European level and strong integration of the European hydrogen sourcing strategy with infrastructure planning.

How do limitations in annual capacity expansion rates constrain the large-scale integration of green hydrogen, and what impact do they have on the overall energy system design?

As shown in *Publication 3*, modelling transformation pathways with high spatial and temporal resolution successfully bridges the research gap between models that use target year optimisation of high shares of renewables and network infrastructure with high temporal resolution, and models with a wider sectoral scope that include transformation pathways, but require strong temporal aggregation. This high temporal resolution provides an accurate representation of a wide range of VRE generation profiles and both short-term and seasonal energy storage, which is particularly important in the context of high levels of domestic electricity and hydrogen production from renewable sources [65]. The extension to transformation pathways with perfect foresight leads to a more cost-efficient system transformation, allowing the model to endogenously account for the cumulative carbon budget as well as to integrate limited capacity expansion rates.

The combination of strong emission reduction targets with limited VRE capacity expansion rates highlights various challenges. Firstly, the national limitation in particular leads to a decrease in large VRE investments in countries with high solar and wind potential, as discussed previously in the context of energy imports. However, this limitation also leads to the capacity targets outlined in the NECP between the EU and its member states being achieved later than planned. This effect can particularly be observed in Germany and Spain, as discussed in the results of *Publication 3*. Similar findings have been observed in other studies comparing capacity expansions for different technologies to short-term targets for 2030 [90]. These high country concentrations, with respect to both the targets and the investments, lead to a strong reliance on individual countries when realizing European energy and climate plans. Additional coordination is therefore required to further spatially diversify the expansion of VRE capacities across Europe.

Secondly, contrasting the unconstrained and constrained VRE capacity expansion rates reveals a significantly higher short-term blue hydrogen production. This can be explained by the model anticipating reduced investment costs for electrolyser stacks in later years and delaying investments into electrolysers. However, in the results of *Publication 3*, this delaying strategy causes a significant investment peak into both PV and electrolyser capacities in the model year 2040. With limited capacity expansion rates, the model correctly plans the necessary scale-up ahead and starts the investments

earlier, but also reaches a lower capacity level in the long term. This effect highlights the indirect risks of strong reliance on blue hydrogen technologies, particularly given that the cost-competitiveness of blue hydrogen in Europe still hinges on achieving high capture rates [92]. This poses a particular challenge for policymakers, who must strike a reasonable balance between further strengthening investor confidence in green hydrogen to close the gap in short-term ambitions for scaling up [93] and ensuring that blue hydrogen can contribute to emission reductions.

Limitations and future work

Given the size of the overall optimisation problem, the chosen approach of using linear programming to identify the least-cost transformation pathways can be a reasonable starting point to inform the overall design of the energy system. However, similar to other modelling approaches, this particular choice has various limitations that must be considered when interpreting the results and drawing conclusions for policy recommendations [5].

Firstly, while a central planner can generally identify the most cost-effective system, its implementation in reality requires consideration of the perspectives and incentives of a wide range of stakeholders and regulatory frameworks. For example, a site-specific assessment of the transition to low-carbon processes in large industrial centres can better capture discrete investment decisions in specific technologies [94]. Similarly, the optimal system from the perspective of a central planner can lead to significant differences in market participants' profitability based on local market values and resource availability [95]. This discrepancy can be addressed, for example, by implementing the model as a bilevel optimisation problem to capture decentralised decision-making processes [96]. However, this approach significantly increases model complexity, rendering the method unsuitable for problems with high spatial and temporal resolution.

Similarly, with respect to the modelling of the transformation pathway, the deterministic nature of the chosen perfect foresight approach does not sufficiently reflect the uncertainties associated with specific investment decisions. In particular uncertainty regarding future carbon prices and price shocks necessitates the adequate capture of decision-makers' myopia [9]. Similarly, deterministic modelling of transformation pathways does not account for the need to respond adaptively to new information. While this could be achieved through methodological improvements towards stochastic or robust optimisation, this would further increase the computational challenge.

The resulting network topology for hydrogen in *Publication 3* indicates a strong preference for connecting large domestic hydrogen production sites to seasonal energy storage with a more decentralised network structure around the corridors. As previously discussed, the importance of pipeline- and ship-based

imports depends heavily on import cost assumptions. As with the adaptability of the pathway, further research is required to determine a robust network topology for the initial short-term build-up. Ideally, investment decisions for pipeline systems should be represented as integer variables to account for different pipeline diameters [97]. Likewise, when planning concrete hydrogen pipelines, a higher spatial resolution is required to accurately model the individual pipelines, adequately model pressure levels and flow restrictions, and further account for maintaining the operational status of the natural gas pipeline network during the transformation process [98]. In addition to gas networks, further considerations have to be included for electrical grids. Here, in particular integrated modelling of inertia and frequency stability requirements can increase the overall amount of curtailment of electricity generation from VREs [99].

Further limitations are connected to the assumptions for the input data. While, in particular, *Publication 3* highlights the crucial role of annual capacity expansion rates, further investigation into the underlying limiting factors is required, which can include dependency on technology and component imports, availability of skilled workers, and national and European policies and incentives [100, 101]. To adequately account for individual limiting factors and dynamic effects, additional country- and technology specific variation of expansion rates need to be considered in future assessments.

5.2 Overcoming computational boundaries for linear ESOMs

Which aspects of ESOMs with a high spatial and temporal resolution cause the computational burden in large-scale applications?

Generally speaking, the main driver of the computational burden can be identified as either the overall size of the model or the number of capacity expansion decisions. In particular, the findings in *Publication 2* suggest that for large-scale capacity expansion models, the overall time taken to solve the model is the main limiting factor. In contrast, for large-scale economic dispatch models, the available shared memory is estimated to become the limiting factor. The results of the computational experiment conducted by Rehfeldt et al. [56] support this finding for economic dispatch models: Their economic dispatch instance for Central Western Europe and for the full European system can be solved in less than 2 hours and less than 24 hours, respectively. However, it should be noted that the experiment was conducted on a 2 TB shared-memory compute node, and no information about the peak memory usage is provided.

In contrast, for the of large-scale capacity expansion problems conducted in the computational experiment *Extended Results* the time to solve the problem instances becomes significantly more

prohibitive. While the problem size in terms of variables and constraints is comparable to that of the economic dispatch problem for the full European system optimised by Rehfeldt et al. [56], the 170 hours required to solve the model instance on shared memory indicate a significantly greater computational burden. Unfortunately, due to the different CPUs and memory configurations, a direct comparison between the two runs is not possible. However, similar excessive computational times of over 300 hours for optimising large-scale capacity expansion pathways have been reported by Kountouris et al. [34].

Taking these two extremes into account, the recommendation for energy system modellers is that only the absolutely necessary expansion variables should be active in the mathematical formulation. To this end, model runs with a downsampled resolution can provide a general idea about the economic competitiveness of individual technologies and allow for a pre-selection. If further reduction of the capacity expansion decision is not possible, an alternative approach is to run the analysis using complexity reduction techniques and provide an additional assessment of the inaccuracies compared to the full temporal resolution, as done in *Publication 3*.

What impact do the decomposition strategy and hardware configuration have on the performance of massively parallel solvers when applied to ESOMs?

Unlike the standard workflow that modellers are accustomed to, the application of PIPS-IPM++ and other block-structured solvers requires additional steps in the workflow as well as a deeper understanding of the model formulation and the available hardware for the computation. The first crucial choice involves the decomposition strategy, where insights from mathematical decomposition approaches, in particular Benders decomposition and Lagrangian relaxation, can be useful.

For both computational experiments in *Publication 2* and the *Extended Results*, a decomposition along the temporal dimension was chosen due to two key considerations. Firstly, this strategy can easily be scaled up to generate a wide range of annotations with a large number of parallel blocks while keeping the number of additional linking constraints relatively low. This simplifies conducting experiments on the scalability of the parallelisation. Secondly, this approach ensures that the blocks are identical in size when optimising for a single target year, as described in *Publication 2*, or roughly similar in size when addressing transformation pathways, as described the in the *Extended Results*. In both cases, using blocks of a similar size and computational burden ensures that no single block limits the overall runtime during the parallel phase. Similar considerations are referred to as granularity and homogeneity for the automatic detection of matrix structures for Lagrangian relaxation [102]. Also, for applications of Benders decomposition to ESOMs, in particular a time based decomposition is

frequently chosen, as it allows splitting of the capacity expansion problem from the economic dispatch problem [103].

For the application of PIPS-IPM++ in particular, the next step is to identify a well-performing solver configuration. This is because a limited number of parallel processes and an insufficient number of parallel cores per process can both lead to computational bottlenecks and diminish the performance benefits. In particular, the hardware layout of the compute nodes and the overall cluster must be considered to optimise for cache locality and NUMA. While the results of the computational experiments in *Publication 2* indicate certain trends, such as the preference for a higher number of blocks for economic dispatch models and a lower number for capacity expansion problems, these results may not necessarily be transferable to other models, especially if they do not utilise an hourly resolution. Throughout the modelling process, a higher emphasis should also be placed on ensuring a concise model formulation. While this can lead to performance benefits in standard IP solvers [67], it is even more relevant for the application of PIPS-IPM++, as the extent of presolving is more limited in order to preserve the underlying block structure.

In what ways can massively parallel solvers provide performance benefits and overcome hardware limitations when applied to capacity expansion pathways?

The computational experiments in *Publication 2* and the *Extended Results* highlight the effectiveness of applying the massively parallel solver PIPS-IPM++ in addressing both large-scale economic dispatch models and capacity expansion models. However, the concrete benefits strongly depend on both the model instance to be solved, as well as the available hardware. The first main benefit is that model instances can be solved in significantly less time if sufficient hardware for parallel processing is available. While the achievable speed-up can range from 5–10 times that of standard IP solvers on shared memory systems, this can translate into a wall-clock time reduction from 170 hours down to 32 hours, as demonstrated in the *Extended Results*. However, this speed-up is also associated with one of the main challenges in applying massively parallel solvers, which is the identification of well-performing configurations. In particular, the findings from *Publication 2* indicate that if suboptimal configurations are chosen, this can easily diminish any performance gains.

The second main benefit of applying massively parallel solvers is connected to their scalability. The ability to run large-scale optimisation problems on distributed memory architectures bypasses the limitations of shared memory systems when the size of the optimisation problem becomes too large by distributing the optimisation across multiple nodes. An example of this can be seen in the *SIMPLE6* instance of the computational experiment by Rehfeldt et al. [56], where the utilised 2 TB compute

node is insufficient to store the optimisation matrix, rendering the instance completely intractable. However, it should be noted that memory limitations with respect to the maximum number of linking variables and constraints can still occur due to the computation of the global Schur complement on the main process. This limitation poses a greater challenge with regard to the number of capacity expansion decisions that can be considered simultaneously and requires further investigation.

Limitations and future work

One of the major limitation of PIPS-IPM++ is that it can only be applied to linear optimisation problems, which restricts its application to specific research questions. While extending the underlying IP algorithm to consider QPs is theoretically possible, it would still be unable to answer research questions requiring integer variables, such as the previously discussed consideration of pipeline diameters in ESOMs. This fundamental aspect of problem types cannot be easily overcome and other approaches such as specific non-linear solvers or iterative model coupling need to be considered. However, in particular the suitability for large-scale LPs should allow the extension of use-cases to transformation pathways with a stochastic component, or applications in the context of European resource adequacy assessment (ERAA), where a capacity expansion model is optimised and subsequently cross-tested against a large number of different weather scenarios. Here, typically only a subset of weather years is crucial for determining the capacity expansion, while a different subset of weather years are determining with respect to the cost associated to the economic dispatch [65]. Although this problem has been previously addressed using HPC and an optimised sub-gradient method [104] it would provide an interesting use-case for the future application of PIPS-IPM++.

Another limitation is the small number of models to which PIPS-IPM++ has been applied so far. Compared to the literature findings for economic dispatch problems, the observed speed-up for capacity expansion models do not demonstrate the same performance increases. Although this can be explained by the number of capacity expansion decisions, which correspond to the overall linking variables included in capacity expansion problems, it nevertheless indicates that further limitations exist. While the successful application of PIPS-IPM++ to the European TIMES model EUSTEM in the the computational experiment by Panos and Hassan [105] indicates a possible transferability to other problem types, more systematic testing of the solver on a wide range of different ESOMs is required, as discussed in more detail in *Publication 2*. As with testing on different models, a better understanding of the impact of specific mathematical formulations on performance is also required. While the *Extended Results* demonstrate that slight modifications to the capacity balance can significantly reduce the optimisation time, the testing of different formulations was by no means exhaustive. Future research

should therefore focus on investigating matrix scaling and preconditioning, as well as ways to reduce the number of linking variables and constraints further.

Access to sufficiently performant hardware can be considered a further possible limitation for applying PIPS-IPM++. While the wider availability of HPC clusters and cloud-computing can address this aspect, so far the typical use-case in the ESOM community is limited to using clusters to run a large set of scenarios in parallel [106], rather than distributed computing applications. Conversely, for the effective application the technical knowledge for the compilation of the solver and required mathematical libraries can pose a challenge. While this limitation can be overcome to a certain degree by providing a readily available software solution via containerisation, the correct setup of decomposition strategies, hardware considerations, and solver configuration are still crucial for obtaining a reasonable performance that outperforms readily available implementations of standard IP methods and need to be adjusted for each optimisation problem individually. Finding this setup requires detailed understanding of the involved computations and effective ways to profile individual parts to identify computational bottlenecks.

Furthermore, there remains significant potential for improvement, not only with regard to possible applications, but also in terms of the further development of parallel solvers. Given the increasing availability of GPU-based parallel processing power, primarily driven by the training and inference of large language models, running compute-heavy sections of the PIPS-IPM++ algorithm or fully porting the algorithms to run on GPUs presents a reasonable next step. In order to encourage the development of an ecosystem around parallel solvers and make them more accessible to new users, it is also necessary to reduce the level of difficulty. This involves improving the understanding of model formulation, the impact on performance and the automation of decomposition strategies, as well as the deployment of solvers – all of which can present challenges to solver adoption. More generally, the additional steps in the workflow, such as model generation, annotation, decomposition and reintegration of the solution for post-processing, can also be challenging, but this can be more easily addressed via tighter integration between the modelling framework and the solver.

6
Conclusions

Taking a step back, this now allows answering the overarching Research Question addressed by this thesis and reflecting on the broader context the individual parts contribute to the research on energy systems.

The narrative of the included publications reflects the experiences of other modellers who have addressed European energy systems via ESOMs. While the first publication in particular enabled a detailed, model-based assessment of the different roles and drivers of energy imports in a European context and demonstrated the value of reimplementing the REMix framework, limitations in the spatial scope and the method of optimising only a target year restricted insights into the network topology and the system's transformation over time, respectively. As with other research questions, attempting to answer a set of specific questions using a model-based assessment reveals limitations relating to particular aspects. These can include the resolution of network infrastructure, the operational patterns of individual technologies, the adequacy of VRE generation profiles and, in this specific case, the representation of long-term capacity expansion pathways. Overcoming these limitations often requires larger, more detailed models, at least to ascertain the validity of specific simplifications and assumptions.

While most previous research has focused on finding methods to reduce complexity in order to address these limitations, in contrast, this thesis developed methods to extend the computational bounds by using the massively parallel processing power of HPC. While this approach involved a steep learning curve and in-depth understanding, in particular the results from the second publication demonstrate that massively parallel solvers can be effectively applied to shift the computational limits for large-scale capacity expansion problems, provided that the correct decomposition strategy is implemented and the proper hardware configuration is identified. Unlike complexity reduction, which allows trade-offs between model dimensions within a quantitative computational limit, the scalability of distributed memory systems enables a qualitative change by circumventing memory limitations and accelerating

the solving of larger optimisation problems. However, it is important to note that utilising massively parallel solvers, such as PIPS-IPM++, and applying complexity reduction methods are not mutually exclusive. In particular, combining carefully selected methods with the performance gains of HPC can significantly increase the level of detail that can be represented, thereby enhancing the explanatory power and insights gained from ESOMs.

This increase in explanatory power was demonstrated in the third publication, which extends the scope to include integrated transformation pathways with perfect foresight and allows the challenges associated with limited technology capacity expansion rates to be evaluated. This publication explores how these challenges interact with the available carbon budget and different hydrogen sources, such as green hydrogen imports and offshore blue hydrogen production. Although complexity reduction methods were still necessary for that specific publication, the extended results included in this thesis demonstrate that optimisation of the full hourly model can be achieved within a similar timeframe through the effective application of PIPS-IPM++, with some further consideration given to the mathematical model formulation.

In summary, the combined publications and extended results of this thesis demonstrate the effectiveness of applying massively parallel solvers to tackle large-scale linear optimisation problems while significantly reducing the solution time. To enable that, this thesis provides the foundational knowledge on the application and performance considerations, outlining how the use of massively parallel solvers can significantly benefit a whole range of related optimisation problems in the field of energy systems. This is of particular value for problem types which include a strong focus on the temporal dimension with limited expansion decisions, such as the stochastic representation of uncertainties. Taken in its completeness, this thesis therefore successfully demonstrates the value of using HPC clusters to enable the computation of energy system transformation pathways with high temporal and spatial detail.

References

[1] S. Dhakal, J.C. Minx, F.L. Toth, A. Abdel-Aziz, M.J. Figueroa Meza, K. Hubacek, I.G.C. Jonckheere, Y.G. Yong-Gun Kim, and G.F. Nemet. Emissions trends and drivers. In Intergovernmental Panel on Climate Change, editor, *Climate Change 2022 - Mitigation of Climate Change*, pages 215–294. Cambridge University Press, 2022. doi: 10.1017/9781009157926.004.

[2] L. Clarke, Y.-M. Wei, A. De La Vega Navarro, A. Garg, A.N. Hahmann, S. Khennas, I.M.L. Azevedo, A. Löschel, A.K. Singh, L. Steg, G. Strbac, and K. Wada. Energy systems. In Intergovernmental Panel on Climate Change, editor, *Climate Change 2022 - Mitigation of Climate Change*, pages 613–746. Cambridge University Press, 2022. doi: 10.1017/9781009157926.008.

[3] Johan Rockström, Owen Gaffney, Joeri Rogelj, Malte Meinshausen, Nebojsa Nakicenovic, and Hans Joachim Schellnhuber. A roadmap for rapid decarbonization. *Science*, 355(6331):1269–1271, 2017.

[4] Dan Tong, Qiang Zhang, Yixuan Zheng, Ken Caldeira, Christine Shearer, Chaopeng Hong, Yue Qin, and Steven J. Davis. Committed emissions from existing energy infrastructure jeopardize 1.5 °c climate target. *Nature*, 572(7769):373–377, 2019. doi: 10.1038/s41586-019-1364-3.

[5] Georgios Savvidis, Kais Siala, Christoph Weissbart, Lukas Schmidt, Frieder Borggrefe, Subhash Kumar, Karen Pittel, Reinhard Madlener, and Kai Hufendiek. The gap between energy policy challenges and model capabilities. *Energy Policy*, 125:503–520, 2019. ISSN 03014215. doi: 10.1016/j.enpol.2018.10.033.

[6] Stefan Pfenninger, Adam Hawkes, and James Keirstead. Energy systems modeling for twenty-first century energy challenges. *Renewable and Sustainable Energy Reviews*, 33:74–86, 2014. ISSN 13640321. doi: 10.1016/j.rser.2014.02.003.

[7] Matteo Giacomo Prina, Giampaolo Manzolini, David Moser, Benedetto Nastasi, and Wolfram

Sparber. Classification and challenges of bottom-up energy system models - a review. *Renewable and Sustainable Energy Reviews*, 129:109917, 2020. ISSN 13640321. doi: 10.1016/j.rser.2020.109917.

[8] Ilkka Keppo and Manfred Strubegger. Short term decisions for long term problems – the effect of foresight on model based energy systems analysis. *Energy*, 35(5):2033–2042, 2010. ISSN 03605442. doi: 10.1016/j.energy.2010.01.019.

[9] Jerry Lambert, Andreas Hanel, Sebastian Fendt, and Hartmut Spliethoff. Evaluation of sector-coupled energy systems using different foresight horizons. *Renewable and Sustainable Energy Reviews*, 184:113562, 2023. ISSN 13640321. doi: 10.1016/j.rser.2023.113562.

[10] Evelina Trutnevyte. Does cost optimization approximate the real-world energy transition? *Energy*, 106:182–193, 2016. ISSN 03605442. doi: 10.1016/j.energy.2016.03.038.

[11] Konstantin Löffler. Social discounting, social costs of carbon, and their use in energy system models. *Environmental Research Letters*, 16(10):104005, 2021. doi: 10.1088/1748-9326/ac228a.

[12] Christian Bussar, Philipp Stöcker, Zhuang Cai, Luiz Moraes Jr., Dirk Magnor, Pablo Wiernes, Niklas van Bracht, Albert Moser, and Dirk Uwe Sauer. Large-scale integration of renewable energies and impact on storage demand in a European renewable power system of 2050—sensitivity study. *Journal of Energy Storage*, 6:1–10, 2016. ISSN 2352152X. doi: 10.1016/j.est.2016.02.004.

[13] Hans Christian Gils, Yvonne Scholz, Thomas Pregger, Diego Luca de Tena, and Dominik Heide. Integrated modelling of variable renewable energy-based power supply in Europe. *Energy*, 123:173–188, 2017. ISSN 03605442. doi: 10.1016/j.energy.2017.01.115.

[14] Hans Christian Gils, Hedda Gardian, and Jens Schmugge. Interaction of hydrogen infrastructures with other sector coupling options towards a zero-emission energy system in Germany. *Renewable Energy*, 180:140–156, 2021. ISSN 09601481. doi: 10.1016/j.renene.2021.08.016.

[15] Fabian Neumann, Elisabeth Zeyen, Marta Victoria, and Tom Brown. The potential role of a hydrogen network in Europe. *Joule*, 7(8):1793–1817, 2023. doi: 10.1016/j.joule.2023.06.016.

[16] Hans-Kristian Ringkjøb, Peter M. Haugan, and Ida Marie Solbrekke. A review of modelling tools for energy and electricity systems with large shares of variable renewables. *Renewable and Sustainable Energy Reviews*, 96:440–459, 2018. ISSN 13640321. doi: 10.1016/j.rser.2018.08.002.

[17] Maximilian Hoffmann, Bruno U. Schyska, Julian Bartels, Tristan Pelser, Johannes Behrens, Manuel Wetzel, Hans Christian Gils, Chuen-Fung Tang, Marius Tillmanns, Jan Stock, André Xhonneux, Leander Kotzur, Aaron Praktiknjo, Thomas Vogt, Patrick Jochem, Jochen Linßen,

Jann M. Weinand, and Detlef Stolten. A review of mixed-integer linear formulations for framework-based energy system models. *Advances in Applied Energy*, 16:100190, 2024. ISSN 26667924. doi: 10.1016/j.adapen.2024.100190.

[18] Leander Kotzur, Lars Nolting, Maximilian Hoffmann, Theresa Groß, Andreas Smolenko, Jan Priesmann, Henrik Büsing, Robin Beer, Felix Kullmann, Bismark Singh, Aaron Praktiknjo, Detlef Stolten, and Martin Robinius. A modeler's guide to handle complexity in energy systems optimization. *Advances in Applied Energy*, 4:100063, 2021. ISSN 26667924. doi: 10.1016/j.adapen.2021.100063.

[19] Kenneth C. Hoffmann and David O. Wood. Energy system modeling and forecasting, 1975.

[20] EG Cazalet. Overview of the SRI-Gulf energy modeling methodology, 1975.

[21] Gregor Czisch and Gregor Giebel. Realisable scenarios for a future electricity supply based 100% on renewable energies. In *Risø International Energy Conference 2007: Energy Solutions for Sustainable Development*, pages 186–195. Risø National Laboratory, 2007.

[22] Mark Z. Jacobson and Mark A. Delucchi. Providing all global energy with wind, water, and solar power, part I: Technologies, energy resources, quantities and areas of infrastructure, and materials. *Energy Policy*, 39(3):1154–1169, 2011. ISSN 03014215. doi: 10.1016/j.enpol.2010.11.040.

[23] Mark A. Delucchi and Mark Z. Jacobson. Providing all global energy with wind, water, and solar power, part II: Reliability, system and transmission costs, and policies. *Energy Policy*, 39(3): 1170–1190, 2011. ISSN 03014215. doi: 10.1016/j.enpol.2010.11.045.

[24] Christian Breyer, Siavash Khalili, Dmitrii Bogdanov, Manish Ram, Ayobami Solomon Oyewo, Arman Aghahosseini, Ashish Gulagi, A. A. Solomon, Dominik Keiner, Gabriel Lopez, Poul Alberg Ostergaard, Henrik Lund, Brian V. Mathiesen, Mark Z. Jacobson, Marta Victoria, Sven Teske, Thomas Pregger, Vasilis Fthenakis, Marco Raugei, Hannele Holttinen, Ugo Bardi, Auke Hoekstra, and Benjamin K. Sovacool. On the history and future of 100% renewable energy systems research. *IEEE Access*, 10:78176–78218, 2022. doi: 10.1109/ACCESS.2022.3193402.

[25] J. P. Deane, G. Drayton, and B. P. Ó Gallachóir. The impact of sub-hourly modelling in power systems with significant levels of renewable generation. *Applied Energy*, 113:152–158, 2014. ISSN 03062619. doi: 10.1016/j.apenergy.2013.07.027.

[26] Jonas Hörsch, Henrik Ronellenfitsch, Dirk Witthaut, and Tom Brown. Linear optimal power flow using cycle flows. *Electric Power Systems Research*, 158:126–135, 2018. ISSN 03787796. doi: 10.1016/j.epsr.2017.12.034.

[27] Katrin Schaber, Florian Steinke, and Thomas Hamacher. Transmission grid extensions for the integration of variable renewable energies in Europe: Who benefits where? *Energy Policy*, 43: 123–135, 2012. ISSN 03014215. doi: 10.1016/j.enpol.2011.12.040.

[28] F. Cebulla, T. Naegler, and M. Pohl. Electrical energy storage in highly renewable European energy systems: Capacity requirements, spatial distribution, and storage dispatch. *Journal of Energy Storage*, 14:211–223, 2017. ISSN 2352152X. doi: 10.1016/j.est.2017.10.004.

[29] T. Brown, D. Schlachtberger, A. Kies, S. Schramm, and M. Greiner. Synergies of sector coupling and transmission reinforcement in a cost-optimised, highly renewable European energy system. *Energy*, 160(Supplement C):720–739, 2018. ISSN 03605442. doi: 10.1016/j.energy.2018.06.222. URL `http://arxiv.org/pdf/1801.05290v2`.

[30] Dilara Gulcin Caglayan, Heidi U. Heinrichs, Martin Robinius, and Detlef Stolten. Robust design of a future 100% renewable European energy supply system with hydrogen infrastructure. *International Journal of Hydrogen Energy*, 46(57):29376–29390, 2021. ISSN 03603199. doi: 10.1016/j.ijhydene.2020.12.197.

[31] Maximilian Pfennig, Diana Böttger, Benedikt Häckner, David Geiger, Christoph Zink, André Bisevic, and Lukas Jansen. Global GIS-based potential analysis and cost assessment of power-to-x fuels in 2050. *Applied Energy*, 347:121289, 2023. ISSN 03062619. doi: 10.1016/j.apenergy.2023.121289.

[32] Michael Moritz, Max Schönfisch, and Simon Schulte. Estimating global production and supply costs for green hydrogen and hydrogen-based green energy commodities. *International Journal of Hydrogen Energy*, 48(25):9139–9154, 2023. ISSN 03603199. doi: 10.1016/j.ijhydene.2022.12.046.

[33] Jana Fakhreddine, Paul E. Dodds, and Isabela Butnar. Global hydrogen trade pathways: A review of modelling advances and challenges. *International Journal of Hydrogen Energy*, 129: 236–252, 2025. ISSN 03603199. doi: 10.1016/j.ijhydene.2025.04.203.

[34] Ioannis Kountouris, Rasmus Bramstoft, Theis Madsen, Juan Gea-Bermúdez, Marie Münster, and Dogan Keles. A unified European hydrogen infrastructure planning to support the rapid scale-up of hydrogen production. *Nature communications*, 15(1):5517, 2024. doi: 10.1038/s41467-024-49867-w.

[35] Tobias Fleiter, Joshua Fragoso, Benjamin Lux, Şirin Alibaş, Khaled Al-Dabbas, Pia Manz, Felix Neuner, Bastian Weißenburger, Matthias Rehfeldt, and Frank Sensfuß. Hydrogen infrastructure in the future CO2-neutral European energy system—how does the demand for hydrogen

affect the need for infrastructure? *Energy Technology*, 13(2), 2025. ISSN 2194-4288. doi: 10.1002/ente.202300981.

[36] Ramachandran Kannan and Hal Turton. A long-term electricity dispatch model with the TIMES framework. *Environmental Modeling & Assessment*, 18(3):325–343, 2013. ISSN 1420-2026. doi: 10.1007/s10666-012-9346-y.

[37] Stefan L. Luxembourg, Steven S. Salim, Koen Smekens, Francesco Dalla Longa, and Bob van der Zwaan. TIMES-Europe: An integrated energy system model for analyzing Europe's energy and climate challenges. *Environmental Modeling & Assessment*, 30(1):1–19, 2025. ISSN 1420-2026. doi: 10.1007/s10666-024-09976-8.

[38] Mark Howells, Holger Rogner, Neil Strachan, Charles Heaps, Hillard Huntington, Socrates Kypreos, Alison Hughes, Semida Silveira, Joe DeCarolis, Morgan Bazillian, and Alexander Roehrl. OSeMOSYS: The open source energy modeling system. *Energy Policy*, 39(10):5850–5870, 2011. ISSN 03014215. doi: 10.1016/j.enpol.2011.06.033.

[39] Karl-Kiên Cao, Jannik Haas, Evelyn Sperber, Shima Sasanpour, Seyedfarzad Sarfarazi, Thomas Pregger, Oussama Alaya, Hendrik Lens, Simon R. Drauz, and Tanja M. Kneiske. Bridging granularity gaps to decarbonize large–scale energy systems—the case of power system planning. *Energy Science & Engineering*, 9(8):1052–1060, 2021. ISSN 2050-0505. doi: 10.1002/ese3.891.

[40] Laura Torralba-Díaz, Christoph Schimeczek, Johannes Kochems, and Kai Hufendiek. Iterative coupling of a fundamental electricity market model and an agent-based simulation model to reduce the efficiency gap. *Energy*, 310:133192, 2024. ISSN 03605442. doi: 10.1016/j.energy.2024.133192.

[41] Felix Nitsch, Manuel Wetzel, Hans Christian Gils, and Kristina Nienhaus. The future role of Carnot batteries in Central Europe: Combining energy system and market perspective. *Journal of Energy Storage*, 85:110959, 2024. ISSN 2352152X. doi: 10.1016/j.est.2024.110959.

[42] Leander Kotzur, Peter Markewitz, Martin Robinius, and Detlef Stolten. Impact of different time series aggregation methods on optimal energy system design. *Renewable Energy*, 117:474–487, 2018. ISSN 09601481. doi: 10.1016/j.renene.2017.10.017.

[43] Leonard Göke and Mario Kendziorski. Adequacy of time-series reduction for renewable energy systems. *Energy*, 238:121701, 2022. ISSN 03605442. doi: 10.1016/j.energy.2021.121701.

[44] Leonard Göke. A graph-based formulation for modeling macro-energy systems. *Applied Energy*, 301:117377, 2021. ISSN 03062619. doi: 10.1016/j.apenergy.2021.117377.

[45] Martha Maria Frysztacki, Gereon Recht, and Tom Brown. A comparison of clustering methods for the spatial reduction of renewable electricity optimisation models of Europe. *Energy Informatics*, 5(1), 2022. doi: 10.1186/s42162-022-00187-7.

[46] Jan Priesmann, Lars Nolting, and Aaron Praktiknjo. Are complex energy system models more accurate? An intra-model comparison of power system optimization models. *Applied Energy*, 255:113783, 2019.

[47] J. F. Benders. Partitioning procedures for solving mixed-variables programming problems. *Numerische Mathematik*, pages 238–252, 1962.

[48] David P. Morton. An enhanced decomposition algorithm for multistage stochastic hydroelectric scheduling. *Annals of Operations Research*, pages 211–235, 1996.

[49] Christian Skar, Gerard Doorman, and Asgeir Tomasgard. Large-scale power system planning using enhanced Benders decomposition. In *2014 Power Systems Computation Conference*, pages 1–7. IEEE, 2014. ISBN 978-83-935801-3-2. doi: 10.1109/PSCC.2014.7038297.

[50] Filippo Pecci and Jesse D. Jenkins. Regularized Benders decomposition for high performance capacity expansion models. *IEEE Transactions on Power Systems*, 40(4):3105–3116, 2025. ISSN 0885-8950. doi: 10.1109/TPWRS.2025.3526413.

[51] Gary L Schultz and Robert R Meyer. An interior point method for block angular optimization. *SIAM Journal on Optimization*, 1(4):583–602, 1991.

[52] Andrzej Ruszczyński. Decomposition methods in stochastic programming. *Mathematical programming*, 79(1):333–353, 1997.

[53] Jacek Gondzio and Andreas Grothey. Exploiting structure in parallel implementation of interior point methods for optimization. *Computational Management Science*, 6(2):135–160, 2009. ISSN 1619-697X. doi: 10.1007/s10287-008-0090-3.

[54] Michael E. Gertz and Stephen J. Wright. Object-oriented software for quadratic programming. *ACM Transactions on Mathematical Software*, pages 58–81, 2003.

[55] Cosmin G. Petra, Olaf Schenk, and Mihai Anitescu. Real time stochastic optimization of complex energy systems on high performance computers. *Computing in Science & Engineering*, 2014.

[56] Daniel Rehfeldt, Hannes Hobbie, David Schönheit, Thorsten Koch, Dominik Möst, and Ambros Gleixner. A massively parallel interior-point solver for LPs with generalized arrowhead structure, and applications to energy system models. *European Journal of Operational Research*, 296(1):60–71, 2022. ISSN 03772217. doi: 10.1016/j.ejor.2021.06.063.

[57] Konstantin Löffler, Karlo Hainsch, Thorsten Burandt, Pao-Yu Oei, Claudia Kemfert, and Christian von Hirschhausen. Designing a global energy system based on 100% renewables for 2050: GENeSYS-MOD: An application of the open-source energy modelling system (OSeMOSYS), 2017.

[58] Fabian Scheller and Thomas Bruckner. Energy system optimization at the municipal level: An analysis of modeling approaches and challenges. *Renewable and Sustainable Energy Reviews*, 105: 444–461, 2019. ISSN 13640321. doi: 10.1016/j.rser.2019.02.005.

[59] Martha Maria Frysztacki, Jonas Hörsch, Veit Hagenmeyer, and Tom Brown. The strong effect of network resolution on electricity system models with high shares of wind and solar. *Applied Energy*, 291:116726, 2021. ISSN 03062619. doi: 10.1016/j.apenergy.2021.116726.

[60] Kais Siala and Mohammad Youssef Mahfouz. Impact of the choice of regions on energy system models. *Energy Strategy Reviews*, 25:75–85, 2019. ISSN 2211467X. doi: 10.1016/j.esr.2019.100362.

[61] Jan Abrell, Süheyb Bilici, Markus Blesl, Ulrich Fahl, Felix Kattelmann, Lena Kittel, Mirjam Kosch, Gunnar Luderer, Drin Marmullaku, Michael Pahle, Robert Pietzcker, Renato Rodrigues, and Jonathan Siegle. Optimal allocation of the EU carbon budget: A multi-model assessment. *Energy Strategy Reviews*, 51:101271, 2024. ISSN 2211467X. doi: 10.1016/j.esr.2023.101271.

[62] S. Hilpert, C. Kaldemeyer, U. Krien, S. Günther, C. Wingenbach, and G. Plessmann. The open energy modelling framework (oemof) - a new approach to facilitate open science in energy system modelling. *Energy Strategy Reviews*, 22:16–25, 2018. ISSN 2211467X. doi: 10.1016/j.esr.2018.07.001.

[63] Stefan Pfenninger. Dealing with multiple decades of hourly wind and pv time series in energy models: A comparison of methods to reduce time resolution and the planning implications of inter-annual variability. *Applied Energy*, 197:1–13, 2017. ISSN 03062619. doi: 10.1016/j.apenergy.2017.03.051.

[64] Michal Kaut, Kjetil T. Midthun, Adrian S. Werner, Asgeir Tomasgard, Lars Hellemo, and Marte Fodstad. Multi-horizon stochastic programming. *Computational Management Science*, 11(1-2): 179–193, 2014. ISSN 1619-697X. doi: 10.1007/s10287-013-0182-6.

[65] Tyler H. Ruggles, Edgar Virgüez, Natasha Reich, Jacqueline Dowling, Hannah Bloomfield, Enrico G.A. Antonini, Steven J. Davis, Nathan S. Lewis, and Ken Caldeira. Planning reliable wind- and solar-based electricity systems. *Advances in Applied Energy*, 15:100185, 2024. ISSN 26667924. doi: 10.1016/j.adapen.2024.100185.

[66] M. Schulze, L. Friedrich, and M. Gautschi. Modeling and optimization of renewables: applying the energy hub approach. In *2008 IEEE International Conference on Sustainable Energy Technologies*, pages 83–88. IEEE, 2008. ISBN 978-1-4244-1887-9. doi: 10.1109/ICSET.2008.4746977.

[67] Diego A. Tejada-Arango, Juha Kiviluoma, and Germán Morales-España. Debunking the speed-fidelity trade-off: Speeding-up large-scale energy models while keeping fidelity. *International Journal of Electrical Power & Energy Systems*, 168:110674, 2025. ISSN 01420615. doi: 10.1016/j.ijepes.2025.110674.

[68] Yvonne Scholz. *Renewable energy based electricity supply at low costs – development of the REMix Model and application for Europe*. PhD thesis, University of Stuttgart, 2012.

[69] Daniel Stetter. *Enhancement of the REMix energy system model: Global renewable energy potentials, optimized power plant siting and scenario validation*. PhD thesis, University of Stuttgart, 2012.

[70] Diego Luca de Tena. *Large scale renewable power integration with electric vehicles: Long term analysis for Germany with a renewable based power supply*. PhD thesis, University of Stuttgart, 2014.

[71] Hans Christian Gils. *Balancing of intermittent renewable power generation by demand response and thermal energy storage*. PhD thesis, University of Stuttgart, 2015.

[72] Felix Cebulla. *Storage demand in highly renewable energy scenarios for Europe: the influence of methodology and data assumptions in model-based assessments*. PhD thesis, University of Stuttgart, 2017.

[73] Karl-Kiên Cao. *Modeling energy scenarios with power-flow constraints – Transparency, challenges and system adequacy*. PhD thesis, University of Stuttgart, 2020.

[74] Tobias Junne. *Constructing and evaluating energy futures – life cycle environmental impacts, material demand and transparency of energy scenarios*. PhD thesis, University of Stuttgart, 2021.

[75] Manuel Wetzel, Eugenio Salvador Arellano Ruiz, Francesco Witte, Jens Schmugge, Shima Sasanpour, Madhura Yeligeti, Fabia Miorelli, Jan Buschmann, Karl-Kiên Cao, Niklas Wulff, Hedda Gardian, Alexander Rubbert, Benjamin Fuchs, Yvonne Scholz, and Hans Christian Gils. REMix: A GAMS-based framework for optimizing energy system models. *Journal of Open Source Software*, 9(99):6330, 2024. doi: 10.21105/joss.06330.

[76] George B Dantzig, Alex Orden, Philip Wolfe, et al. The generalized simplex method for minimizing a linear form under linear inequality restraints. *Pacific Journal of Mathematics*, 5(2): 183–195, 1955.

[77] Robert J. Vanderbei. *Linear Programming*, volume 196. Springer US, Boston, MA, 2014. ISBN 978-1-4614-7629-0. doi: 10.1007/978-1-4614-7630-6.

[78] J. A. J. Hall. Towards a practical parallelisation of the simplex method. *Computational Management Science*, 7(2):139–170, 2010. ISSN 1619-697X. doi: 10.1007/s10287-008-0080-5.

[79] Narendra Karmarkar. A new polynomial-time algorithm for linear programming. In *Proceedings of the sixteenth annual ACM symposium on Theory of computing*, pages 302–311, 1984.

[80] Jacek Gondzio and Robert Sarkissian. Parallel interior-point solver for structured linear programs. *Mathematical Programming*, 96(3):561–584, 2003. ISSN 0025-5610. doi: 10.1007/s10107-003-0379-5.

[81] Robert E Bixby and Matthew J Saltzman. Recovering an optimal LP basis from an interior point solution. *Operations Research Letters*, 15(4):169–178, 1994.

[82] Manuel Bröchin, Bryn Pickering, Tim Tröndle, and Stefan Pfenninger. Harder, better, faster, stronger: understanding and improving the tractability of large energy system models. *Energy, Sustainability and Society*, 14(1), 2024. doi: 10.1186/s13705-024-00458-z.

[83] David Applegate, Mateo Díaz, Oliver Hinder, Haihao Lu, Miles Lubin, Brendan O'Donoghue, and Warren Schudy. Practical large-scale linear programming using primal-dual hybrid gradient. *Advances in Neural Information Processing Systems*, 34:20243–20257, 2021.

[84] David Applegate, Mateo Díaz, Oliver Hinder, Haihao Lu, Miles Lubin, Brendan O'Donoghue, and Warren Schudy. PDLP: A practical first-order method for large-scale linear programming. *arXiv preprint arXiv:2501.07018*, 2025.

[85] Amir Beck. *First-order methods in optimization*. SIAM, 2017.

[86] Haihao Lu and Jinwen Yang. An overview of GPU-based first-order methods for linear programming and extensions, 2025.

[87] Kaihuang Chen, Defeng Sun, Yancheng Yuan, Guojun Zhang, and Xinyuan Zhao. HPR-LP: An implementation of an HPR method for solving linear programming. *arXiv preprint arXiv:2408.12179*, 2024.

[88] Nils-Christian Kempke, Daniel Rehfeldt, and Thorsten Koch. A massively parallel interior-point-method for arrowhead linear programs. *arXiv preprint arXiv:2412.07731*, 2024.

[89] Bob van der Zwaan, Sam Lamboo, and Francesco Dalla Longa. Timmermans' dream: An electricity and hydrogen partnership between Europe and North Africa. *Energy Policy*, 159: 112613, 2021. ISSN 03014215. doi: 10.1016/j.enpol.2021.112613.

[90] Stephan Kigle, Nadja Helmer, and Tapio Schmidt-Achert. Fast enough? the consequences of delayed renewable energy expansion on European hydrogen import needs. *Applied Energy*, 400: 126556, 2025. ISSN 03062619. doi: 10.1016/j.apenergy.2025.126556.

[91] Alejandro Nuñez-Jimenez and Nicola de Blasio. Competitive and secure renewable hydrogen markets: Three strategic scenarios for the European Union. *International Journal of Hydrogen Energy*, 47(84):35553–35570, 2022. ISSN 03603199. doi: 10.1016/j.ijhydene.2022.08.170.

[92] Falko Ueckerdt, Philipp C. Verpoort, Rahul Anantharaman, Christian Bauer, Fiona Beck, Thomas Longden, and Simon Roussanaly. On the cost competitiveness of blue and green hydrogen. *Joule*, 8(1):104–128, 2024. doi: 10.1016/j.joule.2023.12.004.

[93] Adrian Odenweller and Falko Ueckerdt. The green hydrogen ambition and implementation gap. *Nature Energy*, 10(1):110–123, 2025. doi: 10.1038/s41560-024-01684-7.

[94] Marius Neuwirth, Tobias Fleiter, and René Hofmann. Modelling the transformation of energy-intensive industries based on site-specific investment decisions. *Scientific reports*, 14(1):30552, 2024. doi: 10.1038/s41598-024-78881-7.

[95] Jonas Finke, Valentin Bertsch, and Valeria Di Cosmo. Exploring the feasibility of Europe's renewable expansion plans based on their profitability in the market. *Energy Policy*, 177:113566, 2023. ISSN 03014215. doi: 10.1016/j.enpol.2023.113566.

[96] David Yang Shu, Christiane Reinert, Jacob Mannhardt, Ludger Leenders, Jannik Lüthje, Alexander Mitsos, and André Bardow. Overcoming the central planner approach - bilevel optimization of the European energy transition. *iScience*, 27(7):110168, 2024. doi: 10.1016/j.isci.2024.110168.

[97] Markus Reuß, Lara Welder, Johannes Thürauf, Jochen Linßen, Thomas Grube, Lars Schewe, Martin Schmidt, Detlef Stolten, and Martin Robinius. Modeling hydrogen networks for future energy systems: A comparison of linear and nonlinear approaches. *International Journal of Hydrogen Energy*, 44(60):32136–32150, 2019. ISSN 03603199. doi: 10.1016/j.ijhydene.2019.10.080.

[98] Tim Mielich, Rafael Dobler, Jeremias Hollnagel, Okan Akca, and Joachim Müller-Kirchenbauer. Europe's way from natural gas to green hydrogen: Modeling and simulation of the transforming European gas transport infrastructure. *International Journal of Hydrogen Energy*, 135:156–171, 2025. ISSN 03603199. doi: 10.1016/j.ijhydene.2025.04.408.

[99] K. Guerra, P. Haro, R. E. Gutiérrez, and A. Gómez-Barea. Facing the high share of variable renewable energy in the power system: Flexibility and stability requirements. *Applied Energy*, 310:118561, 2022. ISSN 03062619. doi: 10.1016/j.apenergy.2022.118561.

[100] Chris Briggs, Alison Atherton, Jeremy Gill, Rusty Langdon, Jay Rutovitz, and Kriti Nagrath. Building a 'fair and fast' energy transition? renewable energy employment, skill shortages and social licence in regional areas. *Renewable and Sustainable Energy Transition*, 2:100039, 2022. ISSN 2667095X. doi: 10.1016/j.rset.2022.100039.

[101] European Commission. *Clean Energy Technology Observatory, Overall strategic analysis of clean energy technology in the European Union: 2024*. Publications Office, Luxembourg, 2025. ISBN 9789268210154. doi: 10.2760/3507717.

[102] Taghi Khaniyev, Samir Elhedhli, and Fatih Safa Erenay. Structure detection in mixed-integer programs. *INFORMS Journal on Computing*, 30(3):570–587, 2018. ISSN 1091-9856. doi: 10.1287/ijoc.2017.0797.

[103] Leonard Göke, Felix Schmidt, and Mario Kendziorski. Stabilized benders decomposition for energy planning under climate uncertainty. *European Journal of Operational Research*, 316(1): 183–199, 2024. ISSN 03772217. doi: 10.1016/j.ejor.2024.01.016.

[104] Daniel Ávila, Anthony Papavasiliou, Mauricio Junca, and Lazaros Exizidis. Applying high-performance computing to the European resource adequacy assessment. *IEEE Transactions on Power Systems*, 39(2):3785–3797, 2024. ISSN 0885-8950. doi: 10.1109/TPWRS.2023.3304717.

[105] Evangelos Panos and Aymane Hassan. Accelerating the performance of large-scale times models in the modelling of sustainable development goals. In Maryse Labriet, Kari Espegren, George Giannakidis, and Brian Ó Gallachóir, editors, *Aligning the Energy Transition with the Sustainable Development Goals*, volume 101 of *Lecture Notes in Energy*, pages 67–95. Springer Nature Switzerland and Imprint Springer, Cham, 2024. ISBN 9783031588976. doi: 10.1007/978-3-031-58897-6_4.

[106] Tarun Sharma, James Glynn, Evangelos Panos, Paul Deane, Maurizio Gargiulo, Fionn Rogan, and Brian Ó. Gallachóir. High performance computing for energy system optimization models: Enhancing the energy policy tool kit. *Energy Policy*, 128:66–74, 2019. ISSN 03014215. doi: 10.1016/j.enpol.2018.12.055.